LINKING PHENOTYPE TO GENOTYPE IN

PSEUDOMONAS AERUGINOSA

Annapaula Correia

University of East Anglia
Norwich Medical School

This dissertation is submitted for the degree of
Doctor of Philosophy 2017

Abstract

The global transcriptional regulator *mexT*, is a mutational hotspot; the sequence variants commonly seen to co-exist within the *P. aeruginosa* population are: drug susceptible (e.g. PAO1) and chloramphenicol and norfloxacin non-susceptible (nfxC mutant). The nfxC phenotype, selected for on chloramphenicol agar is characterised by reduced virulence. The conversion between PAO1 and *nfxC* phenotypes is associated with an 8-bp repeat sequence in *mexT*. To investigate the effects of the 8-bp repeat on the adaptive mode of survival of *P. aeruginosa,* isogenic mutants were generated: PA (8-bp, two copies) and PAdel (8-bp, one copy). The mutants were characterised using phenotypic microarrays (PM), motility, antibiotic susceptibility, *Galleria* virulence models and RNA-seq in defined media. PM revealed differences in central metabolism indicating that PAdel/PAnfxC were associated with a biological metabolic cost. Strains with the single copy of the 8-bp sequence showed reduced motility and virulence. Transcriptome analysis revealed that *mexT*, in PA, consists of two regulatory elements defined by an intact helix-turn-helix motif (across the repeat region) which is capable of regulating the downstream LysR region via repressor and auto-regulative mechanisms. Whole genome sequencing identified regions of compensatory mutations that were associated with differences in phenotype between PAdel (genetically modified) and PAnfxC (selected). To link phenotype and genotype and to understand the metabolic effects of this mutation, a genome wide metabolic reconstruction was performed. This revealed differences in key metabolic pathways such as glycolysis, gluconeogenesis and oxidative phosphorylation. This study has shown that an 8-bp repeat in *mexT* is a driver of genetic diversity. Regulatory elements linked to the effect of the 8-bp sequence on antibiotic resistance, central metabolism, chemotaxis, motility and virulence have also been identified. These methods can be used to define phenotype in any pair of isogenic mutants, at the genome level, and to investigate the clinical risk of strains.

Acknowledgements

Firstly, I would like to express my sincere gratitude to my primary supervisor Professor John Wain for his continuous support, motivation and knowledge during this PhD. His advice on my research as well as my career has been a tremendous support. I could not have asked for a better supervisor.

I would also like thank the rest of my supervisory committee Dr Justin O'Grady and Professor David Livermore for their insightful comments which have encouraged me to widen my research into different perspectives. My sincere thanks also goes to Dr Jake Malone from the John Innes Centre who gave me access to his laboratory and research facilities. Without his advice on *Pseudomonas aeruginosa* and genetic engineering it would not have been possible to conduct this research.

I would also like to thank Dr Gemma Langridge for her help with the analysis of the results and the writing process. My gratitude also goes to Dr Anna Stincone, Dr Luis de Figueiredo and Dr Stephan Beisken from Discuva Ltd who without their computational biology expertise the metabolic reconstruction would not have been possible.

I would like to extend a thank you to my fellow lab colleagues for making my time in the lab entertaining, especially the good music during those long days working in the lab.

Last but not least I would like to thank my friends and family for their unwavering support and encouragement. Your love and laughter kept me smiling during this PhD.

Declaration

I, Annapaula Correia declare that the work presented in this thesis was undertaken and completed by myself. Where information has been derived from other sources, I confirm that this has been indicated in the work.

Annapaula Correia B.Sc. (Hons)
University of East Anglia
October 2016

Contents

List of Figures

v

List of Tables

1   Introduction

P. aeruginosa is renowned for being a ubiquitous bacterial species which has an extraordinary ability to adapt and colonize various ecological niches. This is reflected in the genetic repertoire of this organism. Isolates have been found in an array of ecological environments, from those adapted to plants and animals to those that thrive in human hosts (Favero et al., 1971, Mena and Gerba, 2009). The adaptability is provided by genes that regulate metabolic pathways with a large number of transcriptional regulators and two-component systems (Stover et al., 2000). It is because of this that *P. aeruginosa* has served as a paradigm for the study of genotype and phenotype (Frank, 2012).

1.1   Classification and taxonomy of *Pseudomonas*

The genus *Pseudomonas* is defined as a Gram negative, rod-shaped γ-proteobacterium that was first described in 1895 (Klein and Migula, 1895, Spiers et al., 2000). Since then it has gone through multiple taxonomic revisions. Early studies based on rRNA-DNA hybridisation led to the formation of five RNA subdivisions whereby rRNA group I included *Pseudomonas aeruginosa* (Palleroni et al., 1973, Palleroni, 1993). The analysis of 16S rRNA gene sequences was later performed on 128 *Pseudomonas* species leading to the classification of seven sub clusters; *P.*

syringae, *P. chlororaphis*, *P. fluorescens*, *P. putida*, *P. stutzeri*, *P. aeruginosa* and *P. pertucinogena* group (Anzai et al., 2000). Debates regarding the poor resolution of phylogenetic analysis and the fact that closely related species cannot be differentiated solely based on the 16S RNA gene, led to the reclassification and identification of subgroups involving 16S rRNA sequence comparison, gene markers (e.g. *gryB*, *rpoD*, *oprI*, *oprF* sequences), housekeeping genes and siderotyping (Figure 1-1) (Bodilis et al., 2006, De Vos et al., 1998, Yamamoto et al., 2000, Frapolli et al., 2007, Ozen and Ussery, 2012, Gomila et al., 2015).

Currently 202 species have been assigned to the genus *Pseudomonas* according to the Approved List of Bacterial Names. The classification method depends not just on 16S rRNA but analysis of cellular fatty acids with physiological and biochemical tests (Tindall et al., 2006).

1.2   Species typing

Typing can involve various techniques depending on the discriminatory power, reproducibility and biological basis for grouping similar strains (Jong Wu et al., 2004). Methods can be divided into those that are related to phenotypic or genotypic analysis.
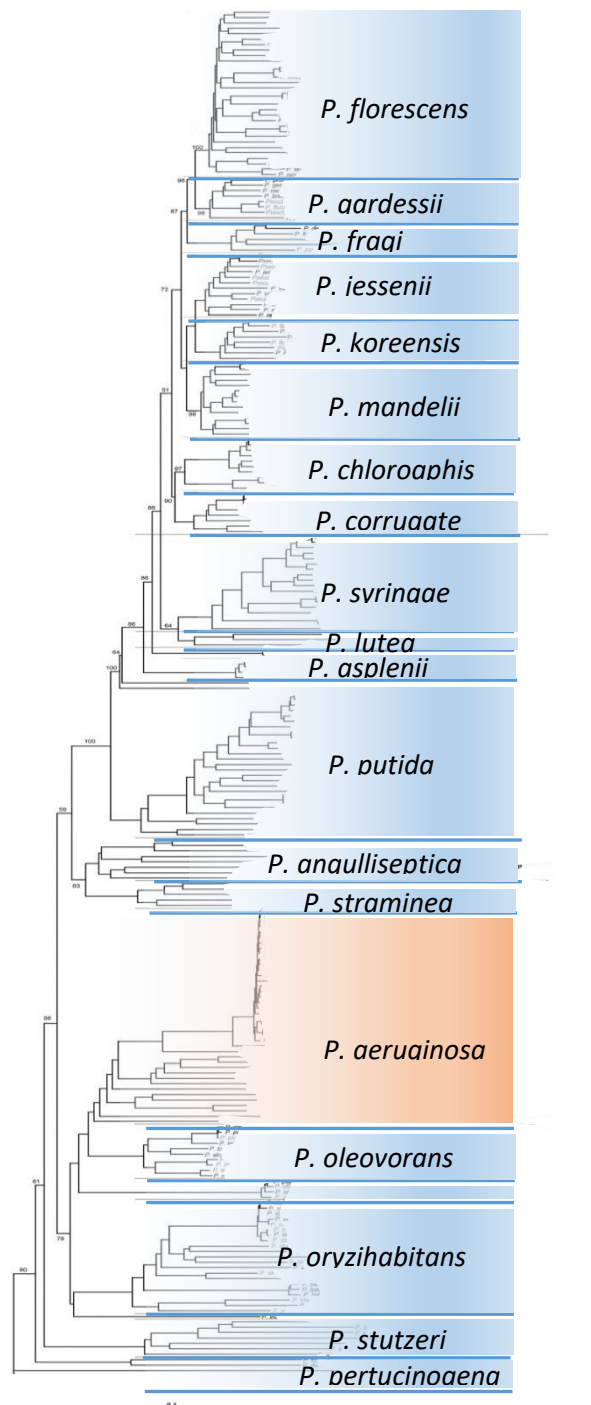
Figure 1-1 Phylogenetic tree of *Pseudomonas*

Figure adapted from (Gomila et al., 2015). Phylogenetic tree of *Pseudomonas* based on the analysis of four concatenated genes (16S rRNA, *gyrB*, *rpoB*, and *rpoD* using neighbor-joining. Numbers indicate bootstrap values for each branch and distance matrices are calculated using the Jukes-Cantor method. The bar indicates sequence divergence.

1.2.1   Phenotypic species typing

Serotyping is based on the phenotypic diversity of the O-polysaccharide moieties on the surface lipopolysaccharide whereby *P. aeruginosa* can be categorized into 20 unique O serotypes according to the International Antigenic Typing System (Knirel, 1990). One example includes serotype O6 which is one of the most frequently isolated strains accounting for 17 to 29 % of *P. aeruginosa* infections in patients (Lu et al., 2014, Estahbanati et al., 2002).

P. aeruginosa is characteristically resistant to specific antibiotics and as such agar incorporated with these antibiotics acts as a selective media for this species. Quantitative analysis of antibiograms using disk zone sizes is another form of phenotypic typing (Giacca and Monti-Bragadin, 1987). Biochemical tests can also identify distinct biotypes of *P. aeruginosa* (Freitas and Barth, 2004). Analysis of carbohydrate utilization rates such as galactose, mannose, mannitol and rhamnose are a method of typing. Although some strains are non-pigmented, *P. aeruginosa* is known for the characteristic blue-green virulence pigment it produces on agar, indicating production of pyocyanin and pyoverdine. Positive results from oxidase and catalase tests are also another indicator of *P. aeruginosa*. These methods of identification are used in water testing as well as clinical laboratories (Penna et al., 2002). Other markers used to identify *P. aeruginosa* include hydrolysis

of urea and haemolysis of blood (Freitas and Barth, 2004) in clinical laboratories.

1.2.2 Molecular species typing

Since traditional phenotypic markers are unstable and do not offer satisfactory resolution power for discrimination of strains, the need for new methods led to the introduction of molecular typing. Some of these techniques included PCR (Polymerase Chain Reaction) based methods such as Random Amplification of Polymorphic DNA (RAPD) and ribotyping (Mahenthiralingam et al., 1996, Syrmis et al., 2004, Blanc et al., 1993). Pulse field gel electrophoresis (PFGE) involves restriction endonuclease analysis of the total genome and has been used as a DNA fingerprinting technique intended for outbreak situations. PFGE restriction profiles however can change according to mutations that modify these restriction sites making this technique impractical (Fothergill et al., 2010). To fulfill these shortcomings, Multi Locus Sequence Typing (MLST) was introduced. This technique is based on allelic variation in housekeeping genes making it highly discriminating (Kidd et al., 2011). Multilocus Variable Number Tandem Repeat Analysis (MLVA) has also successfully been implemented in epidemiological studies and was first developed with the use of seven variable number tandem repeat markers. This has however now been

improved to include new discriminative markers leading to its use as an outbreak detection tool (Maatallah et al., 2013).

Whole genome sequences can provide valuable information on the taxonomic relationships between species (Figure 1-2). These methods have evolved to replace DNA-DNA hybridization methods by creating databases of whole genome sequences. Such methods can include analysis using tetra nucleotide usage patterns, average nucleotide identity and genome-to-genome distance (Gomila et al., 2015).
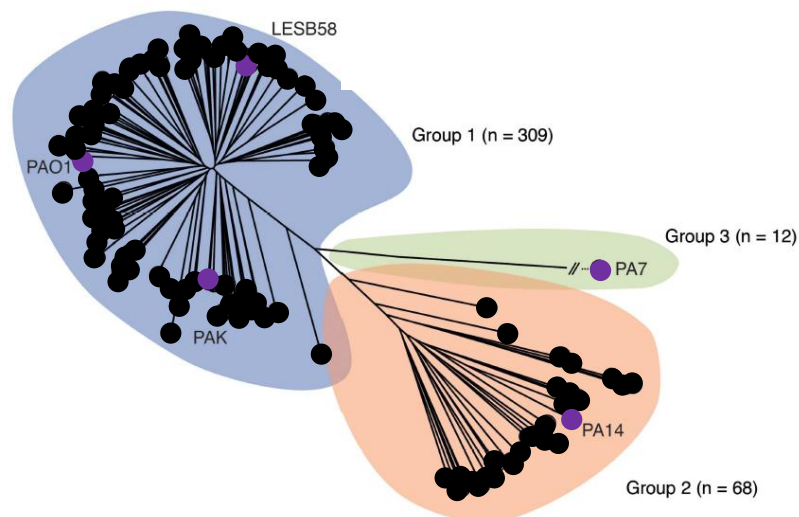
Figure 1-2 Phylogenetic tree of *P. aeruginosa*
Unrooted maximum likelihood tree of 389 *P. aeruginosa* genomes based on variations on SNPs within the core genome as defined by the bioinformatics tool Harvest (100 bootstraps). Genomes include environmental, clinical and animal strains from various sites. Those indicated in purple are reference strains. Strains are divided into three major groups; group 1 (blue), group 2 (pink) and group 3 (green) with the number of strains for each group shown. Purple circles indicate references strains. The phylogenetic tree shows that group 1 strains, including PAO1, are more abundant than those found in group 2, which includes PA14. Figure adapted from Freshchi et al., 2015.

The introduction of standardized matrix assisted laser desorption/ionization time-of-flight mass spectrometry (MALDI-TOF MS) platforms in the medical microbiological practice has revolutionized the way microbial species identification is performed. However, the low resolution and dynamic range of the MALDI-TOF profiles have shown limited applicability for the discrimination of different bacterial strains. This is because only proteins within a small mass-to-charge ratio are detected which mostly only include highly-abundant proteins such as ribosomal proteins. Ultrahigh resolution MALDI-FTICR (Fourier transform ion cyclotron resonance) MS allows the measurement of small proteins at isotopic resolution and can be used to analyse complex mixtures with increased dynamic range (m/z-range from 3497 to about 15 000) and higher precision than MALDI-TOF MS (Fleurbaaij et al., 2016). This is important when associating strains with virulence or antibiotic resistance.

1.3 Methods for integrating genotypic and phenotypic interactions

The genotype–phenotype relationship is one that is important. Understanding the genetic basis of complex traits has been an on-going quest as this relationship is subjected to critical analysis. To elucidate the genetic elements of a bacterium, the typing and characterization of *P. aeruginosa* (as described above) has relied on methods that address defined regions of the bacterial genome. Such methods can include PCR with the aid

of multiplex primer pairs to ensure high throughput sequencing of selected amplified fragments. Another method is hybrid capture whereby DNA fragments from a whole genome library are hybridized to complementary probe sequences, created with a high specificity for matching regions of the test genome. These probes are designed to capture known coding regions and therefore form a bias (Koboldt et al., 2013).

The advent of genomic sequencing in the mid-1990s began to change the way fundamental genotype-phenotype links were made (Lewis et al., 2012). Full genome sequences not only provide comprehensive information about genetic compositions but they also allow analysis of inter- and intra-individual genome variation within a species (Gresham et al., 2008). Differences at the level of DNA sequence are the most abundant source of genomic variation and allow the prediction of phenotype (Lindsey et al., 2016). There is a limit however as to how well phenotypic traits such as virulence and antimicrobial profiles can be predicted since there are no comprehensive whole genome sequence and phenotype databases to compare to. It is therefore essential to perform phenotypic experiments alongside genotypic tests. Genotypic techniques provide a genetic fingerprint that is independent of the physiological state of an organism i.e. the results are not influenced by growth conditions such as media composition or growth phase. Phenotypic techniques, however, can yield more direct functional information that reveals what metabolic activities are

taking place to aid the survival, growth, and development of an organism (Emerson et al., 2008).

Genotyping and phenotyping can be carried out using a range of methods depending on the subject of interest and resources available. Techniques that link genotype to phenotype involve transcriptome studies. Hybridization based technologies such as FISH (Fluorescence in situ hybridization) or microarray based methods suffer limitations. These involve dependence on the existing knowledge of genomic sequences and signal saturation for particular transcripts (with a high abundance and high background noise) due to non-specific hybridization. Recent technological advances have expanded the breadth of transcriptomics. RNA-seq allows genome wide mapping and annotation of the transcriptome, analysis of the functional structure of each gene and quantification of changes in gene expression (Qian et al., 2014).

1.3.1   Data integration

New integration methods are now emerging that aim to bridge the gap between the ability to generate vast amounts of data with an understanding of the regulatory systems involved in the biology of the organism. The primary motivation behind integrated data analysis is to identify key genomic factors and interactions that explain or predict the risk of infection.

New approaches to data integration involve the development of models that predict phenotypic traits and outcomes using omic, transcriptomic, methylomic and metabolomic data (Ritchie et al., 2015). Incorporating omic data with phenotypic data, such as those acquired through high throughput phenotypic microarrays achieves a more thorough and informative interrogation of genotype–phenotype associations than an analysis that relies solely on a single data source. This technique can also compensate for false positives, missing or unreliable information from any single data set. Futhermore, to be able to truly understand the complete biological model of a microorganism, the study of genetic, transcriptomic and proteomic regulation, at different levels, is required.

1.3.2   Methods for cellular modelling

Over the years there has been significant improvement for high throughput methods that characterise phenotype. One such method involves Biolog's Phentoype MicroArray technology which is capable of evaluating nearly 2000 phenotypes in a single experiment using cellular assays, growth kinetics and robotics (Zhou et al., 2003). The advent of genomics and high throughput sequencing has meant that more is now known about the individual molecules and interactions that drive cell function. This combined with the advancement of computational methods has meant that

compressive metabolic network modelling is now possible enabling the prediction of phenotype in defined environments.

Metabolic pathways typically involve reactions comprising of metabolites such as cofactors and by-products. The conversion of nutrients through catabolism into cell components includes the regeneration of cofactors and recycling of by-products. These reactions are dependent on the stoichiometry and rates of the reactions. Manual approaches such as those involving the metabolism reference database BioCyc are unable to assess the feasibility of a given network as metabolic networks require quantitative analysis and are often too large and complex to analyze (Durot et al., 2009).

Recent developments to the BioCyc database now means that this web interface is also capable of incorporating the PathoLogic component of the Pathway Tools software to computationally predict the metabolic network of any organism based on an annotated genome (Caspi et al., 2012). However new methods are required to bridge the gap between predicted and observed metabolic phenotypes. This is where metabolic reconstructions become beneficial. This technique incorporates constraint-based genome scale models of metabolism to identify metabolic fluxes and determine the physiological state of a cell (Durot et al., 2009). It is through comprehensive and precise quantitation of phenotypes, that researchers are able to obtain an unbiased perspective of the effect on cells of genetic

differences, environmental change, exposure to chemicals or drugs, and more.

1.4 *P. aeruginosa* genome structure and diversity

Whole genome sequences of *P. aeruginosa* strains show that this bacterium is larger than most prokaryotic organisms with genome sizes varying between 5.5 to 7 Mbp within species (Schmidt et al., 1996, Lee et al., 2006). The metabolic versatility of *P. aerugionsa* and it's ability to adapt to new environmental conditions would suggest there is variability in the genome content, reflective of where a strain has been isolated from. However despite differences in phenotype among *P. aerguinosa* strains, the core genome of clinical and environmental isolates is highly conserved (Wolfgang et al., 2003, Grosso-Becerra et al., 2014). Within conserved regions, nucleotide diversity is as low as 0.5-0.7% among clonal strains (excluding regions that are subject to diversification). This similarity at the genome level is not observed in bacteria such *Escherichia coli* or even other *Pseudomonas* species. (Lee et al., 2006, Spencer et al., 2003, Cramer et al., 2011).

The accessory genome is the main cause of variability in genome size. It comprises of plasmids or genetic elements that exist external to the chromosome and are acquired through horizontal gene transfer. While the ongoing acquisition of new foreign DNA, mutational events and chromosomal inversions drive genome modification it is the composition of

the accessory genome that accounts for most of the intra- and interclonal genome diversity in *P. aeruginosa* (Klockgether et al., 2011). This diversity leads to the generation of 'high risk clones' which are more prone to disseminate and lead to dominant phenotypes such as those related to antibiotic resistance in clinical settings (Valot et al., 2015).

1.5 Clinical significance of *P. aeruginosa*

Pseudomonas aeruginosa is the causative agent of healthcare associated infections (House of Commons Public Accounts Committee, 2009) and is responsible for approximately 10% of infections (2004, Morrison and Wenzel, 1984) with mortality rates ranging from 18-61% (Vidal et al., 1996, Siegman-Igra et al., 1998, Lodise et al., 2007).

Found to inhabit natural and aquatic environments, in clinical settings this species can colonize a variety of hospital surfaces including taps and medical devices with the ability to cause severe infection as an opportunistic pathogen (Ramsey and Whiteley, 2004, Gellatly and Hancock, 2013b, Bodey et al., 1985). Infections associated with this bacterium include those with artificial prosthesis, severe burns wounds, urinary tract infections, AIDS, lung cancer, chronic obstructive pulmonary disease, bronchiectasis and cystic fibrosis (Kerr and Snelling, 2009, Valderrey et al., 2010, Bouza et al., 2002, Manfredi et al., 2000, Balasubramanian et al., 2013).

P. aeruginosa infections are notoriously difficult to treat due to antibiotic resistance and the ability to evade host defences and form biofilms. This bacterium has intrinsic resistance and the ability to acquire further mechanisms of resistance to antibiotics by adaption (Strateva and Yordanov, 2009). *P. aeruginosa* also employs a range of mechanisms to evade human host immune responses, particularly in acute infection. Flagella, type 4 pili and lipopolysaccharide aid adhesion to host cells (Gellatly and Hancock, 2013a). Exoproteins also have a variety of roles in pathogenesis. Along with virulence, they allow bacteria to interact with the environment and with other microorganisms. There are six secretion systems in *P. aeruginosa*. Some examples of their roles include regulation of cell-surface signalling, haeme uptake, injection of cytotoxins into the host cell and the secretion of effector molecules that are crucial for evading the host phagocytic response (Filloux, 2011, Chakraborty et al., 2013, Lovewell et al., 2014). Virulence factors, capable of degrading and promoting host cell injury, can be categorised into proteases, lipases and phospholipases. Siderophores such as pyocyanin and pyoverdine cause host cell oxidative stress and allow iron chelation (Gellatly and Hancock, 2013a, Smith et al., 2006). Chronic infection arises as the bacterial population adapt in a co-ordinated manner to environmental changes.

1.6   Biofilms

Bacteria can survive as planktonic cells but they predominantly exist as biofilms (Costerton et al., 1987). Bacterial cells that attach to a surface and form an enclosed microbial community within a extracellular polymeric matrix (EPM) are known as biofilms (Hall-Stoodley et al., 2004). *P. aeruginosa* infections caused by implants (i.e. catheters and mechanical ventilators) and those diagnosed in burn victims and cystic fibrosis patients have been attributed to biofilm formation (Hoiby et al., 2011).

While biofilms were first described in 1936 (Zobell and Anderson, 1936), there are a number of hypotheses as to why bacteria form biofilms. The primary reason is defence. Microorganisms inside the EPM are able to avoid antimicrobial agents; in some cases a 100-fold increase in antibiotic concentration is required to kill sessile bacteria compared with the same microbes in planktonic form (Jefferson, 2004). As a biofilm community, organisms can withstand host immune responses such as phagocytosis and endure pH changes and starvation of nutrients. Moreover, subsequent growth and expansion allows nearby planktonic bacteria to attach and form a diverse multi-species biofilm (Jenkinson and Lamont, 2005). Biofilms may grow on sites with a constant supply of nutrients. Therefore growing as a biofilm is preferential for survival and remaining as an attached community (Jefferson, 2004).

Bacteria in biofilms exhibit behaviour similar to a multi-cellular organism; biofilm architecture is built with strain diversification, providing numerous micro-environments in which bacteria can interact with their surroundings. Factors which affect biofilm architecture include cell proliferation and migration in response to environmental nutrients, intercellular signal molecules, EPS structure and fluid channels within the biofilm (Davey et al., 2003, Miller et al., 2012, Sanchez et al., 2013, Pamp and Tolker-Nielsen, 2007, Yang et al., 2011, Parsek and Tolker-Nielsen, 2008). These structures enable bacteria to adjust their metabolic processes to maximize the use of available substrates and to protect themselves from detrimental conditions (Jenkinson and Lamont, 2005).

Biofilm development is a complex process which can be divided into four stages (Figure 1-3): initial attachment, irreversible attachment, maturation and detachment (Renner and Weibel, 2011). Once a bacterium approaches the substrate it is to attach to, initial attachment occurs as electrostatic forces bring the bacterium close enough to allow pili and adhesins to interact with the surface (Hermansson, 1999). Type IV pili and flagella allow irreversible attachment to the surface. Biofilm development is regulated by quorum sensing and as the micro-colony develops and matures it becomes encapsulated by the extracellular matrix, which is composed of proteins, nucleic acids and polysaccharide.
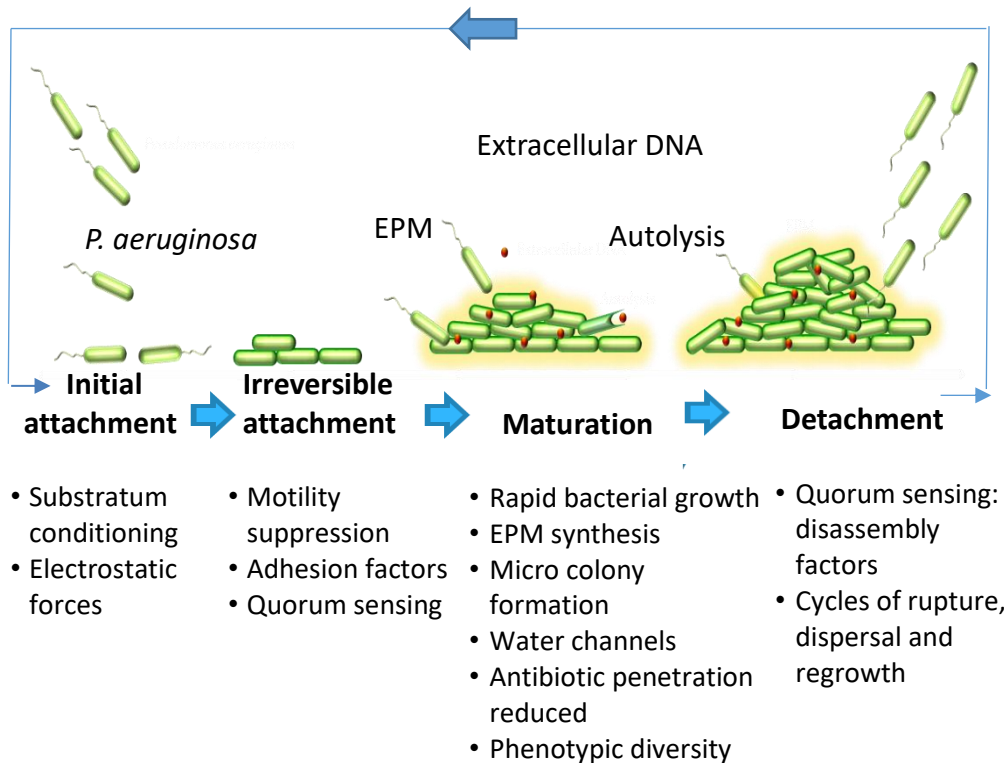
Figure 1-3 Stages of biofilm formation.

Stage 1. Initial attachment brings planktonic cells to the surface via electrostatic forces. Stage 2. Irreversible attachment. Once in close proximity with the surface, adhesive factors such as type VI pili initiate attachment. Stage 3. Maturation. Quorum sensing permits cell aggregate growth and EPM production within the biofilm. The biofilms are interspersed with fluid-filled channels which act as a primitive circulatory system, allowing the exchange of nutrients and waste products. Numerous microenvironments that differ with respect to pH, oxygen concentration, nutrient availability and cell density exist within the biofilm colony and lead to cell diversity. Stage 4. Detachment. Quorum sensing allows the dispersal of cells, ensuring regeneration of the biofilm life cycle.

Throughout biofilm formation, cell differentiation takes place forming oxygen and water filled channels which provide nutrients to cells, deep within the biofilm. The EPS confers biofilm-mediated antimicrobial resistance and acts as a barrier to diffusion of antibiotics. Bacterial diversity

within microenvironments means that metabolically inactive cells residing deep within the biofilm maybe resistant to antimicrobials agents that target actively growing cells (Mah and O'Toole, 2001, Kaplan, 2010).

1.6.1 Regulation of quorum sensing

Quorum sensing (QS) or cell-to-cell communication has a pivotal role in the co-ordination of virulence. It is a process that involves production, detection and response to extracellular signaling molecules known as autoinducers. As the bacterial population density increases, autoinducer concentrations increases in the environment. It is this process that allows groups of bacteria to act in synchronized manner by monitoring changes in cell density and collectively regulating expression of beneficial genes. Processes controlled by QS include bioluminescence, sporulation, competence, antibiotic production, biofilm formation, and virulence factor secretion (Rutherford and Bassler, 2012).

P. aeruginosa utilises two AHL (Acyl Homserine Lactone) based quorum sensing systems; Las and Rhl and a non AHL mechanism, the *Pseudomonas* Quinolone Signal (PQS) system (Figure 1-4). The Las system is comprised of the transcriptional regulator LasR, which is constitly expressed, and its cognate AHL signal molecule, *N*-(3-oxododecanoyl)-L-homoserine lactone (3-oxo-C12-HSL). As cell density increases so do AHL molecules. Upon reaching a high concentration, 3-oxo-C12-HSL binds to the LasR protein and

activates it. The LasR-3- oxo- C12-HSL bound complex can now bind to the promoter sequence (LasBox) and facilitate transcription. Similarly, the Rhl system comprised of RhlR and its cognate AHL, *N*-butyryl-L-homoserine lactone (C4-HSL) activate the Rhl-box (Dandekar and Greenberg, 2013, de Kievit, 2009). Quorum sensing involves multiple signals and receptors with LasR regulating the activity of RhlR and PqsR as well.

P. aeruginosa produces the signalling molecule, 2-heptyl-3-hydroxy-4(1*H*)-quinolone (PQS) by oxidising the precursor 2-heptyl-4-quinolone (HHQ) via pqsH. PQS is positively regulated by the las system but negatively regulated by the Rhl system. In *P. aeruginosa* HHQ is formed via the condensation of anthranilate and a β-keto-fatty acid. Anthranilate is produced from tryptophan degradation via the kynurenine pathway (metabolic pathway: tryptophan to *N*-formylkynurenine to kynurenine to anthranilate) (Olivares et al., 2012).

PQS enhances binding of the LysR-type transcription regulator, PqsR (also known as MvfR) to the *pqsABCDE* operon (Kirisits and Parsek, 2006, Sakuragi and Kolter, 2007). Downstream regulation of this gene involves various targets whereby PqsR mutant strains have been shown to differentially express 141 genes pertaining to transcriptional regulation (Deziel et al., 2005). PQS also acts independently of PqsR to induce expression of the Fur regulon via membrane vesicle formation and iron binding caused by

membrane curvature (Diggle et al., 2007, Bredenbruch et al., 2006, Mashburn and Whiteley, 2005, Schertzer and Whiteley, 2012).

Many global regulators are known to modulate QS dependant genes. RpoS for instance affects 40% of the QS regulon (Schuster et al., 2004, Schuster and Greenberg, 2007) by modulating key transcriptional regulators such as LasR, RhlR and various other QS transcriptional regulators (PA2588, PA4778, PvdS, VqsR and RsaL) (Gilbert et al., 2009). RsaL expression is mediated by the LysR transcriptional regulator (LTR) OxyR and is involved in *las* signalling homeostasis (Wei et al., 2012). RsaL binds to the *lasI* promoters thus preventing LasR activation. Expression of this gene affects 130 genes relating to pyocyanin and hydrogen cyanide. In an intricate network regulated by quorum sensing, this is one example of the role LTRs can play.

1.6.2   Two component systems

Two-component systems (TCS) are signal transduction systems that enable bacteria to respond to specific stimuli. This allows adaption to a variety of environments, stressors and growth conditions. The general structure of a TCS consists of sensory histidine kinase (HK) that is integrated in the membrane and a response regulator (RR) that is situated within the cytoplasm and involved in eliciting a transmitter (Rodrigue et al., 2000, Mitrophanov and Groisman, 2008). While there are variations to this model,

generally once a signal is received, two HK monomers dimerize and cross-phosphorylate at the histidine residue. The phosphate is subsequently transferred to an aspartate residue in the receiver domain of the cognate RR. The receiver domain then catalyzes the phosphotransfer which causes a conformational change. This activates downstream processes which can involve modulation of gene expression or enzymatic activity (Balasubramanian et al., 2013).

P. aeruginosa PAO1 possesses 55 histidine kinases, 89 response regulators and 14 histidine kinases-response regulator hybrid like structures, one of the largest collections of TCS's in any microorganism (Stover et al., 2000). The GacS-GacA system is one TCS that is critical to the regulation of virulence, secondary metabolite, QS and biofilm formation. (Kitten et al., 1998, Pessi et al., 2001). The GacS system is however under the control of two hybrid sensors kinases. The RetS sensor prevents phosphorylation whereas LadS is capable or phosphorylating GacS. Phosphorylated GacA positively regulates the transcription of two small regulatory RNAs, rgRsmZ and rgRsmY, which block the negative regulator RNA-binding protein RsmA. RsmA positively regulates genes of the Type 3 secretion system, type IV pili formation and iron homeostasis while repressing QS, Type 6 secretion and potentially other transcription factors. The GacSA TCS is also involved in antibiotic resistance to three different families of antibiotics, tobramycin, ciprofloxacin and tetracycline, through RsmA/rgRsmZ (Balasubramanian et al., 2013).

1.6.3   Cyclic di-GMP signalling

Cyclic di-GMP (c-di-GMP) is another signalling molecule that has a pivotal role as a secondary messenger. Enzymes responsible for c-di-GMP synthesis are known as diguanylate cyclases (DGCs) and contain the consensus sequence motif GGDEF within the active site. Enzymes with phosphodiesterase activity are governed by EAL domains that catalyse c-di-GMP degradation (Jimenez et al., 2012). Together these enzymes regulate cell phenotype. In simplified terms, high levels of intracellular c-di-GMP levels correlate with a sessile state while low levels are associated with planktonic growth (Ha et al., 2014) as illustrated in Figure 1-4.

1.7   Metabolism

The ability to metabolize various substrates endows *P. aeruginosa* with high environmental adaptability. A knowledge of the metabolic processes that allow bacteria to grow and colonize specific environments are therefore of great importance. However, in most *P. aeruginosa* niche adapted sites these metabolic pathways are not known. For instance, the synthesis of trehalose by *P. aeruginosa* is required for pathogenesis in Arabidopsis, but not in nematodes, insects, or mice. Since trehalose promotes the acquisition of nitrogen-containing nutrients in a process that involves xyloglucan (plant cell wall component), this may allow *P. aeruginosa* to colonise intercellular leaf compartments (Djonovic et al., 2013).

Figure 1-4 The basics of quorum sensing and biofilm genetics
A simplified diagram of the genetics involved in biofilm formation. Lines terminated with an arrow indicate activation but lines terminated with a circle illustrate inhibition. Quorum sensing is regulated by the Las, Rhl and PQS systems. AHL molecules diffuse across the cell membrane or are transported via efflux pumps compared to the PQS signal which is transported via membrane bound vesicles. PQS regulates its own production by controlling the expression of *pqsABCDE, b*ut is also negatively regulated by the Las system, via the transcriptional regulators QscR and VqsR. Biofilm production is additionally linked with increased levels of c-di-GMP which up-regulates expression of genes involved in fimbrial assembly (cup), alginate and EPS (*Pel, Psl*) production. Biofilm production is additionally mediated by *WspR* signalling through its cognate sensor *WspA*.Reduced c-di-GMP levels favors cell motility by increasing expression of genes associated with flagella, acute virulence factors (pyocyanin) and dispersal. The two-component systems, GacS/GacA and RetS/LadS, consists of the histidine kinases which control biofilm associated genes and the AHL systems. Figure from (Correia)

In terms of host-pathogen responses and biofilm development, the nutritional cues for proliferation affect production of extracellular virulence factors, surface motility and alginate production (Palmer et al., 2005, Cutruzzolà and Frankenberg-Dinkel, 2016, Vasil and Ochsner, 1999). *P.*

aeruginosa biofilm formation is prevented and dispersal enhanced by the D-enantiomers of tyrosine, leucine, tryptophan, and methionine. Since this effect was not also observed by the L-enantiomers of these amino acids, it was shown that D-amino acids act by modulating stationary phase cell wall remodeling, indicating that this may be a mechanism by which bacteria adapt to changing environmental conditions (Lam et al., 2009, Moe, 2013).

In a clinical environment, it has been reported that lung mucus which is rich in amino acids promotes the growth of auxtrophic strains during chronic infection (Barth and Pitt, 1995, Jørgensen et al., 2015). Virulence studies also implicate the kynurenine pathway as a source of anthranilate for PQS synthesis (Farrow and Pesci, 2007) and acetyl-CoA as regulator of the type III secretion system (Rietsch and Mekalanos, 2006). Bacterial resistance is concerningly not always associated with a metabolic burden but rather changes in specific pathways. For instance a *Stenotrophomonas maltophilia* mutant that overexpresses a MDR efflux pump is better at metabolising sugars such as gentibiose, dextrin and mannose and formic acid compared to the wild-type (Alonso et al., 2004, Alonso and Martinez, 2000). Carbon sources can also alter the susceptibility to antibiotics. It has been shown that a *P. aeruginosa* mutant with a defective *crc* gene (global regulator of carbon metabolism) is more susceptible to imipenem and fosfomycin. This is because it expresses high levels of the membrane transporters OprD and GlpT, which are involved in transport of basic amino

acids and glycerol-3-phosphate (Martinez and Rojo, 2011, Linares et al., 2006). It is clear that central metabolism has a large impact on bacterial phenotype.

1.8 Respiration

The energy producing system in *P. aeruginosa* is mainly dependant on oxidative substrate catabolism which utilizes the proton motive force for adenosine triphosphate (ATP) synthesis. *P. aeruginosa* is also capable of thriving in anaerobic conditions via external electron acceptors or fermentation of arginine or pyruvate. Catabolite repressor control ensures that *P. aeruginosa* facilitates catabolism of preferred substrates over others in a culture. Preferred sources of carbon or nitrogen include short-chain fatty acids, amino acids and polyamines. Sugars, which are also efficiently metabolized, are less preferred since there are degraded via the Entner-Doudoroff pathway (Entner and Doudoroff, 1952, Goldbourt et al., 2007, Frimmersdorf et al., 2010). This may have an advantage for soil based *P. aeruginosa* where the concentration of organic compounds exceeds sugars, due to decomposing plant and animal matter. *P. aeruginosa* is also capabale of growing on xenobiotics such as *n*-alkanes and (halogenated) aromatic compounds with an ability to produce secondary metabolites (Frimmersdorf et al., 2010).

Aerobic respiration occurs via electron donors and acceptors whereby 17 respiratory dehydrogenases are predicted to be responsible for feeding electrons from respiratory substrates into the quinone pool, including three types of NADH dehydrogenases and a succinate dehydrogenase (Williams et al., 2007). *P. aeruginosa* has five terminal oxidases which catalyse the reduction of molecular oxygen to water (Arai, 2011). Three of them are cytochrome coxidases that receive electrons via the cytochrome bc_1 complex and *c*-type cytochromes; cbb_3-1 oxidase (Cbb3-1), cbb_3-2 oxidase (Cbb3-2), and aa_3 oxidase (Aa3). The remaining two are quinol oxidases that receive electrons from ubiquinol; cytochrome bo_3oxidase (Cyo) and the cyanide-insensitive oxidase (CIO). These terminal oxidases have a specific affinity for oxygen, proton-translocation efficiency and resistance to stresses such as cyanide and reactive nitrogen species (Jo et al., 2014, Arai, 2011).

1.8.1   Regulation of respiration

The redox-responsive transcriptional regulators, ANR (anaerobic regulation of arginine deiminase and nitrate reduction), RoxSR and the stationary phase sigma factor RpoS, are known to regulate terminal oxidase gene expression. In *P. aeruginosa* ANR is an oxygen sensor and global regulator for anaerobic gene expression (Zimmermann et al., 1991, Galimand et al., 1991). RoxSR is a two-component transcriptional regulator that includes RoxR, the

membrane-bound sensor kinase and RoxR, the response regulator (Arai, 2011).

It is thought that the redox status of the respiratory chain acts as a sensing signal of RoxSR in *P. aeruginosa.* The enzyme Cbb3-2, is active under low oxygen conditions and is activated by ANR. This regulator, ANR however represses CIO and Cyo which are low affinity enzymes. RoxSR regulates all five terminal oxidases and other genes related to respiratory function such as *hemB* and *nuoAL* illustrating its important role in respiratory regulation. RpoS plays a role in regulating Aa3 and CIO. The *cox* promoter is activated by the sigma factor RpoS but is simultaneously repressed by the active RoxSR in hypoxic high-cell-density stationary phase cultures. RoxSR and ANR are able to fine tune multiple enzymes capable of terminal oxidase regulation since the redox status is also regulated by nutritional respiratory conditions. Figure 1-5 illustrates the regulatory pathways involved in controlling terminal oxidases (Arai, 2011).
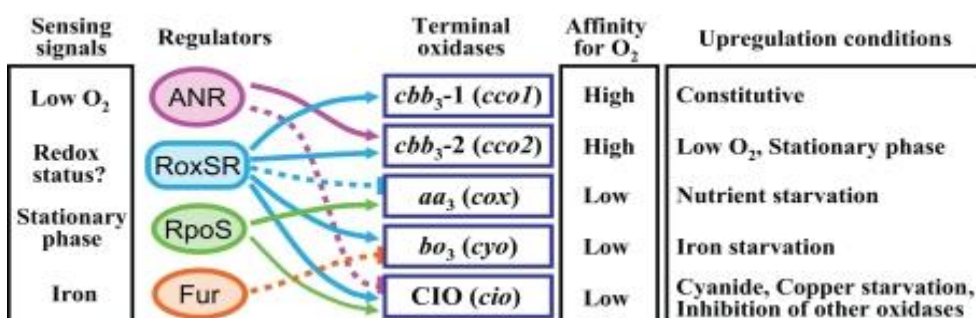
Figure 1-5 Schematic network involving regulators of *P. aeruginosa* terminal oxidases
Figure from (Arai, 2011). On the left; sensing signals for regulators. On the right; terminal oxidase affinity of oxygen and conditions that are required for up-regulation. Arrows show activation whereas dotted lines show inhibition.

1.8.2   Genetics of nitrate metabolism

P. aeruginosa is capable of growing in the absence of oxygen using dissimilatory nitrate respiration whereby nitrogen oxides are used as an alternative terminal electron acceptor in the respiratory chain. This process is known as denitrification whereby soluble nitrate (NO^{-3}) and nitrite (NO^{-2}) are reduced causing the release of nitrous oxide (N_2O) or dinitrogen (N_2) (Arai, 2011).

NO^{-3} reductase catalyzes the first step of denitrification, involving reduction of NO^{-3} to NO^{-2}. There are three types of NO^{-3} reductases, Nar, Nap, and Nas, which are localized to the cytoplasmic membrane, periplasm and cytoplasm (Stover et al., 2000, Berks et al., 1995). The membrane-bound Nar is the enzyme responsible for anaerobic NO^{-3} respiration of *P. aeruginosa* in cystic fibrosis sputum (Palmer et al., 2007). Nar is encoded in the *narK1K2GHJI* gene cluster which comprises the structural subunits of the enzymes (NarG, NarH, and NarI), assembly (NarJ) and NO^{-3}/NO^{-2} transporters (*narK1 and narK2*). The gene cluster is regulated by the two component transcriptional regulator NarXL. Reduction of NO^{-3} by Nar is coupled to quinol oxidation and consumes two protons from the cytoplasm, thereby contributing to the proton gradient across the membrane (Zumft, 1997).

The napEFDABC gene cluster comprises the Nap quinol oxidase which also contributes towards NO^{-3} reduction. The physiological function of this gene

family is however unknown in *P. aeruginosa* but appears to have a role in redox balancing since it does not contribute to the generation of a proton gradient. The *nasC* gene is involved in NO^{-3} assimilation and is clustered with *nirBD* which encodes NO^{-2} reductase (Arai, 2011).

The second step of denitrification involves NO^{-2} reductase and the catalysis of NO^{-2} to nitric oxide (NO) via the *nirSMCFDLGHJEN* gene cluster. This operon consists of nitrite reductase (*nirS*) and cytochromes (*nirM, nirC, nirN*) which mediate electron transfer from the cytochrome complex to nitrite reductase and genes regulating biosynthesis of heme d (*nirFDLGHJE*) (Arai, 2011).

Reduction of NO to N_2O is catalysed by NO reductase and is encoded by the *norCBD* operon. The genes *norB* and *norC* encode cytochrome subunits of NO reductase whereby NorC mediates electron transfer from soluble cytochrome *c* to NorB, which contains the heme catalytic centre. The *nirQOP* operon ensure genes regulating nitrite reductase and NO reductase are tightly regulated to prevent the accumulation of the cytotoxic intermediates (Arai et al., 1997, Arai et al., 1998). This is important during infection when *P. aeruginosa* cells are subjected to nitrosative stress by attack of the host immune system.

Reduction of N_2O to N_2 is the final stage of denitrification and is catalysed by N_2O reductase, a periplasmic enzyme that receives electrons from

cytochrome bc_1 via soluble cytochrome c. While the gene *nosZ* encodes for

the structural N_2O reductase, enzyme activity is also encoded by the

nosRDFYL operon (Arai, 2011).

Denitrification enzymes are induced under anaerobic or low oxygen

conditions in the presence of NO^{-3} or NO^{-2}. Two transcriptional regulators,

ANR and DNR (dissimilatory NO^{-3} respiration regulator), belong to the

CRP/FNR superfamily of transcriptional regulators and are required for full

expression of all denitrification genes (Figure 1-6). Denitrification is also

regulated by the two-component nitrate sensing regulator NarXL and by

quorum-sensing signal molecules (Yoon et al., 2002, Toyofuku et al., 2008).
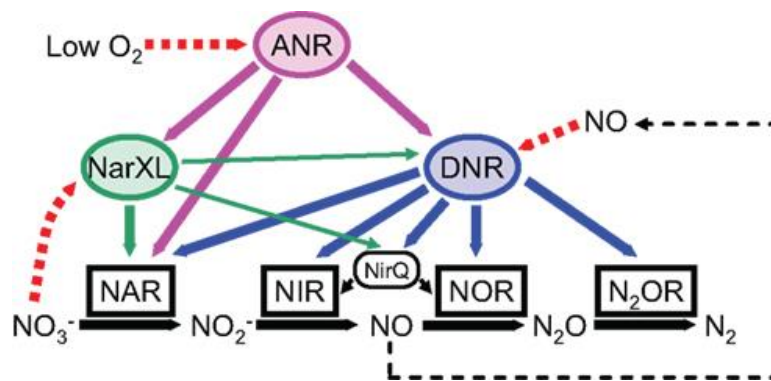
Figure 1-6 A simplified regulatory network illustrating control of denitrification genes in *P. aeruginosa*.
In conditions of low oxygen ANR activates expression of DNR. In the presence of nitric oxide (NO) DNR then can activate expression of the denitrication genes; NAR (nitrate reductase), NIR (nitrite reductase), NirQ, NOR (nitric oxide reductase), N_2OR (nitrous oxide reductase) DNR. ANR, DNR and NarXL (in the presence or nitrate) are capable of activating NAR. The role of NirQ includes the fine tuning of NIR and NOR regulation.

The versatile functions of *P. aeruginosa* involving respiratory and fermentative energy generating systems contribute to the ubiquitous nature of *P. aeruginosa* in both aerobic and anaerobic environments. Moreover the virulence systems highlighted here provide mere insight into the vast complexity of the intricately interlinked regulatory systems of *P. aeruginosa*. Expression of individual virulence and metabolic networks cross-regulate each other whereby signalling cascades fine tune acute and chronic virulence phenotypes. Given the complexity of these global systems and networks, it is expected that the cellular response to stress conditions is elaborate.

1.9   Mode of action of antibiotics

Antibiotics are classified primarily on whether they induce cell death (bactericidal) or inhibit cell growth (bacteriostatic drugs). In addition, antibiotics can be further grouped based on the system or cellular component they interact with. The majority of antibiotics in use today inhibit DNA synthesis, RNA synthesis, protein synthesis or cell wall synthesis (Von Döhren, 2004). Bacteria can develop resistance to antibiotics by preventing antibiotic access to the target site either by mutations that change the antibiotic target or via the modification and thus protection of the target (Billal et al., 2011, Leclercq, 2002) . Bacteria are also capable of destroying or modifying antibiotics, thus resisting their action (Woodford et al., 2011, Johnson and Woodford, 2013, Wright, 2005)

1.9.1   Reduced permeability

Gram-negative bacteria, compared to Gram-positive bacteria are intrinsically less permeable to a number of antibiotics due to the structure of the outer membrane and ability to form a barrier, thus reducing permeability. Hydrophilic antibiotics are capable of passing through the outer membrane via diffusion through outer membrane porin proteins (Blair et al., 2015). To limit antibiotic entry in to the bacterial cell, bacteria down regulate porins or replace them with more selective channels thus reducing the permeability of the outer membrane (Vargiu and Nikaido, 2012). This has been observed in Enterobacteriaceae, *Pseudomonas spp.* and *Acinetobacter spp.*, whereby antibiotic resistance to carbapenems and cephalosporins, which is usually mediated by enzymatic degradation has been facilitated by reductions in porin expression (Blair et al., 2015).

1.9.2   Increased antibiotic efflux

Bacterial efflux pumps are transporters which can actively transport many antibiotics out of the cell and thus play a pivotal role in intrinsic resistance of bacteria to many drugs. *P. aeruginosa* PAO1 has 12 efflux systems of the Resistance-Nodulation-Cell Division (RND) family. Intrinsic multidrug resistance is attributed to its low permeability outer membrane combined with a number of broadly specific multidrug efflux (Mex) systems, of which include MexAB-OprM and MexXY-OprM. In addition to this intrinsic resistance, MexCD-OprJ, MexEF-OprN and MexJK-OprM allow acquired

multidrug resistance via mutations that promote hyper-expression of efflux genes (Figure 1-7) (Schweizer, 2003, Livermore, 2002). These pumps consist of three component systems that include proton motive force driven antiporters, belonging to the RND family (MexB, MexD, MexF and MexY), outer membrane factors (OprM, OprJ and OprN) and periplasmic membrane fusion proteins (MexA, MexC, MexF and MexX) (Morita et al., 2012).

1.10 Efflux mediated cellular activities

As depicted in Figure 1-7, efflux pumps are capable of extruding an array of toxic substances which are not just limited to antibiotics. Efflux pumps are thus involved in various cellular activities, ranging from detoxification of intracellular metabolites, virulence, cell homeostasis and intercellular signal trafficking. While this has now been made evident little is known about how efflux pump expression is affected within innate genetic networks to allow these various functions and ensure adaptability in different environments. The expression of RND pumps can be regulated in response to various external stress factors such as reactive oxygen (MexAB-OprM, MexXY-OprM), reactive nitrogen (MexEF-OprN) compounds that cause stress and damage to the cell membrane (MexCD-OprJ) or those that block ribosome activity (MexXY-OprM) (Morita et al., 2012, Grkovic et al., 2002, Lister et al., 2009, Poole, 2014, Fetar et al., 2011, Dreier and Ruggerone, 2015). Thus, efflux pumps have a key role against cellular stress that provides protection

against antibiotics and naturally occurring signals (Dreier and Ruggerone, 2015).
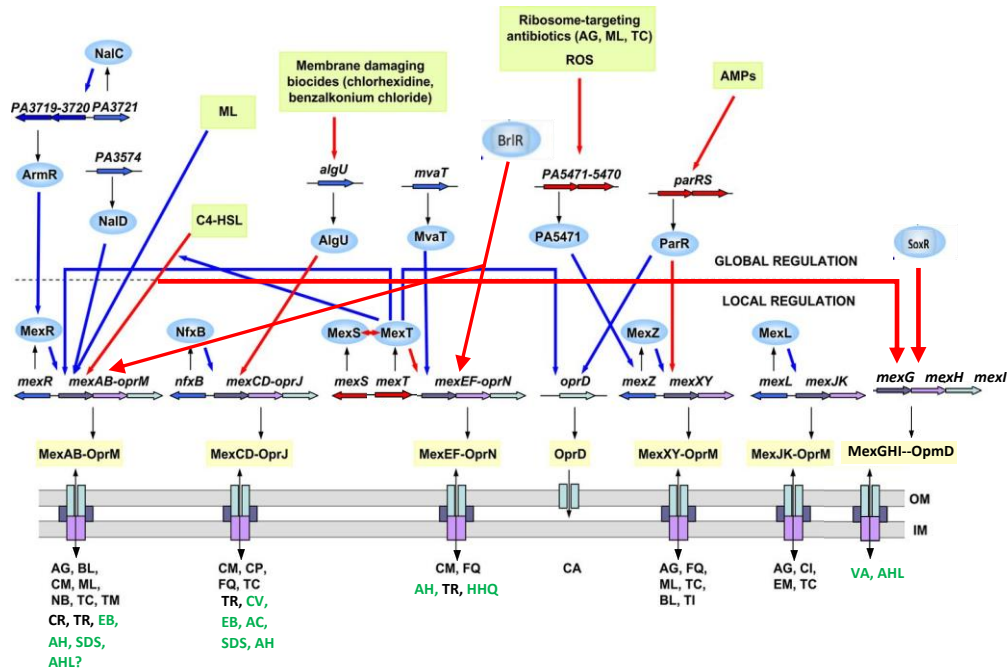
Figure 1-7 Schematic diagram of Mex efflux systems in P. aeruginosa

Overview of characterized Mex pumps in P. aeruginosa and the regulated pathways. Red and blue arrows represent activation and repression, respectively. Substrates for each pump are indicated in black for antimicrobials and green for non-anti-microbials. Abbreviations: AG, aminoglycosides; AMPs, antimicrobial peptides; BL, beta-lactams; CA, carbapenems; CI, ciprofloxacin; CM, chloramphenicol; CP, cationic peptides; EM, erythromycin; FQ, fluoroquinolones; ML, macrolides; NB, novobiocin; TC, tetracycline; TI, ticarcillin; TM, trimethoprim; IM, inner membrane; OM, outer membrane; C4-HSL, N-butyryl-l-homoserine lactone; ROS, reactive oxygen species, VA, vanadium, TR, triclosan. EB, ethidium bromide; AH, aromatic hydrocarbons; SDS, CE, cerulenin; AHL, aceylated homserine lactones; CV, crystal violet; AC, acrifalvine; HHQ, PQS precurosr 4-hydroxy-2-heptylquinoline. Figure adapted from (Schweizer, 2003, Fernández and Hancock, 2012, Fargier et al., 2012, Liao et al., 2013)

1.11   Regulation of MexT

The MexEF-OprN tripartite system is a multi-drug efflux pump, which is activated by the LysR-type transcriptional regulator MexT. The *mexT* gene is located immediately upstream and transcribed in the same direction as the *mexEF-oprN* pump in all *P. aeruginosa* strains. Unlike other RND pumps in *P. aeruginosa*, the *mexEF* system is the only one that is regulated by an activator as the remaining RND systems are regulated by repressors.

It has been reported that MexT regulates two further Mex independent cascade systems. The first involves expression of membrane proteins involved in the transport of antibiotics, such as the MexEF-OprN efflux pump and the imipenem permeable porin OprD. The second is cancellation of quorum-sensing (C4-HSL)-mediated up-regulation of *mexAB-oprM* (Uwate et al., 2013, Maseda et al., 2004). The phenotype of these regulatory pathways is of particular interest in strains termed nfxC-type mutants where MexEF pump induction is known to confer resistance to norfloxacin. In these mutants, an active *mexT* is known to increase expression of *mexEF* and is associated with resistance to chloramphenicol and ciprofloxacin. Reduced C4-HSL production is associated with reduced virulence factor production (pyocyanin, elastase and rhamnolipid), type III secretion, motility and biofilm formation (Maseda et al., 2000, Lamarche and Deziel, 2011, Köhler et al., 1999, Kohler et al., 1997, Kohler et al., 2001). The results obtained from these studies have however relied on reductive science and on a bias of

selected genes using reverse transcription polymerase chain reaction (RT-PCR RT-PCR. It is therefore unclear how the specific regulatory pathways in such mutants regulate phenotype independently of the *mexEF* pump.

Overexpressed *mexT* in wild-type PAO1 and in a *mexEF* deleted isogenic mutant showed that *mexT* regulates diverse virulence phenotypes dependent and independent of the *mexEF-oprN* pump. Figure 1-8 shows that independent of its role in regulating *mexEF-oprN, mexT* also regulates the type III secretion system and early attachment (Tian et al., 2009a). Aside of its role in *mexEF* regulation, this is the first study to identify MexT as a global regulator.
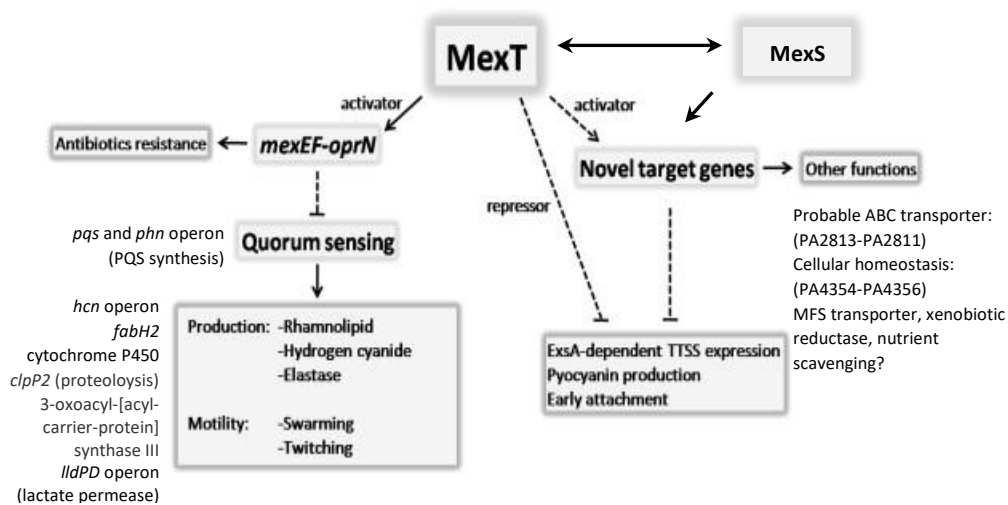
Figure 1-8 Regulatory role of *mexT* on virulence phenotypes, independent and dependant of *mexEF-Oprn*.
A positive effect is illustrated by an arrow while negative effects are indicated by a bar. Solid lines indicate already known links and dashed lines show links that are yet to be determined. Genes associated with phenotype are labelled according to results obtained from microarray data (Jin et al., 2011, Tian et al., 2009a).

The gene *mexS* is located before and adjacent to *mexT,* but divergently transcribed. PAO1 strains overexpressing *mexT* have shown increased transcript level expression of *mexS* and of *mexEF-oprN* when introduced in *trans* on a multicopy plasmid. One study has revealed that *mexS* represses the *mexEF-oprN* efflux pump in a clinical isolate of *P. aeruginosa* while in another study both a functional *mexS* and *mexT* are required for *mexEF-OprN* activation. This discrepancy illustrates the use of different strain backgrounds (Jin et al., 2011).

Further research has led authors to believe that *mexS* is a *mexEF* independent target of *mexT* (Tian et al., 2009a), a theory which has previously been reported (Köhler et al., 1999). While *mexS* can act on *mexT* in a inhibitory manner there are two separate pathways in *mexT*-mediated regulation of *mexEF-oprN* expression, either via *mexS* or by passing *mexS* (Uwate et al., 2013). It is known that antibiotic, disulphide and nitrosative stress causes *mexEF* overexpression via *mexT.* However it has also been shown that overexpression of *mexEF* due to other forms of stress, for instance metabolic stress is caused by a *mexT* independent mechanism (Fetar et al., 2011). While the nature of *mexT* mediated regulation of *mexEF* is not fully understood, it is clear that the role of *mexT* and its regulatory pathways are varied.

1.11.1   MexT, a LysR transcriptional regulator

LysR-type transcriptional regulators (LTTRs) comprise one of the largest groups of prokaryotic transcriptional regulators characterized to date. They are known to regulate biofilm formation, virulence, antibiotic resistance, catabolism and carbon fixation (Vercammen et al., 2015, Kukavica-Ibrulj et al., 2008, McCarthy et al., 2014, Wade et al., 2005). As such, LTTRs are rapidly emerging as a key family of regulators that influence a wide variety of processes in *P. aeruginosa* (Reen et al., 2013, Caille et al., 2014*).* LTTR proteins consist of a conserved helix-turn-helix (HTH) DNA binding motif located in the N-terminal portion of the polypeptide (Brennan & Matthews, 1989; Huffman & Brennan, 2002; Aravind et al., 2005). Those that have the HTH located at the C terminus are transcriptional activators whereas those with the HTH at the N terminus are transcriptional repressors (Pe´rez-Rueda & Collado-Vides, 2000). Dual regulators which activate and repress transcription of itself or the gene(s) it is regulating, consist of a HTH that is located 20–90 amino acids from the N terminus (Maddocks and Oyston, 2008).

The C terminus of LTTRs includes the inducer (co-factor) binding site. Co-factors are usually intermediates formed by metabolic reactions that act as co-inducers by binding to the LTTR to activate or repress transcription (Deghmane et al., 2004, Heroven and Dersch, 2006, Celis, 1999, van Keulen

et al., 2003, Maddocks and Oyston, 2008). LTTRs bind to two distinct binding sites known as the recognition binding site (RBS) and the activation binding site (ABS). The RBS is usually located upstream of the target gene's promoter and can allow regulator binding without a co-inducer. The LTTR binds to the ABS near the −35 region of the target gene. This typically occurs in the presence of a co-effector along with RNA polymerase to regulate transcription (Schell, 1993). A palindromic DNA sequence has been identified to which LTTRs are known to bind (LTTR box); this typically forms part of an imperfect region with dyad symmetry. The sequence ATC-N9-GAT, 250 -275 bp upstream of the *nod* gene in Rhizobium spp was the first identified LTTR box and was referred to as the 'Nod-box' (Goethals et al., 1992). This led to the identification of the LTTR box which consists of the sequence T-N11-A, usually found at the RBS site (Maddocks and Oyston, 2008). The presence of a co-inducer affects the binding affinity of an LTTR to its binding site. The protein without the co-inducer will only bind to the RBS. Once the co-inducer binds to the protein, this causes the ABS site to also bind to the LTTR. This results in bending of DNA as dimeric proteins on the ABS and RBS form a tetramer. As the co-inducer binds, a larger complex with RNA polymerase is formed and transcription is initiated (Maddocks and Oyston, 2008).

The recognition site characteristically contains an LTTR-box, suggesting that this recognition sequence is associated with auto regulatory activity. LTTRs

are divergently transcribed from a promoter that is close or overlapping a promoter of a regulated target gene. This allows simultaneous bidirectional control of transcription enabling LTTRs to repress their own transcription (negative auto regulation), most likely to maintain a constant level (Beck and Warren, 1988). The environmental stimuli for positive autoregulation however remains undefined.

1.12 Objective and Strategy:

The main objectives of this study were to:

- Identify differences in the phenotypic capabilities of different strains of *P. aeruginosa*

- Link genotype to phenotype by integrating data from genomic, transcriptomics and phenotypic results to predict the biological impact of a strain.

Establish phenotype models

↓

Define phenotype in PAO1 lineages

↓

Comparative genomics of PAO1 lineages

↓

Evaluate clinical significance of mutations in clinical strains using epidemiological studies

↓

Identify differences among the isogenic mutants using transcriptomic and phenotypic tests

↓

Integrate phenotypic and genotypic data using novel methods of metabolic reconstruction

Figure 1-9 A schematic view of the research strategy employed in this study

We had access to a range of *P. aeruginosa* strains including four lineages of the laboratory strain PAO1 and clinical strains from Norwich and Norfolk University Hospitals (NNUH) and Public Health England (PHE).

The strategy for investigation, as outlined in Figure 1-9, was as follows:

1. Optimise phenotypic models to characterise PAO1 lineages, as a model organism. One phenotype of interest will include biofilm formation.

2. Use the biofilm model to identify differences in biofilm formation between PAO1 lineages.

3. Identify reasons for variance between PAO1 lineages using comparative genomics.

4. Perform an epidemiological screening test to establish whether mutations present in PAO1 have a clinical significance.

5. Study the genetic mutations of interest in isogenic mutants and investigate the phenotype.

6. Perform comparative transcriptomic analysis on selected strains of interests.

7. Integrate genomic and phenomic data to gain an understanding of the regulatory pathways involved in the mutation of interest.

2 Phenotypic and genotypic variation of *Pseudomonas aeruginosa* PAO1

2.1 Introduction

P. aeruginosa is an incredibly versatile pathogen. Being a ubiquitous environmental organism and a consummate opportunistic pathogen the success of this organism is owed to its metabolic versatility, resistance to antimicrobials and ability to evade host immune responses. Consistent with its remarkable adaptability the *P. aeruginosa* genome is large and complex and is one of the largest bacterial pathogens to infects humans (Ozer et al., 2012). The first strain of *P. aeruginosa* sequenced was PAO1 in 2000 (Stover et al., 2000, Weiss Nielsen et al., 2011). With a genome size of 6.3 Mbp and 5,570 predicted open reading frames (Stover et al., 2000), this reflects the numerous and distinct gene families that this bacterium contains (Kung et al., 2010).

Comparative genomic analysis of clinical strains has revealed that *P. aeruginosa* consists of a relatively conserved core genome with interspersed accessory genetic material (Kung et al., 2010). The accessory genome consists of genes that are not present in all *P. aeruginosa* strains. These tend to cluster in particular loci whereby genomic mutations within these regions of genomic plasticity (Mathee et al., 2008) may contribute towards the niche-based adaptation of particular strains.

The population structure of *P. aeruginosa* in vivo is not fully understood. It is clear however that the adaptation and stress response of *P. aeruginosa* in different conditions is facilitated by the microevolution and genomic diversity of strains (Bezuidt et al., 2013, Fox et al., 2008). Biofilms and static cultures for example consist of multiple types of differentiated cells, even when grown in vitro from a single clonal lineage (Fox et al., 2008). *P. aeruginosa* clearly has the ability to undergo myriad genotypic transformations that provide the natural population with profound phenotypic changes in clinical conditions (Darch et al., 2015, Bianconi et al., 2015, Workentine et al., 2013) some of which have a reproductive advantage.

Phenotypic diversification in *P. aeruginosa* is a common phenomenon that leads to the generation of small colony variants (SCVs) and large colony variants (LCVs). Compared to the wild type, SCVs have a rough small colony morphology and are associated with autoaggregation, hyper-adherence and increased extracellular polymeric matrix (EPM) production (Alhede et al., 2011, Barraud et al., 2006). They show increased sensitivity to fluoroquinolones but reduced susceptibility to the aminoglycosides (Wei et al., 2011). Moreover they show reduced pyocyanin production (Nelson et al., 2010, Haussler et al., 2003, Kirisits et al., 2005).

Slow growth rates are another trait observed in SCVs. Sabra et al. found that for unknown reasons, under iron limited conditions, the growth rate of the

SCV decreased compared to the wild type (Sabra et al., 2014). There is however a debate surrounding the effect of oxygen tension on wild type PAO1 growth. Under increased oxidative stress, *P. aeruginosa* PAO1 has shown reduced growth rates and pyocyanin production in one study (Sabra et al., 2002) but increased growth in another (Alvarez-Ortega and Harwood, 2007). The increased growth observed by Alvarez-Ortega and Harwood may be explained by the high iron concentration used in their growth media, which was nearly double the iron amount utilised by Sambra et al.

SCV development is associated with elevated c-di-GMP levels, which can occur via mutations in *wspF* and those that enhance the activity of the diguanylate cyclase (DGC), which is associated with c-di-GMP synthesis (Hickman et al., 2005). The *yfiBNR* (PA1119 to PA1121) operon has also been identified as a regulator of c-di-GMP, EPS production and autoaggregation via the *pel* and *psl* genes. This operon consists of membrane proteins and a repressed integral membrane DGC which increases c-di-GMP levels and causes SCV formation (Malone et al., 2012, Malone et al., 2010).

LCVs have not been extensively investigated; however this colony variant is comparable to the mucoid phenotype (Li et al., 2005, Lam et al., 1980). A phenotypic switch to a mucoid colony is characterized by the overproduction of the exopolysaccharide alginate (Evans and Linker,

1973, Linker and Jones, 1966) which is known to develop in response to harsh conditions such as oxidative stress (Davey et al., 2003).

P. aeruginosa PAO1 was originally isolated from a wound in Australia in the 1950s (Holloway, 1955, Holloway et al., 1979). Since then PAO1 has been distributed worldwide to major tissue culture collections and has been the major reference for phenotypic and genotypic studies on *P. aeruginosa.* Sequences and their annotations are deposited in the National Center for Biotechnology Information (NCBI) genome database (Refseq. no. NC_002516) and in the *Pseudomonas* Genome Database, which is continuously updated.

The aim of this study was to investigate and identify differences in *P. aeruginosa* PAO1 isolated from different tissue culture collections. To understand the response of *P. aeruginosa* to different environments and its adaptive mode of survival, it is important to first recognise the phenotypic and genotypic differences of the reference strain PAO1.

2.2   Materials and methods

Table 2-1 Strain collection

Strain	Provider	Site of isolation	Phenotype
PAO1-DM	DSMZ	DSMZ 19880	Medium sized colony
PAO1-AM	Jake Malone, JIC	ATCC 15692	Medium sized colony
PAO1-AL	Cambridge	ATCC 15692	Large colony
PAO1-AS	Cambridge	ATCC 15692	Small colony
Pa 11451	Cambridge	NCTC 11451	Unknown
W1236011	NNUH	Water	Unknown
W1236012	NNUH	Water	Unknown
W1236011	NNUH	Water	Unknown
W1236012	NNUH	Water	Unknown
W1236013	NNUH	Water	Unknown
W1236014	NNUH	Water	Unknown
W1236015	NNUH	Water	Unknown
W1236016	NNUH	Water	Unknown
W1236017	NNUH	Water	Unknown
W1236018	NNUH	Water	Unknown
W1236019	NNUH	Water	Unknown
W1236020	NNUH	Water	Unknown
W1236021	NNUH	Water	Unknown
W1236022	NNUH	Water	Unknown
W1236023	NNUH	Water	Unknown
W1236024	NNUH	Water	Unknown
W1236025	NNUH	Water	Unknown
W1236026	NNUH	Water	Unknown
W1236027	NNUH	Water	Unknown
W1236028	NNUH	Water	Unknown
W1236029	NNUH	Water	Unknown
W1236030	NNUH	Water	Unknown
H125160273	PHE	Blood	ST111 MBL* positive
H125180570	PHE	Environment	ST111 MBL* positive (012)
H043280559	PHE	Blood	ST235 MBL* positive

H120420213	PHE	Water	Belfast epidemic strain
H120420202	PHE	Blood	Belfast epidemic
H132500175	PHE	Blood	PA14 clone
H133620473	PHE	Water	PA14 clone
H132640707	PHE	Unknown	PA14 clone VIM†
ENV1	This study	WS1/1 pipe	Unknown
ENV2	This study	WS1/2 pipe	Unknown
ENV3	This study	Sink	Unknown

*MBL (Metallo-β-actamase) and † VIM (Verona integron-encoded metallo-β-lactamase).

2.2.1 Bacterial strains and culture conditions

PAO1 (referred to as PAO1-DM, M meaning medium sized colony) was obtained from the Leibniz Institut DSMZ German Collection of Microorganisms and Cell Cultures. PAO1 strains from the American Type Culture Collection (ATCC) were provided by different laboratories (Table 2-1). PAO1 ATCC (referred to as PAO1-AM), PAO1-ATCC Large (PAO1-AL) and PAO1-ATCC Small (PAO1-AS) were named according to the colony size. NNUH and PHE provided *P. aeruginosa* strains from various sources, as listed in Table 2-1. All strains were stored in glycerol stocks at -80 °C.

2.2.2 Phenotypic characterization

2.2.2.1 Colony morphology

PAO1 variants were cultured on Columbia agar from glycerol stocks and incubated overnight prior to imaging with a Leica MZ16 stereoscopic microscope (Leica, Germany).

2.2.2.2 Growth curve analysis

From frozen stocks, strains were cultured on Columbia agar overnight and in 10 ml Luria Bertani (LB) broth (Oxoid Ltd, Hampshire, UK) the following day at 37 °C. This culturing technique was utilised in all experiments. Overnight cultures were diluted to 1:1000 in fresh LB and re-incubated for 1 h. Cultures were aliquoted in 100 µl volumes and mixed with equal measures of fresh LB in micro-titre plates before incubation at 37 °C with agitation (180 rpm) rpm). Automated optical density readings (600 nm) were taken as a measure of growth using a FLUOstar Omega plate reader (BMG Labtech GmbH, Germany). Experiments were carried out in triplicate and repeated three times.

Growth curves performed with minimal medium (M9) were carried out in the same manner, replacing LB with supplemented M9 (Oxoid). M9 medium was supplemented with 22.2 mM glucose, 2mM $MgSO_4$, 0.1mM $CaCl_2$, 24.4mM casamino acids and 1mM thiamine hydrochloride (Sigma-Aldrich, U.S.).

Bacterial growth was analysed in the presence of oxygen limiting and aerobic conditions. Oxygen-limiting conditions were initiated in a 96 well plate sealed with an adhesive film. Sealed wells were pricked with a sterile needle to imitate aerobic conditions. Automated readings were taken every 7 minutes over the course of 24-28 hours. Growth was analysed using area

under the curve (AUC) analysis, calculated according to the trapezoidal rule (Jones, 1997).

2.2.2.3   Pyocyanin production

PAO1 lineages grown in aerobic conditions (described above), were visually inspected 48 hours after starting the experiment for the characteristic green colour change, indicative of pyocyanin production.

2.2.2.4   Biofilm formation

2.2.2.4.1   Static biofilms

Biofilms were quantified using the mirotiter plate assay method (Merritt et al., 2005). This protocol was modified such that plates were incubated for 48 hr and stained with 1% crystal violet (CV, Sigma-Aldrich) for 30 min.

2.2.2.4.2   Dynamic biofilms

Different models were employed to study biofilm growth. The first was from Cellix Ltd (Dublin, Ireland) and the second from DTU (Technical University of Denmark, Kongens Lyngby, Denmark). Both models are shown in Figure 2-1 and 2-2. PAO1 cultures were cultured in LB and diluted to 10^6 CFU/ml in LB using a spectrophotometer. Each channel within the Cellix biochip was seeded with 5 µl inoculum and the DTU flow cell injected with 250 µl of the

inoculum. Flow cells were then incubated for 1 hour. LB medium was then allowed to flow through the flow cell at a rate of 3 mL/h. Flow cells were incubated at 37 °C for 24 hours using the Cellix model and 48 hours with the DTU model. Biofilms were imaged by staining with SYTO 9 and propidium iodide (Molecular Probes, Inc. U.S.) and visualized using a Leica TCS-4D confocal microscope (Leica, Germany). Images were analysed using COMSTAT (Heydorn et al., 2000) to study biofilm thickness, roughness and surface area parameters to allow architectural comparisons of the different lineages. Roughness measures biofilm heterogeneity while surface area indicates how large a portion of the biofilm is exposed to media flow.
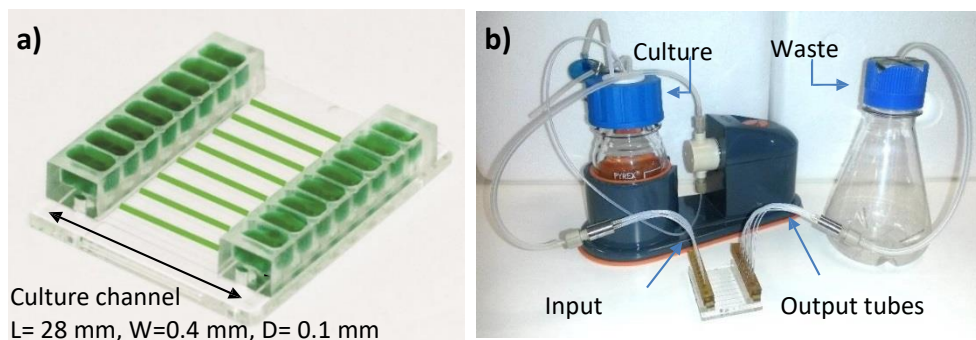
Figure 2-1 Flow cell model 1 by Cellix Ltd.
a) Biofilms were grown in biochips that consisted of 8 channels. Each channel could be inoculated with up to 5 µl.
b) The biofilm model incorporated a Kima pump that passed media from a bottle, through the pump and biochip (seeded with bacteria) and into a waste flask.
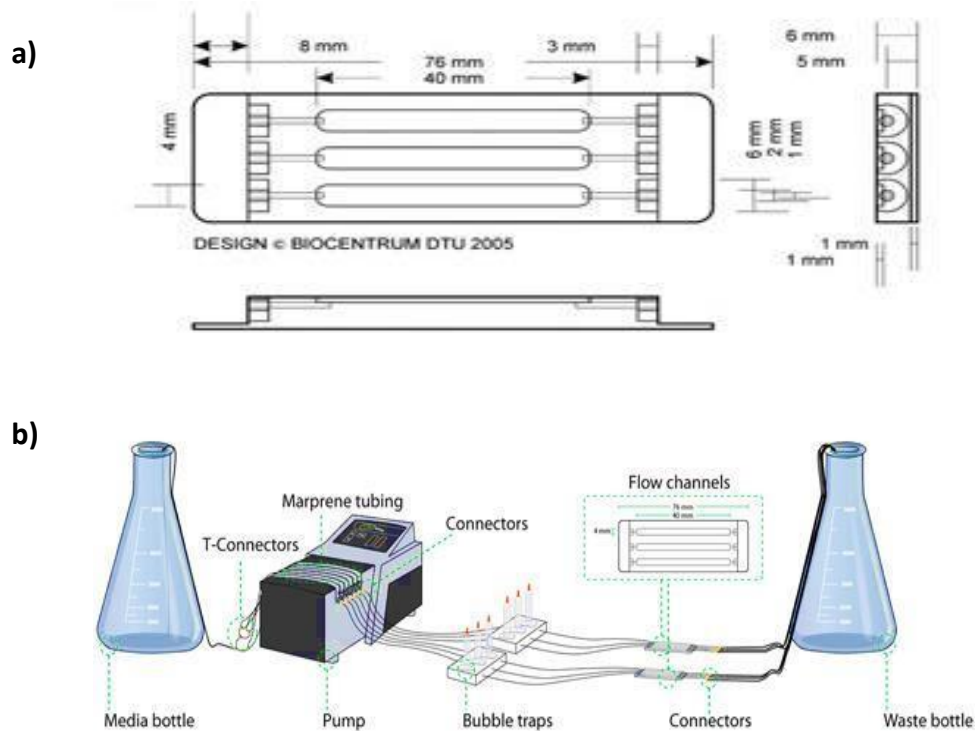
Figure 2-2 Flow cell model 2 from DTU.

a) Biofilms were grown in flow cells consisting of 3 channels. Each channel could be seeded with up to 250 µl of the inoculum.

b) A 16 channel peristaltic pump allowed media to be fed into seeded channels (within the flow cell) and waste collected in the waste bottle. Bubble traps prevented bubbles from being introduced into the flow cell. Figure adapted from (Tolker-Nielsen and Sternberg, 2014).

2.2.2.5   Antimicrobial susceptibility testing

PAO1 lineages were subjected to susceptibility testing against a panel of antibiotics at PHE using the agar dilution method and at NNUH with the Vitek 2 Compact (bioMérieux, France). MICs was determined after 24 hours of growth against; amikacin, gentamicin, tobramycin, aztreonam, ceftazidime, imipenem, meropenem, piperacillin, carbenicillin, colistin and ciprofloxacin.

2.2.2.6 Biotyping

PAO1 sublineages and *P. aeruginosa* 11451 (utilised as a control) were cultivated on Columbia agar. Approximately ten colonies of each strain were subjected to analysis using the Matrix-assisted laser desorption/ionization Mass Spectrometry (MALDI- MS) and BioTyper 3.0 software (Buker, Germany), following previously described protocols (Berrazeg et al., 2013).

2.2.3 Whole genome sequencing

Bacterial cells from 1ml of overnight culture were harvested and DNA extracted using the MagNA Pure bacterial lysis kit and MagNA Pure Compact instrument (Roche). Samples were sent to Nick Loman's group at Birmingham University and underwent Nextera XT sample preparation before deep sequencing on the MiSeq v2 and/or v3 chemistry. Adapter and quality trimming of reads was performed with Trimmomatic. Reads were then mapped onto the reference genome (*P. aeruginosa* PAO1 GenBank accession no. NC002516.2) and variants called using Burrows-Wheeler Aligner-MEM. Variant calling included single nucleotide polymorphisms (SNPs), insertions and deletions (indels), and/or structural variants (such as frameshifts). Variant calling files (VCF) were generated with Samtools mpileup and VarScan. Variants were then annotated with a snpEff Python script to convert the annotated VCF to a table.

2.2.4   Screening of strains

The presence of the 8-bp *mexT* deletion and PA5017 mutation (found in PAO1-AL) were tested in strains from the strain collection (Table 2-1) using PCR (polymerase chain reaction) based techniques. DNA was extracted from strains, as detailed above. To screen strains for the *mexT* 8-bp deletion, DNA extracts were subjected to PCR in the following conditions: 95 °C for 10 sec, 60 °C for 30 sec (45 cycles) followed by melt curve analysis. Strains showing a drop in melting temperature (of approximately 1.5 °C) compared to the negative control (strain known not to harbour the 8-bp deletion) were thought to contain the 8-bp deletion. Mutant and wild type (WT) probe based techniques were used for the PA5017 mutation using the following PCR conditions (95 °C for 5 min, 60 °C for 30 sec, 40 cycles) for amplification of the mutation. Primers and probes are listed in Table 2-2.

Table 2-2 Primer and probe list

Gene	Primer/Probe	Forward sequence	Reverse sequence
PA5017	Primer	GCGACGCAATGTCTCC	CGGTCGATCAGCAGGA
PA5017	Mutant Probe	[6FAM]GCGCTAGAACAGGTGCAG[OQA]	
PA5017	WT Probe	[6FAM]CTGCACCTGTTCCAGCG[OQA]	
8-bp mexT	Primer	CGCAGAGAAACTGTTCCT	GGTACGGACGAACAGC

2.3 Results

2.3.1 Phenotypic results

2.3.1.1 Colony Morphology

All four strains, PAO1-DM, PAO1-AM, PAO1-AL and PAO1-AS exhibited a round colony with a smooth surface and lobated margin (Figure 2-3). As inferred by their names, PAO1-DM and PAO1-AM produced medium sized colonies, 2.5 mm and 3 mm, respectively. PAO1-AL appeared larger (4.5 mm) and PAO1-AS smaller (1mm) than PAO1-AM. Cell density within the colony of PAO1-AL also visually appeared lower while in PAO1-AS cells appeared aggregated.
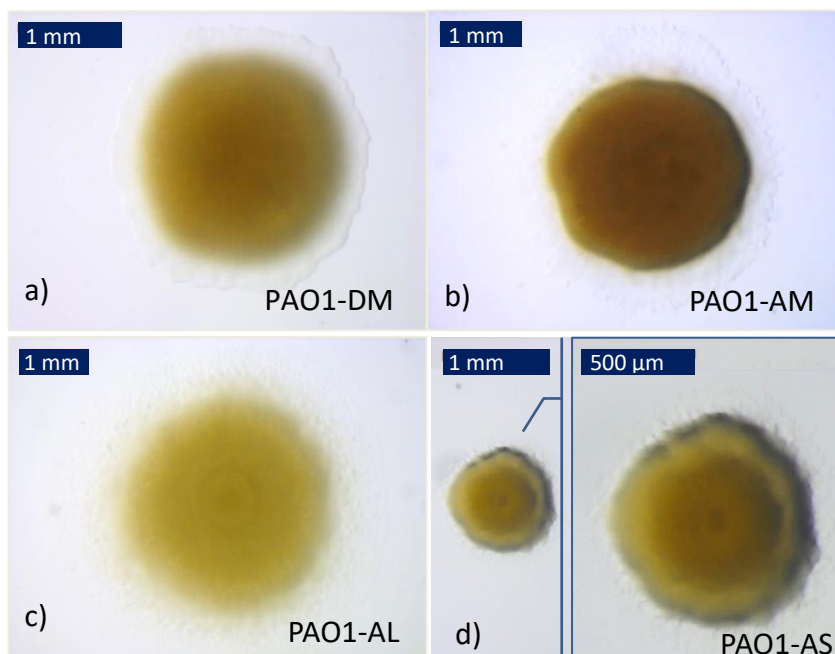
Figure 2-3 Colony morphology of the different PAO1 variants: a) PAO1–DM, b) PAO1–AM, c) PAO1-AL and d) PAO1-AS. Colonies were imaged 24 hours after growth on Columbia agar. PAO1-AS was approximately half the size of PAO1-DM and PAO1-AM. PAO1–AL and PAO1-AS illustrated 3 distinct sub-areas within the colony in contrast to the other colonial variants.

2.3.1.2   Growth curve analysis and pyocyanin formation

Growth of the PAO1 lineages were examined in oxygen limiting and aerobic conditions (Figure 2-4). PAO1-AS showed increased growth in aerobic conditions (as opposed to oxygen limiting conditions) but only after 23 hr, compared to the remaining lineages which showed increased growth after 10 hr. A similar phenotype was seen in supplemented M9. To verify this, colony counts were performed. However, results showed no differences between the lineages in oxygen limiting and aerobic conditions. It is hypothesised that the growth profile of PAO1-AS was actually caused by pellicle formation. Area under the curve analysis revealed that PAO1-AS growth curves were statistically different to the remaining lineages ($P<0.05$) in both LB and defined media. PAO1-AS was also the only lineage that failed to produce pyocyanin in aerobic conditions (Table 2-3).
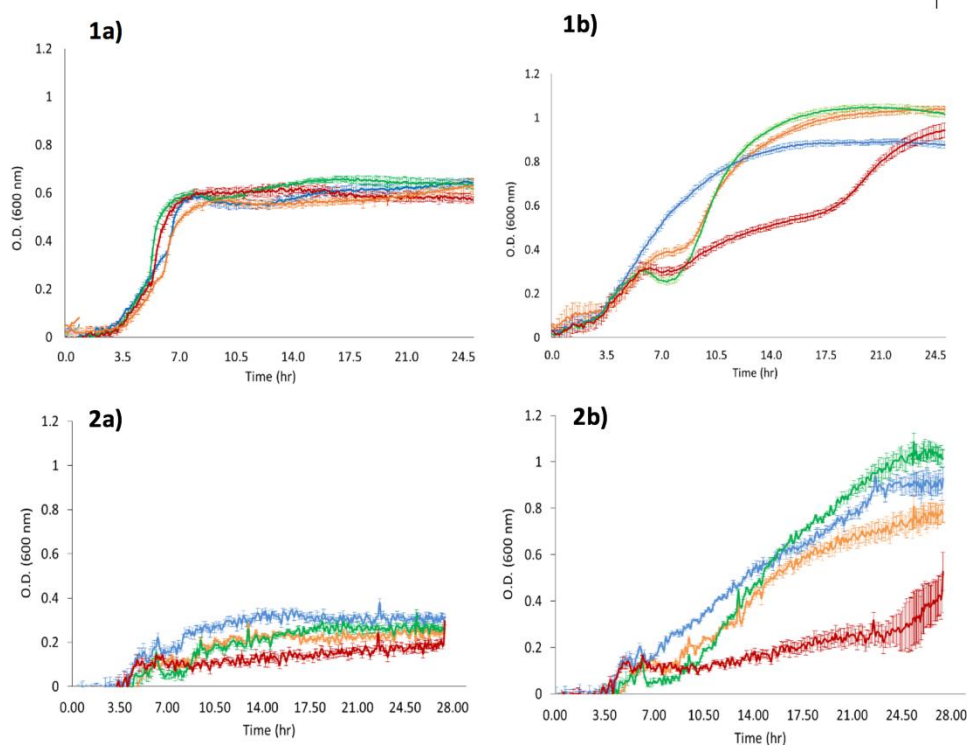
Figure 2-4 Growth curves of PAO1 lineages in 1) LB and 2) defined media (supplemented M9): PAO1-DM (orange), PAO1-AM (blue), PAO1-AL (green) and PAO1-AS (red) investigated under a) oxygen limiting and b) aerobic conditions. Error bars shows standard deviation (n=3).

Table 2-3 Pyocyanin production among the PAO1 lineages.

Lineage	Pyocyanin Production
PAO1-DM	✓
PAO1-AM	✓
PAO1-AL	✓
PAO1-AS	0

PAO1 lineages grown in aerobic conditions were inspected for pyocyanin production, characterised by blue-green pigmentation. PAO1-AS was the only lineage that failed to visually produce pyocyanin. The above image represents the green colour change, characteristic of pyocyanin production

2.3.1.3.1   Static biofilms

Quantifying biofilms using the crystal violet (CV) technique allowed phenotypic characterisation of biofilm growth in a static model. Figure 2-5 shows that PAO1-AS out of all four PAO1 lineages was visibly capable of producing more biofilm (p<0.05).
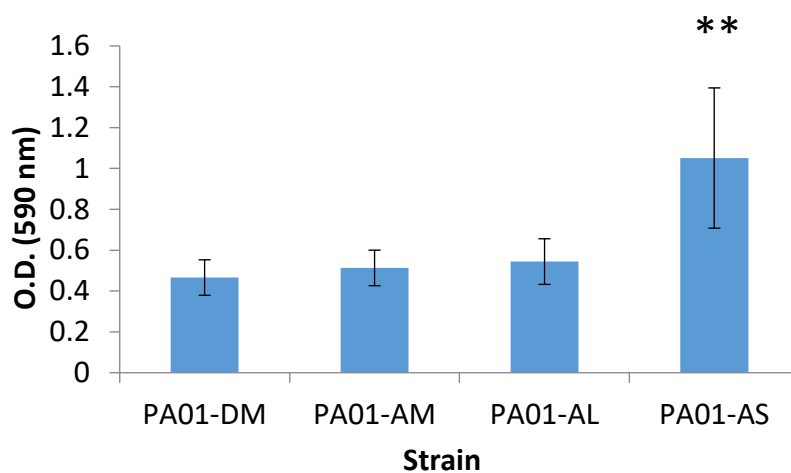
Figure 2-5 CV biofilm assay

PAO1-AS showed higher biofilm forming capabilities compared to PAO1-DM, PAO1-AM and PAO1-AL (**P<0.05). Error bars are standard deviation for experiments performed in triplicate.

2.3.1.3.2   Dynamic biofilms

Strains grown in model 1 initially produced viable biofilms but after two tests (24 hr culture) showed cell death. Images clearly showed biofilm growth. It was hypothesised that during biofilm maturation or the staining process there was an event that lead to cell death. Efforts were made to investigate this (Table 2-4). The design of the Kima pump meant there was no visual

access to check for contamination. The pump cannot be autoclaved but sterilised only by flushing with ethanol. Contaminants present within the pump could have therefore been the reason for bacterial cell death.

Table 2-4 Techniques used to investigate the cause of biofilm death in model 1

Reason for biofilm death	Technique utilised	Result
The seeding process	Bacterial cells prior to seeding and after seeding were subjected to live/dead stain	Cells were viable before and after seeding (1-2h)
Media contaminated by the pump	Bacterial cells were subjected to live/dead stain	Cells were viable
Blockages caused by biofilm growth	Media flow through the output tubes was observed and measured per min	Media flow remained constant at the end of the experiment
	Bacterial cells were subjected to live/dead stain within a channel	The entire length of the channel was stained suggesting that the media, like the stain, would have been able to pass through
	Biofilms were quantified	Biofilms were not thicker than the channel and were not thick enough to causes blockages
Live/dead stain efficacy	Planktonic bacteria with/without ethanol were stained with live/dead stain and visualised	Cell death only observed after treatment with ethanol.
Bacteriophage activated upon cell starvation when cells reach a critical concentration	Biofilm effluent was dropped onto a lawn of *P. aeruginosa*	No effect on *P. aeruginosa* growth
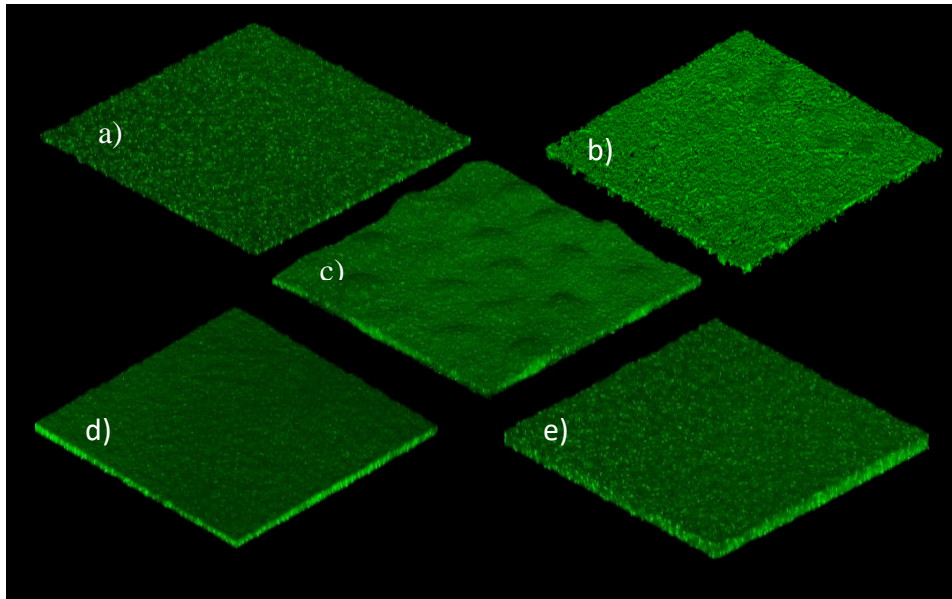
Figure 2-6 i) Biofilm images of different PAO1 lineages: a) PAO1-DM, b) PAO1-AM, c) PA11451, d) PAO1-AL, e) PAO1-AS. Biofilms were imaged 48 hours after seeding.
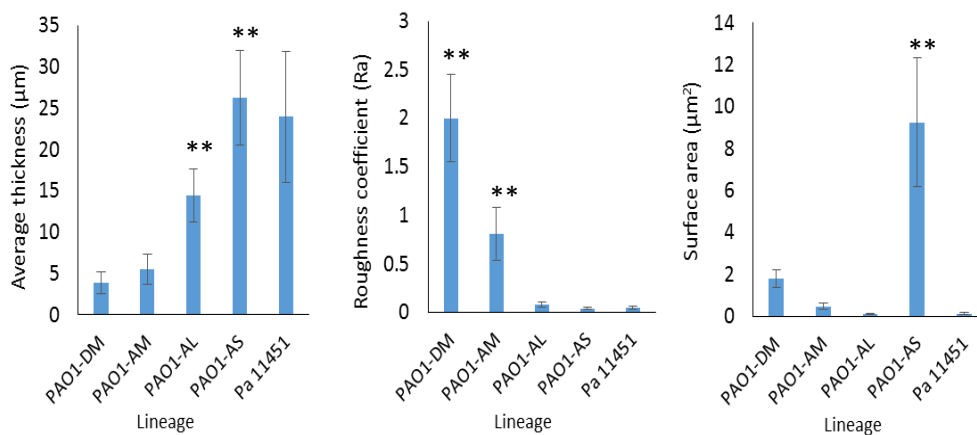
Figure 2-6 ii) Quantification of biofilm structures

Biofilm analysis using COMSTAT showed differences in biofilm structure among the PAO1 lineages. PAO1-AL and PAO1-AS produced thicker biofilms when compared to the remaining PAO1 lineages (**$P < 0.05$). PAO1-DM and PAO1-AM showed increased biofilm roughness (**$P < 0.05$) but PAO1-AS biofilms exhibited an increased surface area to volume ratio (**$P < 0.05$). Error bars indicate standard deviation, n=3.

Flow cell model 2 was optimised to ensure that biofilms produced were matured to a point that would allow comparison between different lineages. Representative images of biofilms from all lineages are illustrated in Figure 2-6 i). Lineages which produced thicker biofilms (PAO1-AL and PAO1-AS) showed reduced roughness suggesting that thicker biofilms are more compact and uniform in terms of distribution of cells within the biofilm (Figure 2-6.ii)).

2.3.1.4 Antimicrobial susceptibility testing

PAO1 lineages were tested against a range of antimicrobials. There was no difference in antimicrobial susceptibility observed among the variants (Figure 2-7).
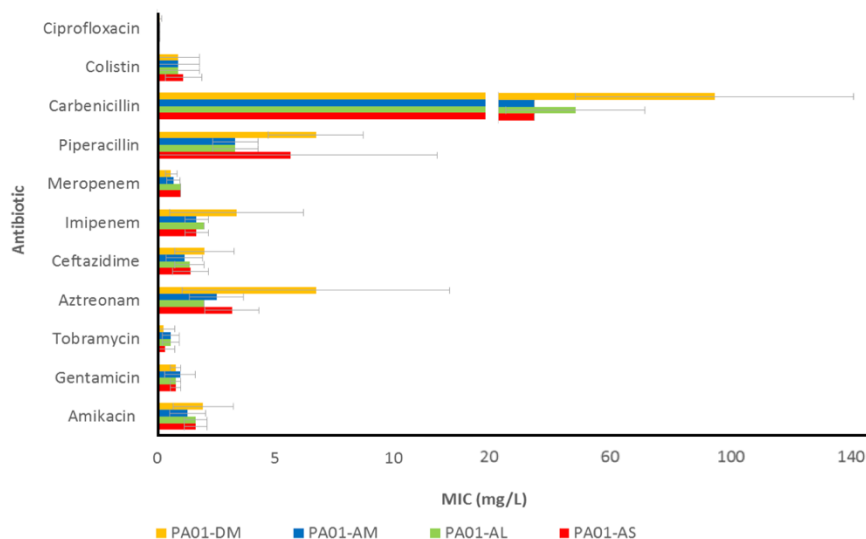
Figure 2-7 Antibiotic minimum inhibitory concentrations for PAO1 lineages.
There were no statistically significant differences observed between susceptibility to antibiotics, among the four PAO1 lineages (n=3).

2.3.1.5   MALDI biotyping
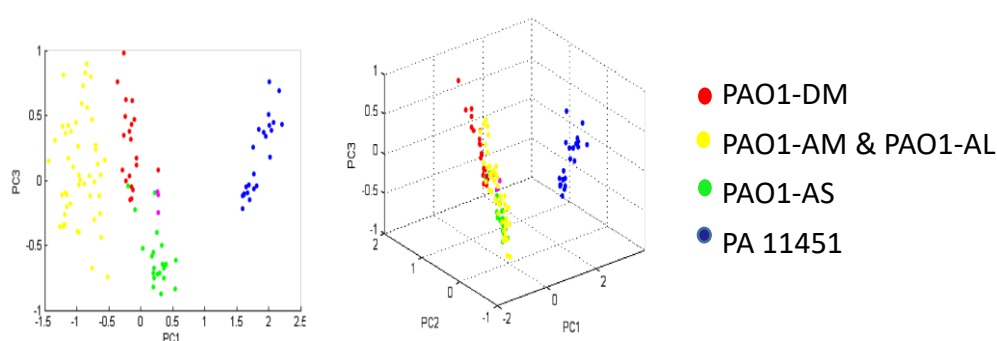
Figure 2-8 MALDI Biotyping for PAO1 lineages

MALDI-MS classifies strains, generating a spectral profile by measuring high abundance proteins, mostly ribosomal proteins. PCA classified the PAO1 lineages into 3 sub-classes. PAO1-DM and PAO1-AS clustered apart. However PAO1-AM and PAO1-AL actually clustered together suggesting similarities between these lineages was not found in the remaining lineages.

All four PAO1 lineages and PA11451 were analysed using MALDI-MS.

PA11451 was included as a control and clustered significantly apart, verifying

that all four PAO1 lineages were not contaminants (Figure 2-8).

2.3.1.6   Summary of phenotypic characterization

Table 2-5 PAO1 lineages and phenotype.
Phenotypic traits among the four PAO1 lineages were compared and graded (low to high, 0, +1, +2) according to strength and deviation from PAO1-AM.

	Phenotype				
Lineage	Biofilm (CV assay)	Biofilm (flow cell)	Increased growth in aerobic conditions	Pyocyanin production	Antimicrobial susceptibility
PAO1-DM	0	0	0	0	0
PAO1-AM	0	0	0	0	0
PAO1-AL	0	+1	0	0	0
PA01-AS	+1	+2	+1	+1	0

Phenotypic comparison (Table 2-5) of the PAO1 lineages showed that PAO1-

AS was the only lineage to exhibit slow growth rates (Fig 2-4) and reduced

pyocyanin production (Table 2-3) in aerobic conditions. CV biofilm assays revealed PAO1-AS as a hyper-biofilm forming lineage (Figure 2-5). This was corroborated by flow cell biofilm analysis which additionally showed that PAO1-AL was also capable of producing a thicker biofilm (Figure 2-6). Since flow cells are the gold standard (Crusz et al., 2012) for quantifying biofilms, biofilm analysis carried out using flow cell technology was considered as a true measure of bacterial growth. MIC data revealed no differences between lineages (Figure 2-7).

2.3.2   Whole genome sequencing

The four PAO1 variants were compared to *P. aeruginosa* PAO1 (GenBank accession no. NC_002516.2). Figure 2-9 shows the lineage specific SNPs and indels among the different variants. Mutations were characterised as low mean synonymous. Non-synoumous mutations were characterised as moderate, modifier and high, meaning missense, indel or frame shift/stop mutations, respectively.

Comparative sequencing revealed two mutations among the four lineages that were categorised as having high strength, non-synonymous effects, both of which were found in the high biofilm-forming strains PAO1-AL and PAO1-AS. It was therefore concluded that the effects of the C→T SNP in PA5017 and the *mexT* 8-bp deletion would be investigated further in the

clinical population since these genes have already been linked to biofilm

related phenotypes (Roy et al., 2012, Favre-Bonté et al., 2003).
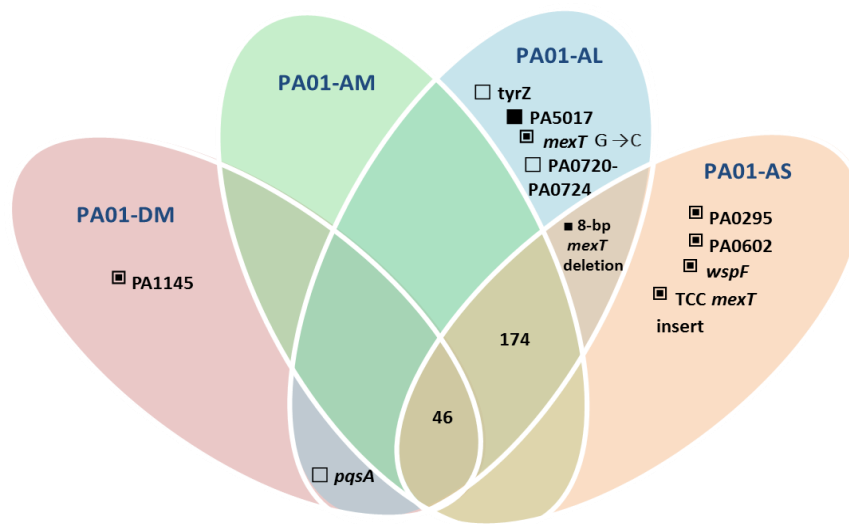
Figure. 2-9 Venn diagram of strain specific SNPs and indels among the PAO1 variants

Mutation strength type has been categorised by low (synonymous mutation, □), moderate (missense variant, ▣), modifier (insertion/deletion, ▨) and high (frameshift/stop gained, ■). * 174 mutations were found in the ATCC variants; PAO1-AM, PAO1-AL and PAO1-AS. * 46 mutations were shared by all PAO1 variants. Details of all mutations are provided in Appendix 8.1.1.

2.3.3   Screening of strains in strain collection

Strains in the strain collection (38 strains) were screened for the PA5017

mutation and *mexT* 8-bp deletion. None of these strains, except PAO1-AL,

had the PA5017 mutation. All strains however (except PAO1-DM and PAO1-

AM) revealed the presence of the *mexT* 8-bp deletion.

2.4 Discussion

The motivation for this work was to define the genetic basis of the different biofilm phenotypes seen in *P. aeruginosa*. Establishment of the biofilm model allowed the identification of differences in biofilm phenotype among four lineages of PAO1: PAO1-DM, PAO1-AM, PAO1-AL and PAO1-AS. PAO1-AL and PAO1-AS exhibited increased biofilm formation compared to PAO1-DM and PAO1-AM. Comparative genomics and further investigation led to the identification of an 8-bp *mexT* deletion, present within both of these hyper-biofilm forming lineages. The data presented here suggests that *mexT* is associated with biofilm formation.

Comparative genomics, compared to the reference genome, revealed that 46 mutations were found in all four PAO1 lineages at identical genomic positions (Figure 2-9 and Appendix 8.1.1), similar to previous findings (Klockgether et al., 2010). Perhaps these sites are hotspots for genomic plasticity. The genome sequencing also revealed 174 mutations unique to the ATCC sublineages. Driven by the individual handling of the strain and microevolution, these mutations probably occurred after the first PAO1 strain was deposited by the original investigators (Holloway, 1955) in public strain collections. Although genomic variations were found among PAO1-DM and PAO1-AM, there were no major phenotypic differences identifed (Table 2-5).

Colony morphology and genomic analysis revealed two sublineages of PAO1 from the ATCC; a larger (PAO1-AL) and a smaller colony variant (PAO1-AS). PAO1-AL was distinguished from PAO1-AM by non-synonymous mutations found in PA5017 and *mexT*. PA5017 has been described as a key component in biofilm dispersal. Similar to the results in this study, a PA5017 knockout previously exhibited increased biofilm production in flow cell experiments (Roy et al., 2012, Li et al., 2007). Consistent with this, the protein encoded by PA5017 has phosphodiesterase activity (Kulasekara et al., 2013) and a role in chemotaxis. Since phosphodiesterase activity is associated with reduced ci-di-GMP activity and increased motility (Simm et al., 2004), inactivation of the phosphodiesterase PA5017 in PAO1-AL was possibly associated with increased biofilm production through increased levels of c-di-GMP.

PAO1-AS contained four mutations that were specific to this strain: single SNPs found in PA0295, PA0602 and *wspF*, and a 3-bp TCC insertion within the *mexT* gene. Mutations within *wspF* affect methylation of the methyl-accepting chemotaxis protein WspA and modulate the biofilm phenotype (Hickman et al., 2005, D'Argenio et al., 2002). This is likely the cause of increased biofilm formation observed in PAO1-AS.

Increased growth in aerobic conditions for all PAO1 lineages apart from PAO1-AS was observed (Fig 2-4). PAO1-AS exhibited an autoaggregative phenotype in liquid media, particularly at the culture surface. Similar to

biofilms, the formation of autoaggregates in liquid culture can create anaerobic pockets (Starkey et al., 2009) which may actually inhibit growth. However, this autoaggregative trait could have produced a pellicle and caused inaccurate O.D. readings. Nevertheless, the data here describe a clear phenotypic difference between PAO1 sublineages. Increased PAO1 growth in aerobic conditions seems logical and compatible with a scenario that ensures propagation in a nutrient rich environment. Perhaps strains with increased biofilm forming capabilities, such as PAO1-AS, behave differently in response to oxidative stress.

MexT, a mutational hotspot, (Klockgether et al., 2010, Luong et al., 2014, Olivas et al., 2012) contained an 8-bp deletion within both PAO1-AL and PAO1-AS, a SNP upstream in PAO1-AL and a TCC insert downstream in PAO1-AS. Both ATCC variants showed increased biofilm capabilities along with an 8-bp deletion in *mexT* (absent in PAO1-DM and PAO1-AM). The phenotype of the SNP in PAO1-AL and TCC insert in PAO1-AS is unknown. The 8-bp deletion within *mexT* has been associated with reduced swarming ability (Luong et al., 2014). Perhaps this mutation is also responsible for the hyper-biofilm forming phenotype observed in PAO1-AL and PAO1-AS. Interestingly, *mexT* mutations also confer resistance to ciprofloxacin yet no differences in antimicrobial susceptibly among the PAO1 lineages were identified. Reduced pyocyanin production is another phenotype seen in strains with this mutation, yet results here indicate that the 8-bp deletion had differing effects on pyocyanin production in aerobic conditions in both lineages. The

additional *mexT* mutations in the ATCC variants may alternatively be having a compensatory effect. Further investigation led to an epidemiological screening of clinical strains in search of the *mexT* 8-bp deletion. Similar to PAO1-AL and PAO1-AS, all samples within the strain collection harboured the 8-bp deletion (Ocampo-Sosa et al., 2012). A sequence alignment of 78 *P. aeruginosa* strains available at NCBI shows that 6 contain a full copy of the *mexT* repetitive sequence (CGGCCAGCCGGCCAGCCGGCCATC) while the remaining harbour a *mexT* 8-bp deletion which has been identified as CGGCCAGC--------CGGCCATC or CGGCCAGCCGGCCA--------TC, both of which reside within the repetitive region. Ocampo found an 8-bp deletion (GCCGGCCA) at position 240 whereas our deletion (CGGCCAGC) was found at position 225 alike to the deletion found in nfxC-type mutants (Maseda et al., 2000). All of these strains have a deletion but due to the repetitive nature of the sequence it is unclear where the exact deletion point is and if these alignments truly represent two distinct types of an 8-bp deletion. Furthermore it is unclear if the epidemiological assay carried out in this study may in fact represent different deletions at multiple sites within the *mexT* gene. This variability between strains highlights the importance of this *mexT* region.

It is well known that pyocyanin production by *P. aeruginosa* is increased in response to iron limitation and oxygen transfer (Kim et al., 2003). In these conditions (aerobic growth tests), this was applicable to all PAO1 lineages apart from PAO1-AS, which failed to produce pyocyanin. There was no

phenotypic link between PAO1-AS and the putative membrane mutations in PA0295 or PA0602. Perhaps these mutations have an impact on growth, transport of small molecules and pyocyanin production since previous findings show ABC transporters have varied roles in molecule transport (Köster, 2001, Brillet et al., 2012). Since *wspF* mutations also cause wrinkled and rough small colony morphologies (Starkey et al., 2009, D'Argenio et al., 2002), it is possible the PA0295 mutation confers a compensatory mechanism by which membrane function is modulated and acts as counter mutation to the *wspF* SNP, therefore producing a smooth round colony.

2.5   Conclusion

Comparative genomics and epidemiology studies led to the identification of an 8-bp deletion in *mexT* as a possible regulator of biofilm formation. Results here indicate that the accumulation of SNPs and the microevolution of *P. aeruginosa* is a multifactorial process with strain dependent effects. Mutations have been identified in naturally occurring variants of the laboratory strain PAO1. Differences in morphology, growth and biofilm phenotype have been shown in strains traditionally perceived to be identical. Phenotypic and genotypic analyses have illustrated that without characterisation, these mutations would have gone unnoticed. Such variations, accumulating over time and sub-culturing, are a cause for concern. It is recommended that researchers routinely perform WGS of their standard strains such as PAO1, publishing these data alongside their experimental results, to allow other researchers to assess the likely impact of any genetic diversity on reproducibility.

3 Phenotypic characterisation of the 8-bp deletion in *mexT* variants

3.1 Introduction

The pathogenicity of *P. aeruginosa* is attributed to a plethora of phenotypes, one of them being antibiotic resistance. *P. aeruginosa* is intrinsically resistant to several antibiotics and has the ability to acquire multi-drug resistance. One such mechanism involves the activation of *mexT*, a regulator of the multi-drug efflux pump MexEF-OprN. Interestingly in PAO1, *mexT* and the MexEF-OprN system are typically quiescent but are both highly induced in mutants which harbour a *mexT* 8-bp deletion (Maseda et al., 2000). NfxC mutants exhibit increased resistance to chloramphenicol, trimethoprim and fluoroquinolones and susceptibility to certain β-lactam and aminoglycoside antibiotics (Maseda et al., 2000, Kohler et al., 1997, Köhler et al., 1997).

While antibiotics were orginally developed for their antimicrobial properties, their biological functions may have different roles in nature and act as intercellular signaling molecules which modulate the collective behavior of microbial populations (Davies, 2006, Linares et al., 2006, Aminov, 2013). It is clear that antimicrobial efflux is not the only function of the MexEF pump; *P. aeruginosa* recovered from an experimental model of rat pneumonia in the absence of antibiotic selection overexpressed MexEF-OprN (Join-Lambert et al., 2001). Interestingly, strains isolated from the intestines of rats during surgical injury conversely showed a lack of *mexE* or

mexF expression due to a mutational loss (acquisition of a stop codon) in *mexT* (Olivas et al., 2012, Luong et al., 2014). Increased *mexEF* expression has also been observed in strains and conditions that function as an antagonist of quorum sensing and virulence, including those involving nitrosative stress (Juhas et al., 2004, Hentzer et al., 2003, Fetar et al., 2011). In agreement with studies performed on nfxC mutants, the induction of the MexEF pump is also associated with reduced levels of homoserine lactone-dependent virulence traits (Kohler et al., 2001) (Favre-Bonté et al., 2003) and reduced expression of TTSS effector proteins (Linares et al., 2005, Olivares et al., 2012). It has been suggested that MexEF-OprN mediates these effects via efflux of cell-signalling intermediates, which ultimately commits the cell to a state of reduced virulence (Kohler et al., 2001). These studies indicate the involvement of a complex regulatory network which is still not fully understood.

The results from the previous chapter revealed an 8-bp deletion within *mexT* as a possible regulator of biofilm formation. NfxC mutants can arise though multifactorial mutations (Sobel et al., 2005, Maseda et al., 2000) yet the physiological effects of this 8-bp deletion alone in *P. aeruginosa* remain to be elucidated. To investigate this mutation further, mutants were engineered solely with the 8-bp deletion to clarify the phenotype of this mutation.

72

3.2 Methods

3.2.1 Bacterial strains and culture conditions

All strains (listed in Table 3-1) were initially grown on Columbia agar (Oxoid,

UK) and then incubated at 37°C for 16h at 180 rpm in M9 medium

supplemented with 22.2 mM glucose, 2mM MgSO$_4$, 0.1mM CaCl$_2$, 24.4mM

casamino acids and 1mM thiamine hydrochloride (Sigma-Aldrich, USA).

Table 3-1 Strains and plamids used in this study

Strain/Plasmid	Genotype or relevant characteristic	Source
Strains		
PA	PA parent with double 8-bp sequence, originally known as PAO1-AM	John Innes Centre
PAdel	PA with single 8-bp sequence (isogenic mutants of PA)	This study
PAnfxC	PA with single 8-bp sequence cultured onto sub MIC chloramphenicol agar	This study
Plasmid		
pTS	8.8-kb broad-host-range cloning/shuttle vector (Tet^r,*oriColE1, sacB)*	Dr Jacob Malone, John Innes Centre

3.2.2   Generation of the isogenic mutant PAdel with the 8-bp deletion

DNA was extracted as per manufacturer's instructions using the Roche MagNA pure Compact system (Roche, Switzerland) and from PA and PAO1-AS. *MexT* was PCR-amplified using Phusion DNA polymerase and Phusion GC Reaction Buffer (New England Biolobs, Massachusetts, U.S.A.) combined with DNTPs and primers listed below (Table 2). PCR conditions: Denaturation: 98 °C (5min), Annealing: 98 °C (10sec), 55 °C (30 sec), Elongation: 72 °C (20sec), (32 cycles) 72 °C (5min) before being left at 10 °C. Plasmid DNA from the suicide vector, pTS, was extracted using the NucleoSpin Plasmid kit (Macherey-Nagel, Germany). Amplified *mexT* DNA was digested with *Mfe I* and *Bam HI* and pTS DNA with *Eco RI* and *Bam HI*, as per manufacturer's instructions (New England Biolabs Ltd, UK). The vector was treated with alkaline phosphatase and ligated with the insert in a ratio of 3:1 (insert to vector) using T4 ligase (New England Biolabs) before incubating overnight at 4 °C. The pTSmexT constructs were individually transformed into *E. coli* DH5α by heat shocking: pTSmexT and *E. coli* DH5α were mixed on ice, heated at 42 °C for 1 min before being placed back onto ice for 2 min. LB broth was added prior to incubation at 37 °C for 2 hrs. This was then plated onto tetraycline agar to confirm the presence of *E. coli* DH5α colonies with the construct and tetracycline resistance marker. Colony PCR (primers listed in Table 3-2) and gel electrophoresis was performed to screen colonies for the required insert. PCR steps included: 95 °C for 5 min, 95 °C

for 30 sec, 55 °C for 30 sec, 72 °C for 2 min (30 cycles) 72 °C 10 min. Overnight PA cultures were washed in 300 mM sucrose. Transformation of the construct into PA was carried out in a Gene Pulser Electroporation System (Bio-Rad, U.S.A.) with the following settings: 200 Ω, 2.5 kV before plating onto sucrose agar.   Colonies with the insert were then confirmed by sequencing (Eurofins Scientific, Luxembourg) and thereafter named PAdel.

Table 3-2 Primers utilised to construct PAdel

Name	Forward sequence	Reverse sequence
mexT	ATGGATCCGTTCGAAGCCGAGACCG	ATGAATTCCTCCTCGTCGACGAAGC
pTS	CGGCAGGTATATGTGATGGG	CCATGAGTGACGACTGAATCCG

3.2.3   Generation of the natural mutant PAnfxC with the 8-bp deletion

To generate PAnfxC, PA overnight cultures were diluted to 10^8 CFU/ml and plated onto LB agar (Oxoid, UK) containing 0.05 µg/ml ciprofloxacin as previously described (Kumar and Schweizer, 2011). Following incubation overnight at 37°C, resistant colonies were screened for the *mexT* 8-bp deletion using colony PCR. Each PCR template was prepared by mixing a single colony with distilled water and heating at 95 °C for 5 min. Each 20 ul PCR reaction consisted of 10 µl Roche Lightcycler 480 SYBR Green I Mastermix (Roche Diagnostics, GmbH, Mannheim, Germany), 0.5 ul (20 µM) forward   (CGCAGAGAAACTGTTCCT)   and   reverse   primer (GGTACGGACGAACAGC) (Sigma-Aldrich, Dorset, UK), 4 µl molecular water

(Sigma-Aldrich) and 5 µl template. DNA amplification was carried out in a Roche LightCycler® 480 Instrument II (Roche) using an initial denaturation step at 95°C for 10 sec followed by 45 cycles of amplification (denaturation at 95°C for 0.5 min, annealing at 60 °C for 30 sec) followed by melt curve analysis. One colony out 18 was identified with a single 8-bp sequence within its genome and was termed PAnfxC.

3.2.4   Antibiotic susceptibility profiles

Antimicrobial susceptibility was tested against a range of antibiotics using the liquid broth micro-dilution method. Cultures were grown at 180 rpm in supplemented M9 at 37 ℃. Cultures were then sub-cultured for 3 hours to achieve a concentration of 2×10^5 CFU/mL. Stock solutions for Gentamicin, Ceftazidime, Meropenem, Piperacillin, Ciprofloxacin and Chloramphenicol (Sigma) were made according to the manufacturer's protocol and two fold serial dilutions of each antibiotic prepared in a 96 well microtiter plate with supplemented M9 media. An equal volume of log phase culture was then added to each well. Plates were incubated overnight at 37°C, and then examined for bacterial growth and turbidity, visually. The minimum inhibitory concentration (MIC) was identified by the lowest concentration of antibiotic that prevented growth.

3.2.5   Motility testing

Swimming, swarming and twitching phenotypes were tested in LB agar concentrations of 0.3%, 0.5% and 1% respectively (O'May and Tufenkji, 2011, Rashid and Kornberg, 2000). For swimming tests, 5 ul of inoculum representing 10^8 CFU/ml, was placed into the center of the agar. For swarm plates, 5ul of the inoculum was placed onto the agar surface. For twitching, the inoculum was pelleted and a toothpick used to inoculate the agar-petri dish interface. Plates were incubated for 18 h at 37°C before the diameters of the motility zones were measured.

3.2.6   Virulence testing

The relative virulence of each *P. aeruginosa* strain was assessed in the *Galleria. mellonella* model according to a protocol modified from McMillan et al. (2015). Briefly, larvae (UK Waxworms Ltd, Sheffield, UK) in groups of 12 were injected with PBS suspensions containing 10 total CFU per larva. In addition, one control group did not undergo any manipulation to control for background larval mortality (no manipulation control) while another group (uninfected control) was injected with PBS only to control for the impact of physical trauma. Larvae were kept in petri dishes in the dark at 37°C for up to 24 h and inspected every 6 h so that percentage survival could be calculated for each group. Larvae were considered dead if they did not move after being stimulated with a sterile inoculation loop. The experiment was

repeated in triplicate and performed by Dr Andre Desbois' research group at the University of Stirling.

3.2.7 Phenotypic microarray

The utilisation of 626 substrates were tested using phenotype microarray (PM) plates and protocols supplied by Biolog Inc, USA. Briefly, strains were serially cultured on Columbia agar twice and incubated at 37°C for 18 hr. Bacterial colonies were suspended in inoculation fluid-0 and dye A, and 100 ul was aliquoted into each well of PM plates 1-2. Sodium succinate, 540 mg/ml (Sigma-Aldrich) and ferric citrate, 0.049 mg/ml (Sigma-Aldrich) were added to the inoculating fluid for PM plates 3, 4 and 6-8. Further optimization of the growth parameters were required for PM plates 3, 6, 7, and 8 to prevent growth in the negative controls. This involved reducing the inoculum and sodium succinate concentration by a 1 in 10 dilution factor for PM plates 3, 6, 7, ad 8. All plates were incubated at 30°C for 96 h in the OmniLog reader.

The signal value (SV) for each substrate was calculated (Homann et al., 2005) and replicates averaged, with negative controls subtracted from the results. Resultant negative values were assigned a value of 0, indicating no growth. To enable fold change (FC) calculations all results (0 and positive) were adjusted by adding a value of 1. The FC was then calculated between PA vs PAdel and PA vs PAnfxC.

The final analysis was carried out by applying a normal distribution to all results from all of the plates (PM1-3, 6-8). This was to see where the major differences were. Results outside of the 95% confidence interval were subjected to a paired Student's T-test and those with a P value of < 0.05 were considered significant.

Uridine and inosine were used to validate some of the Biolog results as these substrates were available in the laboratory. Overnight cultures of the *mexT* variants were grown at 37°C in M9 minimal medium supplemented with 22.2 mM glucose, 2mM MgSO$_4$, 0.1mM CaCl$_2$, 24.4mM casamino acids and 1mM thiamine hydrochloride. Cells were centrifuged and resuspended in M9 minimal medium containing inosine or uridine (30 mM) to a concentration of 10^5 CFU/ml. The optical density of cultures were measured at a wavelength of 600 nm in a FLUOstar Omega plate reader (BMG Labtech GmbH, Germany) over the course of 24 hours. Experiments were performed in triplicate.

3.3 Results

3.3.1 Antimicrobial susceptibility

Variants of *mexT* with the single copy of the 8-bp sequence showed increased resistance to ciprofloxacin and chloramphenicol, a characteristic of nfxC type mutants (Llanes et al., 2011, Li et al., 1994) (Table 3-3). NfxC mutants show increased susceptibility to certain β-lactams, as observed with PAdel and PAnfxC when exposed to piperacillin. Meropenem on the other hand has been linked to reduced susceptibility in strains with an active *mexT*. However, no change was observed with the cephalosporin ceftazidime. Increased susceptibility to the aminoglycoside gentamicin was also observed, as previously reported (Köhler et al., 1999, Kohler et al., 1997).

Table 3-3 Antimicrobial susceptibility profile for PA, PAdel and PAnfxC

Minimum inhibitory concentrations (ug/ml) for gentamcin, ceftazidime, meropenem, piperacillin and ciprofloxacin against PA, PAdel and PAnfxC (n=2).

	Average MIC (ug/ml)		
	PA	PAdel	PAnfxC
Gentamicin	3	1.5	1.5
Ceftazidime	4	4	4
Meropenem	0.125	0.25	0.25
Piperacillin	2	1	1
Ciprofloxacin	256	4096	4096
Chloramphenicol	100	1600	1600

3.3.2   Motility

The absence of the 8-bp sequence in PAdel and PAnfxC significantly reduced swarming and swimming behavior (Figure 3-1). No differences in twitching were identified.
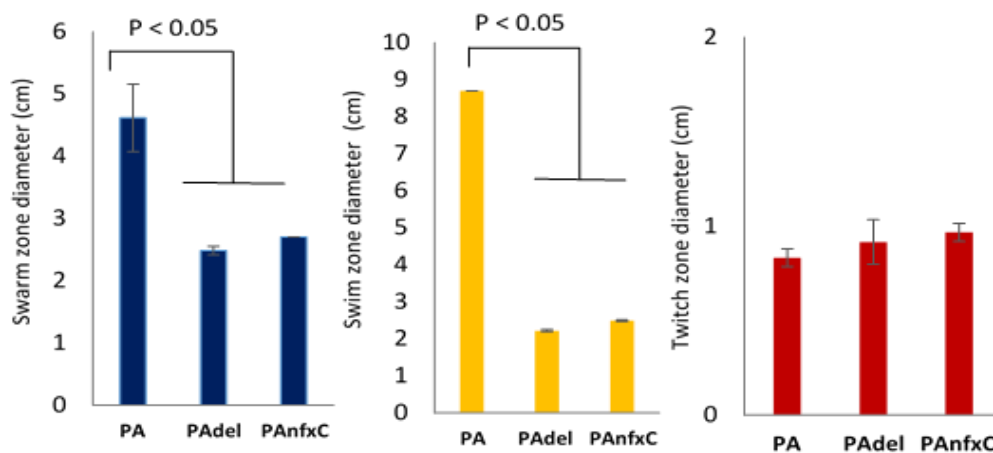
Figure 3-1 Motility phenotype of *mexT* variants
Strains with the 8-bp deletion showed reduced swarming and swimming traits (P< 0.05). Error bars are standard deviation (n=3).

3.3.3   Virulence testing

Strains were exceptionally virulent in the *G. mellonella* model, as it required fewer than 100 cells for death to ensue quickly. To address this, inoculum concentrations were kept consistent, as small variations had an impact on how virulent a strain would appear. Final inoculum concentrations are provided in Figure 3-2.
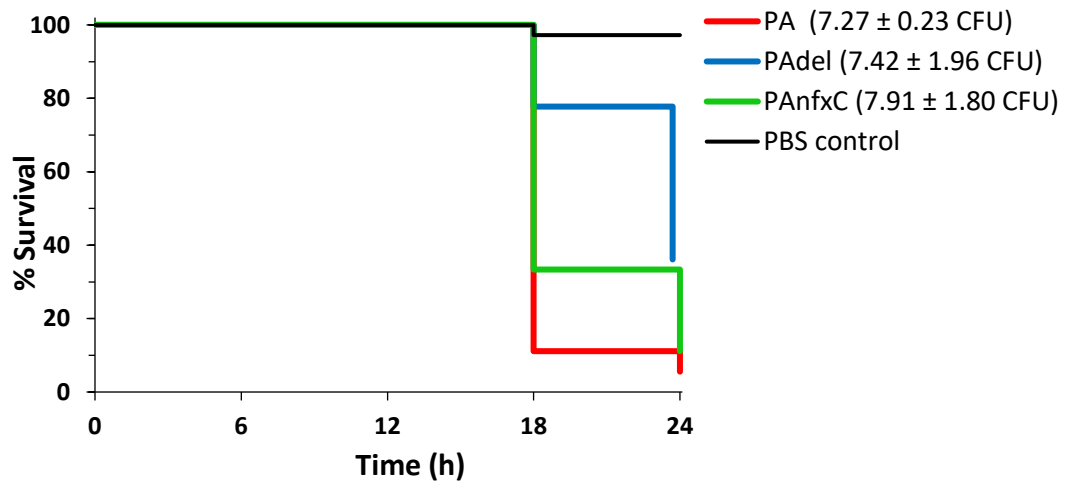
Figure 3-2 Virulence testing of the *mexT* variants in a *G. mellonella* model of infection

Kaplin-Meyer graph (n=12) showing PA was the most virulent among the *mexT* variants (P < 0.005). PAdel was significantly less virulent than PA (P<0.005), however PAnfxC was not significantly virulent compared to PA. Inoculum concentrations are shown in brackets with standard error from the mean.

3.3.4 Phenotypic microarray

Table 3-4 Fold change of 33 substrates differentially utilized by the *mexT* variants. A normal distribution and t-test were applied to the SV (signal value) across all plates and strains (PA vs Padel PA vs PAnfxC). Results where the p value was < 0.05 was indicated by * (n=2).

PM plate	Substrate	Average PA SV	Average PAdel SV	Average PAnfxC SV	Fold change PA vs PAdel	Fold change PA vs PAnfxC
8	Ile-Leu	102.1	1.0	1.0	102.1*	102.1*
6	Ile-His	78.6	1.0	2.6	78.6*	29.8*
8	Leu-Leu-Leu	46.9	1.0	1.9	46.9*	24.7*
7	Ser-Leu	46.4	1.0	1.0	46.4*	46.4*
8	Ser-Gln	52.2	1.1	1.4	45.9*	38.1*
8	Pro-Ser	40.4	1.0	1.0	40.4*	40.4*
6	lle-Trp	32.4	1.0	1.0	32.4*	32.4*
6	Ile-Phe	80.9	2.6	3.6	30.9*	22.8*
6	Glu-Val	23.1	1.0	1.5	23.1*	15.4*
8	Val-Glu	22.1	1.0	1.4	22.1*	15.5*
6	Ile-Val	86.3	4.3	5.1	20.1*	16.9*
8	Thr-Phe	19.2	1.0	1.0	19.2*	19.2*
7	Trp-Tyr	18.4	1.0	1.0	18.4*	18.4*
6	Asp-Trp	17.6	1.0	1.0	17.6*	17.6*
3	Gly-Glu	15.7	1.0	1.0	15.7*	15.7*
6	Asp-Leu	15.6	1.0	1.0	15.6*	15.6*
7	Met-Ile	15.5	1.0	1.0	15.5*	15.5*
7	Trp-Leu	23.8	1.6	1.3	15.2*	18.4*
3	Ala-Gly	17.6	1.2	1.0	15.1*	17.6*
6	His-Val	88.9	5.9	4.0	15.0*	22.2*
8	Leu-Gly-Gly	29.7	2.1	4.0	14.2*	7.4*
6	Glu-Trp	103.5	7.4	9.9	14.0*	10.4*
7	Ser-Phe	75.4	5.4	5.7	14.0*	13.3*
3	L-Leucine	74.3	4.0	1.0	18.6	74.3*
7	Met-Trp	13.1	1.0	1.0	13.1	13.1*
6	Ile-Tyr	110.5	8.5	3.4	13.0	32.4*
6	Gly-Leu	12.8	1.0	1.0	12.8	12.8*
8	Pro-Val	82.9	7.9	5.4	10.5	15.3*
6	Ala-Trp	25.4	2.9	1.5	8.7	16.7*
1	Uridine	45.2	5.8	2.9	7.8	15.6*
6	Glu-Tyr	18.8	3.2	1.0	5.8	18.8*
8	Ala-Ile	43.2	22.6	1.8	1.9	23.4*
3	L-Lysine	91.3	57.9	3.0	1.6	30.9*

Phenotypic microarray results showed that PAdel and PAnfxC were particularly defective in protein, amino acid and nucleoside compound metabolism based on results that lay outside of the 95% confidence level of a normal distribution. The purpose of this statistical analysis was to identify the major differences between the *mexT* variants across all PM plates. Strains with the single copy of the 8-bp sequence also showed a reduced ability to grow on sugars, carboxylic acids and phosphorus based compounds, however these results lay outside of the 95% confidence level of a normal distribution.   Biolog results were validated using uridine and inosine growth in M9. A full list of fold change differences between all substrates tested are listed in Appendix 8.2.1.

Results here also indicated that PAdel and PAnfxC were able to grow in the presence of acids (α-Hydroxy Butyric Acid Phospho-Glycolic Acid). Although reduced metabolism was observed in the presence of glycyl-L-aspartic acid, γ-hydroxy butryic acid and glycl-L- glutamic acid, signal values of approximately 10 indicated inefficient growth and may not be enough to suggest that there was a profound difference in metabolism of these substrates.

A twofold (aprox) difference in the utilization of the central metabolism metabolites such as oxalomalic acid and methyl pyruvate ($p<0.1$) was also observed. Oxalomalic acid, a sodium salt, inhibits both aconitase and NADP-dependent isocitrate dehydrogenase in the conversion of citrate to

isocitrate. The results for this substrate showed that the average SV for PA was 12.6 and for PAdel, 5.9. Again these small signal values among strains may not represent sufficient growth to identify differences. Interestingly, methyl pyruvate, a key player in central metabolism, also supported the growth of PAdel and PAnfxC despite being less metabolically active on other substrate groups.

Although PM results indicated differences in peptide utilisation there were no significant differences in the specific amino acids that form these peptides. This indicates that differences in peptide utilisation maybe caused by transporters that allow import of specific substrates, rather than differences in cytosolic pathways or reactions.

Reduced growth on nucleoside based media was also observed in PAdel and PAnfxC. Differences in uridine metabolism were highly significant when compared to PA. Reduced growth with was also noted on adenosine, cytidine and inosine sources (12 – 5 fold differences) although these were not within the 95% confidence level (listed in Appendix 3-1.2).

Mutants with the single copy of the 8-bp sequence exhibited reduced virulence in the *Galleria mellonella* model. Tryptophan, a known precursor of PQS synthesis (Palmer et al., 2013) illustrated a 3-4 fold reduction in utilization in PAdel and PAnfxC, which may explain the reduced virulence phenotype of these strains. A two to threefold fold reduction was also shown in gelatin utilization in PAdel and PAnfxC suggesting that the reduced

production of virulence factors such as gelatinase and other proteases may hinder the breakdown of peptides and therefore import into the cell. This could also be a contributing factor leading to the reduced metabolism of peptides since virulence factors can be proteases.

3.4 Discussion

The gene, *mexT* is considered a mutational hotspot (Klockgether et al., 2010)

that leads to phenotypic variation. Sequence variants of *mexT* have been

well documented, in terms of *mexT*-mediated regulation of the MexEF-OprN

efflux pump, with several studies having looked at the 8-bp deletion in nfxC

mutants. There is however is no evidence of this being performed on

isogenic mutants but on a strain termed PT149 or PAO-7H (Kohler et al.,

1997) which was originally isolated as an nfxC mutant (selected for on

ciprofloxacin) with a single copy of the 8-bp sequence. It is well known that

various mutations arise in nfxC mutants (Luong et al., 2014, Maseda et al.,

2000, Sobel et al., 2005), not solely in *mexT* but also in neighbouring genes

such as *mexS*, *mexE* and *mexEF* (Köhler et al., 1999, Dumas et al., 2006,

Cosson et al., 2002, Ocampo-Sosa et al., 2012, Llanes et al., 2011). Therefore

the aim was to characterise differences between the parent, the isogenic

mutant PAdel, which was genetically engineered with the 8-bp deletion, and

a naturally selected nfxC mutant, PAnfxC.

Characteristically resistant to chloramphenicol and ciprofloxacin, the

antimicrobial susceptibility profiles of PAdel and PAnfxC were similar to that

of an nfxC mutant (Maseda et al., 2000, Kohler et al., 1997, Köhler et al.,

1997).

The identification of the *mexT* 8-bp deletion in the previous chapter was

linked to the differential regulation of biofilm formation among the PAO1

lineages. Therefore investigation of motility behaviour of all *mexT* variants was also required. Similar to nfxC mutants which are associated with reduced levels of homoserine lactone-dependent virulence traits, reduced motility was also observed in the strains harbouring the 8-bp deletion. Hence, it was anticipated that a difference in biofilm formation would also be identified and so efforts were made to characterise biofilms using standard techniques such as those employed in the first chapter. Contrary to previous studies indicating that *mexT* has a role in attachment (Favre-Bonté et al., 2003, Tian et al., 2009b), in this study a stable phenotype or difference associated with biofilm formation was not found among the *mexT* variants.

Virulence testing in the *G. mellonella* model revealed that PAdel was less virulent than PA. However PAnfxC was not significantly different to PA, a result that differs to previous findings (Olivares et al., 2012). It was hypothesized that differences in compensatory genomic mutations were likely the cause of phenotypic variations between PAdel and PAnfxC, highlighting the importance of isogenic studies. PT149, a commonly studied nfxC mutant, has been shared between laboratories worldwide and has most likely acquired additional mutations beyond the 8-bp deletion over time. With no genome wide data available to contradict this, the phenotype of PT149 is unreliable.

It is generally thought that acquisition of antibiotic resistance and efflux in general is associated with a metabolic burden (Sanchez et al., 2002, Alonso et al., 2004, Piddock, 2006). This theory has been challenged by one study showing that nfxC type mutants co-exist with the wildtype in mixed cultures (Olivares et al., 2012). The 8-bp insertion known to render *mexT* inactive can be likened to a strain termed MPAO1-P2 which had a truncated and inactive form of *mexT*. However, MPAO1-P2 outcompeted MPAO1-P1 (precursor strain of MPAO1-P2 with an active mexT) in competition assays (Luong et al., 2014). The variation in the literature highlights the need for defined media and conditions to corroborate findings. In this study a metabolic burden associated with mutants with the 8-bp deletion was identified. Nucleoside, amino acid, sugar, carbohydrate and phosphate based compounds that supported the growth of the parent strain, did not support the growth of PAdel and PAnfxC. These strains, which display antimicrobial resistance, were however capable of robust growth on acid based compounds.

It seems that PA is adapted to an environment that nurtures growth. A laboratory environment would provide the perfect conditions for such a strain, especially as the 8-bp insertion was originally identified in PAO1-DM and PAO1-AM (Chapter 2). The ability to utilise nucleosides indicates a scavenging phenotype that, when associated with quorum sensing related traits, ensures propagation. Perhaps the generation of the additional 8-bp sequence was also promoted by the specific utilisation of nucleoside based

substrates. PAdel and PAnfxC represent the effect of stress induced responses on *mexT* and as such were capable of thriving in acidic conditions such as those identified by phenotypic microarray tests. It remains unclear whether these phenotypes were *mexEF* dependant.

3.5   Conclusion

There is accumulating evidence that multi-drug efflux pumps have a greater range of function than is usually attributed to them. It was shown that a single 8-bp change in the transcriptional regulator *mexT* is not only capable of mediating antibiotic resistance but also motility, virulence and central metabolism. The phenotype of the 8-bp deletion and its role in nfxC mutants has been clarified. It is hypothesised that differences shown between PAdel and PAnfxC, and previously published nfxC mutants, were likely the result of different compensatory mutations. To identify compensatory mutations, whole genome sequencing is essential. Interrogating the genome sequence and transcriptome will help identify the *mexT* regulon and the role of the *mexEF* pump on the phenotype that has been characterised here.

4 Effect of the *mexT* 8-bp sequence on the transcriptome

4.1 Introduction

The genetic diversity of four colonial variants of PAO1 was previously examined, characterising differences in phenotype based on antibiotic resistance, microaerophilic growth, motility and biofilm formation. This phenotypic diversity was driven by an 8-bp sequence variation found within the LysR transcriptional regulator, *mexT*, a modulator of the MexEF efflux pump.

This gene, *mexT,* is a mutational hotspot (Klockgether et al., 2010) which is known to lead to phenotypic variation in *P. aeruginosa,* yet little is known about the global influence of this mutation and its role in nfxC mutants. The nfxC phenotype is known to occur as a result of mutations within *mexT*, one of them being the 8-bp deletion which is known to activate the gene. The gene *mexT,* classified as a transcriptional regulator is located upstream and in the same orientation as the *mexEF-oprN* pump (Köhler et al., 1999). While other RND pumps are regulated by transcriptional repressors, the MexEF pump is modulated by the transcriptional activator, MexT. Induction of the MexEF-OprN pump is dependent upon an 'active' form of *mexT*, which is essential to the survival of the cell. Thus much research on nfxC mutants has featured the phenotype associated with the *mexEF* efflux pump.

A study looking solely at the *mexT-mexE* intergenic region in *P. aeruginosa* found that the *mexT*-proximal 114-bp region contained a MexT-binding site that comprised of two nod boxes. The protein MexT was capable of binding to the *mexT*-proximal *nod* box but not to the *mexT*-distal *nod* box. The proposal of a *mexT* binding consensus sequence (ATCA(N5)GTCGTA(N4)ACYAT) in an earlier study was therefore ruled out since this sequence contained the *mexT*-distal *nod* box (Tian et al., 2009a). Although the *mexT*-distal *nod* box DNA was −10 to −50 bp from the transcriptional initiation site, a region known to contain a promoter, this region lacked any major promoter-binding sequence known in *P. aeruginosa*. It is was thought that this site may contain a new promoter-binding sequence or is acted on by an uncharacterized sigma factor. Also within the *mexT-mexE* intergenic region is a 13 bp inverted repeat separated by a 10-bp space. This is located in the *mexE*-proximal 27-bp region which has been identified as a repressor-binding site since deletion of this region increased *MexE* production (Maseda et al., 2010).

Increased expression of the MexEF–OprN efflux pump is known to reduce *rhlI* and *rhlAB* transcription which lowers C_4-HSL and surfactant production, respectively. In this case, expression of *lasR* and *rhlR* was not affected (Daniels et al., 2004). Besides the *mexEF-oprN* operon, MexT can activate expression of *mexS* which is characteristically located adjacent to *mexT* and transcribed in the opposite direction (Köhler et al., 1999). There has however been no report of a *nod* box in the promoter region of *mexS*. The regulation

of the *mexT* regulon appears to be complex as it exerts its effects not just on adjacent genes but as global regulator; MexT represses MexAB-OprM thereby decreasing the auto inducer C4-HSL (Uwate et al., 2013, Maseda et al., 2004) whilst induction of the MexEF-OprN efflux pump is associated with reduced levels of virulence factor production (Sobel et al., 2005, Tian et al., 2009b) and transport of cell-signalling intermediates (Tian et al., 2009b). The MexAB–OprM efflux system also contributes to $3O,C_{12}$-HSLsecretion (Pearson et al., 1999). Mutants with the nfxC phenotype are therefore less virulent.

As indicated in chapter 1, independent of MexEF-OprN, MexT can down regulate the TTSS system, pyocyanin formation and early surface attachment (Tian et al., 2009b). It is evident that MexT has a wider role than just regulation of the *mexEF* pump. It is unclear how the MexT regulatory network affects the transcriptome of strains with and without the 8-bp deletion. Understanding the physiological role of the 8-bp sequence and its related stress response is key to understanding this adaptive mode of survival. To investigate this, the aim was to use RNA-seq to compare gene expression levels in a defined medium for two otherwise isogenic *mexT* variants.

4.2   Methods

4.2.1   Whole genome DNA extraction and sequencing

To define all mutations per strain, DNA was extracted from 1 mL of overnight culture using the MagNA pure Bacterial lysis kit with RNAse (Qiagen, Hilden, Germany) on the MagNA Pure Compact instrument (Roche, Switzerland). Nextera XT library preparation was carried out before deep sequencing on the MiSeq with v3 chemistry (Illumina, California, U.S.A).

4.2.2   DNA Single nucleotide variant calls

To identify single nucleotide variants, DNA sequence reads in fastq gzipped format were aligned to the reference genome. The reference genome used was *P. aeruginosa* PAO1, obtained from NCBI Genbank with the accession number NC002516. Reads were aligned to the reference using Bowtie2 (Langmead and Salzberg, 2012) and alignments were sorted, indexed and stored in BAM file format using samtools (Li et al., 2009). Variants (including synonymous and non-synonymous mutations) were called using Bayesian inference with freebayes (Garrison, 2012), using the the samtools calmd setting for BAQ quality filtering. A further filtering step was employed to remove SNPs in windows of very high SNP density. Variants were stored in Samtools VCF file format. Bioinformatics analysis was performed by SequenceAnalysis.co.uk.

4.2.3   RNA Extraction

Five colonies from each strain grown on Columbia agar were used to inoculate 10 ml of Luria-Bertani (LB) broth and incubated at 37°C for 24 hrs. Cultures were diluted to 1:1000 in fresh M9 (supplemented with 22.2 mM glucose, 2mM MgSO4, 0.1 mM CaCl2, 24.4 mM casamino acids and 1mM thiamine hydrochloride) and grown for 24 hr at 37°C, 180 rpm then diluted again 1:100 in fresh M9 and incubated for 5 h to ensure the cells were in log phase. The following steps represent the final protocol used; considerable optimisation was needed to ensure RNA of sufficient quantity and quality were obtained, as detailed in Appendix 8.3.1. The final step of the procedure was to mix cultures with RNAprotect Bacterial Reagent (Qiagen) and centrifuge according to the manufacturer's protocol. Bacterial pellets were stored at –70°C. TE buffer (10 mM Tris, 1 mM EDTA, pH 8.0) containing 15 mg/ml lysozyme (Fisher Scientific Ltd, UK) and proteinase K (Roche, Switzerland) were added to cell pellets and incubated for 10 min at ambient temperature. Samples were then processed using the RNeasy mini Kit (Qiagen) according to the manufacturer's protocol, with the inclusion of on-column DNAse treatment from the RNase free DNase kit (Qiagen). Samples were also treated with DNase using the Turbo DNA-free Kit (Life Technologies Ltd, UK) and washed with the RNeasy mini kit.

4.2.4   **RNA-sequencing** (performed by Genomed, Poland)

Ribo-depletion was performed using the Ribo-Zero rRNA removal kit (Bacteria) (Epicentre, Chicago, U.S.A) and the NEBNext® Ultra™ RNA Library Preparation Kit. Sequencing was carried out on the Hi-Seq (Illumina) using paired-end sequencing (2x 100 bp) and V3 chemistry reagents.

4.2.5   **RNA transcriptomic analysis**

4.2.5.1   **Analysis at Genomed**

Transcriptome reads were aligned to the reference genome as above by Genomed using TopHat (Kim and Salzberg, 2011) and stored in a Samtools bam file format. Analysis results were provided in FPKM value output.

4.2.5.2   **Analysis at UEA**

Reads were counted and normalised in R using simple log fold change, edgeR (Robinson et al., 2010) glm, and edgeR classic formats, as well as using DESeq2 (Love, 2014) methods. Results from the analyses were output as sorted excel files.   DESeq2 output was used for downstream analysis after verification that other transcriptomics methods provided similar results. This was performed by SequenceAnalysis.co.uk (Norwich, UK).

Sequence alignment and Protein family (Pfam) analysis of the *mexT* gene sequence was performed using the NCBI Blast Analysis database

(http://blast.ncbi.nlm.nih.gov/Blast.cgi) and The European Bioinformatics Institute supported protein family database (http://pfam.xfam.org/).

To categorise genes differentially expressed between PA, PAdel and PAnfxC, clusters of orthologous group (COG) analysis was carried out using annotations downloaded from the Pseudomonas Genome Database (Winsor et al., 2016). Some genes have not yet been annotated with COG categories: this included 47 and 132 genes up and down-regulated in PAdel and 43 and 111 genes up and down-regulated in PAnfxC.

4.2.6   Network and metabolic analysis

Pathway analysis was performed using the BioCyc Pathway/Genome Database Collection whereby gene lists with expression values were submitted (Latendresse and Karp, 2011, Paley and Karp, 2006). To analyse networks/pathways and gene enrichment in STRING (http://string-db.org/), log2 fold changes over 1 in genes differently expressed between PA and PAdel or PA and PAnfxC were submitted and the output analysed. Results were filtered and the settings adjusted so that gene associations were made using experimental, co-expression, gene fusion and co-occurrence data only. A medium confidence level of 0.4 was used.

4.3 Results

4.3.1 Comparative genomics
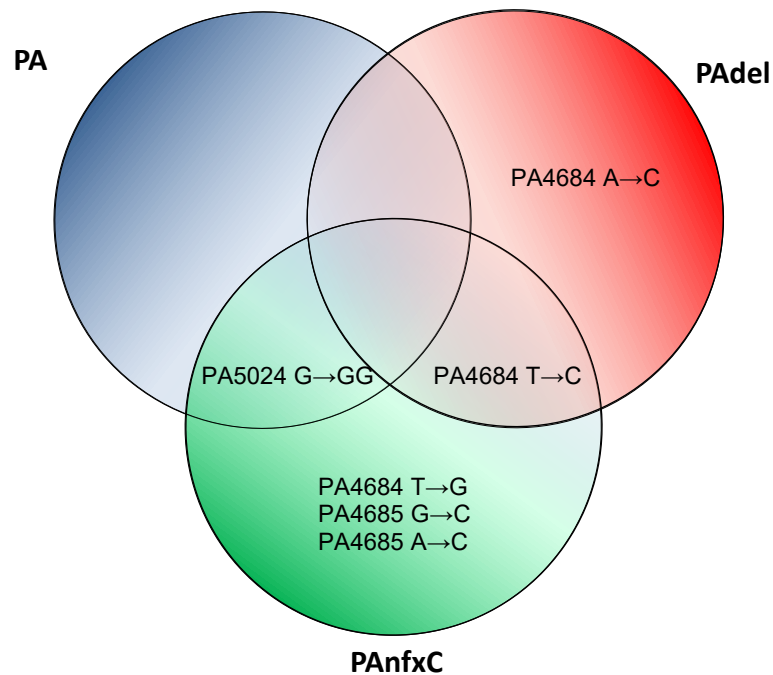
Figure 4-1 Non-synonymous SNPS and indels among the *mex*T variants; PA (double copy of the 8-bp sequence), PAdel and PAnfxC (single copy of the 8-bp sequence). WGS sequencing results identified only non-synonymous among the three *mexT* variants. In PAdel, a side of the 8-bp repeat region, this included 1 mutation in PA4684, unique to this strain. Unique to PAnfxC, a single mutation in PA4684 was identifed, along with two mutations in PA4685 were identified. In PA4684 another mutation was found, present in both PAdel and PAnfxC. A detailed view is available in Appendix 8.3.2.

Figure 4-1 illustrates the non-synonymous SNPS and indels among the *mex*T

variants. The genes PA4684 and PA4685 have not been previously

uncharacterized but appear to be sites of genomic mutational hotspots in *P.*

aeruginosa (Klockgether et al., 2010), perhaps with compensatory functions

for the *mexT* 8-bp deletion. In PA and PAnfxC, a mutation in PA5024 was

found. It is hypothesized that since the generation of PAnfxC occurred after PAdel, a mutation present in PA was passed on to PAnfxC.

4.3.2 Transcriptome results

When compared to the parent strain, 657 genes showed reduced expression with 382 illustrating increased expression in PAdel (Appendix 8.3.3). In PAnfxC there were 568 genes showing reduced expression and 317 showing increased expression compared to the parent (PA). Of these datasets, 547 were commonly down-regulated by both PAdel and PAnfxC with 278 commonly up-regulated. Figure 4-2 shows the similarities in gene expression between PAdel and PAnfxC, whereby differentiation between the two strains was indiscernible according to phylogenetic analysis.

Similar to previous reports of nfxC phenotypic mutants, genes overexpressed in PAdel/PAnfxC included the *mexEF* operon, *mexS* and genes involved with ABC transporters. Down regulated genes included the nitrate respiratory chain and phenazine, rhlamnolipid and hydrogen cyanide production (Tian et al., 2009b, Kohler et al., 2001, Llanes et al., 2011, Uwate et al., 2013, Maseda et al., 2010). New genes implicated by the 8-bp deletion were also identified. These up-regulated genes controlled iron transport, adaption to toxic substances and translation (Figure 4-2 and 4-4). Genes linked to motility, cell adhesion, chemotaxis, oxidative stress and metabolism were down-regulated (Figure 4-2 and 4-5).

Changes between the single and double copy of the of 8-bp sequence in

mexT causes a frame shift. The gene could start in the same place in all *mexT*

variants and finish out of frame or the genes could start in different places

in PA and PAdel/PAnfxC and finish in the same frame. To align raw reads

against the genome, multiple alignment programs were used. All indicated

a dip in expression at position 280700 bp, just before the site of the 8-bp

sequence (Figure 4-3). While it was not entirely clear that the dip in

expression measured by the read alignments was a result of the frame shift

mutation, it was evident that this was not an artefact since the expression

profile of PA still contained the first expression peak, symmetrical to PAdel

and PAnfxC.

Blast analysis revealed that the deletion of the 8-bp sequence in PAdel and

PAnfxC abolished the HTH in *P. aeruginosa* and activated the *lysR* region.

This suggested that the double copy of the 8-bp sequence in PA, was a

repressor of the lysR region. Increased expression was noticed at the N-

terminus of *mexT* in all three *mexT* variants. Further analysis of this region

revealed that there was no stop codon or transcriptional start site sequence

present in this region to explain this expression profile. The 8-bp repeat

sequence however showed high GC content; spikes in GC-content can

represent important compositional factors that define different functional

genomic units, particularly transcription boundaries which are a unique

feature for *in silico* gene identification (Yeramian and Jones, 2003, Zhang et

al., 2004). Interestingly this expression profile was also noticed in PA 11451,

with a stop codon present indicating the presence of two genes (data not

shown.
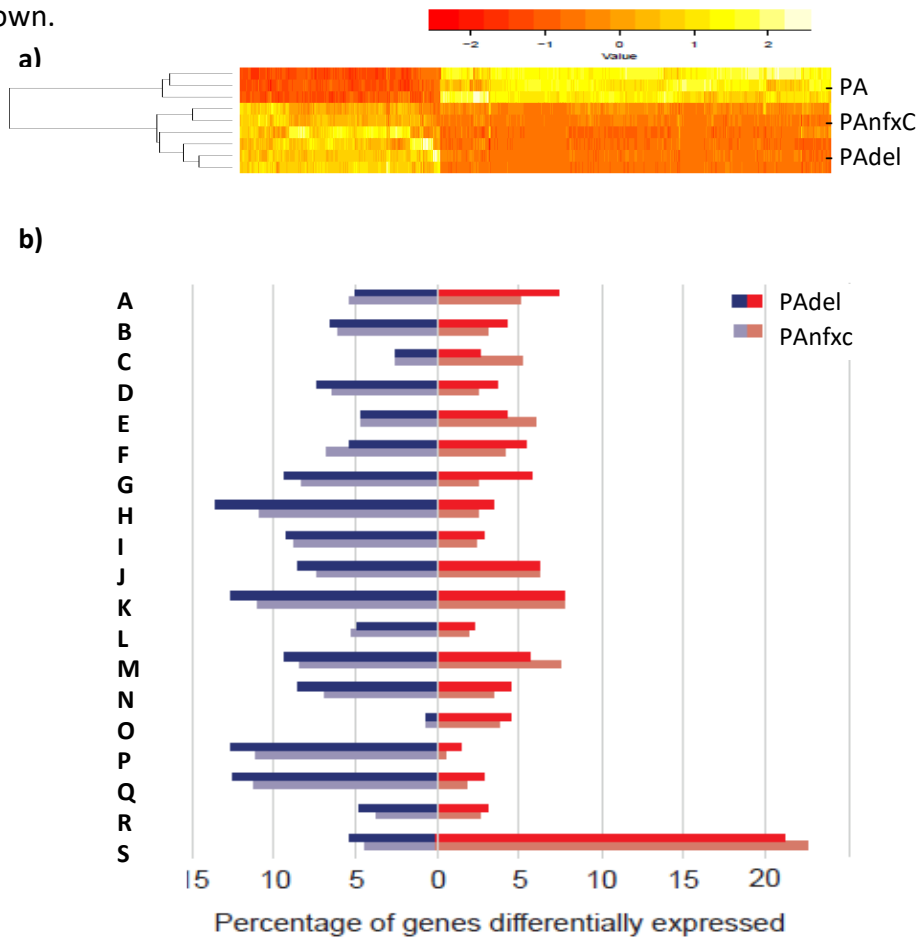
Figure 4-2 Transcriptome results
a) Heat map of the relative expression of genes (RPKM, Reads Per Kilobase of transcript per Million mapped reads values) in PAdel or PAnfxC compared to PA (n=3). Genes that showed ≥ 2-fold changes in expression were hierarchically clustered. **b)** Genes up-regulated (red) and down-regulated (blue) in PAdel and PAnfxC were categorised according to GO term. Bars indicate the percentage of the genome total for each COG category. COG categories are labelled a follows; A: amino acid transport and metabolism; B: carbohydrate transport and metabolism; C: cell cycle control, cell division, chromosome partitioning; D:cell wall/membrane/envelope biogenesis; E: coenzyme transport and metabolism; F: defence mechanisms; G: energy production and conversion; H: function unknown; I: general function prediction only; J: inorganic ion transport and metabolism; K: intracellular trafficking, secretion, and vesicular transport; L: lipid transport and metabolism; M: nucleotide transport and metabolism; N: post-translational modification, protein turnover, chaperones; O: replication, recombination and repair; P: secondary metabolites biosynthesis, transport and catabolism; Q: signal transduction mechanisms; R: transcription; S: translation, ribosomal

102
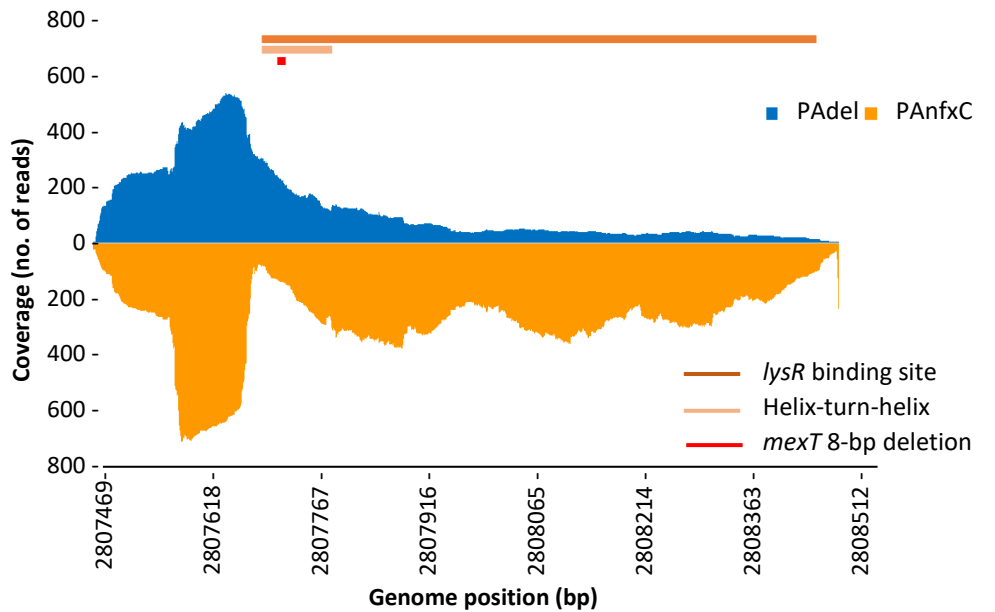
Figure 4-3 Expression of the *mexT* gene in PA and PAdel.
The 8-bp insertion located in the helix-turn helix in PA reduced expression of the *lysR* binding site by 1.7 log2 fold. Two peaks of increased expression in *mexT* of both strains was noticed, the first of which remained unaffected in PA. PAdel and PAnfxC *mexT* expression were similar.

4.3.3 Pathway analysis and metabolic capability of the *mexT* variants

To gain a deeper understanding of the pathways that were differentially regulated between *mexT* variants with the single and double copy of the 8-bp sequence, protein-protein interactions (PPIs) were examined between protein products of all *mexT* influenced genes based on experimental, co-expression, gene fusion and co-occurrence data evidence from the STRING Database33. The PPI network for genes up and down regulated in PAdel are shown in Figure 4-4 and 4-5. The nodes represent proteins and the edges represent the predicted functional associations. A similar method was used to gain an overview of which genes were differently regulated by PAnfxC but

the analysis did not illustrate differences between PAdel and PAnfxC. This may be because although distinct genes were differentially expressed, the regulated pathways may be similar, perhaps due to compensatory mutations.

As expected a subset of genes contributed towards the function of ABC transporters. A large proportion of highly expressed genes in PAdel and PAnfxC were also related to the Ton system (siderophore transport), iron acquisition and heme transport along with sigma and anti-sigma factors associated with these functions (FoxR, FemR, PA4896, PA3410, PA1363). Increased expression of the type III secretion system was also observed along with PQS (pseudomonas quinolone signal) catalytic enzymes. The central gene cluster in Figure 4-4 illustrates the large proportion of genes linked to gene regulation.

Genes down regulated in PAdel compared to PA involved those related to the type II and VI secretion system, pilli assembly, alginate formation and oxidative stress (Figure 4-5).
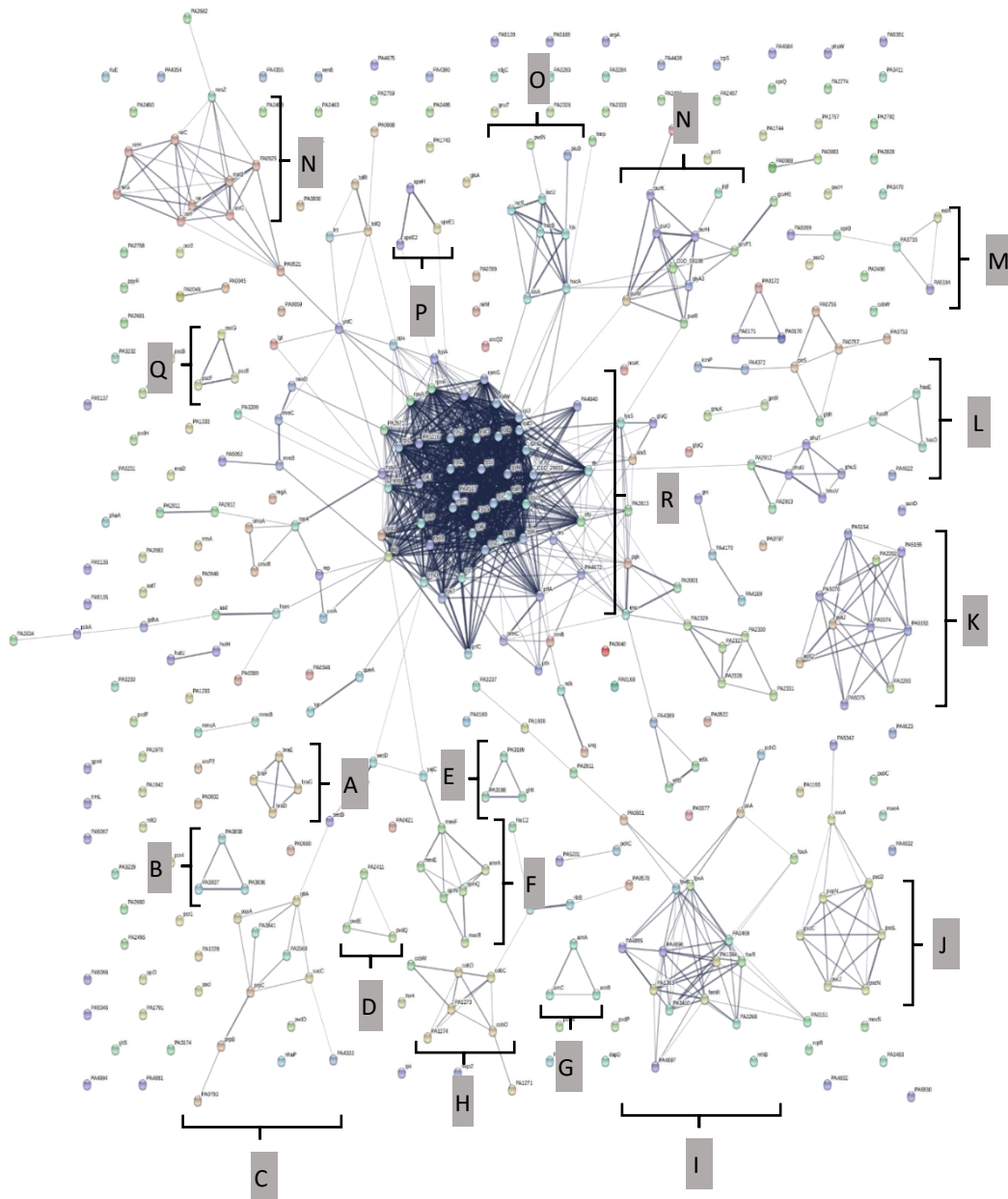
Figure 4-4 Up-regulated genes associated with PAdel

A. Bra group -branched-chain amino acid ABC transporter; Component of the high affinity leucine, isoleucine, valine, transport system (LIV-I), which is operative without Na(+) and is specific for alanine and threonine, in addition to branched-chain amino acids.

B. ABC transporter ATP-binding protein, ABC transporter permease

C. Enzymes related to PQS biosynthetic pathways (methylcitrate synthase, 2-methylisocitrate lyase, citrate synthase, amino acid permease, adenylosuccinate lyase, coenzyme A ligase; formation of anthraniloyl-CoA)

D. Virulence down regulation: Degrades 3-oxo-C12-HSL, one of the two main AHL signal molecules of *P. aeruginosa*, and thereby functions as a quorum quencher, inhibiting the las quorum-sensing system, pyoverdine biosynthesis protein, thioesterase activity

E. ABC sugar transporter permease

F. Antibiotic efflux pump

G. Bi functional enzymes that catalyze the oxidative decarboxylation of UDP-glucuronic acid (UDP-GlcUA) to UDP-4-keto- arabinose (UDP-Ara4O) and the addition of a formyl group to UDP-4-amino-4-deoxy-L-arabinose (UDP-L-Ara4N) to form UDP-L-4-formamido- arabinose (UDP-L-Ara4FN). The modified arabinose is attached to lipid A and is required for resistance to polymyxin and cationic antimicrobial peptides

H. Biosynthesis of corrinoids

I. Iron transport: and sigma factor regulator: ferric pyoverdine receptor, anti-sigma factor, transmembrane sensors, Ferrioxamine receptor, denitrification process

J. Type III secretion apparatus

K. Amino acid (lysine/arginine/ornithine/histidine/octopine) transporter

L. metalloprotease secretion protein and heme uptake

M. Transporters: glucose/carbohydrate outer membrane porin Substrate-selective channel for a variety of different sugars. Involved in the transport of glucose, mannitol, fructose and glycerol (sugars able to support the growth of P.aeruginosa). Facilitates glucose diffusion across the outer membrane

N. purine ribonucleotide biosynthetic process, nucleotide biosynthesis process, glycine biosynthetic processes

O. Iron biding, heat shock proteins

P. Hypothetical: synthesis of the polyamines spermine and spermidine from putrescine

Q. Type III export proteins

R. Gene regulation: 30S and 50 S ribosomal proteins, elongation factors, trigger factors, methyl transferase (translation and termination release factors), bose-phosphate pyrophosphokinase, cell adhesion, type 3 secretion
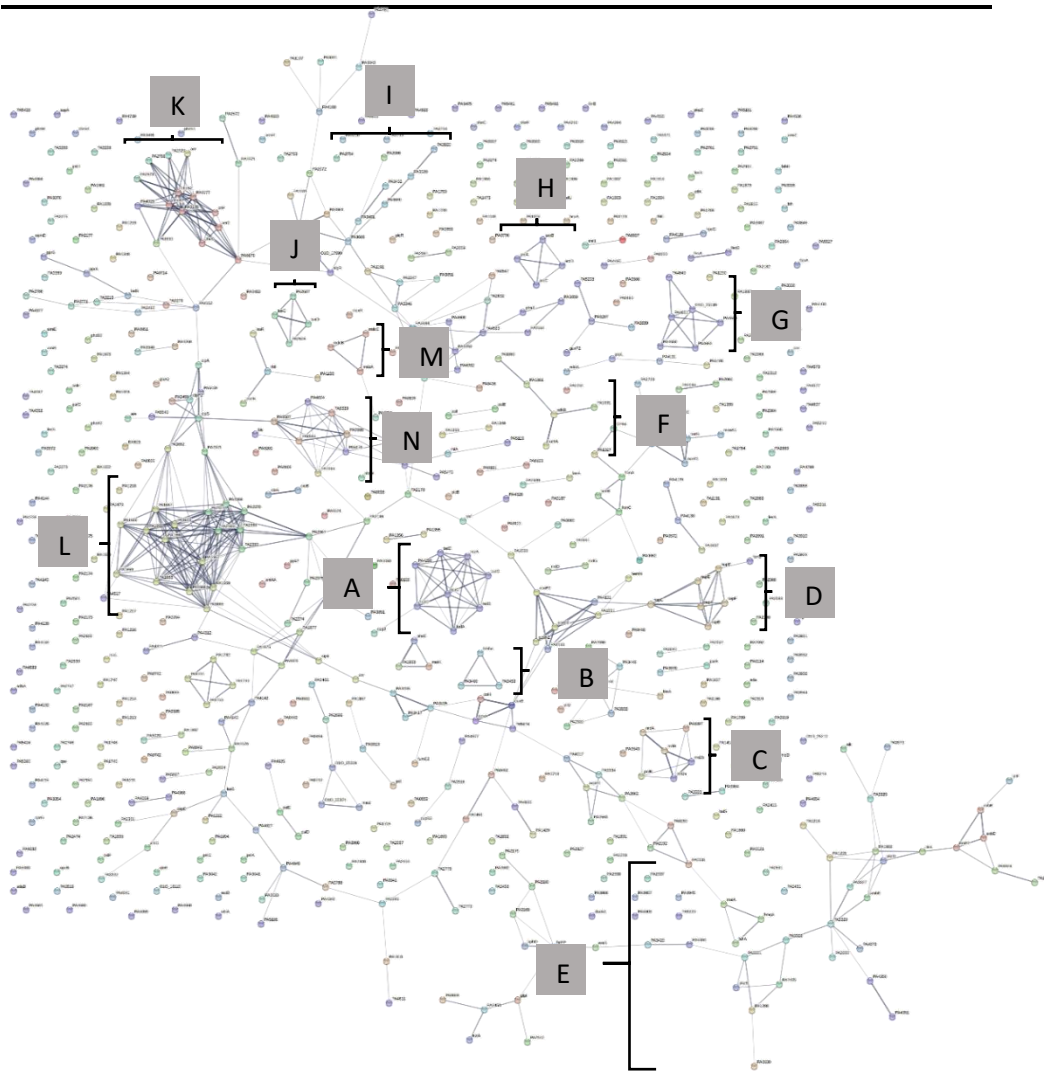
Figure 4-5 Down-regulated gene associations in PAdel

A. Type II secretion system and zinc ion binding

B. Probable glutamine aminotransferase and actyl trasnferase enzymes

C. Anaerobic ribonucleoside triphosphate reductases and cation efflux system protein

D. Nitrate reductase and cytochrome C protein

E. Phytochorme and heme oxygenase, cytochrome C, phenazine production

F. Xanthine dehydrogenase , oxidoreductase

G. Pili assembly

H. Arginine/ ornithine catabolic pathways

I. metal transporting P-type ATPase, epoxide hydrolase, alginate biosynthesis, signal transduction

J. Sulphur transfer

K. Chemotaxis methyltransferase, chemotactic transducers, aerotaxis transducer

L. Protein secetion type VI

M. Malonate metabolism

N. SpoVR like protein, response to oxidative stress

Table 4-1 Up and down regulated pathways in PAdel and PAnfxC (compared to PA).

A detailed view of genes associated with each pathway are shown in Appendix 8.3.4.

Up regulated	Down regulated
Two-component system*	Oxidative phosphorylation†
Purine metabolism†	Bacterial secretion system *
Arginine and proline metabolism *	Biosynthesis of amino acids *
Protein export*	Purine metabolism*
Inter-pathway connection between Pyruvate metabolism and Glyoxylate and dicarboxylate metabolism†	Nitrogen metabolism*
Nitrogen metabolism †	Styrene degradation†
Propanoate metabolism	Aminobenzoate degradation *
Glyoxylate and dicarboxylate metabolism†	Tyrosine metabolism†
Pyruvate metabolism*	Sulphur metabolism *
Inter-pathway connection between Citrate cycle (TCA cycle) and Alanine, aspartate and glutamate metabolism†	Pyruvate metabolism *
Glycine, serine and threonine metabolism [N]	Arginine and proline metabolism [N]
Catalytic complex [N]	Citrate cycle (TCA cycle) [N]
One carbon pool by folate [N]	Glycolysis / Gluconeogenesis [N]
Methane metabolism [N]	
Aminoacyl-tRNA biosynthesis [N]	
Cysteine and methionine metabolism [N]	

Pathways present in *PAdel and PAnfxC, † PAdel only and [N] PAnfxC only.

Pathway analysis (Table 4-1 and Figure 4-6) revealed that deletion of one of the 8-bp sequences had a genome wide effect on the metabolic network of the cell. Genes involved in protein and amino acid metabolism were up regulated in both variants with the single copy of the 8-bp sequence. Down regulated pathways were associated with the bacterial secretion system, amino acid biosynthesis and purine and sulphur metabolism. Differences between PAdel and PAnfxC were few but included those related to folate, tRNA, specific amino acid transport, styrene metabolism and reactions within glycolysis and the TCA (tricarboxylic acid cycle). While STRING analysis can be ideal for identifying differences in pathways the analysis provides an output of the top 10 enriched pathways which is likely to exclude other pathways of interest. Pathway analysis also showed that pyruvate, arginine, proline and nitrogen metabolism were both up and down regulated. Indeed these pathways maybe be differentially regulated, however it is difficult to determine which specific metabolites and bio-reactions within a pathway were differentially expressed.

Figure 4-6 Cell overview of genes differentially regulated by PA and PAdel

Each node in the diagram (such as the small circles and triangles) represents a single metabolite or protein, with each blue line representing a single bioreaction. Catabolic pathways (on the right) are separated from pathways of anabolism and intermediary metabolism (on the left) by the pathways representing glycolysis and tricarboyxylic acid (TCA) cycle. Reactions of small-molecule metabolism that have not been assigned to any pathway have been omitted from the above diagram. Periplasmic pathways and reactions are shown on the right side in between the two membranes. Bioreactions where the difference in expression between PA and PAdel was greater than 1 log2 fold (2) or less than -1 log2 fold (0.5) are shown. Genes down regulated in PAdel are indicated in red and genes up-regulated in purple.
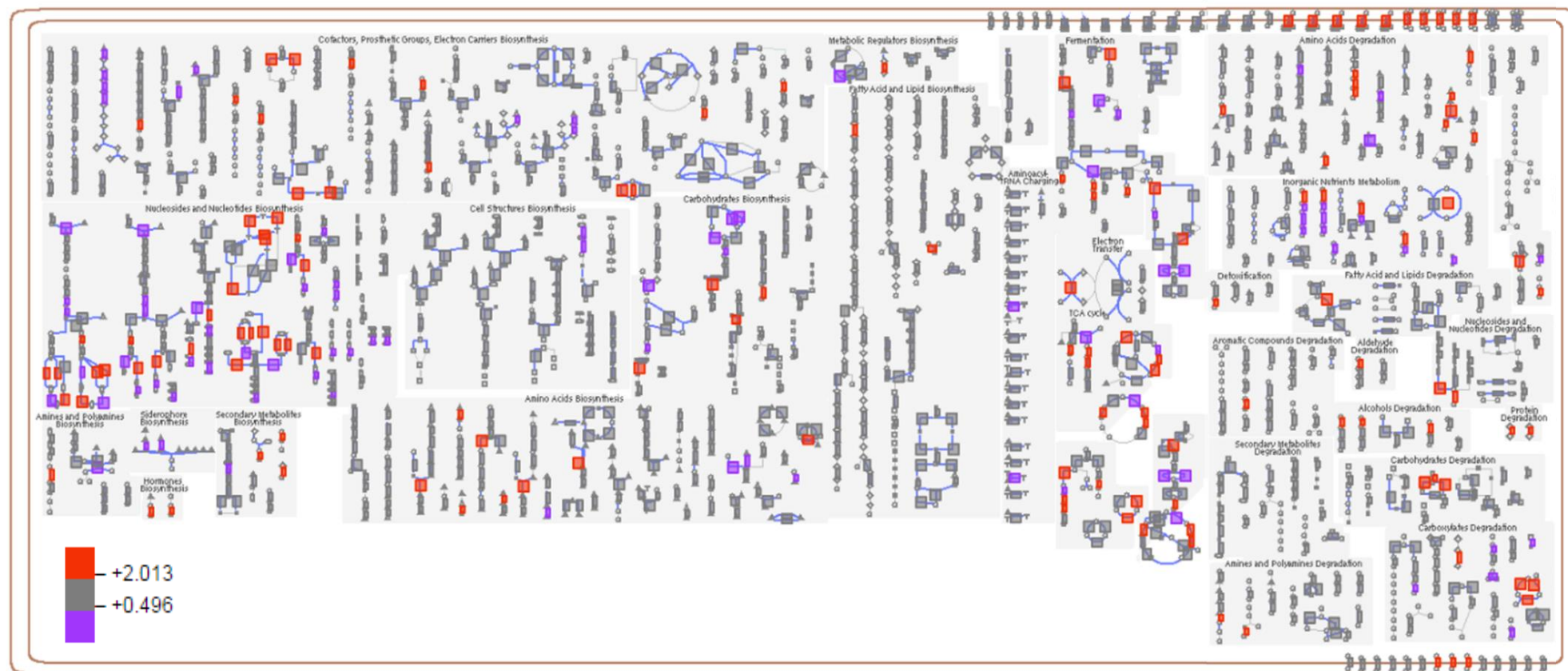
4.4 Discussion

The gene *mexT* is a key regulator of the *mexEF* pump and as such the *mexT* 8-bp deletion has been the foundation for much research in terms of antibiotic resistance and virulence. Sequence variants were identifed: the double copy of the 8-bp sequence (PA), found in most strains of PAO1 and the single copy of the 8-bp sequence (PAdel and PAnfxC) which was found in most clinical isolates. Each appears to be adapted to a very different environment (please see discussion in chapter 3). While nfxC mutants such as PT149 (a derivative of PAO1 selected through antibiotic resistance) are known to harbour an 8-bp deletion it is unclear whether any additional mutations had been selected for aside of the 8-bp sequence without WGS evidence, especially since this strain has been passed between researchers worldwide, a known cause of genetic diversity (Klockgether et al., 2010). To understand the genome wide molecular impact of the deletion, of one copy of the 8-bp sequence, whole genome DNA and RNA sequencing was performed. Transcriptome analysis provided greater insight into the *mexT* regulon and expression of *mexT* itself. The role of the *mexT* 8-bp deletion exceeds that of antibiotic resistance and virulence. Identifying targets other than the *mexEF-oprN*, which may be in high demand in natural environments and known to promote the nfxC phenotype was therefore deemed important.

WGS of the *mexT* variants revealed non-synonymous mutations in known mutational hotspots (Klockgether et al., 2010, Dötsch et al., 2009). As expected, PAnfxC, a strain naturally selected for in the presence of antibiotics contained more mutations compared to PAdel. It would seem that the PA4684 and PA4685 operon were sites of compensatory mutations in strains with a *mexT* 8-bp deletion (P<0.05). While the functions of these genes were unknown it is likely that these mutations caused the phenotypic differences between PAdel and PAnfxC. Despite these mutations, the transcriptome of PAdel and PAnfxC were very similar with 547 genes commonly up regulated by both PA and PAnfxC and 278 commonly down regulated.

Mutants with the nfxC phenotype and *mexT* 8-bp deletion are deemed to have an active *mexT*, since the MexEF-OprN efflux system is over expressed (Maseda et al., 2000, Tian et al., 2009b, Kumar and Schweizer, 2011, Kohler et al., 2001). Contrary to other studies (Köhler et al., 1999, Olivares et al., 2014), this study shows that the transcriptional levels of *mexT* in PAdel and PAnfxC were not comparable to those of the wild type (Olivares et al., 2012). PAdel and PAnfxC displayed increased expression of *mexT* by 1.2 log 2 fold compared to PA. Although the *lysR* region (identified through sequence alignment) was inactive in PA, this study shows that the N-terminus was still active suggesting that *mexT* may actually be functional in the wild type (Figure 4-3). Furthermore the number of genes exhibiting reduced expression (11.7%) was nearly two times more than those displaying

increased expression (6.8%) in PAdel and PAnfxC (Figure 4-2). A set of genes differentially expressed in an nfxC mutant and its isogenic mutant overexpressing MexT (Tian et al., 2009a) were also analysed. It was found that 50.5% of the genes mentioned by Tian (2009a) showed no difference in expression between PA and PAdel (O'Gara et al.). These results show that although the 8-bp insert prevents expression of the *mexEF* pump it does not in fact render m*exT* inactive in PA.

Protein family analysis revealed that the deletion of the 8-bp sequence abolishes the HTH that lies within the lysR region of PAdel. The consequential activation of the *lysR* domain was reflected in the expression of genes pertaining to gene activation (30S and 50S ribosomal proteins, elongation factors, trigger factors). In PA, it is clear that the double copy of the 8-bp sequence acts as a repressor; an intact HTH reduces expression of the *mexT* lysR region. In line with previous research on LTTRs and if the HTH is considered the site of another gene (as indicated by the increase in gene expression within this region of *mexT*), the HTH in *mexT* is located 66 amino acids from the N terminus, indicative of a repressor with auto regulative functions (Maddocks and Oyston, 2008).

Since two peaks of expression across *mexT* was observed it is hypothesised that *mexT* consists of two entities. While it unclear what effect this has on *mexT* gene regulation, a GC spike found in the region of the 8-bp sequence may have a bi regulative function (Yeramian and Jones, 2003, Zhang et al.,

2004. RNA-seq analysis also revealed that the *mexT* binding site consensus sequence (Tian et al., 2009a, Köhler et al., 1999) was identified solely in the mexT-*mexEF* intergenic region and could not be used to identify *mexT* dependent genes.

Co-factors have the ability to modify the LysR-type regulator protein conformation resulting in numerous protein targets with the ability to act as an activator or repressor (Maddocks and Oyston, 2008). MexT may also bind to a modified binding site under different conditions whereby different co-factors modify the conformation of the LTTR causing the protein to bind to different targets depending on the conformation. To date the co-factor(s) of MexT have not been identified. Differences in phenotypic microarray substrates in chapter 3 may provide some insight into this. Studies have previously shown that small repeated genomic sequences (e.g. miniature inverted-repeat transposable elements (MITEs), repetitive extragenic palindromic (REP) sequences have the potential to fold into secondary structures at the DNA and or RNA level whereby gene expression is regulated (Croucher et al., 2011). Repeated sequences have varied roles in bacterial cell physiology and cell-host interactions. MITEs for instance inactivate genes via insertions within a protein coding sequence (Delihas, 2011). The 8-bp duplicated sequence in *mexT* is located on a helix-turn-helix ensuring access to transcriptional regulators (Aravind et al., 2005). Perhaps the 8-bp insertion forms a hairpin loop which exerts a supercoiling effect on the helix-turn-helix. Differences in sigma factor expression (*algU* and iron scavenging

genes) and small RNAs were also found between strains harbouring the double and single copy of the 8-bp sequence, which may have had differential effects as a global regulator.

Variants with the single copy of the m*exT* 8-bp sequence showed increased resistance to ciprofloxacin and chloramphenicol, indicative of overexpression of the MexEF pump (Llanes et al., 2011, Li et al., 1994) which, in turn, reduces expression of the carbapenem-specific OprD porin protein (Ochs et al., 1999, Livermore, 1992) thus endowing the mutant strains with reduced susceptibility to meropenem.

We also observed increased susceptibility to gentamicin and pipercillin, as previously reported (Köhler et al., 1999, Kohler et al., 1997). β-lactam hyper susceptibility in *nfxC*-type mutant cells is caused by MexT-mediated cancellation of C4-HSL-mediated enhancement of *MexAB-OprM* expression (Maseda et al., 2004). In this study however, no significant change in *mexAB* expression was found between strains which may explain why the MIC of ceftazidime remained the same; MexAB activity is associated with ceftazidime resistance (Du et al., 2010). It is not clear why piperacillin, also a beta lactam remained affected. It is possible that there may be other mechanisms of resistance against β-lactams, which may work in concert in these strains.

Reduced virulence factor production and swarming is a phenotype commonly seen in strains with a non-functional *mexT* (Luong et al., 2014,

Olivas et al., 2012). Overproduction of *MexEF–OprN* correlates with reduced C$_4$-HSL concentrations, controlled by the *las* and *rhl* quorum sensing systems (Kohler et al., 2001). This study showed reduced expression of all genes in the *las* and *rhl* operon in PAdel and PAnfxc, except *rhlG* and *las*). This would explain the reduced swimming, swarming and virulence observed in these strains (Kohler et al., 2000, Kohler et al., 2001). *RhlG* does not affect C4-HSL production (Campos-Garcia et al., 1998) but it was not clear why *lasI* expression remained the same in all *mexT* variants. Type III and VI secretion in nfxC mutants are known to be reduced (Olivares et al., 2012, Jin et al., 2011). The work here shows that this was not the case. Type III secretion was increased in PAdel and PAnfxC with type II secretion also increased in PAdel. Reduced PQS production is associated with increased *mexEF* expression (Tian et al., 2009a). In previous studies, reduced virulence factor production in nfxC mutants was linked to reduced levels of intracellular PQS, due to extrusion of HHQ (4-hydroxy-2-heptylquinoline) though the pump or reduced amounts of its metabolic precursor, kynurenine (via the anthrialnte pathway). Genes related to the PQS operon (*pqsB, pqsC, pqsD and pqsE*) in this study were not significantly different in PA and PAdel/PAnfxC, apart from *pqsA* which actually showed a twofold increase in expression in PAdel and PAnfxC (P< 0.05). Chapter 3 revealed a threefold reduction in tryptophan utilization (Biolog results from chapter3), a known precursor of PQS synthesis yet no differences were found in expression of genes encoding anthranilate synthases *(trpEG, phnAB, kyn)* (Knoten et al., 2014, Palmer et

al., 2013). It is speculated that since *mexAB-oprM*, the majority of the *pqs* operon genes and genes encoding typtophan degradation are not differently expressed between *mexT* variants, reduced virulence and motility in PA is not due to quorum sensing specific genes but instead quorum sensing regulatory pathways associated with *lasR* and genes in the phenazine operon (which are down regulated) (Dietrich et al., 2006).

Transcriptome analysis revealed the reduced expression of genes in the *alg* operon (*algZ, algR, algA, algB)*, *che* operon (*cheB, cheY*), *mcpA, wspA* (*wspR, wspD, wspF, wspC, wspE, wspb* > 1.5 fold difference) and *pil* operon (*pilU, pilM*). These genes affect alginate production (Baynham et al., 1999), flagella assembly and polysaccharide production. Genes regulating chemotaxis (*cheB* and *mcpA)* (Ferrandez et al., 2002, Garcia-Fontana et al., 2014) and phosphodiesterase activity and hence motility (McCarter and Gomelsky, 2015) were also down regulated. Perhaps these traits are the reason for the reduced virulence and motility traits reported in *mexT* mutants (Lamarche and Deziel, 2011, Kohler et al., 2001).

Figure 4-6 reflects the effects of the 8-bp deletion across various metabolic pathways. Phenotypic microarray results from Chapter 3 showed that PAdel and PAnfxC were defective in protein, amino acid, nucleoside, sugar, carboxylic acid and phosphorus based compound metabolism. Overexpression of *mexEF-oprN* in PAdel is linked to decreased amounts of the outer membrane OprD porin (Ochs et al., 1999), an important

mechanism which prevents transport of amino acids, proteins and drugs. A 0.8 log2 fold difference in *oprD* expression between PAdel and PAnfxC compared to PA was observed. RNA-seq data additionally showed that within the *bra* (branched-chain amino acid transport protein) operon, two integral membrane proteins (BraD and BraE) and two ATP-binding proteins (BraF and BraG) expected to be part of the LIV (leucine, isoleucine, valine, alanine, threonine, and possibly serine) transport system were highly expressed in PAdel and PAnfxC (Hoshino et al., 1992, Adams et al., 1990, Hosie et al., 2002). In agreement, reduced growth of PAdel and PAnfxC was observed in the presence of L-valine, isoleucine (plate 3 but not2) and L-serine (plate1 but not 3).

Glycolysis and the TCA cycle, key components of central metabolism were deferentially regulated by the *mexT* variants. It would seem that although variants with the 8-bp deletion were associated with a metabolic burden, PAdel and PAnfxC were more capable of metabolizing methyl pyruvate. In contrast PA3416 and PA3417 which are associated with pyruvate decarboxylation (to acetyl CoA) were up regulated in PA. Various other discrepancies were observed. For instance, although PAdel and PAnfxC showed reduced growth on carboxylic acids the *mqo* gene responsible for the oxidation of malate to oxaloacetate was up regulated. These discrepancies represent the need for improved methods to identify specific bioreactions within pathways that are differentially altered, an issue that was previously highlighted in Table 4-1.

In Chapter 3 it was shown that nucleoside media did not support the growth of the *mexT* mutants (PAdel and PAnfxC) and this result was corroborated by the reduced expression of genes regulating purine metabolism (*xdhA, xdhB*) inosine, guanosine and adenosine biosynthesis (*purB, purH, spuA, nrdD, nrdB, ndk, dut*).

Another function of ABC (ATP-binding cassette) transporters is the related uptake of iron. (Koster, 2001, Brillet et al., 2012, Danese et al., 2004). This was a prominent feature observed in the 8-bp deleted mutants whereby genes associated with the Ton family, heme uptake and associated sigma factors were highly expressed in mutants with the 8-bp deletion.

It is thought that mutants with the single copy of the 8-bp sequence are adapted to anaerobic environments as elements of the nitrate respiratory chain were deferentially regulated (Olivares et al., 2012, Olivares et al., 2014). In this study, nitrate to nitrite conversion was down regulated by genes not only belonging to the *nar* but also *nap* operon whereas genes converting nitrite to nitrogen such as those involving the *nir* and *nos* operon were highly expressed. One study hypothesized that the increased oxygen consumption rate of nfxC mutants in aerobic conditions may actually lead to a decrease in environmental oxygen in cultures, thus enabling cells to sense this environmental change and activate the nitrate respiratory chain to prevent the deleterious effect associated with overexpression of MexEF-OprN (Olivares et al., 2014). This is interesting since genes down regulated

119

by the *mexT* mutants in this study involved those related to oxidative stress,

superoxide radical degradation and cytochrome C (*cco* and *cox* operon), key

regulators of aerobic respiration.

4.5   Conclusion

Different opinions have been expressed as to whether strains containing one or two copies of the 8-bp sequence in *mexT* are "wild types" or "mutants". Although PA is the parent in this study, it would seem incongruous that a strain would arise where functionality is blocked in the first instance. Transcriptome analysis indicated that *mexT* is actually an auto regulative repressor rather than an activator with an interesting expression profile suggesting that *mexT* may actually consist of two regulatory elements. It was also shown that the 8-bp insertion does not inactivate *mexT*. A comprehensive list of differentially expressed genes were also identified, that contributed towards the phenotype of PAdel and PAnfxC, acknowledging differences between strains as the result of compensatory mutations. Results also indicated that the majority of proteins are interconnected using String analysis. This could explain how the regulation of distinct genes in multiple pathways may have a similar phenotypic effect, if they act on a similar set of genes in key pathways in PAdel and PAnfxC. This chapter has defined the link between the 8-bp sequence and antibiotic resistance, motility, virulence and metabolism through gene expression networks. Cellular processes are regulated by complex networks of functionally interacting genes. Differential activity of genes in these networks largely determines the state of the cell and cellular phenotypes.

Understanding these processes using metabolic reconstruction will allow

assessment of the impact of such strains in clinical environments.

5 Genome scale metabolic reconstruction of *Pseudomonas aeruginosa*

5.1 Introduction

The metabolic versatility of *P. aeruginosa* and its ability to thrive in a range of natural environments renders the systemic study of this microorganism crucial to the understanding of it's flexibile nature. Chapter 3 and 4 showed that there were differences in the metabolic capability of *P. aeruginosa* based on a genomic 8-bp sequence difference. Phenotypic results showed that growth on nucleosides, amino-acids and peptides were not supported. Transcriptomic data showed that there were more down-regulated genes than there were up-regulated genes relating to metabolism in an array of metabolic sub-systems. Unravelling the myriad of systems and pathways that contribute towards phenotype and disease is one of the most important applications. In order to elucidate the basic principles of metabolic versatility and identify the differences in pathways between PA and PAdel, a genome-scale reconstruction is required.

The combination of genomic data with biochemical knowledge leads to the generation of genome scale metabolic network models. With the aid of experimental phenotypic data and computational analysis these models allow the exploration and prediction of physiological responses in context of defined environments and genetic constraints (Heinemann et al., 2005, Oberhardt et al., 2010, Oberhardt et al., 2008). These models have

previously been successfully implemented and yielded clinically relevant results. Examples include drug target discovery, early diagnosis of diseased phenotypes and the metabolic engineering of cells to enable the production of metabolites of industrial interest (Beste et al., 2007, Jamshidi and Palsson, 2007, Triana et al., 2014, Bro et al., 2006, Bordbar and Palsson, 2012).

The availability of sequenced genomes has greatly improved over the years along with the continuous and updated annotation of genes. The first genome-scale metabolic reconstruction of *P. aeruginosa* PAO1 accounted for 1056 genes, 1030 proteins and 883 reactions. The model was tested against Biolog PM and genome scale transposon knockout data and led to the re-annotation of several open reading frames. These metabolic models allow the prediction of a microbe's entire metabolic map, starting with the whole genome sequence (Cuevas et al., 2016). This is the first step in the metabolic reconstruction process, creating a draft model. Assembled genome sequences can be annotated by software such as Rapid Annotation Subsystem Technology (RAST), PROKKA, BG7, Blast2Go and BASys (Aziz et al., 2008, Overbeek et al., 2014, Seemann, 2014, Tobes et al., 2015, Conesa et al., 2005, Van Domselaar et al., 2005). Protein and RNA encoding genes are assigned functional roles along with Enzyme Commission numbers (E.C.), in doing so functional roles are associated to enzymes and then to reactions. The cofactors specific to each enzyme are also annotated. Unknown cofactors are annotated as standard cofactors (e.g. NAD+) which can lead to

inaccuracies in the model (Cuevas et al., 2016, Henry et al., 2010). These connections can be obtained from public resources such as EXPASY, the KEGG dataset, MetaCyc and BRENDA (Gasteiger et al., 2003, Kanehisa et al., 2004, Caspi et al., 2014, Schomburg et al., 2002).

The draft model which consists of a list of reaction equations, compounds and compartments is then converted to a stoichiometric matrix. This is also known as constraint based modelling as this matrix only contains reactions and associated metabolites present within the model. In doing so, the boundaries and feasible space which contribute towards phenotype are defined (Cuevas et al., 2016).

Predicting the phenotypic response and fluxes through a reaction in a metabolic network allow the confirmation of biochemical reactions. Confirmation of complete biochemical reactions present within a microorganism and prediction of a phenotypic response requires phenotypic, transcriptomic, proteomic, fluxomic, taxonomic, or metagenomic verification (Fondi and Liò, 2015). These results are then applied along with constraint based modelling, to predict the fluxes through a reaction in a process called flux balance analysis (FBA). The processes involved in metabolic reconstruction are outlined in Figure 5-1.

FBA is the linear programming technique that uses metabolic models to simulate growth and predict the phenotypic response imposed by environmental factors. Cell growth is simulated by estimating ATP

consumption and biomass (e.g. amino acids, lipids, nucleotides and cofactors) whereby the product of a biomass reaction is one gram of biomass (Henry et al., 2010). FBA and growth simulation are performed using defined media compositions which act as another form of constraint set upon the model (Cuevas et al., 2016).

ASSEMBLED GENOME
▼
ANNOTATION SERVER
RAST, metaSHARK, AUTOGRAPH
▼
PRELIMINARY MODEL
Model SEED, SuBliMinaL Toolbox
▼
MODEL REFINEMENT
Gap-filling and removal/addition of reactions from the model
▼
DRAFT RECONSTRUCTION MODEL
▼
FBA ◄ **Phenomic data**
(OptFlux,
MeaNetX, RAVEN,
COBRA,
▼
REFINED MODEL
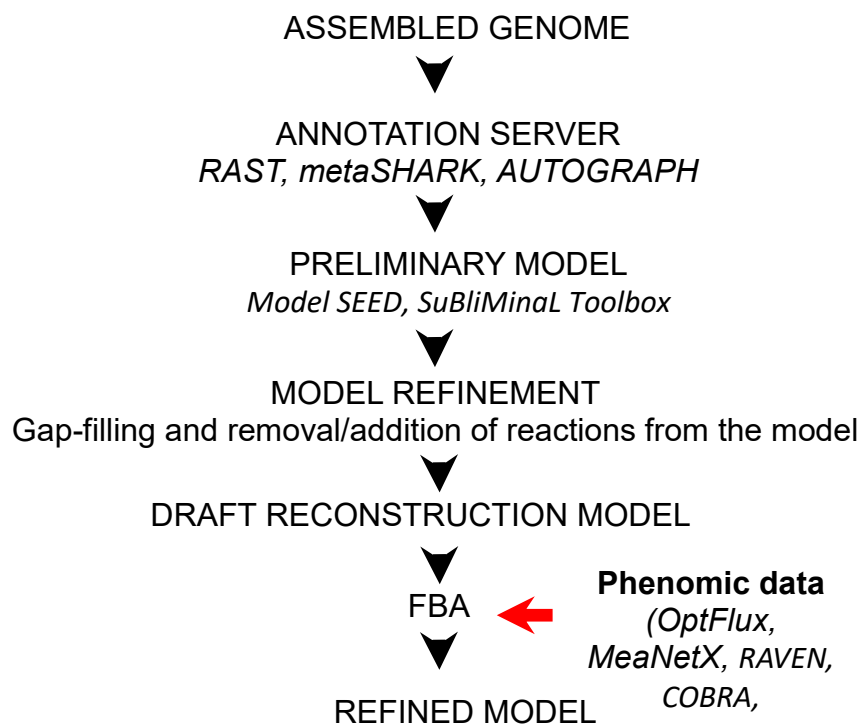
Figure 5-1 Metabolic Reconstruction pipeline and programs available
The genome sequence is first annotated using RAST, metaSHARK or AUTOGRAPH. The annotated sequence can then be imported into *Model SEED or SuBliMinaL Toolbox*. A preliminary metabolic model is generated using annotated genes and reactions. The model is then refined, by adding additional missing or mis-annotated reactions to create a draft reconstruction. FBA is then used to simulate biomass and link phenotype predictions. Further refinement of the model leads to fitting phenomic data such as Biolog PM and/or transcriptomic data into the model.

In this study the aim was to identify the differences in the metabolic capability of PA and PAdel by incorporating genotypic and phenotypic data. FBA was used to represent metabolic states, leading to the identification of pathways specific to each strain.

5.2 Methods

5.2.1 Genome annotation and curation

Whole genome sequences for PA were assembled using Velvet Optimser and submitted as FASTA sequences into RAST (http://rast.nmpdr.org/), using the below parameters listed in Table 5.1. The automatic process can run into problems such as gene candidates that overlap RNAs, or genes that are embedded within genes. These issues are automatically corrected by RAST, by the deletion of gene candidates. The pipeline also involved fixing frameshifts and blasting large gaps for missing genes to prevent errors. Protein encoding genes were identified and assigned functions based on FIGfams/kmers. Upon completion, the RAST-annotated genome was automatically imported into Model SEED (http://modelseed.org/) to perform preliminary reconstructions.

Table 5-1 RAST annotation settings

Settings	
RAST annotation scheme	Classic RAST
Gene caller	RASt
FIGfam (protein family) version	Release70
Automatically fix error	Yes
Fix frameshifts	Yes
Backfill gaps	Yes
Reference genome	PAO1 GenBank accession no. NC002516.2
Verbosity level	0

5.2.2   Preliminary reconstruction

In this study, RAST was used to generate annotations and connect biochemical reactions to E.C. numbers, encoded by Model SEED. Model SEED underlies the RAST platform as a single database and both of these publically available sources are frequently updated. While EC numbers are not capable of covering all reactions, using a single database platform was useful in preventing errors in the reconstruction process since they use the same annotation conventions and nomenclature and are therefore more consistent (Cuevas et al., 2016).

In Model Seed preliminary reconstructions were performed. Out of 190 carbon sources available on the Biolog PM plates, 159 were available on Model SEED (listed in Table 5.2). Preliminary reconstructions were carried out only on carbon sources that PA was capable of utilising, based on Biolog PM results. To identify these carbon sources, an arbitrary cut-off was applied. To identify growth on a substrate, the signal value (SV) had to be greater than half of the maximum signal value for any substrate in that PM plate. For instance in PM 1 the highest SV produced was 261.58. Therefore any substrate that had a signal value greater than 130.79 (half of 261.58) was categorized as showing growth. The maximum SV in PM2 was 228.67 therefore the cut-off for growth of substrates in PM2 was 114.33. Substrates

categorized as showing growth were assigned a value of 1 and are listed in Table 5.2 as 'Observed growth'.

Each reconstruction consisted of a reaction network with gene-protein-reaction-enzyme associations, predicting Gibbs free energy for organism specific biomass reactions involving cofactors, lipids, proteins, DNA, RNA and cell wall components. Biomass was predicted using the Biomass Composition Reaction (BCR) where the quantity of all metabolite molecules required to generate 1 g of biomass was calculated. The small metabolite molecules that contributed towards biomass varied depending upon the metabolic pathways present in the model (e.g bacterial cell wall type and electron transport chain). Each metabolite was associated with a specific condition that had to be satisfied if the metabolite was to be included in the model. Since some metabolites were universal they were included in all models (e.g. nucleotides and amino acids). Some, however were only included in the model if the genome annotation included evidence for the functional role associated with the utilisation and synthesis of that metabolite (Henry et al., 2010).

5.2.3   Merging the preliminary reconstruction models

Once reconstructions for each substrate were complete, the models were merged into a single one using a Java script. This merged model represented all reactions and compartments relative to the genome and PM carbon

sources. This process can incur inconsistencies such as those relating to unbalanced reactions which can lead to the false synthesis of ATP or protons (Thiele and Palsson, 2010). The merged model was therefore also validated using the Systems Biology Markup Language (SBML) validator (http://sbml.org/validator/). Unbalanced reactions or those causing errors were removed.

5.2.4 Simulating multiple growth phenotypes using FBA

The annotated genome from RAST and the merged model were then imported into K-base (https://kbase.us/). The merged model was imported as a "FBA model" in a SBML format. The biomass reaction identifier was called "Biomass0" since this was reserved as the identifier used to represent biomass in the model. Media compositions representing PM carbon sources were imported from the "Public" K-base database. Phenotypic data was also imported as a "Phenotype set" in a tab-separated value format. This file consisted of identifiers for each carbon media composition and a phenotype consisting of either 1 (growth) or 0 (no growth) based on the cut-off previously described. Table 5-2 illustrates the file used to import the Phenotype dataset.

The simulation of growth phenotype was performed in a set of media conditions. The draft metabolic model was therefore curated using PM growth in specific media conditions allowing the identification of differences

between growth predictions and experimental PM growth. This was performed to test the accuracy of the draft model in replicating experimental phenotypes. Growth of the model was simulated using FBA for each media composition in the phenotype dataset (Table 5-2). The lower bounds of exchange reactions were set to -1000 mmol $g^{-1} \times h^{-1}$, to mimic non-limiting conditions. The model was subjected to gap filling to allow some reconciliation of the model with PM data.

Table 5-2 Phenotype data set imported into K-base

Gene knockout (geneko) referred to a list of genes knocked out. Since the parent (PA) was being studied here, this was left blank. Workspace information or medilaws included the workspace narrative details used to import media compositions. Additional compounds and their workspace ID could also be added alongside primary media formulations if required. Observed growth indicated growth using PM microarrays results after applying the cut-off.

Geneko	Mediaws	Media	Additional compounds	Observed growth
	annapaula:1471110739173	Carbon-1-2-Propanediol		0
	annapaula:1471110739173	Carbon-2-3-Butanediol		0
	annapaula:1471110739173	Carbon-2-3-Butanone		0
	annapaula:1471110739173	Carbon-2-Deoxy-Adenosine		0
	annapaula:1471110739173	Carbon-2-Deoxy-D-Ribose		0
	annapaula:1471110739173	Carbon-2-Hydroxy-Benzoic-Acid		0
	annapaula:1471110739173	Carbon-3-Hydroxy-2-Butanone		0
	annapaula:1471110739173	Carbon-4-Hydroxy-Benzoic-Acid		1
	annapaula:1471110739173	Carbon-4-Hydroxy-L-Proline-trans		1
	annapaula:1471110739173	Carbon-a-D-Glucose		1
	annapaula:1471110739173	Carbon-a-D-Lactose		0
	annapaula:1471110739173	Carbon-a-Hydroxy-Butyric-Acid		0
	annapaula:1471110739173	Carbon-a-Keto-Butyric-Acid		0
	annapaula:1471110739173	Carbon-a-Keto-Glutaric-Acid		1
	annapaula:1471110739173	Carbon-a-Keto-Valeric-Acid		0
	annapaula:1471110739173	Carbon-a-Methyl-D-Galactoside		0
	annapaula:1471110739173	Carbon-a-Methyl-D-Glucoside		0
	annapaula:1471110739173	Carbon-Acetamide		0
	annapaula:1471110739173	Carbon-Acetic-Acid		1

annapaula:1471110739173	Carbon-Acetoacetic-Acid	0
annapaula:1471110739173	Carbon-Adenosine	0
annapaula:1471110739173	Carbon-Adonitol	0
annapaula:1471110739173	Carbon-Amygdalin	0
annapaula:1471110739173	Carbon-Arbutin	0
annapaula:1471110739173	Carbon-b-D-Allose	0
annapaula:1471110739173	Carbon-b-Hydroxy-Butyric-Acid	1
annapaula:1471110739173	Carbon-b-Methyl-D-Galactoside	0
annapaula:1471110739173	Carbon-b-Methyl-D-Glucoside	0
annapaula:1471110739173	Carbon-b-Phenylethylamine	0
annapaula:1471110739173	Carbon-Butylamine-sec	0
annapaula:1471110739173	Carbon-Butyric-Acid	1
annapaula:1471110739173	Carbon-Capric-Acid	0
annapaula:1471110739173	Carbon-Caproic-Acid	1
annapaula:1471110739173	Carbon-Chondroitin-Sulfate-C	0
annapaula:1471110739173	Carbon-Citraconic-Acid	0
annapaula:1471110739173	Carbon-Citric-Acid	1
annapaula:1471110739173	Carbon-D-Alanine	1
annapaula:1471110739173	Carbon-d-Amino-Valeric-Acid	1
annapaula:1471110739173	Carbon-D-Arabinose	0
annapaula:1471110739173	Carbon-D-Arabitol	1
annapaula:1471110739173	Carbon-D-Aspartic-Acid	0
annapaula:1471110739173	Carbon-D-Cellobiose	0
annapaula:1471110739173	Carbon-D-Fructose	1
annapaula:1471110739173	Carbon-D-Fructose-6-Phosphate	0
annapaula:1471110739173	Carbon-D-Galactonic-Acid-g-Lactone	0
annapaula:1471110739173	Carbon-D-Galactose	0
annapaula:1471110739173	Carbon-D-Galacturonic-Acid	0
annapaula:1471110739173	Carbon-D-Gluconic-Acid	1
annapaula:1471110739173	Carbon-D-Glucosamine	0
annapaula:1471110739173	Carbon-D-Glucosaminic-Acid	0
annapaula:1471110739173	Carbon-D-Glucose-1-Phosphate	0
annapaula:1471110739173	Carbon-D-Glucose-6-Phosphate	0
annapaula:1471110739173	Carbon-D-Glucuronic-Acid	0
annapaula:1471110739173	Carbon-D-L-a-Glycerol-Phosphate	0
annapaula:1471110739173	Carbon-D-L-Carnitine	1
annapaula:1471110739173	Carbon-D-L-Citramalic-Acid	1
annapaula:1471110739173	Carbon-D-L-Malic-Acid	1
annapaula:1471110739173	Carbon-D-L-Octopamine	1
annapaula:1471110739173	Carbon-D-Lactitol	0
annapaula:1471110739173	Carbon-D-Malic-Acid	0
annapaula:1471110739173	Carbon-D-Mannitol	1
annapaula:1471110739173	Carbon-D-Mannose	0
annapaula:1471110739173	Carbon-D-Melezitose	0

annapaula:1471110739173	Carbon-D-Melibiose	0
annapaula:1471110739173	Carbon-D-Psicose	0
annapaula:1471110739173	Carbon-D-Raffinose	0
annapaula:1471110739173	Carbon-D-Ribose	0
annapaula:1471110739173	Carbon-D-Saccharic-Acid	0
annapaula:1471110739173	Carbon-D-Serine	0
annapaula:1471110739173	Carbon-D-Sorbitol	0
annapaula:1471110739173	Carbon-D-Tagatose	0
annapaula:1471110739173	Carbon-D-Tartaric-Acid	0
annapaula:1471110739173	Carbon-D-Threonine	0
annapaula:1471110739173	Carbon-D-Trehalose	0
annapaula:1471110739173	Carbon-D-Xylose	0
annapaula:1471110739173	Carbon-Dextrin	0
annapaula:1471110739173	Carbon-Dihydroxy-Acetone	0
annapaula:1471110739173	Carbon-Dulcitol	0
annapaula:1471110739173	Carbon-Ethanolamine	1
annapaula:1471110739173	Carbon-Formic-Acid	0
annapaula:1471110739173	Carbon-Fumaric-Acid	1
annapaula:1471110739173	Carbon-g-Amino-Butyric-Acid	1
annapaula:1471110739173	Carbon-g-Hydroxy-Butyric-Acid	0
annapaula:1471110739173	Carbon-Gelatin	0
annapaula:1471110739173	Carbon-Gentiobiose	0
annapaula:1471110739173	Carbon-Glycerol	1
annapaula:1471110739173	Carbon-Glycine	0
annapaula:1471110739173	Carbon-Glycogen	0
annapaula:1471110739173	Carbon-Glycolic-Acid	0
annapaula:1471110739173	Carbon-Glycyl-L-Aspartic-Acid	0
annapaula:1471110739173	Carbon-Glycyl-L-Glutamic-Acid	0
annapaula:1471110739173	Carbon-Glycyl-L-Proline	1
annapaula:1471110739173	Carbon-Glyoxylic-Acid	0
annapaula:1471110739173	Carbon-i-Erythritol	0
annapaula:1471110739173	Carbon-Inosine	1
annapaula:1471110739173	Carbon-Inulin	0
annapaula:1471110739173	Carbon-Inulin	0
annapaula:1471110739173	Carbon-Itaconic-Acid	1
annapaula:1471110739173	Carbon-L-Alanine	1
annapaula:1471110739173	Carbon-L-Alanyl-Glycine	0
annapaula:1471110739173	Carbon-L-Arabinose	0
annapaula:1471110739173	Carbon-L-Arabitol	0
annapaula:1471110739173	Carbon-L-Arginine	1
annapaula:1471110739173	Carbon-L-Asparagine	1
annapaula:1471110739173	Carbon-L-Aspartic-Acid	1
annapaula:1471110739173	Carbon-L-Fucose	0
annapaula:1471110739173	Carbon-L-Glutamic-Acid	1

annapaula:1471110739173	Carbon-L-Glutamine	1
annapaula:1471110739173	Carbon-L-Histidine	1
annapaula:1471110739173	Carbon-L-Homoserine	0
annapaula:1471110739173	Carbon-L-Isoleucine	1
annapaula:1471110739173	Carbon-L-Lactic-Acid	1
annapaula:1471110739173	Carbon-L-Leucine	1
annapaula:1471110739173	Carbon-L-Lysine	1
annapaula:1471110739173	Carbon-L-Lyxose	0
annapaula:1471110739173	Carbon-L-Malic-Acid	1
annapaula:1471110739173	Carbon-L-Methionine	0
annapaula:1471110739173	Carbon-L-Ornithine	1
annapaula:1471110739173	Carbon-L-Phenylalanine	0
annapaula:1471110739173	Carbon-L-Proline	1
annapaula:1471110739173	Carbon-L-Pyroglutamic-Acid	1
annapaula:1471110739173	Carbon-L-Rhamnose	0
annapaula:1471110739173	Carbon-L-Serine	1
annapaula:1471110739173	Carbon-L-Sorbose	0
annapaula:1471110739173	Carbon-L-Tartaric-Acid	0
annapaula:1471110739173	Carbon-L-Threonine	0
annapaula:1471110739173	Carbon-L-Valine	0
annapaula:1471110739173	Carbon-Lactulose	0
annapaula:1471110739173	Carbon-Laminarin	0
annapaula:1471110739173	Carbon-m-Inositol	0
annapaula:1471110739173	Carbon-m-Tartaric-Acid	0
annapaula:1471110739173	Carbon-Malonic-Acid	1
annapaula:1471110739173	Carbon-Maltose	0
annapaula:1471110739173	Carbon-Maltotriose	0
annapaula:1471110739173	Carbon-Mannan	0
annapaula:1471110739173	Carbon-Mucic-Acid	0
annapaula:1471110739173	Carbon-N-Acetyl-b-D-Mannosamine	0
annapaula:1471110739173	Carbon-N-Acetyl-D-Galactosamine	0
annapaula:1471110739173	Carbon-N-Acetyl-D-Glucosamine	1
annapaula:1471110739173	Carbon-N-Acetyl-L-Glutamic-Acid	1
annapaula:1471110739173	Carbon-N-Acetyl-Neuraminic-Acid	0
annapaula:1471110739173	Carbon-Oxalic-Acid	0
annapaula:1471110739173	Carbon-Oxalomalic-Acid	0
annapaula:1471110739173	Carbon-Palatinose	0
annapaula:1471110739173	Carbon-Pectin	0
annapaula:1471110739173	Carbon-Propionic-Acid	1
annapaula:1471110739173	Carbon-Putrescine	1
annapaula:1471110739173	Carbon-Pyruvic-Acid	1
annapaula:1471110739173	Carbon-Quinic-Acid	1
annapaula:1471110739173	Carbon-Salicin	0
annapaula:1471110739173	Carbon-Sebacic-Acid	1

annapaula:1471110739173	Carbon-Stachyose	0
annapaula:1471110739173	Carbon-Succinic-Acid	1
annapaula:1471110739173	Carbon-Sucrose	0
annapaula:1471110739173	Carbon-Thymidine	0
annapaula:1471110739173	Carbon-Tween-20	1
annapaula:1471110739173	Carbon-Tween-80	1
annapaula:1471110739173	Carbon-Tyramine	1
annapaula:1471110739173	Carbon-Uridine	0
annapaula:1471110739173	Carbon-Xylitol	0

Missing or miss-annotated reactions can cause problems that prevent the model from accurately predicting and generating biomass. Such irregularities include imbalanced and irregular formulations (e.g. undefined compounds, thermodynamics and reactions). To prevent this, reactions within the model were compared to those present within the K-base biochemistry database. Attempts were made to find the minimal set of reactions required to produce biomass and growth. These reactions were then incorporated into the model. This is known as gap filling (Henry et al., 2010).

5.2.5 Identification of different pathways in PA and PAdel

To identify the pathways which were differentially regulated, FBA was performed with the draft model, incorporating RNA expression results. Prior to RNA extraction, bacterial cells were grown in supplemented M9 including disodium phosphate, monopotassium phosphate, ammonium chloride, sodium chloride, glucose, casamino acids, and thiamine hydrochloride. This

media composition was not available on K-base. Instead the closest media resembling supplemented M9 was used, Argonne LB media. Details for this media composition are included in Table 5-3. Transcriptome data included normalized RNA-seq results for each gene in PA and PAdel (Appendix 8.3.3)**.** FBA was also performed using the following parameters; expression threshold: 0.5 and expression uncertainty: 0.1. Reactions with gene expression values in the percentile above this threshold were considered on, or off if they were below. The 'expression of uncertainty' described the range of uncertainty for reaction classifications based on the gene expression threshold. Reactions below the level of uncertainty were described as unknown. FBA was consequently performed using the draft reconstruction model, gene expression results for PA and PAdel, the parameters described above and growth conditions incorporating Argonne LB media. The results from the FBA for PA and PAdel were then compared. Figure 5-2 shows a summary of the metabolic reconstruction method.

Table 5-3 Media composition for Argonne LB media.

The min uptake for all compounds was -100 mol/g cell dry weight (CDW) hr and the max uptake 100 mol/g CDW hr.

Compound	Name	Formula	Charge
cpd00001	H2O	H2O	0
cpd00007	O2	O2	0
cpd00009	Phosphate	HO4P	-2
cpd00013	NH3	H4N	1
cpd00018	AMP	C10H13N5O7P	-1
cpd00023	L-Glutamate	C5H8NO4	-1
cpd00027	D-Glucose	C6H12O6	0
cpd00028	Heme	C34H30FeN4O4	-2
cpd00030	Mn2+	Mn	2
cpd00033	Glycine	C2H5NO2	0
cpd00034	Zn2+	Zn	2
cpd00035	L-Alanine	C3H7NO2	0
cpd00039	L-Lysine	C6H15N2O2	1
cpd00041	L-Aspartate	C4H6NO4	-1
cpd00046	CMP	C9H13N3O8P	-1
cpd00048	Sulfate	O4S	-2
cpd00051	L-Arginine	C6H15N4O2	1
cpd00054	L-Serine	C3H7NO3	0
cpd00058	Cu2+	Cu	2
cpd00060	L-Methionine	C5H11NO2S	0
cpd00063	Ca2+	Ca	2
cpd00065	L-Tryptophan	C11H12N2O2	0
cpd00066	L-Phenylalanine	C9H11NO2	0
cpd00067	H+	H	1
cpd00069	L-Tyrosine	C9H11NO3	0
cpd00091	UMP	C9H12N2O9P	-1
cpd00092	Uracil	C4H4N2O2	0
cpd00099	Cl-	Cl	-1
cpd00107	L-Leucine	C6H13NO2	0
cpd00119	L-Histidine	C6H9N3O2	0
cpd00126	GMP	C10H13N5O8P	-1
cpd00129	L-Proline	C5H8NO2	-1
cpd00149	Co2+	Co	2
cpd00156	L-Valine	C5H11NO2	0
cpd00161	L-Threonine	C4H9NO3	0
cpd00182	Adenosine	C10H13N5O4	0
cpd00184	Thymidine	C10H14N2O5	0
cpd00205	K+	K	1
cpd00215	Pyridoxal	C8H9NO3	0

cpd00218	Niacin	C6H4NO2	-1
cpd00220	Riboflavin	C17H20N4O6	0
cpd00226	HYXN	C5H4N4O	0
cpd00239	H2S	H2S	0
cpd00244	Ni2+	Ni	2
cpd00246	Inosine	C10H12N4O5	0
cpd00249	Uridine	C9H12N2O6	0
cpd00254	Mg	Mg	2
cpd00311	Guanosine	C10H13N5O5	0
cpd00322	L-Isoleucine	C6H13NO2	0
cpd00381	L-Cystine	C6H12N2O4S2	0
cpd00393	Folate	C19H17N7O6	-2
cpd00438	Deoxyadenosine	C10H13N5O3	0
cpd00531	Hg2+	Hg	2
cpd00541	Lipoate	C8H13O2S2	-1
cpd00644	PAN	C9H16NO5	-1
cpd00654	Deoxycytidine	C9H13N3O4	0
cpd00793	Thiamine phosphate	C12H17N4O4PS	0
cpd00971	Na+	Na	1
cpd01012	Cd2+	Cd	2
cpd01048	Arsenate	HO4As	-2
cpd03424	Vitamin B12	C61H86CoN13O14PR	6
cpd10515	Fe2+	Fe	2
cpd10516	fe3	Fe	3
cpd11574	Molybdate	H2MoO4	0
cpd11595	chromate	H2O4Cr	-2

ASSEMBLED GENOME SEQUENCE

▼

ANNOTATION SERVER
RAST

▼

PRELIMINARY MODELS
Model SEED

▼

MODEL REFINEMENT
(*Merging of the preliminary models and
refinement using SMBL validator*)

▼

DRAFT RECONSTRUCTION MODEL
(K-base gap-filling and manual removal/addition of reactions
from the model)

▼

FBA ◄━━ **Addition of Biolog and
RNA-seq data**
(K-base)

▼

REFINED MODEL
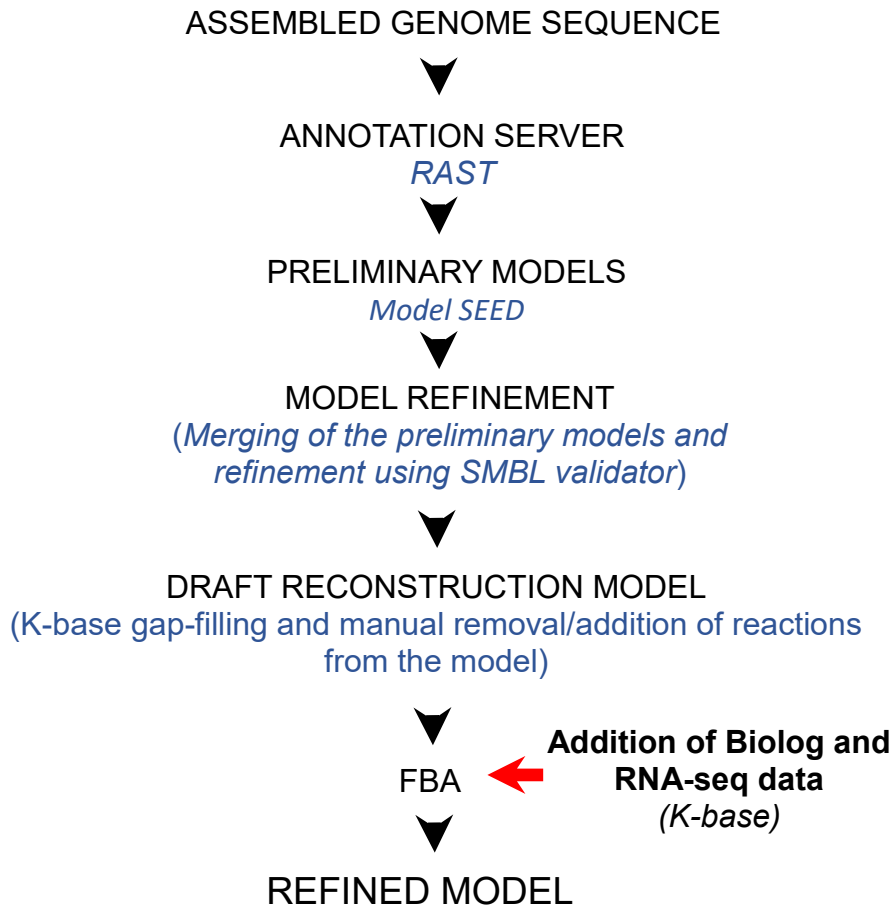
Figure 5-2 Summary of the metabolic reconstruction pipeline
The assembled genome sequence was first annotated in RAST and automatically imported into Model SEED. Preliminary models were then generated in Model Seed whereby intracellular and transport reactions were assigned genes according to RAST annotations and organism-specific biomass reactions. The preliminary models were merged and refined using SMBL validator. Missing or mis-annotated reactions were also added to create a draft reconstruction. FBA was then carried out to simulate biomass with Biolog and transcriptomic data to create the refined model.

5.3   Results

5.3.1   Genome annotation and curation

P. aeruginosa FASTA sequences were aligned to *P. aeruginosa* PAO1 GenBank accession no. NC002516.2. The curated and annotated *P. aeruginosa* PAO1 genome was 6,191,479 bp in size. There were 5711 coding sequences and 63 RNAs. The RAST annotation results are shown in Figure 5-3.
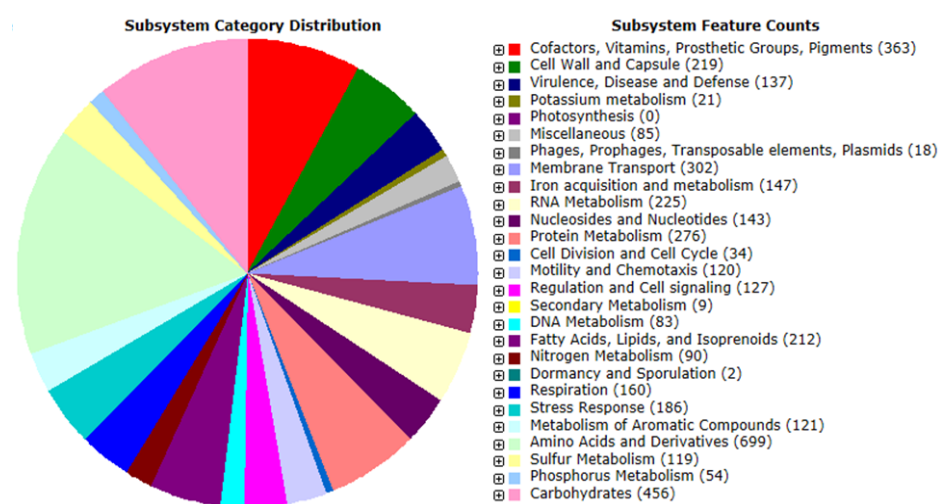
Figure 5-3 RAST genome annotation results
Results from the subsystem analysis revealed numerous genes were annotated with function relating to metabolism.

5.3.2 *P. aeruginosa* PAO1 model validation

Table 5-4 Experimental and computational growth incorporated in the model and used to predict growth phenotype.
0 indicates no growth and 1 means growth. Predicted growth rates were compared to those experimentally determined and allocated a class according to how consistent the results were; CAP—correct positive (the model was predicted to grow and showed this), CN—Correct negative (the model was predicted to not grow and did not), FP—False positive (model was predicted to grow, but it did not) and FN — False negative (model was predicted not to grow, but it did). If a cut-off of 0 had been used, a tick was assigned showing observed and predicted growth was consistent, leaving 40 inconsistent results.

Media	Observed PM SV	Observed growth	*In silico* growth	Phenotype class	
1-2-Propanediol	21.53	0	0	CN	✓
2-3-Butanediol	16.83	0	0	CN	✓
2-Deoxy-Adenosine	0.00	0	0	CN	✓
2-Deoxy-D-Ribose	11.19	0	0	CN	✓
3-Hydroxy-2-Butanone	7.45	0	0	CN	✓
Acetamide	21.90	0	0	CN	✓
Adenosine	43.36	0	0	CN	✓
α-D-Lactose	0.00	0	0	CN	✓
Adonitol	0.00	0	0	CN	✓
Amygdalin	0.00	0	0	CN	✓
Arbutin	0.00	0	0	CN	✓
ß-Methyl-D-Glucoside	0.00	0	0	CN	✓
Chondroitin-Sulfate-C	0.00	0	0	CN	✓
Citraconic Acid	0.00	0	0	CN	✓
D-Arabinose	0.00	0	0	CN	✓
D-Aspartic Acid	0.00	0	0	CN	✓
D-Cellobiose	0.00	0	0	CN	✓
D-Fructose-6-Phosphate	0.00	0	0	CN	✓
D-Galactose	0.00	0	0	CN	✓
D-Galacturonic Acid	0.00	0	0	CN	✓
D-Glucosaminic Acid	0.00	0	0	CN	✓
D-Glucose-1-Phosphate	0.00	0	0	CN	✓
D-Glucose-6-Phosphate	0.17	0	0	CN	✓
D-Glucuronic Acid	0.00	0	0	CN	✓
4-Hydroxy-Benzoic Acid	247.13	1	1	CP	✓
4-Hydroxy-L-Proline-trans	244.90	1	1	CP	✓

Media	Observed PM SV	Observed growth	*In silico* growth	Phenotype class	
Acetic Acid	219.48	1	1	CP	✓
α-D-Glucose	244.53	1	1	CP	✓
ß-Hydroxy-Butyric Acid	218.93	1	1	CP	✓
Caproic Acid	228.37	1	1	CP	✓
Citric Acid	238.60	1	1	CP	✓
D-Alanine	132.00	1	1	CP	✓
D-Arabitol	207.02	1	1	CP	✓
D-Fructose	226.80	1	1	CP	✓
D-Gluconic Acid	258.02	1	1	CP	✓
D-L-Citramalic Acid	176.03	1	1	CP	✓
D-L-Malic Acid	241.25	1	1	CP	✓
D-L-Octopamine	248.10	1	1	CP	✓
D-Mannitol	230.00	1	1	CP	✓
Ethanolamine	235.34	1	1	CP	✓
Fumaric Acid	246.23	1	1	CP	✓
γ-Amino-Butyric Acid	255.97	1	1	CP	✓
Glycerol	206.24	1	1	CP	✓
Glycyl-L-Proline	235.93	1	1	CP	✓
Inosine	151.61	1	1	CP	✓
Itaconic Acid	248.54	1	1	CP	✓
L-Alanine	208.00	1	1	CP	✓
L-Arginine	226.71	1	1	CP	✓
L-Asparagine	259.19	1	1	CP	✓
L-Aspartic Acid	245.06	1	1	CP	✓
L-Glutamic Acid	239.91	1	1	CP	✓
L-Glutamine	261.58	1	1	CP	✓
L-Histidine	246.28	1	1	CP	✓
L-Isoleucine	222.24	1	1	CP	✓
L-Lactic Acid	114.84	1	1	CP	✓
L-Leucine	158.18	1	1	CP	✓
L-Lysine	144.87	1	1	CP	✓
L-Malic Acid	235.20	1	1	CP	✓
L-Ornithine	147.09	1	1	CP	✓
L-Proline	258.74	1	1	CP	✓
L-Pyroglutamic Acid	253.21	1	1	CP	✓
L-Serine	93.92	1	1	CP	✓
Malonic Acid	172.91	1	1	CP	✓
N-Acetyl-D-Glucosamine	190.58	1	1	CP	✓
N-Acetyl-L-Glutamic Acid	245.16	1	1	CP	✓
Propionic Acid	241.90	1	1	CP	✓
Putrescine	211.50	1	1	CP	✓

Media	Observed PM SV	Observed growth	*In silico* growth	Phenotype class	
Quinic Acid	244.66	1	1	CP	✓
Pyruvic Acid	165.49	1	1	CP	✓
Sebacic Acid	211.58	1	1	CP	✓
Succinic Acid	175.11	1	1	CP	✓
Tween-20	185.15	1	1	CP	✓
Tween-80	230.83	1	1	CP	✓
Tyramine	249.32	1	1	CP	✓
δ-Amino Valeric Acid	237.53	1	1	CP	✓
2-3-Butanone	14.47	0	1	FP	✓
Acetoacetic Acid	4.52	0	1	FP	✓
α-Hydroxy-Butyric Acid	8.75	0	1	FP	✓
α-Keto-Butyric Acid	13.15	0	1	FP	✓
α-Keto-Valeric Acid	7.02	0	1	FP	✓
Capric Acid	33.06	0	1	FP	✓
Dextrin	4.60	0	1	FP	✓
D-Glucosamine	14.65	0	1	FP	✓
Dihydroxy-Acetone	19.64	0	1	FP	✓
D-L-a-Glycerol-Phosphate	17.58	0	1	FP	✓
D-Malic Acid	1.46	0	1	FP	✓
D-Raffinose	1.68	0	1	FP	✓
D-Ribose	25.99	0	1	FP	✓
D-Serine	2.27	0	1	FP	✓
D-Tartaric Acid	0.19	0	1	FP	✓
D-Threonine	1.14	0	1	FP	✓
D-Trehalose	52.72	0	1	FP	✓
Dulcitol	4.55	0	1	FP	✓
D-Xylose	1.78	0	1	FP	✓
Formic Acid	7.87	0	1	FP	✓
Gelatin	29.44	0	1	FP	✓
Gentiobiose	0.79	0	1	FP	✓
γ-Hydroxy-Butyric Acid	8.79	0	1	FP	✓
Glycine	16.23	0	1	FP	✓
Glycogen	2.15	0	1	FP	✓
Glycyl-L-Aspartic Acid	8.83	0	1	FP	✓
Glycyl-L-Glutamic Acid	15.64	0	1	FP	✓
i-Erythritol	1.58	0	1	FP	✓
L-Alanyl-Glycine	43.59	0	1	FP	✓
L-Arabinose	2.61	0	1	FP	✓
L-Lyxose	70.77	0	1	FP	✓
L-Methionine	1.84	0	1	FP	✓
L-Phenylalanine	36.11	0	1	FP	✓

Media	Observed PM SV	Observed growth	*In silico* growth	Phenotype class	
L-Threonine	6.69	0	1	FP	✓
L-Valine	47.00	0	1	FP	✓
L-Tartaric Acid	5.45	0	1	FP	✓
N-Acetyl-D-Galactosamine	1.37	0	1	FP	✓
Oxalomalic Acid	11.63	0	1	FP	✓
Palatinose	2.37	0	1	FP	✓
Pectin	2.72	0	1	FP	✓
Salicin	0.21	0	1	FP	✓
Sec-Butylamine	1.14	0	1	FP	✓
Thymidine	1.26	0	1	FP	✓
Uridine	44.24	0	1	FP	✓
Butyric Acid	110.73	1	0	FN	
D-L-Carnitine	153.10	1	0	FN	
α-Keto-Glutaric Acid	250.82	1	0	FN	
2-Hydroxy-Benzoic Acid	0.00	0	1	FP	
α-Methyl-D-Galactoside	0.00	0	1	FP	
α-Methyl-D-Glucoside	0.00	0	1	FP	
ß-D-Allose	0.00	0	1	FP	
ß-Methyl-D-Galactoside	0.00	0	1	FP	
ß-Phenylethylamine	0.00	0	1	FP	
D-Galactonic Acid-γ-Lactone	0.00	0	1	FP	
D-Lactitol	0.00	0	1	FP	
D-Mannose	0.00	0	1	FP	
D-Melezitose	0.00	0	1	FP	
D-Melibiose	0.00	0	1	FP	
D-Psicose	0.00	0	1	FP	
D-Saccharic Acid	0.00	0	1	FP	
D-Sorbitol	0.00	0	1	FP	
D-Tagatose	0.00	0	1	FP	
Glycolic Acid	0.00	0	1	FP	
Glyoxylic Acid	0.00	0	1	FP	
Inulin	0.00	0	1	FP	
Lactulose	0.00	0	1	FP	
Laminarin	0.00	0	1	FP	
L-Arabitol	0.00	0	1	FP	
L-Fucose	0.00	0	1	FP	
L-Homoserine	0.00	0	1	FP	
L-Rhamnose	0.00	0	1	FP	
L-Sorbose	0.00	0	1	FP	
Maltose	0.00	0	1	FP	

Media	Observed PM SV	Observed growth	*In silico* growth	Phenotype class
Mannan	0.00	0	1	FP
Maltotriose	0.00	0	1	FP
M-Tartaric Acid	0.00	0	1	FP
Mucic Acid	0.00	0	1	FP
N-Acetyl-b-D-Mannosamine	0.00	0	1	FP
N-Acetyl-Neuraminic Acid	0.00	0	1	FP
Oxalic Acid	0.00	0	1	FP
Stachyose	0.00	0	1	FP
Sucrose	0.00	0	1	FP
Xylitol	0.00	0	1	FP

To assess the accuracy of the model and the ability to predict growth, simulated growth was compared to PM growth using *in silico* prediction. Among the 192 carbon substrates utilised on the Biolog PM Carbon plates, 159 carbon sources had a metabolic reaction assigned in the model. The carbon sources were appropriate for *in silico* predictions, but predicting the FBA for substrates in the Nitrogen (PM3), Phosphorus (PM4) and Peptide Nitrogen (PM6-8) plates could not be performed. This meant that that refinement of the model incorporating substrates in PM3-8 to improve the accuracy of the model, could not be performed at this present time. The experimental media utilised for growth in PM3, 4 and 6-8 were supplemented with succinate instead of glucose. The media composition on Model Seed and K-base required modifications which when applied caused the program to fail since these programs are still in the early developmental stages and there is no reaction data available for every co-factor in each

cellular compartment of the model. There were additionally no media compositions available for substrates in the Peptide-Nitrogen plates. This may be because the reactions assigned to dipeptides and tripeptides are mostly unknown.

Carbon sources that were included in the model are listed in Table 5-4 along with their experimental and computational growth phenotype. Simulation of growth was performed using FBA in K-Base. Experimental growth was determined using a cut-off whereby SV's (signal values) for each substrate, greater than half of the maximum SV in the corresponding plate were considered as growth. This cut-off led to an underestimation of the overall agreement between PM outcomes and computational predictions. For example 2-3-Butanone had a signal value of 14.47 which was below the cut-off and was assigned a 'False Positive' phenotype according to the model. A cutoff of 0 would have provided a better indication of growth. To improve the accuracy of the model, new reconstructions (represented by an SBML file for each carbon source) could have been added to the model for carbon sources above the cut-off of 0. This was not carried at the time since each SBML file (representing a FBA for each carbon source) already in the model covered most of the reactions available in the metabolic framework. A cut-off of '0' meant that 120 out of 192 carbon sources were consistent with the experimental data, confirming the accuracy of the model. A tick confirmed an agreement between the experimental and computational results if a cut-off of 0 had been applied. This is shown in Table 5-4.

5.3.3   Integrating transcriptomics with the metabolic model

Omics-derived data was used to refine, validate and integrate with the merged metabolic model. FBA was performed, as described in the methods using the merged metabolic model and gene expression values to associate genes to a metabolic pathway or reaction. The final model carried out on supplemented LB media included 156 compounds and 1673 reactions. Results showed that PA had a biomass of 30.27 g and PAdel a biomass of 20.17, demonstrating that the model grew less with the mutant strain (PAdel). Exchange (transporter) based reactions most likely also contributed to this result since there were 3 less compounds available to PAdel (compared to PA) with 1 more compound excreted (Table 5-5 and 5-6). Although there were less compounds available to PAdel, 29 were involved in uptake (2 more than PAdel). This could be caused by differences in the catabolism and anabolism of compounds available in the media. Transporters are difficult to annotate because there are very similar to each other and only differ in substrate specificity. This may have been a contributing factor (Marger and Saier, 1993, Saier, 1994). During gap-filling it is also important to recognize that not all reactions are equal. Transporters for instance and non-KEGG reactions are penalized along with missing structures or unknown thermodynamic values (Henry et al., 2010).

Reactions were categorised as 'on' (meaning active), 'off' (meaning inactive) or 'unknown'. A full list of reactions in each strain are available upon request.

The reaction states in both PA and PAdel were identical; 615 were active, 613 were inactive and 448 were unknown. Out of the 1673 reactions, 372 were found to be different between PA and PAdel. Unknown reactions were omitted, including those that had been identified as unknown for one strain but active/inactive for another. The analysis was therefore performed using reactions that were specifically identified as 'on' and 'off'. This left 18 reactions that were categorically different between PA and PAdel, all of which were active in PA but inactive in PAdel. Details of these reactions are listed in Table 5-7 along with gene associations.

Table 5-5 Compound exchange results

Available compounds refers to compounds and co-factors in the media that were present and could be metabolised by the cell. Uptake refers to compounds that were capable of entering the cell. Excretion indicates the number of compounds that were expelled from the cell. Exchange reactions were classified as blocked (not present in the model), negative (excretion), negative variable (a zero maximal, and a negative minimal, meaning it can either be zero, or it can go from right to left), positive (uptake), positive variable (reaction has a positive maximal, and a zero minimal, meaning that it can either be zero, or it can go from left to right) and variable (means that the reaction has positive maximal and negative minimal values, meaning that it can go in either direction).

Overview of compounds	PA	PAdel
Available	111	108
Uptake	27	29
Excretion	18	19
Reaction classification of compound exchanges (transporters) that varied between PA and PAdel		
Negative	1	1
Negative variable	1	3
Blocked	3	1
Positive	1	3
Positive variable	3	2
Variable	2	1

Table 5-6 Differences in compound exchange reactions (transporters).
All exchanges are related to the extracellular compartment of the cell. The state of the exchange was described as being involved in UP (uptake) or EX (excretion) or being IA (inactive). Exchange reactions were classified as blocked (not present in the model), negative (excretion), negative variable (a zero maximal, and a negative minimal, meaning it can either be zero, or it can go from right to left), positive (uptake), positive variable (reaction has a positive maximal, and a zero minimal, meaning that it can either be zero, or it can go from left to right) and variable (means that the reaction has positive maximal and negative minimal values, meaning that it can go in either direction). Max flux defined the maximum allowed uptake/excretion of a compound while the min flux defined the minimum allowed uptake or excretion of a compound. Results highlighted in yellow showed differences in reaction classification between strains. The remaining results did not show a differences in reaction classifications but there were differences in reaction states between strains.

Compound	compound ID	Compound charge	Max flux	Min flux	PA reaction states	PA reaction classification	PAdel reaction state	PAdel reaction classification
Urea	cpd00073	0	0	-1000	EX	**Negative variable**	EX	**Negative**
L-Proline	cpd00129	0	100	-100	UP	**Variable**	UP	**Positive**
3-Hydroxybutanoate	cpd00797	-1	0	-1000	IA	**Blocked**	IA	**Negative variable**
L-Arginine	cpd00051	1	100	-100	EX	**Variable**	UP	**Positive variable**
Fe2+	cpd10515	2	100	-100	IA	**Positive variable**	UP	**Positive**
L-Methionine	cpd00060	0	100	-100	UP	**Positive**	UP	**Positive variable**
Xanthine	cpd00309	0	0	-1000	EX	**Negative**	EX	**Negative variable**
Fe3	cpd10516	3	100	-100	UP	**Positive variable**	UP	**Positive**
Hypoxanthine	cpd00226	0	100	-100	IA	**Blocked**	EX	**Variable**
Uracil	cpd00092	0	100	-100	UP	**Positive variable**	IA	**Blocked**
4-Hydroxy-benzylalcohol	cpd15378	0	0	-1000	IA	**Blocked**	IA	**Negative variable**
H+	cpd00067	1	100	-100	UP	Variable	EX	Variable
L-Glutamate	cpd00023	-1	100	-100	EX	Variable	UP	Variable
Acetoacetate	cpd00142	-1	0	-1000	IA	Negative variable	EX	Negative variable
O2	cpd00007	0	100	-100	EX	Variable	UP	Variable
CO2	cpd00011	0	0	-1000	IA	Negative variable	EX	Negative variable

Table 5-7 Predicted pathways that are active in PA and inactive in PAdel. All reactions were related to the cytosol compartment (c0). Each K-base reaction has been assigned a KEGG ID, gene and Enzyme Commission number (E.C.). Gene expression values have also been provided for PA and PAdel. All of the below 18 reactions were inactive in PAdel but active in PA. A full list of reactions for each strain are available upon request.

Reaction ID	Pathway	Reaction name	Kegg ID	Reaction	Gene	PAdel gene expression	PA gene expression	E. C. Number
rxn02201	-Folate biosynthesis	2-amino-4-hydroxy-6-hydroxymethyl-7,8-dihydropteridine-diphosphate:4-aminobenzoate 2-amino-4-hydroxydihydropteridine-6-methenyltransferase	R03067	ABEE + 7,8-Dihydropterin pyrophosphate <=> PPi + Dihydropteroate	PA3361	99.24	6201.84	2.5.1.15
rxn00953	-Glycine, serine and threonine metabolism -Cysteine and methionine metabolism -Antibiotic biosynthesis -Amino acids biosynthesis	L-Serine hydro-lyase (adding homocysteine)	R01290	Serine + L-Homocysteine <=> H2O + Cystathionine	PA5208	439.71	1623.38	4.2.1.22

Reaction ID	Pathway	Reaction name	Kegg ID	Reaction	Gene	PAdel gene expression	PA gene expression	E. C. Number
rxn01268	-Antibiotic biosynthesis -Biosynthesis of amino acids -Novobiocin biosynthesis -Biosynthesis of secondary metabolites	Prephenate:NAD+ oxidoreductase(decarboxylating)	R01728	NAD + Prephenate <=> NADH + CO2 + 4-Hydroxyphenylpyruvate	PA1784	255.57	1480.71	1.3.1.12 1.3.1.43 1.3.1.52
rxn00068	---	Fe2+:NAD+ oxidoreductase	R00092	NAD + H+ + 2 Fe2+ <=> NADH + 2 fe3	PA2079	390.75	342.82	1.16.1.7
rxn01269	-Phenylalanine, tyrosine and tryptophan biosynthesis -Biosynthesis of secondary metabolites - Antibiotic biosynthesis	Prephenate:NADP+ oxidoreductase(decarboxylating)	R01730	TPN + Prephenate <=> TPNH + CO2 + 4-Hydroxyphenylpyruvate	PA1784	255.57	1480.71	1.3.1.13 1.3.1.43
rxn00555	-Antibiotic biosynthesis -Alanine, aspartate and glutamate metabolism -Amino sugar and nucleotide sugar metabolism -Metabolic pathways	L-glutamine:D-fructose-6-phosphate isomerase (deaminating)	R00768	L-Glutamine + Neuberg ester <=> GLU + D-Glucosamine phosphate	PA1263 or PA5473	644.65 or 579.12	482.72 or 1560.20	2.6.1.16

Reaction ID	Pathway	Reaction name	Kegg ID	Reaction	Gene	PAdel gene expression	PA gene expression	E. C. Number
rxn01642	-Histidine metabolism	4-imidazolone-5-propanoate amidohydrolase	R02288	H2O + 4-Imidazolone-5-propanoate <=> N-Formimino-L-glutamate	PA4108	409.48	1730.16	3.5.2.7
rxn02971	-Benzoate degradation -Microbial metabolism in diverse environments -Degradation of aromatic compounds	5-oxo-2,5-dihydrofuran-2-acetate delta3-delat2-isomerase	R06990	Muconolactone <=> 3-Oxoadipate enol-lactone	PA1733	674.40	1322.15	5.3.3.4
rxn02200	-Folate biosynthesis	2-amino-4-hydroxy-6-hydroxymethyl-7,8-dihydropteridine:4-aminobenzoate 2-amino-4-hydroxydihydropteridine-6-methenyltransferase	R03066	ABEE + 6-hydroxymethyl dihydropterin <=> H2O + Dihydropteroate	PA3361	99.24	6201.84	2.5.1.15
rxn03380	---	L-Serine hydro-lyase (adding homocysteine)	R04942	Serine + Selenohomocysteine <=> H2O + Selenocystathionine	PA5208	439.71	1623.38	4.2.1.22

Reaction ID	Pathway	Reaction name	Kegg ID	Reaction	Gene	PAdel gene expression	PA gene expression	E. C. Number
rxn05909	-Glycine, serine and threonine metabolism - Antibiotic biosynthesis	L-serine hydro-lyase (adding hydrogen sulfide, L-cysteine-forming)	R00891	Serine + H2S <=> H2O + L-Cysteine	PA5208	439.71	1623.38	4.2.1.22
rxn00056	Porphyrin and chlorophyll metabolism	Fe(II):oxygen oxidoreductase	R00078	O2 + 4 H+ + 4 Fe2+ <=> 2 H2O + 4 fe3	PA2079	390.75	342.82	1.16.3.1
rxn07841	-Zeatin biosynthesis -Biosynthesis of secondary metabolites -Histidine metabolism	2-Isopentenyl-diphosphate:ATP delta2-isopentenyltransferase	R08051	ATP + DMAPP <=> PPi + Isopentenyl-ATP	PA3361	99.24	6201.84	
rxn02473	-Biosynthesis of secondary metabolites -Biosynthesis of amino acids	D-erythro-1-(Imidazol-4-yl)glycerol 3-phosphate hydro-lyase	R03457	D-erythro-imidazol-glycerol-phosphate <=> H2O + Imidazole-acetol phosphate	PA0524 or PA5208	5031.17 or 439.71	1321.39 or 1623.38	4.2.1.19
rxn05596		Potassium transport out via proton antiport		H+[e] + K+ <=> H+ + K+[e]	PA2618 or PA1228	481.36 or 77.11	1940.00 or 34.74	TC-2.A.37 2.A.37
rxn00567	-Nitrogen metabolism -Microbial metabolism in diverse environments	Nitric-oxide:ferricytochrome-c oxidoreductase	R00783	H2O + Cytochrome c3+ + NO <=> 2 H+ + Nitrite + Cytochrome c2+	PA2193	124.30	1484.07	1.7.2.1
rxn07842	-Zeatin biosynthesis	2-Isopentenyl-diphosphate:ADP delta2-isopentenyltransferase	R08052	ADP + DMAPP <=> PPi + Isopentenyl-ADP	PA3361	99.24	6201.84	

5.4 Discussion

In this study computational systems biology was integrated with genomic and phenomic data to predict the impact of the *mexT* 8-bp repeat sequence on metabolic capability. Differences in the metabolic pathways relating to glycolysis, gluconeogenesis, oxidative phosphorylation and biomass were identified, illustrating the complex processes underlying *P. aeruginosa* adaption.

A draft metabolic reconstruction model incorporating constraint-based modelling was created using the parent strain (PA) combined with its genomic and PM (phenotypic microarray) derived data. A high cut-off value was initially chosen for cellular growth to allow differentiation between growth phenotypes in PA and PAdel. Although 75% of the PM substrates were accurately predicted using *in silico* modelling and despite modification of the cut-off value there were still discrepancies. These inconsistencies were most likely caused by missing or mis-annotated genes in the initial draft reconstruction which prevented the model from testing specific carbon sources. The identification of these gaps or missing transport reactions is a necessary refinement of the model in the future. To overcome this, genomic annotations need improvement and the reactions involved in the metabolism of specific substrates need to be defined better.

According to the RNA-seq results from chapter 4 and the Panther Gene Ontology database (http://www.pantherdb.org/) it was shown that 99 of the up-regulated genes in PAdel were linked to metabolic processes and 31 genes linked to transporters. Down-regulated genes related to metabolism accounted for 125 genes while 26 were linked to transporters. It was unclear from this data which pathways and transporters were specifically altered since RNA-seq identifies genes that are differentially regulated but it does assign these to a pathway. The draft metabolic model was therefore used to refine and integrate omics derived data. FBA was performed and growth simulated using supplemented LB media to validate the model. The modified metabolically reconstructed model contained 156 compounds and 1673 reactions, the largest, up-to-date and most refined model reported for any Pseudomonad (or even any strain) (Oberhardt et al., 2008). PA showed increased growth and produced a larger biomass of 30.27 g compared to 20.17 g by PAdel. Pathway analysis also identified 18 reactions unique to PA, confirming previous findings from Chapter 3 and 4 using PM and transcriptomic results, that PA is more metabolically active compared to PAdel. This also highlights the predictive capability of this method.

Reactions that displayed differences between strains were related to virulence, antibiotic and amino acid biosynthesis and the ability to metabolise in diverse environments. These reactions are likely to increase

the efficiency of metabolism by influencing processes such as glycolysis, gluconeogenesis and oxidative phosphorylation. All of these gene-reaction associations showed a ≥2 fold change difference in gene expression between the parent and mutant strain. The exception was the oxido-reductase reactions which were assigned to PA2079 where the difference in expression between PA and PAdel was 0.9 fold change. The reason for this maybe that the model was refined using stoichiometric results and gap filling or there was an annotation issue. Again, further refinement of the model will reveal gaps in the metabolic framework which can be corrected to increase the accuracy.

Analysis of compounds exchanged through transporters revealed differences in 11 exchange reactions between PA and PAdel. These compounds were not identified in the pathway analysis suggesting these differences are due to the catabolism and metabolism of cofactors within reactions altering between compartments.

RNA-seq data showed that there were more transporters up-regulated then there were down-regulated in PAdel. This would explain the results observed in Table 5-5 and 5-6 whereby PAdel was predicted to contain 2 less blocked reactions, 2 more positive and 2 more negative variable reactions, contributing to the increased uptake and excretion of compounds during efflux.

Biolog phenotypic analysis indicated that PAdel was not capable of efficiently growing on nucleoside based media. In agreement, the model showed uracil (formed from uridine) was involved in uptake in PA while this pathway was blocked in PAdel. Furthermore hypoxanthine, also a constituent of nucleic acids (inosine) was up-taken but also excreted by PAdel. Hypoxanthine was therefore expected to be linked to uptake in PA, yet this reaction was actually completely blocked. PM results illustrated that growth on butyric-acid based media was marginally increased in PAdel. Results from the hydroxyl-butanoate compound exchange (a hydroxyl-butryic derivative) in the model suggest that this maybe because this reaction was blocked in PA but excreted by PAdel. L-arginine and L-proline are amino acids that are synthesised by similar pathways yet is unclear why L-proline and L-arginine were involved in uptake in PAdel but only L-proline was transported into PA. Iron related compounds were also positively transported into PAdel but by PA there were variably up-taken suggesting a form of siderophore regulation pertaining to increased virulence, as previously observed.

The D-fructose-6-phosphate isomerase pathway with L-glutamine in PAdel was inactive within the cell in the model. This may be caused by the positive flux caused by glutamate import through transporters. Glutamine is formed by the condensation of glutamate and ammonia. Since hydrolysis of urea produces ammonia in the predicted media, ammonia was capable

of reacting with glutamate to produce glutamine which could then pass into glycolysis via D-fructose-6-phosphate isomerase. This may explain why no difference was observed between PA and PAdel when grown solely on L-glutamine or L-glutamate media (PM data).

Further refinement is underway to increase the accuracy of the metabolic model. This includes the modification of the draft model to incorporate the genomic content and specific mutations found in PAdel and PAnfxC. The removal of inaccurate annotations, inconsistent phenotypes (observed vs predicted) and un-balanced reactions will increase the predictive capability. The incorporation of new reactions, thermodynamic information and related compounds to the modelling database will allow the addition of new media compositions relating to sources in PM 4-8, further increasing the complexity and predictability power of the model. The metabolic reconstruction was performed using supplemented LB (Argonne LB) since the media composition required to mimic supplemented M9 (which was used experimentally) could not be performed. Model SEED and K-base are not in their present form compressive nor flexible enough to perform the detailed analysis required to define differences in the metabolic and regulatory network. It does however provide a way of predicting differences in pathway utilisation among mutants.

5.5   Conclusion

This study has shown that using metabolic reconstruction the pathways unique to PA and PAdel have been defined. The acquisition of antibiotic resistance caused by the deletion of an 8-bp sequence in the transcription regulator *mexT* is associated with increased efflux of metabolites which inactivates specific cytosolic pathways that are no longer required. It is this process that contributes towards the reduced metabolic capability of PAdel. Reduced pathway activity relating to iron transport intraceullarly and via transporters may explain the reduced virulence phenotype previously observed. This metabolic model is the most up to date version for *P. aeruginosa* PAO1, integrating genotypic and phenotypic data to successfully predict biomass or growth in defined media.

6 Final Discussion

The aim of this thesis was to identify and characterise mutations that cause diversity in the *Pseudomonas aeruginosa* population. In doing so it is hoped that high risk strains can be identified to aid new diagnostics techniques. To investigate this hypothesis a collection of *P. aeruginosa* PAO1 strains were used as a test population. A region consisting of repeats of the sequence CGGCCAGC found within the transcriptional regulation *mexT* was identified as a key driver of genetic diversity. A single copy of this *mexT* 8-bp sequence was linked to increased antimicrobial resistance, reduced motility, virulence and ability to grow on specific substrates. It was also shown that the transcriptional effects of this repeat region were not solely constrained to *mexT* but also the whole genome, with the majority of genes differentially expressed linked to the phenotype and the metabolic capability of the cell. These results clearly show a difference in the niche adapted response caused by this *mexT* mutation.

Since the advent of sequencing, the falling costs of genome sequencing along with the vast amounts of data it generates, has meant that this technique has large potential not just in diagnostics and routine surveillance but in linking phenotype to genotype. The databases required to understand the effects of mutations on phenotype is however still lagging behind. Comparative genomics was used in this study and

combined with phenotypic analysis revealed differences among variants of the strain PAO1, which prior to this study were all thought to be the same. While *mexT* was identified as a mutational hotspot, the deletion of an 8-bp sequence was of particular interest since this was found only in the hyperbiofilm forming strains. To elucidate the role of this mutation (8-bp deletion) alone, an isogenic mutant was created termed PAdel, along with a naturally selected mutant also found to harbour the 8-bp deletion, called PAnfxC.

Phenotypic analysis of the parent strain compared to mutants with the single copy of the 8-bp sequence showed reduced virulence, motility and antimicrobial susceptibility. Previous studies have shown that *mexT* has a role in biofilm formation (Tian et al., 2009b, Favre-Bonté et al., 2003). In this study although a difference in motility (probably due to chemotaxis) was found, there was no reproducible difference in biofilm formation between the parent and mutant strains. Whole genome sequencing results revealed that compensatory mutations may be responsible for this. These results highlight the need for researchers to publish the whole genome sequences of isogenic mutants alongside their results to ensure reproducibility and thorough analysis of results.

The effect of a mutation on the phenotype of a cell can be predicted based on the nucleotide and codon change. We are approaching an era where

predictive modelling has the ability to not just predict the effect of a mutation on phenotype but predict the composite phenotype from multiple mutations. This is part of the planned future work that will increase predictability of clinically relevant phenotypes such as antibiotic susceptibility, virulence, motility and spread of infection.

Transcriptomic data showed that the single copy of the 8-bp sequence activates the LysR encoding region of the *mexT* gene in PAdel and PAnfxC whilst the double copy reduces expression across the LysR region. Expression across the whole coding sequence of *mexT* revealed that this gene may in fact consist of two genes since a dip in expression was identified across the 8-bp sequence region in PA. There was however no shine-dalgarno sequence ahead of this region to prove this hypothesis. It is likely that *mexT* in PAO1 consists of a single gene with a novel form of gene regulation. Since the 8-bp sequence lies on a helix-turn-helix it is concluded that *mexT* actually has an auto-regulative function and is a repressor that represses the *lysR* region in PA. The helix-turn-helix is located 66 amino acids from the N-terminus confirming this is a site for auto-regulatory elements. This repetitive *mexT* region may also encode RNAse activity and enable transcript degradation along the 3' region, another mechanism that aids repressor activity.

It is clear that *mexT* is a key regulator capable of altering the cell phenotype through regulation of the 8-bp sequence. PAnfxC was selected from a population primarily thought to consist of cells with the double copy of the 8-bp sequence. The phenotypic switch from PA to PAnfxC is a clear indicator of this, endowing the strain with antimicrobial resistance and reduced virulence when selected for in an antibiotic related environment. It would seem that strains with the single copy of the 8-bp sequence are adapted to clinically relevant environments. Transcriptomic data showed that genes associated with iron uptake were up-regulated in PAdel and PAnfxC, indicating adaption to sites of human infection which have a rich supply of blood. Genes up-regulated also included those required for survival in toxic environments, suggesting an adaption to antibiotic exposure.

Since antibiotic use is a selective pressure for the single copy of the 8-bp sequence, it would explain why all strains screened for this *mexT* genotype had the 8-bp deletion. This was because strains in this screen were all collected from sites of human contact. Collecting environmental strains from unpopulated areas would be beneficial in identifying the true genetic diversity of *mexT*. Identifying the conditions required to switch the single copy of the 8-bp sequence back to the double copy is also the next step. Controlling the conditions that promote growth in niche adapted sites will aid the treatment of *P. aeruginosa* infections.

In this thesis the techniques required to link phenotype to genotype have also been described. Using whole genome genomics and transcriptomics along with high throughput phenotypic methods, the metabolic capability and effect of the 8-bp sequence has been defined. Key pathways relating to glycolysis, gluconeogenesis and oxidative phosphorylation were predicted to be differentially regulated by PA and PAdel. This explains the reasons for the reduced metabolic activity identified in PAdel and PAnfxC, based on phenotypic microarray results. In line with the theory that strains with the single copy of the 8-bp sequence are clinically adapted, it would seem that PA with the duplicate copy of the sequence is adapted to nutrient rich environments. Metabolic reconstructions identified peptide utilisation and bacteriocin production related pathways that were active in PA but inactive in PAdel and PAnfxC. *P. aeruginoisa* is commonly isolated from soil and aquatic environments, both of which are nutritionally and ecologicaly versatile. Survival in such environments is dependant on competition with other microbes. Increased utilisation of nutrients and production of bacteriocins against other inhabiting bacteria would be beneficial in such environments.

Future work will lead to the use of computational modelling to predict regulatory pathways that affect not just the metabolic capability but clinically relevant phenotypes such a virulence, biofilm formation and antibiotic resistance. Since the *mexT* variants in this study were shown to

co-exist in a population, community based modelling using for instance single cell genome sequencing and transcriptomics could identify the genetic and environmental cues of phenotypic diversity particularly in biofilms where cell expansion and clonal diversity is common. This could also be applied to multi-species community based modelling and aid the prediction of antibiotic treatment and resistance over time. Understanding the metabolic profile of a cell may also have a role in diagnostics to identify the stage of infection.

The predictive capability of such models is increased with the addition of phenomic based data such as high throughput genome-wide transposon mutant libraries which identify gene essentiality. This will form part of the future work on this study. The effects of a single 8-bp sequence within an isogenic mutant have been characterised in this study. Incorporating numerous strains from different environments and using biologically relevant conditions will allow us to truly understand the genetic diversity of *P. aeruginosa* and predict the clinical outcome of high risk strains.

Papers and Presentations from this Thesis

Papers:
A.Correia, J., Malone, A. Desbois, D. Livermore, J. O'Grady, L. Crossman, J. Wain, G. Langridge. (2016). "Significance of an 8-bp variation in a global regulator, mexT, in Pseudomonas aeruginosa' " Proceedings of the National Academy of Sciences. (In preparation)

Presentations:
'Genome wide impact of antibiotic resistance mutations', Antimicrobial Society for Microbiology 2016

Conference papers:
'Significance of an 8-bp variation in a global regulator, *mexT* in *Pseudomonas aeruginosa*' Antimicrobial Society for Microbiology 2016

*'*Significance of the regulator *mexT* in *Pseudomonas aeruginosa*', University of East Anglia Post Graduate conference 2016

'Variability of *Pseudomonas aeruginosa* PAO1', Society of General Microbiology Annual Conference 2014

'*Pseudomonas aeruginosa* genetic variation' One Bug One Drug Conference 2013

7 References

2004. National Nosocomial Infections Surveillance (NNIS) System Report, data summary from January 1992 through June 2004, issued October 2004. *Am J Infect Control,* 32**,** 470-85.

ADAMS, M. D., WAGNER, L. M., GRADDIS, T. J., LANDICK, R., ANTONUCCI, T. K., GIBSON, A. L. & OXENDER, D. L. 1990. Nucleotide sequence and genetic characterization reveal six essential genes for the LIV-I and LS transport systems of Escherichia coli. *Journal of Biological Chemistry,* 265**,** 11436-11443.

ALHEDE, M., KRAGH, K. N., QVORTRUP, K., ALLESEN-HOLM, M., VAN GENNIP, M., CHRISTENSEN, L. D., JENSEN, P. O., NIELSEN, A. K., PARSEK, M., WOZNIAK, D., MOLIN, S., TOLKER-NIELSEN, T., HOIBY, N., GIVSKOV, M. & BJARNSHOLT, T. 2011. Phenotypes of non-attached Pseudomonas aeruginosa aggregates resemble surface attached biofilm. *PLoS One,* 6**,** e27943.

ALONSO, A. & MARTINEZ, J. L. 2000. Cloning and characterization of SmeDEF, a novel multidrug efflux pump from Stenotrophomonas maltophilia. *Antimicrob Agents Chemother,* 44**,** 3079-86.

ALONSO, A., MORALES, G., ESCALANTE, R., CAMPANARIO, E., SASTRE, L. & MARTINEZ, J. L. 2004. Overexpression of the multidrug efflux pump SmeDEF impairs Stenotrophomonas maltophilia physiology. *J Antimicrob Chemother,* 53**,** 432-4.

ALVAREZ-ORTEGA, C. & HARWOOD, C. S. 2007. Responses of Pseudomonas aeruginosa to low oxygen indicate that growth in the cystic fibrosis lung is by aerobic respiration. *Mol Microbiol,* 65**,** 153-65.

AMINOV, R. I. 2013. Biotic acts of antibiotics. *Front Microbiol,* 4**,** 241.

ANZAI, Y., KIM, H., PARK, J. Y., WAKABAYASHI, H. & OYAIZU, H. 2000. Phylogenetic affiliation of the pseudomonads based on 16S rRNA sequence. *Int J Syst Evol Microbiol,* 50 Pt 4**,** 1563-89.

ARAI, H. 2011. Regulation and Function of Versatile Aerobic and Anaerobic Respiratory Metabolism in Pseudomonas aeruginosa. *Front Microbiol,* 2**,** 103.

ARAI, H., KODAMA, T. & IGARASHI, Y. 1997. Cascade regulation of the two CRP/FNR-related transcriptional regulators (ANR and DNR) and the denitrification enzymes in Pseudomonas aeruginosa. *Mol Microbiol,* 25**,** 1141-8.

ARAI, H., KODAMA, T. & IGARASHI, Y. 1998. The role of the nirQOP genes in energy conservation during anaerobic growth of Pseudomonas aeruginosa. *Biosci Biotechnol Biochem,* 62**,** 1995-9.

ARAVIND, L., ANANTHARAMAN, V., BALAJI, S., BABU, M. M. & IYER, L. M. 2005. The many faces of the helix-turn-helix domain: transcription regulation and beyond. *FEMS Microbiol Rev,* 29**,** 231-62.

AZIZ, R. K., BARTELS, D., BEST, A. A., DEJONGH, M., DISZ, T., EDWARDS, R. A., FORMSMA, K., GERDES, S., GLASS, E. M., KUBAL, M., MEYER, F., OLSEN, G. J., OLSON, R., OSTERMAN, A. L., OVERBEEK, R. A., MCNEIL, L. K., PAARMANN, D., PACZIAN, T., PARRELLO, B., PUSCH, G. D., REICH, C., STEVENS, R., VASSIEVA, O., VONSTEIN, V., WILKE, A. & ZAGNITKO, O. 2008.

The RAST Server: rapid annotations using subsystems technology. *BMC Genomics,* 9**,** 75.

BALASUBRAMANIAN, D., SCHNEPER, L., KUMARI, H. & MATHEE, K. 2013. A dynamic and intricate regulatory network determines Pseudomonas aeruginosa virulence. *Nucleic Acids Res,* 41**,** 1-20.

BARRAUD, N., HASSETT, D. J., HWANG, S.-H., RICE, S. A., KJELLEBERG, S. & WEBB, J. S. 2006. Involvement of Nitric Oxide in Biofilm Dispersal of Pseudomonas aeruginosa. *Journal of Bacteriology,* 188**,** 7344-7353.

BARTH, A. L. & PITT, T. L. 1995. Auxotrophic variants of Pseudomonas aeruginosa are selected from prototrophic wild-type strains in respiratory infections in patients with cystic fibrosis. *J Clin Microbiol,* 33**,** 37-40.

BAYNHAM, P. J., BROWN, A. L., HALL, L. L. & WOZNIAK, D. J. 1999. Pseudomonas aeruginosa AlgZ, a ribbon-helix-helix DNA-binding protein, is essential for alginate synthesis and algD transcriptional activation. *Mol Microbiol,* 33**,** 1069-80.

BECK, C. F. & WARREN, R. A. 1988. Divergent promoters, a common form of gene organization. *Microbiol Rev,* 52**,** 318-26.

BERKS, B. C., FERGUSON, S. J., MOIR, J. W. & RICHARDSON, D. J. 1995. Enzymes and associated electron transport systems that catalyse the respiratory reduction of nitrogen oxides and oxyanions. *Biochim Biophys Acta,* 1232**,** 97-173.

BESTE, D. J., HOOPER, T., STEWART, G., BONDE, B., AVIGNONE-ROSSA, C., BUSHELL, M. E., WHEELER, P., KLAMT, S., KIERZEK, A. M. & MCFADDEN, J. 2007. GSMN-TB: a web-based genome-scale network model of Mycobacterium tuberculosis metabolism. *Genome Biol,* 8**,** R89.

BEZUIDT, O. K., KLOCKGETHER, J., ELSEN, S., ATTREE, I., DAVENPORT, C. F. & TUMMLER, B. 2013. Intraclonal genome diversity of Pseudomonas aeruginosa clones CHA and TB. *BMC Genomics,* 14**,** 416.

BIANCONI, I., JEUKENS, J., FRESCHI, L., ALCALA-FRANCO, B., FACCHINI, M., BOYLE, B., MOLINARO, A., KUKAVICA-IBRULJ, I., TUMMLER, B., LEVESQUE, R. C. & BRAGONZI, A. 2015. Comparative genomics and biological characterization of sequential Pseudomonas aeruginosa isolates from persistent airways infection. *BMC Genomics,* 16**,** 1105.

BILLAL, D. S., FENG, J., LEPROHON, P., LEGARE, D. & OUELLETTE, M. 2011. Whole genome analysis of linezolid resistance in Streptococcus pneumoniae reveals resistance and compensatory mutations. *BMC Genomics,* 12**,** 512.

BLAIR, J. M. A., WEBBER, M. A., BAYLAY, A. J., OGBOLU, D. O. & PIDDOCK, L. J. V. 2015. Molecular mechanisms of antibiotic resistance. *Nat Rev Micro,* 13**,** 42-51.

BLANC, D. S., SIEGRIST, H. H., SAHLI, R. & FRANCIOLI, P. 1993. Ribotyping of Pseudomonas aeruginosa: discriminatory power and usefulness as a tool for epidemiological studies. *J Clin Microbiol,* 31**,** 71-7.

BODEY, G. P., JADEJA, L. & ELTING, L. 1985. Pseudomonas bacteremia. Retrospective analysis of 410 episodes. *Arch Intern Med,* 145**,** 1621-9.

BODILIS, J., HEDDE, M., ORANGE, N. & BARRAY, S. 2006. OprF polymorphism as a marker of ecological niche in Pseudomonas. *Environ Microbiol,* 8**,** 1544-51.

BORDBAR, A. & PALSSON, B. O. 2012. Using the reconstructed genome-scale human metabolic network to study physiology and pathology. *Journal of Internal Medicine,* 271**,** 131-141.

BOUZA, E., BURILLO, A. & MUNOZ, P. 2002. Catheter-related infections: diagnosis and intravascular treatment. *Clin Microbiol Infect,* 8**,** 265-74.

BREDENBRUCH, F., GEFFERS, R., NIMTZ, M., BUER, J. & HAUSSLER, S. 2006. The Pseudomonas aeruginosa quinolone signal (PQS) has an iron-chelating activity. *Environ Microbiol,* 8**,** 1318-29.

BRILLET, K., RUFFENACH, F., ADAMS, H., JOURNET, L., GASSER, V., HOEGY, F., GUILLON, L., HANNAUER, M., PAGE, A. & SCHALK, I. J. 2012. An ABC transporter with two periplasmic binding proteins involved in iron acquisition in Pseudomonas aeruginosa. *ACS Chem Biol,* 7**,** 2036-45.

BRO, C., REGENBERG, B., FORSTER, J. & NIELSEN, J. 2006. In silico aided metabolic engineering of Saccharomyces cerevisiae for improved bioethanol production. *Metab Eng,* 8**,** 102-11.

CAILLE, O., ZINCKE, D., MERIGHI, M., BALASUBRAMANIAN, D., KUMARI, H., KONG, K.-F., SILVA-HERZOG, E., NARASIMHAN, G., SCHNEPER, L., LORY, S. & MATHEE, K. 2014. Structural and Functional Characterization of Pseudomonas aeruginosa Global Regulator AmpR. *Journal of Bacteriology,* 196**,** 3890-3902.

CAMPOS-GARCIA, J., CARO, A. D., NAJERA, R., MILLER-MAIER, R. M., AL-TAHHAN, R. A. & SOBERON-CHAVEZ, G. 1998. The Pseudomonas aeruginosa rhlG gene encodes an NADPH-dependent beta-ketoacyl reductase which is specifically involved in rhamnolipid synthesis. *J Bacteriol,* 180**,** 4442-51.

CASPI, R., ALTMAN, T., BILLINGTON, R., DREHER, K., FOERSTER, H., FULCHER, C. A., HOLLAND, T. A., KESELER, I. M., KOTHARI, A., KUBO, A., KRUMMENACKER, M., LATENDRESSE, M., MUELLER, L. A., ONG, Q., PALEY, S., SUBHRAVETI, P., WEAVER, D. S., WEERASINGHE, D., ZHANG, P. & KARP, P. D. 2014. The MetaCyc database of metabolic pathways and enzymes and the BioCyc collection of Pathway/Genome Databases. *Nucleic Acids Res,* 42**,** D459-71.

CASPI, R., ALTMAN, T., DREHER, K., FULCHER, C. A., SUBHRAVETI, P., KESELER, I. M., KOTHARI, A., KRUMMENACKER, M., LATENDRESSE, M., MUELLER, L. A., ONG, Q., PALEY, S., PUJAR, A., SHEARER, A. G., TRAVERS, M., WEERASINGHE, D., ZHANG, P. & KARP, P. D. 2012. The MetaCyc database of metabolic pathways and enzymes and the BioCyc collection of pathway/genome databases. *Nucleic Acids Research,* 40**,** D742-D753.

CELIS, R. T. 1999. Repression and activation of arginine transport genes in Escherichia coli K 12 by the ArgP protein. *J Mol Biol,* 294**,** 1087-95.

CHAKRABORTY, R., BRAUN, V., HANTKE, K. & CORNELIS, P. 2013. *Iron Uptake in Bacteria with Emphasis on E. coli and Pseudomonas*, Springer Netherlands.

CONESA, A., GOTZ, S., GARCIA-GOMEZ, J. M., TEROL, J., TALON, M. & ROBLES, M. 2005. Blast2GO: a universal tool for annotation, visualization and analysis in functional genomics research. *Bioinformatics,* 21**,** 3674-6.

CORREIA, A. Biofilm Formation. Unpublished image.

COSSON, P., ZULIANELLO, L., JOIN-LAMBERT, O., FAURISSON, F., GEBBIE, L., BENGHEZAL, M., VAN DELDEN, C., CURTY, L. K. & KÖHLER, T. 2002. Pseudomonas aeruginosa Virulence Analyzed in a Dictyostelium discoideum Host System. *Journal of Bacteriology,* 184**,** 3027-3033.

COSTERTON, J. W., CHENG, K. J., GEESEY, G. G., LADD, T. I., NICKEL, J. C., DASGUPTA, M. & MARRIE, T. J. 1987. Bacterial biofilms in nature and disease. *Annu Rev Microbiol,* 41**,** 435-64.

CRAMER, N., KLOCKGETHER, J., WRASMAN, K., SCHMIDT, M., DAVENPORT, C. F. & TUMMLER, B. 2011. Microevolution of the major common Pseudomonas aeruginosa clones C and PA14 in cystic fibrosis lungs. *Environ Microbiol,* 13**,** 1690-704.

CROUCHER, N. J., VERNIKOS, G. S., PARKHILL, J. & BENTLEY, S. D. 2011. Identification, variation and transcription of pneumococcal repeat sequences. *BMC Genomics,* 12**,** 120.

CRUSZ, S. A., POPAT, R., RYBTKE, M. T., CAMARA, M., GIVSKOV, M., TOLKER-NIELSEN, T., DIGGLE, S. P. & WILLIAMS, P. 2012. Bursting the bubble on bacterial biofilms: a flow cell methodology. *Biofouling,* 28**,** 835-42.

CUEVAS, D. A., EDIRISINGHE, J., HENRY, C. S., OVERBEEK, R., O'CONNELL, T. G. & EDWARDS, R. A. 2016. From DNA to FBA: How to Build Your Own Genome-Scale Metabolic Model. *Frontiers in Microbiology,* 7**,** 907.

CUTRUZZOLÀ, F. & FRANKENBERG-DINKEL, N. 2016. Origin and Impact of Nitric Oxide in Pseudomonas aeruginosa Biofilms. *Journal of Bacteriology,* 198**,** 55-65.

D'ARGENIO, D. A., CALFEE, M. W., RAINEY, P. B. & PESCI, E. C. 2002. Autolysis and Autoaggregation in Pseudomonas aeruginosa Colony Morphology Mutants. *Journal of Bacteriology,* 184**,** 6481-6489.

DANDEKAR, A. A. & GREENBERG, E. P. 2013. Microbiology: Plan B for quorum sensing. *Nat Chem Biol,* 9**,** 292-3.

DANESE, I., HAINE, V., DELRUE, R. M., TIBOR, A., LESTRATE, P., STEVAUX, O., MERTENS, P., PAQUET, J. Y., GODFROID, J., DE BOLLE, X. & LETESSON, J. J. 2004. The Ton system, an ABC transporter, and a universally conserved GTPase are involved in iron utilization by Brucella melitensis 16M. *Infect Immun,* 72**,** 5783-90.

DANIELS, R., VANDERLEYDEN, J. & MICHIELS, J. 2004. Quorum sensing and swarming migration in bacteria. *FEMS Microbiol Rev,* 28**,** 261-89.

DARCH, S. E., MCNALLY, A., HARRISON, F., CORANDER, J., BARR, H. L., PASZKIEWICZ, K., HOLDEN, S., FOGARTY, A., CRUSZ, S. A. & DIGGLE, S. P. 2015. Recombination is a key driver of genomic and phenotypic diversity in a Pseudomonas aeruginosa population during cystic fibrosis infection. *Scientific Reports,* 5**,** 7649.

DAVEY, M. E., CAIAZZA, N. C. & O'TOOLE, G. A. 2003. Rhamnolipid surfactant production affects biofilm architecture in Pseudomonas aeruginosa PAO1. *J Bacteriol,* 185**,** 1027-36.

DAVIES, J. 2006. Are antibiotics naturally antibiotics? *J Ind Microbiol Biotechnol,* 33**,** 496-9.

DE KIEVIT, T. R. 2009. Quorum sensing in Pseudomonas aeruginosa biofilms. *Environ Microbiol,* 11**,** 279-88.

DE VOS, D., BOUTON, C., SARNIGUET, A., DE VOS, P., VAUTERIN, M. & CORNELIS, P. 1998. Sequence diversity of the oprI gene, coding for major outer membrane lipoprotein I, among rRNA group I pseudomonads. *J Bacteriol,* 180**,** 6551-6.

DEGHMANE, A. E., GIORGINI, D., MAIGRE, L. & TAHA, M. K. 2004. Analysis in vitro and in vivo of the transcriptional regulator CrgA of Neisseria meningitidis upon contact with target cells. *Mol Microbiol,* 53**,** 917-27.

DELIHAS, N. 2011. Impact of small repeat sequences on bacterial genome evolution. *Genome Biol Evol,* 3**,** 959-73.

DEZIEL, E., GOPALAN, S., TAMPAKAKI, A. P., LEPINE, F., PADFIELD, K. E., SAUCIER, M., XIAO, G. & RAHME, L. G. 2005. The contribution of MvfR to Pseudomonas aeruginosa pathogenesis and quorum sensing circuitry regulation: multiple quorum sensing-regulated genes are modulated without affecting lasRI, rhlRI or the production of N-acyl-L-homoserine lactones. *Mol Microbiol,* 55**,** 998-1014.

DIETRICH, L. E., PRICE-WHELAN, A., PETERSEN, A., WHITELEY, M. & NEWMAN, D. K. 2006. The phenazine pyocyanin is a terminal signalling factor in the quorum sensing network of Pseudomonas aeruginosa. *Mol Microbiol,* 61**,** 1308-21.

DIGGLE, S. P., MATTHIJS, S., WRIGHT, V. J., FLETCHER, M. P., CHHABRA, S. R., LAMONT, I. L., KONG, X., HIDER, R. C., CORNELIS, P., CAMARA, M. & WILLIAMS, P. 2007. The Pseudomonas aeruginosa 4-quinolone signal molecules HHQ and PQS play multifunctional roles in quorum sensing and iron entrapment. *Chem Biol,* 14**,** 87-96.

DJONOVIC, S., URBACH, J. M., DRENKARD, E., BUSH, J., FEINBAUM, R., AUSUBEL, J. L., TRAFICANTE, D., RISECH, M., KOCKS, C., FISCHBACH, M. A., PRIEBE, G. P. & AUSUBEL, F. M. 2013. Trehalose biosynthesis promotes Pseudomonas aeruginosa pathogenicity in plants. *PLoS Pathog,* 9**,** e1003217.

DÖTSCH, A., POMMERENKE, C., BREDENBRUCH, F., GEFFERS, R. & HÄUSSLER, S. 2009. Evaluation of a microarray-hybridization based method applicable for discovery of single nucleotide polymorphisms (SNPs) in the Pseudomonas aeruginosa genome. *BMC Genomics,* 10**,** 1-13.

DREIER, J. & RUGGERONE, P. 2015. Interaction of antibacterial compounds with RND efflux pumps in Pseudomonas aeruginosa. *Frontiers in Microbiology,* 6**,** 660.

DU, S. J., KUO, H. C., CHENG, C. H., FEI, A. C. Y., WEI, H. W. & CHANG, S. K. 2010. Molecular mechanisms of ceftazidime resistance in Pseudomonas aeruginosa isolates from canine and human infections. *Veterinární Medicína,* 55**,** 172-182.

DUMAS, J. L., VAN DELDEN, C., PERRON, K. & KOHLER, T. 2006. Analysis of antibiotic resistance gene expression in Pseudomonas aeruginosa by quantitative real-time-PCR. *FEMS Microbiol Lett,* 254**,** 217-25.

DUROT, M., BOURGUIGNON, P.-Y. & SCHACHTER, V. 2009. Genome-scale models of bacterial metabolism: reconstruction and applications. *Fems Microbiology Reviews,* 33**,** 164-190.

EMERSON, D., AGULTO, L., LIU, H. & LIU, L. 2008. Identifying and Characterizing Bacteria in an Era of Genomics and Proteomics. *BioScience,* 58**,** 925-936.

ENTNER, N. & DOUDOROFF, M. 1952. Glucose and gluconic acid oxidation of Pseudomonas saccharophila. *J Biol Chem,* 196**,** 853-62.

ESTAHBANATI, H. K., KASHANI, P. P. & GHANAATPISHEH, F. 2002. Frequency of Pseudomonas aeruginosa serotypes in burn wound infections and their resistance to antibiotics. *Burns,* 28**,** 340-8.

EVANS, L. R. & LINKER, A. 1973. Production and Characterization of the Slime Polysaccharide of Pseudomonas aeruginosa. *Journal of Bacteriology,* 116**,** 915-924.

FARROW, J. M. & PESCI, E. C. 2007. Two Distinct Pathways Supply Anthranilate as a Precursor of the Pseudomonas Quinolone Signal. *Journal of Bacteriology,* 189**,** 3425-3433.

FAVERO, M. S., CARSON, L. A., BOND, W. W. & PETERSEN, N. J. 1971. Pseudomonas aeruginosa: growth in distilled water from hospitals. *Science,* 173**,** 836-8.

FAVRE-BONTÉ, S., KÖHLER, T. & VAN DELDEN, C. 2003. Biofilm formation by Pseudomonas aeruginosa: role of the C4-HSL cell-to-cell signal and inhibition by azithromycin. *Journal of Antimicrobial Chemotherapy,* 52**,** 598-604.

FERRANDEZ, A., HAWKINS, A. C., SUMMERFIELD, D. T. & HARWOOD, C. S. 2002. Cluster II che genes from Pseudomonas aeruginosa are required for an optimal chemotactic response. *J Bacteriol,* 184**,** 4374-83.

FETAR, H., GILMOUR, C., KLINOSKI, R., DAIGLE, D. M., DEAN, C. R. & POOLE, K. 2011. mexEF-oprN multidrug efflux operon of Pseudomonas aeruginosa: regulation by the MexT activator in response to nitrosative stress and chloramphenicol. *Antimicrob Agents Chemother,* 55**,** 508-14.

FILLOUX, A. 2011. Protein Secretion Systems in Pseudomonas aeruginosa: An Essay on Diversity, Evolution, and Function. *Frontiers in Microbiology,* 2**,** 155.

FLEURBAAIJ, F., KRAAKMAN, M. E. M., CLAAS, E. C. J., KNETSCH, C. W., VAN LEEUWEN, H. C., VAN DER BURGT, Y. E. M., VELDKAMP, K. E., VOS, M. C., GOESSENS, W., MERTENS, B. J., KUIJPER, E. J., HENSBERGEN, P. J. & NICOLARDI, S. 2016. Typing Pseudomonas aeruginosa Isolates with Ultrahigh Resolution MALDI-FTICR Mass Spectrometry. *Analytical Chemistry,* 88**,** 5996-6003.

FONDI, M. & LIÒ, P. 2015. Multi -omics and metabolic modelling pipelines: Challenges and tools for systems microbiology. *Microbiological Research,* 171**,** 52-64.

FOTHERGILL, J. L., WHITE, J., FOWERAKER, J. E., WALSHAW, M. J., LEDSON, M. J., MAHENTHIRALINGAM, E. & WINSTANLEY, C. 2010. Impact of Pseudomonas aeruginosa genomic instability on the application of typing methods for chronic cystic fibrosis infections. *J Clin Microbiol,* 48**,** 2053-9.

FOX, A., HAAS, D., REIMMANN, C., HEEB, S., FILLOUX, A. & VOULHOUX, R. 2008. Emergence of secretion-defective sublines of Pseudomonas aeruginosa PAO1 resulting from spontaneous mutations in the vfr global regulatory gene. *Appl Environ Microbiol,* 74**,** 1902-8.

FRANK, D. W. 2012. Research Topic on Pseudomonas aeruginosa, Biology, Genetics, and Host–Pathogen Interactions. *Frontiers in Microbiology,* 3**,** 20.

FRAPOLLI, M., DEFAGO, G. & MOENNE-LOCCOZ, Y. 2007. Multilocus sequence analysis of biocontrol fluorescent Pseudomonas spp. producing the antifungal compound 2,4-diacetylphloroglucinol. *Environ Microbiol,* 9**,** 1939-55.

FREITAS, A. L. & BARTH, A. L. 2004. Typing of Pseudomonas aeruginosa from hospitalized patients: a comparison of susceptibility and biochemical profiles with genotype. *Braz J Med Biol Res,* 37**,** 77-82.

FRIMMERSDORF, E., HORATZEK, S., PELNIKEVICH, A., WIEHLMANN, L. & SCHOMBURG, D. 2010. How Pseudomonas aeruginosa adapts to various environments: a metabolomic approach. *Environ Microbiol,* 12**,** 1734-47.

GALIMAND, M., GAMPER, M., ZIMMERMANN, A. & HAAS, D. 1991. Positive FNR-like control of anaerobic arginine degradation and nitrate respiration in Pseudomonas aeruginosa. *J Bacteriol,* 173**,** 1598-606.

GARCIA-FONTANA, C., CORRAL LUGO, A. & KRELL, T. 2014. Specificity of the CheR2 methyltransferase in Pseudomonas aeruginosa is directed by a C-terminal pentapeptide in the McpB chemoreceptor. *Sci Signal,* 7**,** ra34.

GARRISON, E. M., G. 2012. Haplotype-based variant detection from short-read sequencing. *arXiv Prepr. arXiv1207.3907 9*

GASTEIGER, E., GATTIKER, A., HOOGLAND, C., IVANYI, I., APPEL, R. D. & BAIROCH, A. 2003. ExPASy: The proteomics server for in-depth protein knowledge and analysis. *Nucleic Acids Res,* 31**,** 3784-8.

GELLATLY, S. L. & HANCOCK, R. E. 2013a. Pseudomonas aeruginosa: new insights into pathogenesis and host defenses. *Pathog Dis,* 67**,** 159-73.

GELLATLY, S. L. & HANCOCK, R. E. W. 2013b. Pseudomonas aeruginosa: new insights into pathogenesis and host defenses. *Pathogens and Disease,* 67**,** 159-173.

GIACCA, M. & MONTI-BRAGADIN, C. 1987. Multivariate analysis of antibiograms for typing Pseudomonas aeruginosa. *Eur J Clin Microbiol,* 6**,** 552-8.

GILBERT, K. B., KIM, T. H., GUPTA, R., GREENBERG, E. P. & SCHUSTER, M. 2009. Global position analysis of the Pseudomonas aeruginosa quorum-sensing transcription factor LasR. *Mol Microbiol,* 73**,** 1072-85.

GOLDBOURT, A., DAY, L. A. & MCDERMOTT, A. E. 2007. Assignment of congested NMR spectra: carbonyl backbone enrichment via the Entner-Doudoroff pathway. *J Magn Reson,* 189**,** 157-65.

GOMILA, M., PENA, A., MULET, M., LALUCAT, J. & GARCIA-VALDES, E. 2015. Phylogenomics and systematics in Pseudomonas. *Front Microbiol,* 6**,** 214.

GRESHAM, D., DUNHAM, M. J. & BOTSTEIN, D. 2008. Comparing whole genomes using DNA microarrays. *Nat Rev Genet,* 9**,** 291-302.

GRKOVIC, S., BROWN, M. H. & SKURRAY, R. A. 2002. Regulation of Bacterial Drug Export Systems. *Microbiology and Molecular Biology Reviews,* 66**,** 671-701.

GROSSO-BECERRA, M. V., SANTOS-MEDELLIN, C., GONZALEZ-VALDEZ, A., MENDEZ, J. L., DELGADO, G., MORALES-ESPINOSA, R., SERVIN-GONZALEZ, L., ALCARAZ, L. D. & SOBERON-CHAVEZ, G. 2014. Pseudomonas aeruginosa clinical and environmental isolates constitute a single population with high phenotypic diversity. *BMC Genomics,* 15**,** 318.

HA, D. G., RICHMAN, M. E. & O'TOOLE, G. A. 2014. Deletion mutant library for investigation of functional outputs of cyclic diguanylate metabolism in Pseudomonas aeruginosa PA14. *Appl Environ Microbiol,* 80**,** 3384-93.

HALL-STOODLEY, L., COSTERTON, J. W. & STOODLEY, P. 2004. Bacterial biofilms: from the Natural environment to infectious diseases. *Nat Rev Micro,* 2**,** 95-108.

HAUSSLER, S., ZIEGLER, I., LOTTEL, A., VON GOTZ, F., ROHDE, M., WEHMHOHNER, D., SARAVANAMUTHU, S., TUMMLER, B. & STEINMETZ, I. 2003. Highly adherent small-colony variants of Pseudomonas aeruginosa in cystic fibrosis lung infection. *J Med Microbiol,* 52**,** 295-301.

HEINEMANN, M., KUMMEL, A., RUINATSCHA, R. & PANKE, S. 2005. In silico genome-scale reconstruction and validation of the Staphylococcus aureus metabolic network. *Biotechnol Bioeng,* 92**,** 850-64.

HENRY, C. S., DEJONGH, M., BEST, A. A., FRYBARGER, P. M., LINSAY, B. & STEVENS, R. L. 2010. High-throughput generation, optimization and analysis of genome-scale metabolic models. *Nat Biotech,* 28**,** 977-982.

HENTZER, M., WU, H., ANDERSEN, J. B., RIEDEL, K., RASMUSSEN, T. B., BAGGE, N., KUMAR, N., SCHEMBRI, M. A., SONG, Z., KRISTOFFERSEN, P., MANEFIELD, M., COSTERTON, J. W., MOLIN, S., EBERL, L., STEINBERG, P., KJELLEBERG, S., HOIBY, N. & GIVSKOV, M. 2003. Attenuation of Pseudomonas aeruginosa virulence by quorum sensing inhibitors. *EMBO J,* 22**,** 3803-15.

HEROVEN, A. K. & DERSCH, P. 2006. RovM, a novel LysR-type regulator of the virulence activator gene rovA, controls cell invasion, virulence and motility of Yersinia pseudotuberculosis. *Mol Microbiol,* 62**,** 1469-83.

HEYDORN, A., NIELSEN, A. T., HENTZER, M., STERNBERG, C., GIVSKOV, M., ERSBØLL, B. K. & MOLIN, S. 2000. Quantification of biofilm structures by the novel computer program comstat. *Microbiology,* 146**,** 2395-2407.

HICKMAN, J. W., TIFREA, D. F. & HARWOOD, C. S. 2005. A chemosensory system that regulates biofilm formation through modulation of cyclic diguanylate levels. *Proceedings of the National Academy of Sciences of the United States of America,* 102**,** 14422-14427.

HOIBY, N., CIOFU, O., JOHANSEN, H. K., SONG, Z. J., MOSER, C., JENSEN, P. O., MOLIN, S., GIVSKOV, M., TOLKER-NIELSEN, T. & BJARNSHOLT, T. 2011. The clinical impact of bacterial biofilms. *Int J Oral Sci,* 3**,** 55-65.

HOLLOWAY, B. W. 1955. Genetic Recombination in Pseudomonas aeruginosa. *Journal of General Microbiology,* 13**,** 572-581.

HOLLOWAY, B. W., KRISHNAPILLAI, V. & MORGAN, A. F. 1979. Chromosomal genetics of Pseudomonas. *Microbiological Reviews,* 43**,** 73-102.

HOMANN, O. R., CAI, H., BECKER, J. M. & LINDQUIST, S. L. 2005. Harnessing natural diversity to probe metabolic pathways. *PLoS Genet,* 1**,** e80.

HOSHINO, T., KOSE-TERAI, K. & SATO, K. 1992. Solubilization and reconstitution of the Pseudomonas aeruginosa high affinity branched-chain amino acid transport system. *Journal of Biological Chemistry,* 267**,** 21313-21318.

HOSIE, A. H. F., ALLAWAY, D., GALLOWAY, C. S., DUNSBY, H. A. & POOLE, P. S. 2002. Rhizobium leguminosarum Has a Second General Amino Acid Permease with Unusually Broad Substrate Specificity and High Similarity to Branched-Chain Amino Acid Transporters (Bra/LIV) of the ABC Family. *Journal of Bacteriology,* 184**,** 4071-4080.

HOUSE OF COMMONS PUBLIC ACCOUNTS COMMITTEE 2009. Reducing healthcare associated infection in hospitals in England. .

JAMSHIDI, N. & PALSSON, B. Ø. 2007. Investigating the metabolic capabilities of Mycobacterium tuberculosis H37Rv using the in silico strain iNJ 661 and proposing alternative drug targets. *BMC Systems Biology,* 1**,** 1-20.

JEFFERSON, K. K. 2004. What drives bacteria to produce a biofilm? *FEMS Microbiol Lett,* 236**,** 163-73.

JENKINSON, H. F. & LAMONT, R. J. 2005. Oral microbial communities in sickness and in health. *Trends Microbiol,* 13**,** 589-95.

JIMENEZ, P. N., KOCH, G., THOMPSON, J. A., XAVIER, K. B., COOL, R. H. & QUAX, W. J. 2012. The multiple signaling systems regulating virulence in Pseudomonas aeruginosa. *Microbiol Mol Biol Rev,* 76**,** 46-65.

JIN, Y., YANG, H., QIAO, M. & JIN, S. 2011. MexT Regulates the Type III Secretion System through MexS and PtrC in Pseudomonas aeruginosa. *Journal of Bacteriology,* 193**,** 399-410.

JO, J., PRICE-WHELAN, A. & DIETRICH, L. E. 2014. An aerobic exercise: defining the roles of Pseudomonas aeruginosa terminal oxidases. *J Bacteriol,* 196**,** 4203-5.

JOHNSON, A. P. & WOODFORD, N. 2013. Global spread of antibiotic resistance: the example of New Delhi metallo-beta-lactamase (NDM)-mediated carbapenem resistance. *J Med Microbiol,* 62**,** 499-513.

JOIN-LAMBERT, O. F., MICHEA-HAMZEHPOUR, M., KOHLER, T., CHAU, F., FAURISSON, F., DAUTREY, S., VISSUZAINE, C., CARBON, C. & PECHERE, J. 2001. Differential selection of multidrug efflux mutants by trovafloxacin and ciprofloxacin in an experimental model of Pseudomonas aeruginosa acute pneumonia in rats. *Antimicrob Agents Chemother,* 45**,** 571-6.

JONES, N. H. 1997. Finding the area under a curve using JMP and a trapezoidal rule. *SAS Institute, Cary, NC, USA*.

JONG WU, J., CHUN LEE, Y., NING LEAW, S., CHU LIN, M. & CHAIN CHANG, T. 2004. Evaluation of an impedance method for subtyping of P seudomonas aeruginosa. *Diagnostic Microbiology and Infectious Disease,* 48**,** 181-189.

JØRGENSEN, K. M., WASSERMANN, T., JOHANSEN, H. K., CHRISTIANSEN, L. E., MOLIN, S., HØIBY, N. & CIOFU, O. 2015. Diversity of metabolic profiles of cystic fibrosis Pseudomonas aeruginosa during the early stages of lung infection. *Microbiology,* 161**,** 1447-1462.

JUHAS, M., WIEHLMANN, L., HUBER, B., JORDAN, D., LAUBER, J., SALUNKHE, P., LIMPERT, A. S., VON GOTZ, F., STEINMETZ, I., EBERL, L. & TUMMLER, B. 2004. Global regulation of quorum sensing and virulence by VqsR in Pseudomonas aeruginosa. *Microbiology,* 150**,** 831-41.

KANEHISA, M., GOTO, S., KAWASHIMA, S., OKUNO, Y. & HATTORI, M. 2004. The KEGG resource for deciphering the genome. *Nucleic Acids Res,* 32**,** D277-80.

KAPLAN, J. B. 2010. Biofilm dispersal: mechanisms, clinical implications, and potential therapeutic uses. *J Dent Res,* 89**,** 205-18.

KERR, K. G. & SNELLING, A. M. 2009. Pseudomonas aeruginosa: a formidable and ever-present adversary. *J Hosp Infect,* 73**,** 338-44.

KIDD, T. J., GRIMWOOD, K., RAMSAY, K. A., RAINEY, P. B. & BELL, S. C. 2011. Comparison of Three Molecular Techniques for Typing Pseudomonas aeruginosa Isolates in Sputum Samples from Patients with Cystic Fibrosis. *Journal of Clinical Microbiology,* 49**,** 263-268.

KIM, D. & SALZBERG, S. L. 2011. TopHat-Fusion: an algorithm for discovery of novel fusion transcripts. *Genome Biol,* 12**,** R72.

KIM, E. J., SABRA, W. & ZENG, A. P. 2003. Iron deficiency leads to inhibition of oxygen transfer and enhanced formation of virulence factors in cultures of Pseudomonas aeruginosa PAO1. *Microbiology,* 149**,** 2627-34.

KIRISITS, M. J. & PARSEK, M. R. 2006. Does Pseudomonas aeruginosa use intercellular signalling to build biofilm communities? *Cell Microbiol,* 8**,** 1841-9.

KIRISITS, M. J., PROST, L., STARKEY, M. & PARSEK, M. R. 2005. Characterization of Colony Morphology Variants Isolated from Pseudomonas aeruginosa Biofilms. *Applied and Environmental Microbiology,* 71**,** 4809-4821.

KITTEN, T., KINSCHERF, T. G., MCEVOY, J. L. & WILLIS, D. K. 1998. A newly identified regulator is required for virulence and toxin production in Pseudomonas syringae. *Mol Microbiol,* 28**,** 917-29.

KLEIN, L. & MIGULA, W. 1895. *Arbeiten aus dem bakteriologischen Institut der Technischen Hochschule zu Karlsruhe*, Nemnich.

KLOCKGETHER, J., CRAMER, N., WIEHLMANN, L., DAVENPORT, C. F. & TUMMLER, B. 2011. Pseudomonas aeruginosa Genomic Structure and Diversity. *Front Microbiol,* 2**,** 150.

KLOCKGETHER, J., MUNDER, A., NEUGEBAUER, J., DAVENPORT, C. F., STANKE, F., LARBIG, K. D., HEEB, S., SCHOCK, U., POHL, T. M., WIEHLMANN, L. & TUMMLER, B. 2010. Genome diversity of Pseudomonas aeruginosa PAO1 laboratory strains. *J Bacteriol,* 192**,** 1113-21.

KNIREL, Y. A. 1990. Polysaccharide Antigens of Pseudomonas Aeruginosa. *Critical Reviews in Microbiology,* 17**,** 273-304.

KNOTEN, C. A., WELLS, G., COLEMAN, J. P. & PESCI, E. C. 2014. A conserved suppressor mutation in a tryptophan auxotroph results in dysregulation of Pseudomonas quinolone signal synthesis. *J Bacteriol,* 196**,** 2413-22.

KOBOLDT, D. C., STEINBERG, K. M., LARSON, D. E., WILSON, R. K. & MARDIS, E. R. 2013. The next-generation sequencing revolution and its impact on genomics. *Cell,* 155**,** 27-38.

KOHLER, T., CURTY, L. K., BARJA, F., VAN DELDEN, C. & PECHERE, J. C. 2000. Swarming of Pseudomonas aeruginosa is dependent on cell-to-cell signaling and requires flagella and pili. *J Bacteriol,* 182**,** 5990-6.

KÖHLER, T., EPP, S. F., CURTY, L. K. & PECHÈRE, J.-C. 1999. Characterization of MexT, the Regulator of the MexE-MexF-OprN Multidrug Efflux System of Pseudomonas aeruginosa. *Journal of Bacteriology,* 181**,** 6300-6305.

KOHLER, T., MICHEA-HAMZEHPOUR, M., HENZE, U., GOTOH, N., CURTY, L. K. & PECHERE, J. C. 1997. Characterization of MexE-MexF-OprN, a positively regulated multidrug efflux system of Pseudomonas aeruginosa. *Mol Microbiol,* 23**,** 345-54.

KÖHLER, T., MICHEA-HAMZEHPOUR, M., PLESIAT, P., KAHR, A. L. & PECHERE, J. C. 1997. Differential selection of multidrug efflux systems by quinolones in Pseudomonas aeruginosa. *Antimicrobial Agents and Chemotherapy,* 41**,** 2540-3.

KOHLER, T., VAN DELDEN, C., CURTY, L. K., HAMZEHPOUR, M. M. & PECHERE, J. C. 2001. Overexpression of the MexEF-OprN multidrug efflux system affects cell-to-cell signaling in Pseudomonas aeruginosa. *J Bacteriol,* 183**,** 5213-22.

KOSTER, W. 2001. ABC transporter-mediated uptake of iron, siderophores, heme and vitamin B12. *Res Microbiol,* 152**,** 291-301.

KÖSTER, W. 2001. ABC transporter-mediated uptake of iron, siderophores, heme and vitamin B12. *Research in Microbiology,* 152**,** 291-301.

KUKAVICA-IBRULJ, I., SANSCHAGRIN, F., PETERSON, A., WHITELEY, M., BOYLE, B., MACKAY, J. & LEVESQUE, R. C. 2008. Functional genomics of PycR, a LysR family transcriptional regulator essential for maintenance of Pseudomonas aeruginosa in the rat lung. *Microbiology,* 154**,** 2106-18.

KULASEKARA, B. R., KAMISCHKE, C., KULASEKARA, H. D., CHRISTEN, M., WIGGINS, P. A. & MILLER, S. I. 2013. *c-di-GMP heterogeneity is generated by the chemotaxis machinery to regulate flagellar motility*.

KUMAR, A. & SCHWEIZER, H. P. 2011. Evidence of MexT-independent overexpression of MexEF-OprN multidrug efflux pump of Pseudomonas aeruginosa in presence of metabolic stress. *PLoS One,* 6**,** e26520.

KUNG, V. L., OZER, E. A. & HAUSER, A. R. 2010. The accessory genome of Pseudomonas aeruginosa. *Microbiol Mol Biol Rev,* 74**,** 621-41.

LAM, H., OH, D.-C., CAVA, F., TAKACS, C. N., CLARDY, J., DE PEDRO, M. A. & WALDOR, M. K. 2009. D-Amino Acids Govern Stationary Phase Cell Wall Remodeling in Bacteria. *Science,* 325**,** 1552-1555.

LAM, J., CHAN, R., LAM, K. & COSTERTON, J. W. 1980. Production of mucoid microcolonies by Pseudomonas aeruginosa within infected lungs in cystic fibrosis. *Infect Immun,* 28**,** 546-56.

LAMARCHE, M. G. & DEZIEL, E. 2011. MexEF-OprN efflux pump exports the Pseudomonas quinolone signal (PQS) precursor HHQ (4-hydroxy-2-heptylquinoline). *PLoS One,* 6**,** e24310.

LANGMEAD, B. & SALZBERG, S. L. 2012. Fast gapped-read alignment with Bowtie 2. *Nat Methods,* 9**,** 357-9.

LATENDRESSE, M. & KARP, P. D. 2011. Web-based metabolic network visualization with a zooming user interface. *BMC Bioinformatics,* 12**,** 1-9.

LECLERCQ, R. 2002. Mechanisms of resistance to macrolides and lincosamides: nature of the resistance elements and their clinical implications. *Clin Infect Dis,* 34**,** 482-92.

LEE, D. G., URBACH, J. M., WU, G., LIBERATI, N. T., FEINBAUM, R. L., MIYATA, S., DIGGINS, L. T., HE, J., SAUCIER, M., DEZIEL, E., FRIEDMAN, L., LI, L., GRILLS, G., MONTGOMERY, K., KUCHERLAPATI, R., RAHME, L. G. & AUSUBEL, F. M. 2006. Genomic analysis reveals that Pseudomonas aeruginosa virulence is combinatorial. *Genome Biol,* 7**,** R90.

LEWIS, N. E., NAGARAJAN, H. & PALSSON, B. O. 2012. Constraining the metabolic genotype-phenotype relationship using a phylogeny of in silico methods. *Nat Rev Microbiol,* 10**,** 291-305.

LI, H., HANDSAKER, B., WYSOKER, A., FENNELL, T., RUAN, J., HOMER, N., MARTH, G., ABECASIS, G. & DURBIN, R. 2009. The Sequence Alignment/Map format and SAMtools. *Bioinformatics,* 25**,** 2078-9.

LI, X. Z., LIVERMORE, D. M. & NIKAIDO, H. 1994. Role of efflux pump(s) in intrinsic resistance of Pseudomonas aeruginosa: resistance to tetracycline, chloramphenicol, and norfloxacin. *Antimicrob Agents Chemother,* 38**,** 1732-41.

LI, Y., XIA, H., BAI, F., XU, H., YANG, L., YAO, H., ZHANG, L., ZHANG, X., BAI, Y., SARIS, P. E. J., TOLKER-NIELSEN, T. & QIAO, M. 2007. Identification of a new gene PA5017 involved in flagella-mediated motility, chemotaxis and biofilm formation in Pseudomonas aeruginosa. *FEMS Microbiology Letters,* 272**,** 188-195.

LI, Z., KOSOROK, M. R., FARRELL, P. M., LAXOVA, A., WEST, S. E., GREEN, C. G., COLLINS, J., ROCK, M. J. & SPLAINGARD, M. L. 2005. Longitudinal development of mucoid Pseudomonas aeruginosa infection and lung disease progression in children with cystic fibrosis. *JAMA,* 293**,** 581-8.

LINARES, J. F., GUSTAFSSON, I., BAQUERO, F. & MARTINEZ, J. L. 2006. Antibiotics as intermicrobial signaling agents instead of weapons. *Proceedings of the National Academy of Sciences,* 103**,** 19484-19489.

LINARES, J. F., LOPEZ, J. A., CAMAFEITA, E., ALBAR, J. P., ROJO, F. & MARTINEZ, J. L. 2005. Overexpression of the multidrug efflux pumps MexCD-OprJ and MexEF-OprN is associated with a reduction of type III secretion in Pseudomonas aeruginosa. *J Bacteriol,* 187**,** 1384-91.

LINDSEY, R. L., POUSEELE, H., CHEN, J. C., STROCKBINE, N. A. & CARLETON, H. A. 2016. Implementation of Whole Genome Sequencing (WGS) for Identification and Characterization of Shiga Toxin-Producing Escherichia coli (STEC) in the United States. *Frontiers in Microbiology,* 7.

LINKER, A. & JONES, R. S. 1966. A new polysaccharide resembling alginic acid isolated from pseudomonads. *J Biol Chem,* 241**,** 3845-51.

LISTER, P. D., WOLTER, D. J. & HANSON, N. D. 2009. Antibacterial-resistant Pseudomonas aeruginosa: clinical impact and complex regulation of chromosomally encoded resistance mechanisms. *Clin Microbiol Rev,* 22**,** 582-610.

LIVERMORE, D. M. 1992. Interplay of impermeability and chromosomal beta-lactamase activity in imipenem-resistant Pseudomonas aeruginosa. *Antimicrob Agents Chemother,* 36**,** 2046-8.

LIVERMORE, D. M. 2002. Multiple Mechanisms of Antimicrobial Resistance in Pseudomonas aeruginosa: Our Worst Nightmare? *Clinical Infectious Diseases,* 34**,** 634-640.

LLANES, C., KOHLER, T., PATRY, I., DEHECQ, B., VAN DELDEN, C. & PLESIAT, P. 2011. Role of the MexEF-OprN efflux system in low-level resistance of Pseudomonas aeruginosa to ciprofloxacin. *Antimicrob Agents Chemother,* 55**,** 5676-84.

LODISE, T. P., JR., PATEL, N., KWA, A., GRAVES, J., FURUNO, J. P., GRAFFUNDER, E., LOMAESTRO, B. & MCGREGOR, J. C. 2007. Predictors of 30-day mortality among patients with Pseudomonas aeruginosa bloodstream infections: impact of delayed appropriate antibiotic selection. *Antimicrob Agents Chemother,* 51**,** 3510-5.

LOVE, M. I., ANDERS, S. & HUBER, W. 2014. Differential analysis of count data - the DESeq2 package. . *Genome Biology,* 15.

LOVEWELL, R. R., PATANKAR, Y. R. & BERWIN, B. 2014. Mechanisms of phagocytosis and host clearance of Pseudomonas aeruginosa. *American Journal of Physiology - Lung Cellular and Molecular Physiology,* 306**,** L591-L603.

LU, Q., EGGIMANN, P., LUYT, C.-E., WOLFF, M., TAMM, M., FRANÇOIS, B., MERCIER, E., GARBINO, J., LATERRE, P.-F., KOCH, H., GAFNER, V., RUDOLF, M. P., MUS, E., PEREZ, A., LAZAR, H., CHASTRE, J. & ROUBY, J.-J. 2014. Pseudomonas aeruginosa serotypes in nosocomial pneumonia: prevalence and clinical outcomes. *Critical Care,* 18**,** R17.

LUONG, P. M., SHOGAN, B. D., ZABORIN, A., BELOGORTSEVA, N., SHROUT, J. D., ZABORINA, O. & ALVERDY, J. C. 2014. Emergence of the P2 phenotype in

Pseudomonas aeruginosa PAO1 strains involves various mutations in mexT or mexF. *J Bacteriol,* 196**,** 504-13.

MAATALLAH, M., BAKHROUF, A., HABEEB, M. A., TURLEJ-ROGACKA, A., IVERSEN, A., POURCEL, C., SIOUD, O. & GISKE, C. G. 2013. Four genotyping schemes for phylogenetic analysis of Pseudomonas aeruginosa: comparison of their congruence with multi-locus sequence typing. *PLoS One,* 8**,** e82069.

MADDOCKS, S. E. & OYSTON, P. C. 2008. Structure and function of the LysR-type transcriptional regulator (LTTR) family proteins. *Microbiology,* 154**,** 3609-23.

MAH, T. F. & O'TOOLE, G. A. 2001. Mechanisms of biofilm resistance to antimicrobial agents. *Trends Microbiol,* 9**,** 34-9.

MAHENTHIRALINGAM, E., CAMPBELL, M. E., FOSTER, J., LAM, J. S. & SPEERT, D. P. 1996. Random amplified polymorphic DNA typing of Pseudomonas aeruginosa isolates recovered from patients with cystic fibrosis. *J Clin Microbiol,* 34**,** 1129-35.

MALONE, J. G., JAEGER, T., MANFREDI, P., DOTSCH, A., BLANKA, A., BOS, R., CORNELIS, G. R., HAUSSLER, S. & JENAL, U. 2012. The YfiBNR signal transduction mechanism reveals novel targets for the evolution of persistent Pseudomonas aeruginosa in cystic fibrosis airways. *PLoS Pathog,* 8**,** e1002760.

MALONE, J. G., JAEGER, T., SPANGLER, C., RITZ, D., SPANG, A., ARRIEUMERLOU, C., KAEVER, V., LANDMANN, R. & JENAL, U. 2010. YfiBNR mediates cyclic di-GMP dependent small colony variant formation and persistence in Pseudomonas aeruginosa. *PLoS Pathog,* 6**,** e1000804.

MANFREDI, R., NANETTI, A., FERRI, M. & CHIODO, F. 2000. Pseudomonas spp. complications in patients with HIV disease: an eight-year clinical and microbiological survey. *Eur J Epidemiol,* 16**,** 111-8.

MARGER, M. D. & SAIER, M. H., JR. 1993. A major superfamily of transmembrane facilitators that catalyse uniport, symport and antiport. *Trends Biochem Sci,* 18**,** 13-20.

MARTINEZ, J. L. & ROJO, F. 2011. Metabolic regulation of antibiotic resistance. *FEMS Microbiol Rev,* 35**,** 768-89.

MASEDA, H., SAITO, K., NAKAJIMA, A. & NAKAE, T. 2000. Variation of the mexT gene, a regulator of the MexEF-OprN efflux pump expression in wild-type strains of Pseudomonas aeruginosa. *FEMS Microbiology Letters,* 192**,** 107-112.

MASEDA, H., SAWADA, I., SAITO, K., UCHIYAMA, H., NAKAE, T. & NOMURA, N. 2004. Enhancement of the mexAB-oprM efflux pump expression by a quorum-sensing autoinducer and its cancellation by a regulator, MexT, of the mexEF-oprN efflux pump operon in Pseudomonas aeruginosa. *Antimicrob Agents Chemother,* 48**,** 1320-8.

MASEDA, H., UWATE, M. & NAKAE, T. 2010. Transcriptional regulation of the mexEF-oprN multidrug efflux pump operon by MexT and an unidentified repressor in nfxC-type mutant of Pseudomonas aeruginosa. *FEMS Microbiol Lett,* 311**,** 36-43.

MASHBURN, L. M. & WHITELEY, M. 2005. Membrane vesicles traffic signals and facilitate group activities in a prokaryote. *Nature,* 437**,** 422-5.

MATHEE, K., NARASIMHAN, G., VALDES, C., QIU, X., MATEWISH, J. M., KOEHRSEN, M., ROKAS, A., YANDAVA, C. N., ENGELS, R., ZENG, E., OLAVARIETTA, R., DOUD, M., SMITH, R. S., MONTGOMERY, P., WHITE, J. R., GODFREY, P. A., KODIRA, C., BIRREN, B., GALAGAN, J. E. & LORY, S. 2008. Dynamics of Pseudomonas aeruginosa genome evolution. *Proc Natl Acad Sci U S A,* 105**,** 3100-5.

MCCARTER, L. L. & GOMELSKY, M. 2015. Fifty ways to inhibit motility via cyclic di-GMP: the emerging Pseudomonas aeruginosa swarming story. *J Bacteriol,* 197**,** 406-9.

MCCARTHY, R. R., MOOIJ, M. J., REEN, F. J., LESOUHAITIER, O. & O'GARA, F. 2014. A new regulator of pathogenicity (bvlR) is required for full virulence and tight microcolony formation in Pseudomonas aeruginosa. *Microbiology,* 160**,** 1488-500.

MENA, K. D. & GERBA, C. P. 2009. Risk assessment of Pseudomonas aeruginosa in water. *Rev Environ Contam Toxicol,* 201**,** 71-115.

MERRITT, J. H., KADOURI, D. E. & O'TOOLE, G. A. 2005. Growing and analyzing static biofilms. *Curr Protoc Microbiol,* Chapter 1**,** Unit 1B 1.

MILLER, J. K., BADAWY, H. T., CLEMONS, C., KREIDER, K. L., WILBER, P., MILSTED, A. & YOUNG, G. 2012. Development of the Pseudomonas aeruginosa mushroom morphology and cavity formation by iron-starvation: a mathematical modeling study. *J Theor Biol,* 308**,** 68-78.

MITROPHANOV, A. Y. & GROISMAN, E. A. 2008. Signal integration in bacterial two-component regulatory systems. *Genes Dev,* 22**,** 2601-11.

MOE, L. A. 2013. Amino acids in the rhizosphere: From plants to microbes. *American Journal of Botany,* 100**,** 1692-1705.

MORITA, Y., TOMIDA, J. & KAWAMURA, Y. 2012. MexXY multidrug efflux system of Pseudomonas aeruginosa. *Front Microbiol,* 3**,** 408.

MORRISON, A. J., JR. & WENZEL, R. P. 1984. Epidemiology of infections due to Pseudomonas aeruginosa. *Rev Infect Dis,* 6 Suppl 3**,** S627-42.

NELSON, L. K., STANTON, M. M., ELPHINSTONE, R. E., HELWERDA, J., TURNER, R. J. & CERI, H. 2010. Phenotypic diversification in vivo: Pseudomonas aeruginosa gacS- strains generate small colony variants in vivo that are distinct from in vitro variants. *Microbiology,* 156**,** 3699-709.

O'MAY, C. & TUFENKJI, N. 2011. The Swarming Motility of Pseudomonas aeruginosa Is Blocked by Cranberry Proanthocyanidins and Other Tannin-Containing Materials. *Applied and Environmental Microbiology,* 77**,** 3061-3067.

OBERHARDT, M. A., GOLDBERG, J. B., HOGARDT, M. & PAPIN, J. A. 2010. Metabolic Network Analysis of Pseudomonas aeruginosa during Chronic Cystic Fibrosis Lung Infection. *Journal of Bacteriology,* 192**,** 5534-5548.

OBERHARDT, M. A., PUCHAŁKA, J., FRYER, K. E., MARTINS DOS SANTOS, V. A. P. & PAPIN, J. A. 2008. Genome-Scale Metabolic Network Analysis of the Opportunistic Pathogen Pseudomonas aeruginosa PAO1. *Journal of Bacteriology,* 190**,** 2790-2803.

OCAMPO-SOSA, A. A., CABOT, G., RODRIGUEZ, C., ROMAN, E., TUBAU, F., MACIA, M. D., MOYA, B., ZAMORANO, L., SUAREZ, C., PENA, C., DOMINGUEZ, M. A., MONCALIAN, G., OLIVER, A. & MARTINEZ-MARTINEZ, L. 2012. Alterations of OprD in carbapenem-intermediate and -susceptible strains of

Pseudomonas aeruginosa isolated from patients with bacteremia in a Spanish multicenter study. *Antimicrob Agents Chemother,* 56**,** 1703-13.

OCHS, M. M., MCCUSKER, M. P., BAINS, M. & HANCOCK, R. E. 1999. Negative regulation of the Pseudomonas aeruginosa outer membrane porin OprD selective for imipenem and basic amino acids. *Antimicrob Agents Chemother,* 43**,** 1085-90.

OLIVARES, J., ALVAREZ-ORTEGA, C., LINARES, J. F., ROJO, F., KOHLER, T. & MARTINEZ, J. L. 2012. Overproduction of the multidrug efflux pump MexEF-OprN does not impair Pseudomonas aeruginosa fitness in competition tests, but produces specific changes in bacterial regulatory networks. *Environ Microbiol,* 14**,** 1968-81.

OLIVARES, J., ÁLVAREZ-ORTEGA, C. & MARTINEZ, J. L. 2014. Metabolic Compensation of Fitness Costs Associated with Overexpression of the Multidrug Efflux Pump MexEF-OprN in Pseudomonas aeruginosa. *Antimicrobial Agents and Chemotherapy,* 58**,** 3904-3913.

OLIVAS, A. D., SHOGAN, B. D., VALUCKAITE, V., ZABORIN, A., BELOGORTSEVA, N., MUSCH, M., MEYER, F., TRIMBLE, W. L., AN, G., GILBERT, J., ZABORINA, O. & ALVERDY, J. C. 2012. Intestinal tissues induce an SNP mutation in Pseudomonas aeruginosa that enhances its virulence: possible role in anastomotic leak. *PLoS One,* 7**,** e44326.

OVERBEEK, R., OLSON, R., PUSCH, G. D., OLSEN, G. J., DAVIS, J. J., DISZ, T., EDWARDS, R. A., GERDES, S., PARRELLO, B., SHUKLA, M., VONSTEIN, V., WATTAM, A. R., XIA, F. & STEVENS, R. 2014. The SEED and the Rapid Annotation of microbial genomes using Subsystems Technology (RAST). *Nucleic Acids Res,* 42**,** D206-14.

OZEN, A. I. & USSERY, D. W. 2012. Defining the Pseudomonas genus: where do we draw the line with Azotobacter? *Microb Ecol,* 63**,** 239-48.

OZER, E. A., ALLEN, J. P. & HAUSER, A. R. 2012. Draft genome sequence of the Pseudomonas aeruginosa bloodstream isolate PABL056. *J Bacteriol,* 194**,** 5999.

PALEY, S. M. & KARP, P. D. 2006. The Pathway Tools cellular overview diagram and Omics Viewer. *Nucleic Acids Research,* 34**,** 3771-3778.

PALLERONI, N. J. 1993. Pseudomonas classification. A new case history in the taxonomy of gram-negative bacteria. *Antonie Van Leeuwenhoek,* 64**,** 231-51.

PALLERONI, N. J., KUNISAWA, R. & CONTOPOULOU, R. 1973. Nucleic Acid Homologies in the Genus Pseudomonas. *International Journal of Systematic and Evolutionary Microbiology,* 23**,** 333-339.

PALMER, G. C., JORTH, P. A. & WHITELEY, M. 2013. The role of two Pseudomonas aeruginosa anthranilate synthases in tryptophan and quorum signal production. *Microbiology,* 159**,** 959-69.

PALMER, K. L., MASHBURN, L. M., SINGH, P. K. & WHITELEY, M. 2005. Cystic Fibrosis Sputum Supports Growth and Cues Key Aspects of Pseudomonas aeruginosa Physiology. *Journal of Bacteriology,* 187**,** 5267-5277.

PAMP, S. J. & TOLKER-NIELSEN, T. 2007. Multiple roles of biosurfactants in structural biofilm development by Pseudomonas aeruginosa. *J Bacteriol,* 189**,** 2531-9.

PARSEK, M. R. & TOLKER-NIELSEN, T. 2008. Pattern formation in Pseudomonas aeruginosa biofilms. *Curr Opin Microbiol,* 11**,** 560-6.

PEARSON, J. P., VAN DELDEN, C. & IGLEWSKI, B. H. 1999. Active efflux and diffusion are involved in transport of Pseudomonas aeruginosa cell-to-cell signals. *J Bacteriol,* 181**,** 1203-10.

PENNA, V. T. C., MARTINS, S. A. M. & MAZZOLA, P. G. 2002. Identification of bacteria in drinking and purified water during the monitoring of a typical water purification system. *BMC Public Health,* 2**,** 1-11.

PESSI, G., WILLIAMS, F., HINDLE, Z., HEURLIER, K., HOLDEN, M. T. G., CÁMARA, M., HAAS, D. & WILLIAMS, P. 2001. The Global Posttranscriptional Regulator RsmA Modulates Production of Virulence Determinants andN-Acylhomoserine Lactones in Pseudomonas aeruginosa. *Journal of Bacteriology,* 183**,** 6676-6683.

PIDDOCK, L. J. 2006. Multidrug-resistance efflux pumps - not just for resistance. *Nat Rev Microbiol,* 4**,** 629-36.

POOLE, K. 2014. Stress responses as determinants of antimicrobial resistance in Pseudomonas aeruginosa: multidrug efflux and more. *Can J Microbiol,* 60**,** 783-91.

QIAN, X., BA, Y., ZHUANG, Q. & ZHONG, G. 2014. RNA-Seq Technology and Its Application in Fish Transcriptomics. *OMICS : a Journal of Integrative Biology,* 18**,** 98-110.

RAMSEY, M. M. & WHITELEY, M. 2004. Pseudomonas aeruginosa attachment and biofilm development in dynamic environments. *Mol Microbiol,* 53**,** 1075-87.

RASHID, M. H. & KORNBERG, A. 2000. Inorganic polyphosphate is needed for swimming, swarming, and twitching motilities of Pseudomonas aeruginosa. *Proc Natl Acad Sci U S A,* 97**,** 4885-90.

REEN, F. J., BARRET, M., FARGIER, E., O'MUINNEACHAIN, M. & O'GARA, F. 2013. Molecular evolution of LysR-type transcriptional regulation in Pseudomonas aeruginosa. *Mol Phylogenet Evol,* 66**,** 1041-9.

RENNER, L. D. & WEIBEL, D. B. 2011. Physicochemical regulation of biofilm formation. *MRS Bull,* 36**,** 347-355.

RIETSCH, A. & MEKALANOS, J. J. 2006. Metabolic regulation of type III secretion gene expression in Pseudomonas aeruginosa. *Mol Microbiol,* 59**,** 807-20.

RITCHIE, M. D., HOLZINGER, E. R., LI, R., PENDERGRASS, S. A. & KIM, D. 2015. Methods of integrating data to uncover genotype-phenotype interactions. *Nat Rev Genet,* 16**,** 85-97.

ROBINSON, M. D., MCCARTHY, D. J. & SMYTH, G. K. 2010. edgeR: a Bioconductor package for differential expression analysis of digital gene expression data. *Bioinformatics,* 26**,** 139-40.

RODRIGUE, A., QUENTIN, Y., LAZDUNSKI, A., MÉJEAN, V. & FOGLINO, M. 2000. Cell signalling by oligosaccharides. Two-component systems in Pseudomonas aeruginosa: why so many? *Trends in Microbiology,* 8**,** 498-504.

ROY, A. B., PETROVA, O. E. & SAUER, K. 2012. The Phosphodiesterase DipA (PA5017) Is Essential for Pseudomonas aeruginosa Biofilm Dispersion. *Journal of Bacteriology,* 194**,** 2904-2915.

RUTHERFORD, S. T. & BASSLER, B. L. 2012. Bacterial Quorum Sensing: Its Role in Virulence and Possibilities for Its Control. *Cold Spring Harbor Perspectives in Medicine,* 2.

SABRA, W., HADDAD, A. M. & ZENG, A. P. 2014. Comparative physiological study of the wild type and the small colony variant of Pseudomonas aeruginosa 20265 under controlled growth conditions. *World J Microbiol Biotechnol,* 30**,** 1027-36.

SABRA, W., KIM, E. J. & ZENG, A. P. 2002. Physiological responses of Pseudomonas aeruginosa PAO1 to oxidative stress in controlled microaerobic and aerobic cultures. *Microbiology,* 148**,** 3195-202.

SAIER, M. H., JR. 1994. Computer-aided analyses of transport protein sequences: gleaning evidence concerning function, structure, biogenesis, and evolution. *Microbiol Rev,* 58**,** 71-93.

SAKURAGI, Y. & KOLTER, R. 2007. Quorum-sensing regulation of the biofilm matrix genes (pel) of Pseudomonas aeruginosa. *J Bacteriol,* 189**,** 5383-6.

SANCHEZ, P., LINARES, J. F., RUIZ-DIEZ, B., CAMPANARIO, E., NAVAS, A., BAQUERO, F. & MARTINEZ, J. L. 2002. Fitness of in vitro selected Pseudomonas aeruginosa nalB and nfxB multidrug resistant mutants. *J Antimicrob Chemother,* 50**,** 657-64.

SANCHEZ, Z., TANI, A., SUZUKI, N., KARIYAMA, R., KUMON, H. & KIMBARA, K. 2013. Assessment of change in biofilm architecture by nutrient concentration using a multichannel microdevice flow system. *J Biosci Bioeng,* 115**,** 326-31.

SCHELL, M. A. 1993. Molecular biology of the LysR family of transcriptional regulators. *Annu Rev Microbiol,* 47**,** 597-626.

SCHERTZER, J. W. & WHITELEY, M. 2012. A bilayer-couple model of bacterial outer membrane vesicle biogenesis. *MBio,* 3.

SCHMIDT, K. D., TUMMLER, B. & ROMLING, U. 1996. Comparative genome mapping of Pseudomonas aeruginosa PAO with P. aeruginosa C, which belongs to a major clone in cystic fibrosis patients and aquatic habitats. *J Bacteriol,* 178**,** 85-93.

SCHOMBURG, I., CHANG, A. & SCHOMBURG, D. 2002. BRENDA, enzyme data and metabolic information. *Nucleic Acids Res,* 30**,** 47-9.

SCHUSTER, M. & GREENBERG, E. P. 2007. Early activation of quorum sensing in Pseudomonas aeruginosa reveals the architecture of a complex regulon. *BMC Genomics,* 8**,** 287.

SCHUSTER, M., HAWKINS, A. C., HARWOOD, C. S. & GREENBERG, E. P. 2004. The Pseudomonas aeruginosa RpoS regulon and its relationship to quorum sensing. *Mol Microbiol,* 51**,** 973-85.

SCHWEIZER, H. P. 2003. Efflux as a mechanism of resistance to antimicrobials in Pseudomonas aeruginosa and related bacteria: unanswered questions. *Genet Mol Res,* 2**,** 48-62.

SEEMANN, T. 2014. Prokka: rapid prokaryotic genome annotation. *Bioinformatics,* 30**,** 2068-9.

SIEGMAN-IGRA, Y., RAVONA, R., PRIMERMAN, H. & GILADI, M. 1998. Pseudomonas aeruginosa bacteremia: an analysis of 123 episodes, with particular emphasis on the effect of antibiotic therapy. *Int J Infect Dis,* 2**,** 211-5.

SIMM, R., MORR, M., KADER, A., NIMTZ, M. & RÖMLING, U. 2004. GGDEF and EAL domains inversely regulate cyclic di-GMP levels and transition from sessility to motility. *Molecular Microbiology,* 53**,** 1123-1134.

SMITH, E. E., BUCKLEY, D. G., WU, Z., SAENPHIMMACHAK, C., HOFFMAN, L. R., D'ARGENIO, D. A., MILLER, S. I., RAMSEY, B. W., SPEERT, D. P., MOSKOWITZ, S. M., BURNS, J. L., KAUL, R. & OLSON, M. V. 2006. Genetic adaptation by Pseudomonas aeruginosa to the airways of cystic fibrosis patients. *Proc Natl Acad Sci U S A,* 103**,** 8487-92.

SOBEL, M. L., NESHAT, S. & POOLE, K. 2005. Mutations in PA2491 (mexS) Promote MexT-Dependent mexEF-oprN Expression and Multidrug Resistance in a Clinical Strain of Pseudomonas aeruginosa. *Journal of Bacteriology,* 187**,** 1246-1253.

SPENCER, D. H., KAS, A., SMITH, E. E., RAYMOND, C. K., SIMS, E. H., HASTINGS, M., BURNS, J. L., KAUL, R. & OLSON, M. V. 2003. Whole-genome sequence variation among multiple isolates of Pseudomonas aeruginosa. *J Bacteriol,* 185**,** 1316-25.

SPIERS, A. J., BUCKLING, A. & RAINEY, P. B. 2000. The causes of Pseudomonas diversity. *Microbiology,* 146 (Pt 10)**,** 2345-50.

STARKEY, M., HICKMAN, J. H., MA, L., ZHANG, N., DE LONG, S., HINZ, A., PALACIOS, S., MANOIL, C., KIRISITS, M. J., STARNER, T. D., WOZNIAK, D. J., HARWOOD, C. S. & PARSEK, M. R. 2009. Pseudomonas aeruginosa rugose small-colony variants have adaptations that likely promote persistence in the cystic fibrosis lung. *J Bacteriol,* 191**,** 3492-503.

STOVER, C. K., PHAM, X. Q., ERWIN, A. L., MIZOGUCHI, S. D., WARRENER, P., HICKEY, M. J., BRINKMAN, F. S. L., HUFNAGLE, W. O., KOWALIK, D. J., LAGROU, M., GARBER, R. L., GOLTRY, L., TOLENTINO, E., WESTBROCK-WADMAN, S., YUAN, Y., BRODY, L. L., COULTER, S. N., FOLGER, K. R., KAS, A., LARBIG, K., LIM, R., SMITH, K., SPENCER, D., WONG, G. K. S., WU, Z., PAULSEN, I. T., REIZER, J., SAIER, M. H., HANCOCK, R. E. W., LORY, S. & OLSON, M. V. 2000. Complete genome sequence of Pseudomonas aeruginosa PAO1, an opportunistic pathogen. *Nature,* 406**,** 959-964.

STRATEVA, T. & YORDANOV, D. 2009. Pseudomonas aeruginosa – a phenomenon of bacterial resistance. *Journal of Medical Microbiology,* 58**,** 1133-1148.

SYRMIS, M. W., O'CARROLL, M. R., SLOOTS, T. P., COULTER, C., WAINWRIGHT, C. E., BELL, S. C. & NISSEN, M. D. 2004. Rapid genotyping of Pseudomonas aeruginosa isolates harboured by adult and paediatric patients with cystic fibrosis using repetitive-element-based PCR assays. *J Med Microbiol,* 53**,** 1089-96.

THIELE, I. & PALSSON, B. O. 2010. A protocol for generating a high-quality genome-scale metabolic reconstruction. *Nat. Protocols,* 5**,** 93-121.

TIAN, Z.-X., FARGIER, E., MAC AOGÁIN, M., ADAMS, C., WANG, Y.-P. & O'GARA, F. 2009a. Transcriptome profiling defines a novel regulon modulated by the LysR-type transcriptional regulator MexT in Pseudomonas aeruginosa. *Nucleic Acids Research,* 37**,** 7546-7559.

TIAN, Z.-X., MAC AOGÁIN, M., O'CONNOR, H. F., FARGIER, E., MOOIJ, M. J., ADAMS, C., WANG, Y.-P. & O'GARA, F. 2009b. MexT modulates virulence determinants in Pseudomonas aeruginosa independent of the MexEF-OprN efflux pump. *Microbial Pathogenesis,* 47**,** 237-241.

TINDALL, B. J., KAMPFER, P., EUZEBY, J. P. & OREN, A. 2006. Valid publication of names of prokaryotes according to the rules of nomenclature: past history and current practice. *Int J Syst Evol Microbiol,* 56**,** 2715-20.

TOBES, R., PAREJA-TOBES, P., MANRIQUE, M., PAREJA-TOBES, E., KOVACH, E., ALEKHIN, A. & PAREJA, E. 2015. Gene calling and bacterial genome annotation with BG7. *Methods Mol Biol,* 1231**,** 177-89.

TOLKER-NIELSEN, T. & STERNBERG, C. 2014. Methods for Studying Biofilm Formation: Flow Cells and Confocal Laser Scanning Microscopy. *In:* FILLOUX, A. & RAMOS, J.-L. (eds.) *Pseudomonas Methods and Protocols.* New York, NY: Springer New York.

TOYOFUKU, M., NOMURA, N., KUNO, E., TASHIRO, Y., NAKAJIMA, T. & UCHIYAMA, H. 2008. Influence of the Pseudomonas quinolone signal on denitrification in Pseudomonas aeruginosa. *J Bacteriol,* 190**,** 7947-56.

TRIANA, J., MONTAGUD✝, A., SIURANA, M., FUENTE, D., URCHUEGUÍA, A., GAMERMANN, D., TORRES, J., TENA, J., DE CÓRDOBA, P. F. & URCHUEGUÍA, J. F. 2014. Generation and Evaluation of a Genome-Scale Metabolic Network Model of Synechococcus elongatus PCC7942. *Metabolites,* 4**,** 680-698.

UWATE, M., ICHISE, Y. K., SHIRAI, A., OMASA, T., NAKAE, T. & MASEDA, H. 2013. Two routes of MexS-MexT-mediated regulation of MexEF-OprN and MexAB-OprM efflux pump expression in Pseudomonas aeruginosa. *Microbiol Immunol,* 57**,** 263-72.

VALDERREY, A. D., POZUELO, M. J., JIMENEZ, P. A., MACIA, M. D., OLIVER, A. & ROTGER, R. 2010. Chronic colonization by Pseudomonas aeruginosa of patients with obstructive lung diseases: cystic fibrosis, bronchiectasis, and chronic obstructive pulmonary disease. *Diagn Microbiol Infect Dis,* 68**,** 20-7.

VALOT, B., GUYEUX, C., ROLLAND, J. Y., MAZOUZI, K., BERTRAND, X. & HOCQUET, D. 2015. What It Takes to Be a Pseudomonas aeruginosa? The Core Genome of the Opportunistic Pathogen Updated. *PLoS One,* 10**,** e0126468.

VAN DOMSELAAR, G. H., STOTHARD, P., SHRIVASTAVA, S., CRUZ, J. A., GUO, A., DONG, X., LU, P., SZAFRON, D., GREINER, R. & WISHART, D. S. 2005. BASys: a web server for automated bacterial genome annotation. *Nucleic Acids Res,* 33**,** W455-9.

VAN KEULEN, G., RIDDER, A. N., DIJKHUIZEN, L. & MEIJER, W. G. 2003. Analysis of DNA binding and transcriptional activation by the LysR-type transcriptional regulator CbbR of Xanthobacter flavus. *J Bacteriol,* 185**,** 1245-52.

VARGIU, A. V. & NIKAIDO, H. 2012. Multidrug binding properties of the AcrB efflux pump characterized by molecular dynamics simulations. *Proc Natl Acad Sci U S A,* 109**,** 20637-42.

VASIL, M. L. & OCHSNER, U. A. 1999. The response of Pseudomonas aeruginosa to iron: genetics, biochemistry and virulence. *Mol Microbiol,* 34**,** 399-413.

VERCAMMEN, K., WEI, Q., CHARLIER, D., DOTSCH, A., HAUSSLER, S., SCHULZ, S., SALVI, F., GADDA, G., SPAIN, J., RYBTKE, M. L., TOLKER-NIELSEN, T., DINGEMANS, J., YE, L. & CORNELIS, P. 2015. Pseudomonas aeruginosa LysR PA4203 regulator NmoR acts as a repressor of the PA4202 nmoA gene, encoding a nitronate monooxygenase. *J Bacteriol,* 197**,** 1026-39.

VIDAL, F., MENSA, J., ALMELA, M., MARTINEZ, J. A., MARCO, F., CASALS, C., GATELL, J. M., SORIANO, E. & JIMENEZ DE ANTA, M. T. 1996. Epidemiology and outcome of Pseudomonas aeruginosa bacteremia, with special emphasis on the influence of antibiotic treatment. Analysis of 189 episodes. *Arch Intern Med,* 156**,** 2121-6.

VON DÖHREN, H. 2004. Antibiotics: Actions, origins, resistance, by C. Walsh. 2003. Washington, DC: ASM Press. 345 pp. $99.95 (hardcover). *Protein Science : A Publication of the Protein Society,* 13**,** 3059-3060.

WADE, D. S., CALFEE, M. W., ROCHA, E. R., LING, E. A., ENGSTROM, E., COLEMAN, J. P. & PESCI, E. C. 2005. Regulation of Pseudomonas Quinolone Signal Synthesis in Pseudomonas aeruginosa. *Journal of Bacteriology,* 187**,** 4372-4380.

WEI, Q., LE MINH, P. N., DÖTSCH, A., HILDEBRAND, F., PANMANEE, W., ELFARASH, A., SCHULZ, S., PLAISANCE, S., CHARLIER, D., HASSETT, D., HÄUSSLER, S. & CORNELIS, P. 2012. Global regulation of gene expression by OxyR in an important human opportunistic pathogen. *Nucleic Acids Research,* 40**,** 4320-4333.

WEI, Q., TARIGHI, S., DOTSCH, A., HAUSSLER, S., MUSKEN, M., WRIGHT, V. J., CAMARA, M., WILLIAMS, P., HAENEN, S., BOERJAN, B., BOGAERTS, A., VIERSTRAETE, E., VERLEYEN, P., SCHOOFS, L., WILLAERT, R., DE GROOTE, V. N., MICHIELS, J., VERCAMMEN, K., CRABBE, A. & CORNELIS, P. 2011. Phenotypic and genome-wide analysis of an antibiotic-resistant small colony variant (SCV) of Pseudomonas aeruginosa. *PLoS One,* 6**,** e29276.

WEISS NIELSEN, M., STERNBERG, C., MOLIN, S., REN & REGENBERG, B. 2011. Pseudomonas aeruginosa and Saccharomyces cerevisiae Biofilm in Flow Cells. e2383.

WILLIAMS, H. D., ZLOSNIK, J. E. & RYALL, B. 2007. Oxygen, cyanide and energy generation in the cystic fibrosis pathogen Pseudomonas aeruginosa. *Adv Microb Physiol,* 52**,** 1-71.

WINSOR, G. L., GRIFFITHS, E. J., LO, R., DHILLON, B. K., SHAY, J. A. & BRINKMAN, FIONA S. L. 2016. Enhanced annotations and features for comparing thousands of Pseudomonas genomes in the Pseudomonas genome database. *Nucleic Acids Research,* 44**,** D646-D653.

WOLFGANG, M. C., KULASEKARA, B. R., LIANG, X., BOYD, D., WU, K., YANG, Q., MIYADA, C. G. & LORY, S. 2003. Conservation of genome content and virulence determinants among clinical and environmental isolates of Pseudomonas aeruginosa. *Proc Natl Acad Sci U S A,* 100**,** 8484-9.

WOODFORD, N., TURTON, J. F. & LIVERMORE, D. M. 2011. Multiresistant Gram-negative bacteria: the role of high-risk clones in the dissemination of antibiotic resistance. *FEMS Microbiol Rev,* 35**,** 736-55.

WORKENTINE, M. L., SIBLEY, C. D., GLEZERSON, B., PURIGHALLA, S., NORGAARD-GRON, J. C., PARKINS, M. D., RABIN, H. R. & SURETTE, M. G. 2013. Phenotypic heterogeneity of Pseudomonas aeruginosa populations in a cystic fibrosis patient. *PLoS One,* 8**,** e60225.

WRIGHT, G. D. 2005. Bacterial resistance to antibiotics: enzymatic degradation and modification. *Adv Drug Deliv Rev,* 57**,** 1451-70.

YAMAMOTO, S., KASAI, H., ARNOLD, D. L., JACKSON, R. W., VIVIAN, A. & HARAYAMA, S. 2000. Phylogeny of the genus Pseudomonas: intrageneric

structure reconstructed from the nucleotide sequences of gyrB and rpoD genes. *Microbiology,* 146 (Pt 10)**,** 2385-94.

YANG, L., HU, Y., LIU, Y., ZHANG, J., ULSTRUP, J. & MOLIN, S. 2011. Distinct roles of extracellular polymeric substances in Pseudomonas aeruginosa biofilm development. *Environ Microbiol,* 13**,** 1705-17.

YERAMIAN, E. & JONES, L. 2003. GeneFizz: A web tool to compare genetic (coding/non-coding) and physical (helix/coil) segmentations of DNA sequences. Gene discovery and evolutionary perspectives. *Nucleic Acids Res,* 31**,** 3843-9.

YOON, S. S., HENNIGAN, R. F., HILLIARD, G. M., OCHSNER, U. A., PARVATIYAR, K., KAMANI, M. C., ALLEN, H. L., DEKIEVIT, T. R., GARDNER, P. R., SCHWAB, U., ROWE, J. J., IGLEWSKI, B. H., MCDERMOTT, T. R., MASON, R. P., WOZNIAK, D. J., HANCOCK, R. E., PARSEK, M. R., NOAH, T. L., BOUCHER, R. C. & HASSETT, D. J. 2002. Pseudomonas aeruginosa anaerobic respiration in biofilms: relationships to cystic fibrosis pathogenesis. *Dev Cell,* 3**,** 593-603.

ZHANG, L., KASIF, S., CANTOR, C. R. & BROUDE, N. E. 2004. GC/AT-content spikes as genomic punctuation marks. *Proceedings of the National Academy of Sciences of the United States of America,* 101**,** 16855-16860.

ZHOU, L., LEI, X.-H., BOCHNER, B. R. & WANNER, B. L. 2003. Phenotype MicroArray Analysis of Escherichia coli K-12 Mutants with Deletions of All Two-Component Systems. *Journal of Bacteriology,* 185**,** 4956-4972.

ZIMMERMANN, A., REIMMANN, C., GALIMAND, M. & HAAS, D. 1991. Anaerobic growth and cyanide synthesis of Pseudomonas aeruginosa depend on anr, a regulatory gene homologous with fnr of Escherichia coli. *Mol Microbiol,* 5**,** 1483-90.

ZOBELL, C. E. & ANDERSON, D. Q. 1936. Observations on the multiplication of bacteria in different volumes of stored sea water and the influence of oxygen tension and solid surfaces. *The Biological Bulletin,* 71**,** 324-342.

8 Appendicies

8.1 Chapter 2

8.1.1 Whole genome sequencing results

SNP and indel differences among PAO1 lineages: The four PAO1 lineages were compared to *P. aeruginosa* PAO1 (GenBank accession no. NC002516.2). Results indicated in: orange are strain specific mutations, green are mutations found in the ATCC lineages and blue are mutations found in all PAO1 lineages. *167 mutations were found within bacteriophage linked genes only in the ATCC lineages. Genes with variation were named or denoted as PA number; other SNPs were denoted by P_ positions within the genome. 0 is indicated when there was no sequence coverage.

Position	PAO1-DM	PAO1-AM	PAO1-AL	PAO1-AS	Gene name	Encoded product	Ref	Alt	Effect	AA change
332051				✓	PA0295	Probable periplasmic polyamine binding protein	A	G	missense	p.Phe258Ser/c.773T>C
66 3845				✓	PA0602	Probable binding protein component of ABC transporter	G	A	missense	p.Val111Ile/c.331G>A
720551			✓		tyrZ	Tyrosyl-tRNA synthetase 2	A	G	synonymous	p.Gly65Gly/c.195A>G
790429			✓		PA0720	Helix destabilizing protein of bacteriophage Pf1	C	T	synonymous	p.Gly88Gly/c.264C>T
790447			✓		PA0720	Helix destabilizing protein of bacteriophage Pf1	G	A	synonymous	p.Gln94Gln/c.282G>A
792152			✓		PA0724	Probable coat protein A of bacteriophage Pf1	T	C	synonymous	p.Asn261Asn/c.783T>C

Position					Gene	Description	Ref	Alt	Effect	Change
792275	0		✓		PA0724	Probable coat protein A of bacteriophage Pf1	C	T	synonymous	p.Asn302Asn/c.906C>T
1078735	✓		✓		pqsA	Probable coenzyme A ligase	C	T	synonymous	p.Leu92Leu/c.274C>T
1237197	✓				PA1145	Probable transcriptional regulator	T	C	missense	p.Leu185Pro/c.554T>C
2807665			✓		mexT	Transcriptional regulator	G	C	missense	p.Arg66Pro/c.197G>C
2807693			✓	✓	mexT	Transcriptional regulator	TCGGCCAGC	T	frameshift	p.Arg76fs/c.226 233delCGGCCAGC
2807985				✓	mexT	Transcriptional regulator	G	GTCC	inframe insertion	p.Val173 Leu174insValLeu/c.518 519insTCC
4144991				✓	wspF	Probable methylesterase	T	G	missense	p.Gln319Pro/c.956A>C
5642054			✓		PA5017	conserved hypothetical protein	C	T	stop gained	p.Gln349*/c.1045C>T
183697		✓	✓	✓	PA0159	probable transcriptional regulator	T	G	missense	p.Cys310Trp/c.930T>G
2342110		✓	✓	✓			C	CT	intergenic region	
2807982		✓	✓	✓	mexT	Transcriptional regulator	T	A	missense	p.Phe172Ile/c.514T>A
4869855		✓	✓	✓	PA4341	Probable transcriptional regulator	T	G	missense	p.Glu158Asp/c.474A>C
5036891		✓	✓	✓			A	C	intergenic region	
5071543		✓	✓	✓			AACTG	A	intergenic region	
6079222		✓	✓	✓	dgcB	DgcB, Dimethylglycine catabolism	A	G	synonymous	p.Leu393Leu/c.1179A>G
789170-795768*		✓	✓	✓	PA0717-PA0727 coaB	coat protein B of bacteriophage Pf1, hypothetical protein from bacteriophage Pf1				
169283	✓	✓	✓	✓			CG	C	intergenic region	
411125	✓	✓	✓	✓			AC	A	intergenic region	

Position					Gene	Protein	Ref	Alt	Effect	Notation
413850	✓	✓	✓	✓			T	C	intergenic region	
667028	✓	✓	✓	✓			G	GC	intergenic region	
740419	✓	✓	✓	✓	PA0683	Probable type II secretion system protein	G	GC	frameshift	p.Val73 Arg74fs/c.218 219insC
816529	✓	✓	✓	✓			G	GC	intergenic region	
891099	0	✓	0	✓			A	AC	intergenic region	
1116213	✓	✓	✓	✓			G	GC	intergenic region	
1215657	✓	✓	✓	✓			A	AG	intergenic region	
1275766	✓	✓	✓	✓	napA	Periplasmic nitrate reductase protein NapA	GA	G	frameshift	p.Phe11fs/c.32delT
1440622	✓	✓	0	✓	PA1327	Probable protease	CA	C	frameshift	p.Lys640fs/c.1918delA
1445357	✓	✓	✓	✓			A	AG	intergenic region	
1467482	✓	✓	✓	✓			A	AGC	intergenic region	
1467483	✓	✓	✓	✓			C	G	intergenic region	
1589438	✓	✓	✓	✓	PA1459	Probable methyltransferase	G	C	missense	p.Gly34Ala/c.101G>C
1835045	✓	✓	✓	✓	masA	Enolase-phosphatase E-1	G	GC	frameshift	p.Ser218 Ser219fs/c.654 655insC
2169348	✓	✓	✓	✓			A	AG	intergenic region	
2186927	✓	✓	✓	✓			G	GC	intergenic region	
2195457	✓	✓	✓	✓			G	GC	intergenic region	
2239547	✓	✓	✓	✓			T	G	intergenic region	
2239555	✓	✓	✓	✓			A	AG	intergenic region	
2355771	✓	✓	✓	✓			A	AG	intergenic region	

2356681	✓	✓	✓	✓	PA2141	Hypothetical protein	GC	G	frameshift	p.Ala172fs/c.515delC
2532046	✓	✓	✓	✓			G	GC	intergenic region	
2669175	✓	✓	✓	✓	pvdJ	Pyoverdine biosynthesis	G	C	missense	p.Pro819Ala/c.2455C>G
2753522	✓	✓	✓	✓			G	GC	intergenic region	
3016844	✓	✓	✓	✓			G	GC	intergenic region	
3083196	✓	✓	✓	✓			A	AG	intergenic region	
3919508	✓	✓	✓	✓			G	GC	intergenic region	
4212201	✓	✓	✓	✓	PA3760	N-Acetyl-D-Glucosamine phosphotransferase system transporter	A	G	missense	p.His636Arg/c.1907A>G
4344266	✓	✓	✓	✓	narK1	Nitrite extrusion protein 1	A	G	synonymous	p.Leu190Leu/c.570T>C
4448855	✓	✓	✓	✓			C	G	intergenic region	
4448856	✓	✓	✓	✓			G	C	intergenic region	
4539468	✓	✓	✓	✓			G	GC	intergenic region	
4888194	✓	✓	✓	✓			A	AG	intergenic region	
4924552	✓	✓	✓	✓	PA4394	Hypothetical protein	C	G	missense	p.Val178Leu/c.532G>C
4924553	✓	✓	✓	✓	PA4394	Hypothetical protein	G	C	synonymous	p.Pro177Pro/c.531C>G
5033101	✓	✓	✓	✓			G	GC	intergenic region	
5472415	✓	✓	✓	✓			C	CG	intergenic region	
5655220	✓	✓	✓	✓	PA5024	Conserved hypothetical protein	C	CCGG	inframe insertion	p.Ala222 Gly223insAlaGly/c.666 667insCGG
5743461	✓	✓	✓	✓	hutU	Urocanase	C	G	synonymous	p.Thr431Thr/c.1293G>C
5743462	✓	✓	✓	✓	hutU	Urocanase	G	C	missense	p.Thr431Arg/c.1292C>G

6098781	✓	✓	✓	✓	soxA	Sarcosine oxidase alpha subunit	G	C	synonymous	p.Gly586Gly/c.1758G>C
6115455	✓	✓	✓	✓	mtr	Tryptophan permease	T	G	missense	p.Lys286Asn/c.858A>C
816529	✓	✓	✓	✓	PA0748	Still frameshift probable transcriptional regulator	G	GC		

8.2 Chapter 3

8.2.1 Fold change between test groups PA vs PAdel and PA vs PAnfxC

Signal values for each strain with replicate results (n=2). Negative controls were subtracted from the tests. A value of 1 was added to all results to ensure the fold change could be calculated. A student t-test was applied to SV (signal value) results with p-values shown.

PM plate	Substrate	Rep 1 PA SV	Rep 2 PA SV	PA average SV	Rep 1 PAdel SV	Rep 2 PAdel SV	PAdel average SV	Rep 1 PAnfxC SV	Rep 2 PAnfxC SV	PAnfxC average SV	PA vs PAdel fold change	PA vs Padel p-value	PA vs PanfxC fold change	Pa vs Padel p-value
1	Uridine	45.8	44.7	45.2	5.2	6.5	5.8	4.1	1.7	2.9	7.8	0.000	15.6	0.001
1	Inosine	159.0	146.2	152.6	29.7	28.0	28.9	33.1	31.5	32.3	5.3	0.003	4.7	0.003
1	D-Ribose	25.3	28.6	27.0	5.1	7.3	6.2	6.9	4.3	5.6	4.4	0.009	4.8	0.010
1	Adenosine	41.5	47.2	44.4	19.7	20.9	20.3	19.7	15.7	17.7	2.2	0.015	2.5	0.017
1	D-Malic Acid	2.7	2.3	2.5	2.9	3.5	3.2	1.0	1.0	1.0	0.8	0.199	2.5	0.017
1	D,L-Malic Acid	243.2	241.3	242.3	242.7	231.5	237.1	235.4	235.1	235.3	1.0	0.463	1.0	0.019
1	L-Serine	100.1	89.8	94.9	57.1	53.7	55.4	55.8	50.1	52.9	1.7	0.018	1.8	0.019
1	Glycyl-L-Aspartic Acid	9.4	10.2	9.8	1.0	4.8	2.9	4.1	2.3	3.2	3.4	0.069	3.1	0.023
1	Mono Methyl Succinate	170.9	175.1	173.0	196.0	185.0	190.5	187.4	190.7	189.1	0.9	0.097	0.9	0.026
1	Glycyl-L-Glutamic Acid	18.6	14.6	16.6	3.1	7.6	5.4	6.1	3.6	4.8	3.1	0.064	3.4	0.037
1	D-Fructose	228.9	226.7	227.8	220.3	202.2	211.3	208.7	197.4	203.1	1.1	0.210	1.1	0.051
1	Tween 40	239.0	241.9	240.5	237.7	236.9	237.3	229.7	233.4	231.6	1.0	0.166	1.0	0.063
1	L-Asparagine	265.3	255.1	260.2	244.9	231.7	238.3	241.5	234.2	237.8	1.1	0.120	1.1	0.071
1	D-Trehalose	64.8	42.7	53.7	10.4	12.5	11.4	20.3	1.0	10.6	4.7	0.062	5.0	0.099
1	Pyruvic Acid	188.3	144.7	166.5	219.9	228.0	223.9	231.4	223.4	227.4	0.7	0.122	0.7	0.111

1	Tyramine	252.4	248.2	250.3	193.2	194.7	193.9	216.4	174.6	195.5	1.3	0.002	1.3	0.121
1	Fumaric Acid	248.1	246.4	247.2	253.9	238.8	246.4	252.5	249.8	251.2	1.0	0.921	1.0	0.130
1	L-Glutamic Acid	240.6	241.2	240.9	240.5	214.8	227.6	231.4	218.8	225.1	1.1	0.410	1.1	0.130
1	α-Hydroxy Butyric Acid	9.0	10.6	9.8	34.6	27.1	30.9	35.4	20.4	27.9	0.3	0.032	0.3	0.137
1	Methyl Pyruvate	18.3	80.7	49.5	126.7	112.6	119.7	127.2	120.6	123.9	0.4	0.160	0.4	0.141
1	Tween 20	177.3	195.0	186.2	226.6	198.9	212.7	206.4	204.4	205.4	0.9	0.247	0.9	0.164
1	L-Threonine	5.4	10.0	7.7	4.7	2.0	3.4	1.0	3.5	2.2	2.3	0.249	3.4	0.174
1	D-Gluconic Acid	259.3	258.7	259.0	259.0	250.4	254.7	256.7	251.5	254.1	1.0	0.422	1.0	0.205
1	L-Aspartic Acid	240.4	251.7	246.1	235.0	228.9	232.0	236.7	219.3	228.0	1.1	0.160	1.1	0.225
1	α-D-Glucose	246.6	244.5	245.5	246.4	238.2	242.3	244.1	242.8	243.4	1.0	0.524	1.0	0.230
1	Acetic Acid	212.4	228.6	220.5	209.6	195.7	202.7	214.4	188.8	201.6	1.1	0.236	1.1	0.339
1	1,2-Propanediol	8.1	37.0	22.5	58.7	46.3	52.5	76.0	33.1	54.5	0.4	0.197	0.4	0.341
1	Glycerol	192.2	222.3	207.2	241.4	217.1	229.2	228.8	223.0	225.9	0.9	0.373	0.9	0.348
1	Glycolic Acid	1.0	1.0	1.0	1.0	8.3	4.7	3.6	28.7	16.2	0.2	0.423	0.1	0.350
1	α-Keto-Butyric Acid	18.2	10.1	14.1	38.6	29.9	34.2	57.2	16.6	36.9	0.4	0.078	0.4	0.386
1	L-Malic Acid	244.7	227.7	236.2	210.4	220.7	215.5	233.0	204.0	218.5	1.1	0.173	1.1	0.402
1	D-Threonine	1.0	3.3	2.1	1.0	1.0	1.0	1.0	1.0	1.0	2.1	0.423	2.1	0.423
1	α-Hydroxy Glutaric Acid-γ-Lactone	1.1	1.0	1.1	1.0	1.0	1.0	1.0	1.0	1.0	1.1	0.423	1.1	0.423
1	Thymidine	3.5	1.0	2.3	1.0	5.0	3.0	1.0	1.0	1.0	0.8	0.782	2.3	0.423
1	D,L-α-Glycerol-Phosphate	26.1	11.1	18.6	3.7	16.7	10.2	15.7	2.8	9.3	1.8	0.487	2.0	0.445
1	2-Aminoethanol	267.5	205.2	236.3	197.3	204.0	200.6	217.7	193.3	205.5	1.2	0.372	1.2	0.453
1	N-Acetyl-DGlucosamine	217.5	165.7	191.6	231.5	187.5	209.5	221.2	206.3	213.8	0.9	0.651	0.9	0.497
1	Propionic Acid	242.0	243.8	242.9	243.4	238.1	240.8	245.6	219.1	232.3	1.0	0.526	1.0	0.510
1	α-Keto-Glutaric Acid	245.3	258.3	251.8	256.3	241.1	248.7	245.6	248.7	247.2	1.0	0.784	1.0	0.555
1	L-Arabinose	3.9	3.3	3.6	2.9	3.8	3.4	3.6	3.1	3.3	1.1	0.721	1.1	0.558

1	L-Glutamine	264.9	260.3	262.6	253.2	258.1	255.6	264.6	250.6	257.6	1.0	0.174	1.0	0.566
1	Formic Acid	12.4	5.3	8.9	10.1	21.8	15.9	16.7	8.0	12.3	0.6	0.411	0.7	0.599
1	L-Lyxose	73.9	69.6	71.8	63.6	52.8	58.2	74.9	58.6	66.7	1.2	0.144	1.1	0.610
1	p-Hydroxy Phenyl Acetic Acid	268.6	249.9	259.2	250.9	260.5	255.7	262.6	239.1	250.8	1.0	0.769	1.0	0.632
1	D-Glucose-6-Phosphate	1.0	1.3	1.2	1.0	7.1	4.0	1.0	1.8	1.4	0.3	0.445	0.8	0.651
1	D-Mannitol	229.9	232.1	231.0	236.2	224.0	230.1	230.8	230.1	230.4	1.0	0.899	1.0	0.678
1	Succinic Acid	180.8	171.5	176.1	173.7	141.8	157.7	182.2	157.9	170.0	1.1	0.383	1.0	0.687
1	Bromo Succinic Acid	77.8	93.6	85.7	97.9	94.0	95.9	92.1	86.5	89.3	0.9	0.337	1.0	0.711
1	D-Serine	1.7	4.8	3.3	6.9	5.0	5.9	2.2	3.3	2.7	0.6	0.284	1.2	0.776
1	L-Proline	263.5	256.0	259.7	258.1	258.7	258.4	262.0	254.0	258.0	1.0	0.755	1.0	0.782
1	D-Alanine	193.8	72.2	133.0	176.2	60.9	118.6	168.5	48.0	108.2	1.1	0.879	1.2	0.800
1	Acetoacetic Acid	1.0	10.0	5.5	11.3	1.6	6.4	3.7	5.2	4.5	0.9	0.902	1.2	0.838
1	Dulcitol	10.1	1.0	5.5	4.8	10.5	7.6	8.0	1.0	4.5	0.7	0.736	1.2	0.869
1	Citric Acid	246.9	232.3	239.6	233.5	241.1	237.3	244.3	231.6	238.0	1.0	0.805	1.0	0.881
1	Tween 80	232.4	231.3	231.8	234.7	228.5	231.6	234.7	229.8	232.2	1.0	0.941	1.0	0.891
1	L-Alanyl-Glycine	80.0	9.1	44.6	143.2	126.0	134.6	1.0	102.2	51.6	0.3	0.132	0.9	0.920
1	Glycyl-L-Proline	252.7	221.1	236.9	237.2	240.3	238.8	244.8	226.2	235.5	1.0	0.919	1.0	0.945
1	D-Xylose	4.6	1.0	2.8	1.0	6.7	3.8	4.5	1.0	2.7	0.7	0.781	1.0	0.988
1	L-Lactic Acid	116.4	115.3	115.8	106.6	109.0	107.8	119.5	112.2	115.9	1.1	0.026	1.0	0.997
1	L-Alanine	210.0	208.0	209.0	217.6	197.8	207.7	205.2	212.8	209.0	1.0	0.907	1.0	1.000
1	Adonitol	1.0	1.0	1.0	1.0	1.1	1.0	1.0	1.0	1.0	1.0	0.423	1.0	N/A
1	α-Methyl-DGalactoside	1.0	1.0	1.0	1.0	1.5	1.2	1.0	1.0	1.0	0.8	0.423	1.0	N/A
1	D-Galactose	1.0	1.0	1.0	1.0	1.8	1.4	1.0	1.0	1.0	0.7	0.423	1.0	N/A
1	D-Melibiose	1.0	1.0	1.0	1.0	2.4	1.7	1.0	1.0	1.0	0.6	0.423	1.0	N/A
1	L-Rhamnose	1.0	1.0	1.0	1.0	1.0	1.0	1.0	1.0	1.0	1.0	N/A	1.0	N/A

1	D-Glucose-1-Phosphate	1.0	1.0	1.0	1.0	1.0	1.0	1.0	1.0	1.0	1.0	N/A	1.0	N/A
1	D-Psicose	1.0	1.0	1.0	1.0	1.0	1.0	1.0	1.0	1.0	1.0	N/A	1.0	N/A
1	D-Sorbitol	1.0	1.0	1.0	1.0	1.0	1.0	1.0	1.0	1.0	1.0	N/A	1.0	N/A
1	Glyoxylic Acid	1.0	1.0	1.0	1.0	1.0	1.0	1.0	1.0	1.0	1.0	N/A	1.0	N/A
1	D-Glucosaminic Acid	1.0	1.0	1.0	1.0	1.0	1.0	1.0	1.0	1.0	1.0	N/A	1.0	N/A
1	D-Aspartic Acid	1.0	1.0	1.0	1.0	1.0	1.0	1.0	1.0	1.0	1.0	N/A	1.0	N/A
1	D-Galacturonic Acid	1.0	1.0	1.0	1.0	1.0	1.0	1.0	1.0	1.0	1.0	N/A	1.0	N/A
1	Glucuronamide	1.0	1.0	1.0	1.0	1.0	1.0	1.0	1.0	1.0	1.0	N/A	1.0	N/A
1	2-Deoxy Adenosine	1.0	1.0	1.0	1.0	1.0	1.0	1.0	1.0	1.0	1.0	N/A	1.0	N/A
1	D-Mannose	1.0	1.0	1.0	1.0	1.0	1.0	1.0	1.0	1.0	1.0	N/A	1.0	N/A
1	M-Inositol	1.0	1.0	1.0	1.0	1.0	1.0	1.0	1.0	1.0	1.0	N/A	1.0	N/A
1	D-Glucuronic Acid	1.0	1.0	1.0	1.0	1.0	1.0	1.0	1.0	1.0	1.0	N/A	1.0	N/A
1	M-Tartaric Acid	1.0	1.0	1.0	1.0	1.0	1.0	1.0	1.0	1.0	1.0	N/A	1.0	N/A
1	Sucrose	1.0	1.0	1.0	1.0	1.0	1.0	1.0	1.0	1.0	1.0	N/A	1.0	N/A
1	Maltose	1.0	1.0	1.0	1.0	1.0	1.0	1.0	1.0	1.0	1.0	N/A	1.0	N/A
1	α-D-Lactose	1.0	1.0	1.0	1.0	1.0	1.0	1.0	1.0	1.0	1.0	N/A	1.0	N/A
1	m-Hydroxy Phenyl Acetic Acid	1.0	1.0	1.0	1.0	1.0	1.0	1.0	1.0	1.0	1.0	N/A	1.0	N/A
1	Lactulose	1.0	1.0	1.0	1.0	1.0	1.0	1.0	1.0	1.0	1.0	N/A	1.0	N/A
1	D-Galactonic Acid-γ-Lactone	1.0	1.0	1.0	1.0	1.0	1.0	1.0	1.0	1.0	1.0	N/A	1.0	N/A
1	D-Saccharic Acid	1.0	1.0	1.0	1.0	1.0	1.0	1.0	1.0	1.0	1.0	N/A	1.0	N/A
1	Mucic Acid	1.0	1.0	1.0	1.0	1.0	1.0	1.0	1.0	1.0	1.0	N/A	1.0	N/A
1	L-Fucose	1.0	1.0	1.0	1.0	1.0	1.0	1.0	1.0	1.0	1.0	N/A	1.0	N/A
1	Phenylethylamine	1.0	1.0	1.0	1.0	1.0	1.0	1.0	1.0	1.0	1.0	N/A	1.0	N/A

1	L-Galactonic Acid-γ-Lactone	1.0	1.0	1.0	1.0	1.0	1.0	1.0	1.0	1.0	1.0	N/A	1.0	N/A
1	β-Methyl-D Glucoside	1.0	1.0	1.0	1.0	1.0	1.0	1.0	1.0	1.0	1.0	N/A	1.0	N/A
1	Tricarballylic Acid	1.0	1.0	1.0	1.0	1.0	1.0	1.0	1.0	1.0	1.0	N/A	1.0	N/A
1	Maltotriose	1.0	1.0	1.0	1.0	1.0	1.0	1.0	1.0	1.0	1.0	N/A	1.0	N/A
1	N-Acetyl-β-DMannosamine	1.0	1.0	1.0	1.0	1.0	1.0	1.0	1.0	1.0	1.0	N/A	1.0	N/A
1	D-Fructose-6-Phosphate	1.0	1.0	1.0	1.0	1.0	1.0	1.0	1.0	1.0	1.0	N/A	1.0	N/A
1	D-Cellobiose	1.0	1.0	1.0	1.0	1.0	1.0	1.0	1.0	1.0	1.0	N/A	1.0	N/A
2	D-Fucose	1.5	1.4	1.4	1.9	1.0	1.5	3.3	3.3	3.3	1.0	0.960	0.4	0.001
2	δ-Amino Valeric Acid	241.7	235.4	238.5	193.8	199.7	196.7	201.5	202.6	202.1	1.2	0.010	1.2	0.008
2	Butyric Acid	110.7	112.8	111.7	129.3	142.4	135.9	148.3	156.1	152.2	0.8	0.068	0.7	0.010
2	D-Tartaric Acid	1.4	1.0	1.2	4.1	1.0	2.6	3.8	3.4	3.6	0.5	0.476	0.3	0.012
2	β-Hydroxy Butyric Acid	218.9	220.9	219.9	240.5	239.3	239.9	247.8	242.2	245.0	0.9	0.003	0.9	0.014
2	Malonic Acid	176.1	171.7	173.9	146.8	134.5	140.7	139.2	130.2	134.7	1.2	0.037	1.3	0.016
2	D-Arabitol	210.9	205.2	208.0	183.9	186.3	185.1	186.9	177.1	182.0	1.1	0.018	1.1	0.044
2	Itaconic Acid	251.4	247.7	249.5	263.7	253.3	258.5	256.8	258.6	257.7	1.0	0.244	1.0	0.058
2	Sebacic Acid	217.2	208.0	212.6	179.2	174.5	176.8	186.2	171.9	179.0	1.2	0.020	1.2	0.059
2	L-Arginine	229.7	225.7	227.7	220.8	219.6	220.2	215.1	207.2	211.1	1.0	0.070	1.1	0.064
2	a-Keto-Valeric Acid	8.3	7.7	8.0	9.9	6.9	8.4	17.2	13.1	15.2	1.0	0.836	0.5	0.077
2	γ-Hydroxy Butyric Acid	10.5	9.1	9.8	4.8	1.5	3.1	4.8	6.8	5.8	3.1	0.064	1.7	0.081
2	N-Acetyl-Lglutamic Acid	244.2	248.2	246.2	259.0	248.5	253.7	252.6	253.2	252.9	1.0	0.311	1.0	0.081
2	Gelatin	26.5	34.4	30.4	19.0	5.2	12.1	9.8	17.7	13.8	2.5	0.148	2.2	0.096
2	L-Alaninamide	34.5	24.8	29.7	16.9	15.5	16.2	17.1	14.8	16.0	1.8	0.110	1.9	0.110
2	Oxalomalic Acid	14.2	11.1	12.6	5.3	6.4	5.9	8.6	8.2	8.4	2.2	0.055	1.5	0.115
2	Dihydroxy Acetone	22.8	18.5	20.6	11.3	12.6	11.9	14.5	15.8	15.2	1.7	0.062	1.4	0.137

2	L-Pyroglutamic Acid	252.2	256.2	254.2	274.9	255.4	265.1	260.2	266.9	263.6	1.0	0.387	1.0	0.141
2	D.L-Octopamine	257.3	240.9	249.1	209.9	157.5	183.7	207.6	148.1	177.9	1.4	0.140	1.4	0.147
2	L-Valine	61.4	34.6	48.0	11.4	17.3	14.4	22.5	12.3	17.4	3.3	0.134	2.8	0.167
2	Putrescine	220.0	205.0	212.5	187.4	175.2	181.3	191.9	160.0	175.9	1.2	0.084	1.2	0.174
2	Hydroxy-LProline	249.0	242.8	245.9	234.0	236.3	235.1	240.1	230.6	235.4	1.0	0.084	1.0	0.205
2	L-Histidine	249.8	244.8	247.3	258.8	253.6	256.2	257.0	251.0	254.0	1.0	0.131	1.0	0.227
2	Caproic Acid	233.4	225.3	229.4	220.5	223.8	222.1	223.7	225.2	224.4	1.0	0.238	1.0	0.352
2	γ-Amino Butyric Acid	263.6	250.3	257.0	243.5	244.2	243.9	252.4	238.5	245.4	1.1	0.188	1.0	0.352
2	Glycine	25.2	9.3	17.2	1.0	9.1	5.0	11.5	1.0	6.3	3.4	0.304	2.8	0.368
2	L-Phenylalanine	42.3	31.9	37.1	27.2	23.5	25.4	33.2	27.2	30.2	1.5	0.168	1.2	0.371
2	5-Keto-Dgluconic Acid	8.1	1.0	4.5	4.9	4.5	4.7	7.7	9.6	8.7	1.0	0.967	0.5	0.375
2	L-Isoleucine	231.4	215.1	223.2	210.2	212.0	211.1	216.9	209.2	213.1	1.1	0.278	1.0	0.377
2	4-Hydroxy Benzoic Acid	252.9	243.4	248.1	246.5	232.5	239.5	246.3	233.3	239.8	1.0	0.417	1.0	0.409
2	L-Ornithine	155.3	140.8	148.1	146.3	122.8	134.5	155.6	155.2	155.4	1.1	0.429	1.0	0.418
2	Citramalic Acid	179.0	175.1	177.0	172.7	163.8	168.3	176.7	160.7	168.7	1.1	0.214	1.0	0.420
2	Melibionic Acid	1.1	1.0	1.0	1.0	1.0	1.0	1.0	1.0	1.0	1.0	0.423	1.0	0.423
2	Laminarin	1.0	1.0	1.0	1.6	1.0	1.3	1.0	2.3	1.6	0.8	0.423	0.6	0.423
2	Mannan	1.0	1.0	1.0	3.6	1.0	2.3	4.2	1.0	2.6	0.4	0.423	0.4	0.423
2	Citraconic Acid	1.0	1.0	1.0	1.0	1.0	1.0	1.0	1.6	1.3	1.0	N/A	0.8	0.423
2	Xylitol	1.0	1.0	1.0	1.0	1.0	1.0	1.0	1.2	1.1	1.0	N/A	0.9	0.423
2	D-Arabinose	1.0	1.0	1.0	1.0	1.0	1.0	1.0	1.1	1.0	1.0	N/A	1.0	0.423
2	γ-Cyclodextrin	1.0	1.0	1.0	1.0	1.0	1.0	1.0	1.1	1.1	1.0	N/A	0.9	0.423
2	α-Methyl-DMannoside	1.0	1.0	1.0	1.0	1.0	1.0	1.0	1.5	1.2	1.0	N/A	0.8	0.423
2	β-Methyl-Dglucuronic Acid	1.0	1.0	1.0	1.0	1.0	1.0	1.0	1.1	1.0	1.0	N/A	1.0	0.423
2	Acetamide	32.3	13.5	22.9	10.0	9.6	9.8	11.3	15.5	13.4	2.3	0.298	1.7	0.427

2	Sorbic Acid	165.6	145.5	155.6	142.0	153.9	148.0	146.7	144.9	145.8	1.1	0.581	1.1	0.435
2	Sec-Butylamine	2.9	1.4	2.1	1.0	5.1	3.1	9.0	1.9	5.5	0.7	0.714	0.4	0.461
2	Salicin	1.0	1.4	1.2	1.0	1.0	1.0	1.0	1.0	1.0	1.2	0.423	1.2	0.470
2	D,L-Carnitine	159.3	148.9	154.1	145.0	154.5	149.8	150.3	148.9	149.6	1.0	0.603	1.0	0.485
2	β-Methyl-DXyloside	1.0	1.4	1.2	2.0	1.0	1.5	1.0	3.7	2.3	0.8	0.638	0.5	0.491
2	Gentiobiose	1.0	2.6	1.8	1.0	1.0	1.0	1.0	1.3	1.1	1.8	0.423	1.6	0.499
2	Quinic Acid	253.2	238.1	245.7	250.7	253.6	252.2	254.8	248.9	251.8	1.0	0.488	1.0	0.526
2	Glycogen	1.0	5.3	3.1	8.9	2.5	5.7	8.3	3.1	5.7	0.6	0.576	0.6	0.532
2	2,3-Butanediol	24.6	11.1	17.8	14.3	19.0	16.7	31.8	18.1	25.0	1.1	0.885	0.7	0.535
2	2,3-Butanone	18.4	12.6	15.5	12.6	8.6	10.6	15.0	10.7	12.9	1.5	0.303	1.2	0.548
2	3-0-β-D-Galactopyranosyl-Darabinose	13.3	5.6	9.4	7.7	2.8	5.2	2.8	9.2	6.0	1.8	0.452	1.6	0.563
2	D-Glucosamine	14.0	17.3	15.7	10.7	8.1	9.4	9.7	16.6	13.2	1.7	0.096	1.2	0.585
2	2-Deoxy-DRibose	9.2	15.1	12.2	15.5	8.9	12.2	11.2	18.1	14.7	1.0	0.998	0.8	0.639
2	D-Lactic Acid Methyl Ester	10.0	7.0	8.5	3.9	5.1	4.5	7.4	13.1	10.2	1.9	0.130	0.8	0.646
2	3-Hydroxy 2-Butanone	13.3	3.6	8.4	8.3	6.5	7.4	11.0	10.7	10.9	1.1	0.853	0.8	0.670
2	Succinamic Acid	224.2	235.1	229.7	235.3	219.7	227.5	221.9	230.8	226.4	1.0	0.838	1.0	0.685
2	L-Lysine	153.7	138.1	145.9	142.1	124.8	133.5	131.9	149.0	140.5	1.1	0.398	1.0	0.685
2	Pectin	4.6	2.8	3.7	8.4	2.3	5.3	1.0	11.1	6.1	0.7	0.661	0.6	0.694
2	Palatinose	2.9	3.8	3.4	7.4	1.0	4.2	1.0	8.4	4.7	0.8	0.824	0.7	0.755
2	N-Acetyl-D Galactosamine	1.2	3.5	2.4	1.0	1.0	1.0	2.2	1.7	2.0	2.4	0.347	1.2	0.756
2	I-Erythritol	1.0	4.2	2.6	5.0	1.0	3.0	1.0	6.1	3.5	0.9	0.889	0.7	0.780
2	L-Methionine	4.7	1.0	2.8	1.6	1.0	1.3	1.3	6.1	3.7	2.2	0.489	0.8	0.806

2	Capric Acid	38.0	30.1	34.1	21.7	32.0	26.9	27.7	45.4	36.6	1.3	0.384	0.9	0.821
2	Dextrin	1.0	10.2	5.6	8.5	1.0	4.7	5.1	8.1	6.6	1.2	0.897	0.9	0.859
2	L-Tartaric Acid	10.9	2.0	6.4	1.5	1.8	1.7	5.8	7.9	6.9	3.8	0.397	0.9	0.935
2	D-Raffinose	1.0	4.4	2.7	1.0	1.0	1.0	1.0	4.0	2.5	2.7	0.423	1.1	0.939
2	L-Leucine	171.5	146.9	159.2	160.2	172.3	166.3	157.8	159.7	158.7	1.0	0.657	1.0	0.974
2	α-Cyclodextrin	1.0	1.0	1.0	1.6	1.0	1.3	1.0	1.0	1.0	0.8	0.423	1.0	N/A
2	D-Ribono-1,4- Lactone	1.0	1.0	1.0	1.0	1.0	1.0	1.0	1.0	1.0	1.0	N/A	1.0	N/A
2	N-Acetyl-DGlucosaminitol	1.0	1.0	1.0	1.0	1.0	1.0	1.0	1.0	1.0	1.0	N/A	1.0	N/A
2	L-Homoserine	1.0	1.0	1.0	1.0	1.0	1.0	1.0	1.0	1.0	1.0	N/A	1.0	N/A
2	L-Glucose	1.0	1.0	1.0	1.0	1.0	1.0	1.0	1.0	1.0	1.0	N/A	1.0	N/A
2	Stachyose	1.0	1.0	1.0	1.0	1.0	1.0	1.0	1.0	1.0	1.0	N/A	1.0	N/A
2	Chondroitin Sulfate C	1.0	1.0	1.0	1.0	1.0	1.0	1.0	1.0	1.0	1.0	N/A	1.0	N/A
2	Maltitol	1.0	1.0	1.0	1.0	1.0	1.0	1.0	1.0	1.0	1.0	N/A	1.0	N/A
2	β-Cyclodextrin	1.0	1.0	1.0	1.0	1.0	1.0	1.0	1.0	1.0	1.0	N/A	1.0	N/A
2	Turanose	1.0	1.0	1.0	1.0	1.0	1.0	1.0	1.0	1.0	1.0	N/A	1.0	N/A
2	Sedoheptulosan	1.0	1.0	1.0	1.0	1.0	1.0	1.0	1.0	1.0	1.0	N/A	1.0	N/A
2	Oxalic Acid	1.0	1.0	1.0	1.0	1.0	1.0	1.0	1.0	1.0	1.0	N/A	1.0	N/A
2	D-Melezitose	1.0	1.0	1.0	1.0	1.0	1.0	1.0	1.0	1.0	1.0	N/A	1.0	N/A
2	D-Tagatose	1.0	1.0	1.0	1.0	1.0	1.0	1.0	1.0	1.0	1.0	N/A	1.0	N/A
2	Lactitol	1.0	1.0	1.0	1.0	1.0	1.0	1.0	1.0	1.0	1.0	N/A	1.0	N/A
2	β-Methyl-DGalactoside	1.0	1.0	1.0	1.0	1.0	1.0	1.0	1.0	1.0	1.0	N/A	1.0	N/A
2	L-Arabitol	1.0	1.0	1.0	1.0	1.0	1.0	1.0	1.0	1.0	1.0	N/A	1.0	N/A
2	3-Methyl Glucose	1.0	1.0	1.0	1.0	1.0	1.0	1.0	1.0	1.0	1.0	N/A	1.0	N/A
2	N-Acetyl-Neuraminic Acid	1.0	1.0	1.0	1.0	1.0	1.0	1.0	1.0	1.0	1.0	N/A	1.0	N/A

2	a-Methyl-DGlucoside	1.0	1.0	1.0	1.0	1.0	1.0	1.0	1.0	1.0	1.0	N/A	1.0	N/A
2	Amygdalin	1.0	1.0	1.0	1.0	1.0	1.0	1.0	1.0	1.0	1.0	N/A	1.0	N/A
2	β-D-Allose	1.0	1.0	1.0	1.0	1.0	1.0	1.0	1.0	1.0	1.0	N/A	1.0	N/A
2	L-Sorbose	1.0	1.0	1.0	1.0	1.0	1.0	1.0	1.0	1.0	1.0	N/A	1.0	N/A
2	2-Hydroxy Benzoic Acid	1.0	1.0	1.0	1.0	1.0	1.0	1.0	1.0	1.0	1.0	N/A	1.0	N/A
2	Arbutin	1.0	1.0	1.0	1.0	1.0	1.0	1.0	1.0	1.0	1.0	N/A	1.0	N/A
2	Inulin	1.0	1.0	1.0	1.0	1.0	1.0	1.0	1.0	1.0	1.0	N/A	1.0	N/A
3	Adenosine	136.5	136.0	136.2	9.2	12.9	11.0	13.6	14.7	14.1	12.3	0.000	9.6	0.000
3	L-Lysine	90.7	91.9	91.3	58.2	57.7	57.9	4.9	1.0	3.0	1.6	0.000	30.9	0.001
3	L-Isoleucine	171.9	167.2	169.5	74.3	76.4	75.3	76.2	77.2	76.7	2.2	0.001	2.2	0.001
3	L-Valine	43.1	43.1	43.1	16.0	18.0	17.0	18.1	19.4	18.7	2.5	0.001	2.3	0.001
3	Ala-Leu	132.9	139.8	136.4	13.2	21.1	17.2	14.8	13.0	13.9	7.9	0.002	9.8	0.001
3	Inosine	75.6	73.1	74.3	24.0	29.7	26.8	31.4	30.9	31.1	2.8	0.004	2.4	0.001
3	Ala-Gly	18.1	17.1	17.6	1.0	1.3	1.2	1.0	1.0	1.0	15.1	0.001	17.6	0.001
3	N-Acetyl-DMannosamine	3.0	2.9	3.0	1.0	1.0	1.0	1.0	1.0	1.0	3.0	0.001	3.0	0.001
3	Glycine	1.0	1.0	1.0	7.0	3.7	5.3	5.2	5.0	5.1	0.2	0.120	0.2	0.001
3	Gly-Glu	16.4	15.0	15.7	1.0	1.0	1.0	1.0	1.0	1.0	15.7	0.002	15.7	0.002
3	L-Tryptophan	66.9	63.7	65.3	24.0	16.1	20.0	12.3	17.9	15.1	3.3	0.009	4.3	0.004
3	Ala-Gln	113.8	129.2	121.5	10.9	40.9	25.9	7.1	9.8	8.4	4.7	0.030	14.4	0.005
3	D,L-α-Amino-Nbutyric Acid	11.2	10.3	10.7	1.0	4.0	2.5	4.5	4.1	4.3	4.3	0.034	2.5	0.006
3	D-Lysine	1.5	1.6	1.5	1.0	1.0	1.0	1.0	1.0	1.0	1.5	0.011	1.5	0.011
3	Ala-Thr	9.9	10.0	10.0	1.0	1.0	1.0	1.0	2.8	1.9	10.0	0.000	5.2	0.013
3	Ala-Asp	15.5	18.0	16.7	4.2	1.0	2.6	1.0	3.8	2.4	6.5	0.020	7.0	0.016
3	Uridine	98.3	76.1	87.2	17.2	14.0	15.6	13.6	14.4	14.0	5.6	0.024	6.2	0.022

3	Cytidine	37.0	26.8	31.9	1.0	5.5	3.3	6.5	3.9	5.2	9.7	0.036	6.1	0.037
3	L-Cysteine	17.7	13.8	15.8	8.1	9.2	8.7	6.1	5.0	5.6	1.8	0.074	2.8	0.038
3	D,L-Lactamide	142.1	133.7	137.9	173.2	164.4	168.8	168.2	180.4	174.3	0.8	0.036	0.8	0.039
3	L-Leucine	90.6	57.9	74.3	7.0	1.0	4.0	1.0	1.0	1.0	18.6	0.052	74.3	0.046
3	Met-Ala	25.1	25.3	25.2	1.0	5.2	3.1	2.0	11.4	6.7	8.1	0.009	3.8	0.058
3	Ala-His	130.7	144.0	137.3	68.7	86.8	77.7	63.8	12.6	38.2	1.8	0.034	3.6	0.064
3	L-Alanine	52.9	56.9	54.9	42.7	32.4	37.6	43.3	34.3	38.8	1.5	0.089	1.4	0.082
3	α-Amino-Nvaleric Acid	14.6	16.0	15.3	6.8	3.6	5.2	7.9	11.2	9.6	2.9	0.028	1.6	0.085
3	N-Acetyl-DGlucosamine	186.3	172.6	179.4	159.4	156.4	157.9	159.6	154.0	156.8	1.1	0.092	1.1	0.093
3	N-Acetyl-D,Lglutamic Acid	113.9	120.9	117.4	133.0	135.3	134.1	135.0	128.3	131.7	0.9	0.045	0.9	0.099
3	Uric Acid	27.4	22.6	25.0	32.2	27.9	30.1	31.3	32.1	31.7	0.8	0.257	0.8	0.110
3	Ethanolamine	161.0	156.9	159.0	141.3	154.6	148.0	153.7	153.2	153.5	1.1	0.255	1.0	0.118
3	L-Tyrosine	79.5	75.8	77.6	53.2	49.7	51.4	61.8	39.5	50.6	1.5	0.009	1.5	0.140
3	Adenine	12.6	8.7	10.7	14.6	15.8	15.2	18.4	14.5	16.4	0.7	0.153	0.6	0.169
3	L-Ornithine	138.7	121.6	130.2	118.6	108.5	113.5	114.4	112.2	113.3	1.1	0.236	1.1	0.189
3	D-Asparagine	1.0	1.0	1.0	7.3	2.3	4.8	6.5	2.8	4.6	0.2	0.267	0.2	0.192
3	Gly-Gln	114.0	39.7	76.9	3.3	8.3	5.8	9.4	9.1	9.2	13.2	0.197	8.3	0.210
3	Ammonia	12.1	10.0	11.1	14.0	7.3	10.6	9.2	9.4	9.3	1.0	0.913	1.2	0.226
3	Thymine	7.9	2.8	5.3	1.0	1.0	1.0	1.0	1.0	1.0	5.3	0.235	5.3	0.235
3	L-Pyroglutamic Acid	162.2	168.0	165.1	170.1	168.0	169.0	175.8	168.1	171.9	1.0	0.328	1.0	0.293
3	Histamine	107.3	112.3	109.8	105.0	106.8	105.9	102.8	107.3	105.1	1.0	0.282	1.0	0.295
3	L-Phenylalanine	32.8	31.2	32.0	30.7	15.3	23.0	29.4	11.7	20.6	1.4	0.367	1.6	0.327
3	L-Aspartic Acid	107.9	102.8	105.4	114.8	104.6	109.7	103.4	99.4	101.4	1.0	0.527	1.0	0.348
3	Gly-Asn	14.5	15.2	14.9	8.5	15.2	11.9	14.5	10.8	12.7	1.3	0.469	1.2	0.363
3	Putrescine	134.6	123.0	128.8	132.7	124.4	128.6	123.2	121.3	122.2	1.0	0.977	1.1	0.380

3	Ethylenediamine	4.9	1.0	2.9	6.9	10.8	8.8	14.0	3.6	8.8	0.3	0.166	0.3	0.401
3	Tyramine	153.7	146.6	150.2	162.7	157.1	159.9	154.2	153.3	153.8	0.9	0.163	1.0	0.418
3	Allantoin	14.2	12.7	13.4	3.9	13.3	8.6	19.8	13.6	16.7	1.6	0.418	0.8	0.418
3	L-Homoserine	1.0	1.0	1.0	4.4	1.9	3.1	1.0	1.3	1.2	0.3	0.231	0.9	0.423
3	Guanosine	1.0	1.3	1.1	1.0	1.0	1.0	1.0	1.0	1.0	1.1	0.423	1.1	0.423
3	L-Threonine	1.0	1.0	1.0	4.3	1.0	2.6	1.0	1.0	1.0	0.4	0.423	1.0	0.423
3	Nitrite	1.0	1.0	1.0	5.6	1.0	3.3	3.7	1.0	2.3	0.3	0.423	0.4	0.423
3	Urea	1.0	1.0	1.0	13.1	1.0	7.0	6.3	1.0	3.7	0.1	0.423	0.3	0.423
3	L-Histidine	183.1	173.2	178.1	192.5	184.6	188.5	202.2	178.1	190.1	0.9	0.242	0.9	0.455
3	Guanine	23.6	23.0	23.3	25.5	43.5	34.5	21.9	37.3	29.6	0.7	0.339	0.8	0.497
3	L-Arginine	133.5	126.2	129.9	137.1	116.3	126.7	131.9	106.1	119.0	1.0	0.799	1.1	0.502
3	L-Serine	16.3	10.7	13.5	25.2	13.9	19.5	16.5	15.1	15.8	0.7	0.444	0.9	0.513
3	L-Glutamine	169.0	164.0	166.5	164.7	166.1	165.4	180.2	164.8	172.5	1.0	0.700	1.0	0.536
3	L-Glutamic Acid	149.9	132.3	141.1	144.8	149.4	147.1	136.2	135.1	135.6	1.0	0.574	1.0	0.597
3	N-Acetyl-DGalactosamine	2.3	1.0	1.7	1.0	1.0	1.0	1.0	1.5	1.3	1.7	0.407	1.3	0.625
3	L-Proline	148.9	140.4	144.7	158.8	149.2	154.0	156.7	142.1	149.4	0.9	0.281	1.0	0.630
3	δ-Amino-Nvaleric Acid	129.4	124.7	127.0	135.1	128.7	131.9	125.2	134.8	130.0	1.0	0.349	1.0	0.633
3	Xanthine	60.9	66.7	63.8	67.8	68.6	68.2	61.9	71.3	66.6	0.9	0.276	1.0	0.667
3	L-Asparagine	132.3	130.3	131.3	131.6	128.4	130.0	134.1	124.5	129.3	1.0	0.551	1.0	0.719
3	γ-Amino-Nbutyric Acid	137.3	126.1	131.7	120.9	132.0	126.4	139.3	130.0	134.6	1.0	0.573	1.0	0.722
3	D-Glutamic Acid	129.3	127.0	128.2	126.9	124.6	125.8	139.0	122.7	130.9	1.0	0.285	1.0	0.774
3	D-Alanine	27.9	24.6	26.2	17.2	26.8	22.0	29.2	20.5	24.8	1.2	0.495	1.1	0.792
3	Uracil	3.4	1.0	2.2	2.1	1.7	1.9	2.6	1.0	1.8	1.2	0.815	1.2	0.797
3	Acetamide	60.1	32.9	46.5	48.9	46.1	47.5	47.4	48.5	48.0	1.0	0.947	1.0	0.922
3	Ala-Glu	43.0	40.7	41.8	112.8	65.6	89.2	1.0	74.7	37.9	0.5	0.183	1.1	0.924

3	Agmatine	153.0	148.7	150.9	166.2	140.7	153.4	164.2	137.5	150.8	1.0	0.862	1.0	0.998
3	Formamide	1.0	1.0	1.0	3.0	1.0	2.0	1.0	1.0	1.0	0.5	0.423	1.0	N/A
3	Xanthosine	1.0	1.0	1.0	1.0	1.0	1.0	1.0	1.0	1.0	1.0	N/A	1.0	N/A
3	Gly-Met	1.0	1.0	1.0	1.0	1.0	1.0	1.0	1.0	1.0	1.0	N/A	1.0	N/A
3	Cytosine	1.0	1.0	1.0	1.0	1.0	1.0	1.0	1.0	1.0	1.0	N/A	1.0	N/A
3	Parabanic Acid	1.0	1.0	1.0	1.0	1.0	1.0	1.0	1.0	1.0	1.0	N/A	1.0	N/A
3	ε-Amino-Ncaproic Acid	1.0	1.0	1.0	1.0	1.0	1.0	1.0	1.0	1.0	1.0	N/A	1.0	N/A
3	D-Glucosamine	1.0	1.0	1.0	1.0	1.0	1.0	1.0	1.0	1.0	1.0	N/A	1.0	N/A
3	Alloxan	1.0	1.0	1.0	1.0	1.0	1.0	1.0	1.0	1.0	1.0	N/A	1.0	N/A
3	β-Phenylethylamine	1.0	1.0	1.0	1.0	1.0	1.0	1.0	1.0	1.0	1.0	N/A	1.0	N/A
3	D-Mannosamine	1.0	1.0	1.0	1.0	1.0	1.0	1.0	1.0	1.0	1.0	N/A	1.0	N/A
3	Thymidine	1.0	1.0	1.0	1.0	1.0	1.0	1.0	1.0	1.0	1.0	N/A	1.0	N/A
3	D-Galactosamine	1.0	1.0	1.0	1.0	1.0	1.0	1.0	1.0	1.0	1.0	N/A	1.0	N/A
3	N-Amylamine	1.0	1.0	1.0	1.0	1.0	1.0	1.0	1.0	1.0	1.0	N/A	1.0	N/A
3	Hyroxylamine	1.0	1.0	1.0	1.0	1.0	1.0	1.0	1.0	1.0	1.0	N/A	1.0	N/A
3	Methylamine	1.0	1.0	1.0	1.0	1.0	1.0	1.0	1.0	1.0	1.0	N/A	1.0	N/A
3	Glucuronamide	1.0	1.0	1.0	1.0	1.0	1.0	1.0	1.0	1.0	1.0	N/A	1.0	N/A
3	N-Butylamine	1.0	1.0	1.0	1.0	1.0	1.0	1.0	1.0	1.0	1.0	N/A	1.0	N/A
3	D,L-α-Amino- Caprylic Acid	1.0	1.0	1.0	1.0	1.0	1.0	1.0	1.0	1.0	1.0	N/A	1.0	N/A
3	D-Serine	1.0	1.0	1.0	1.0	1.0	1.0	1.0	1.0	1.0	1.0	N/A	1.0	N/A
3	Ethylamine	1.0	1.0	1.0	1.0	1.0	1.0	1.0	1.0	1.0	1.0	N/A	1.0	N/A
3	D-Aspartic Acid	1.0	1.0	1.0	1.0	1.0	1.0	1.0	1.0	1.0	1.0	N/A	1.0	N/A
3	D-Valine	1.0	1.0	1.0	1.0	1.0	1.0	1.0	1.0	1.0	1.0	N/A	1.0	N/A
3	L-Citrulline	1.0	1.0	1.0	1.0	1.0	1.0	1.0	1.0	1.0	1.0	N/A	1.0	N/A
3	L-Methionine	1.0	1.0	1.0	1.0	1.0	1.0	1.0	1.0	1.0	1.0	N/A	1.0	N/A

3	N-Phthaloyl-Lglutamic Acid	1.0	1.0	1.0	1.0	1.0	1.0	1.0	1.0	1.0	1.0	N/A	1.0	N/A
3	Biuret	1.0	1.0	1.0	1.0	1.0	1.0	1.0	1.0	1.0	1.0	N/A	1.0	N/A
3	Nitrate	1.0	1.0	1.0	1.0	1.0	1.0	1.0	1.0	1.0	1.0	N/A	1.0	N/A
4	Hypophosphite	22.3	22.9	22.6	8.5	11.2	9.8	8.5	9.2	8.8	2.3	0.011	2.6	0.001
4	Cytidine- 2'-monophosphate	234.1	232.7	233.4	252.5	249.9	251.2	258.0	259.1	258.6	0.9	0.007	0.9	0.001
4	Guanosine- 2'-monophosphate	234.2	231.9	233.1	249.8	253.8	251.8	256.3	255.8	256.0	0.9	0.015	0.9	0.003
4	Uridine- 2'-monophosphate	231.8	234.6	233.2	254.9	253.4	254.2	260.9	261.7	261.3	0.9	0.006	0.9	0.003
4	Phospho-Glycolic Acid	105.3	100.1	102.7	189.6	176.1	182.9	201.9	191.0	196.5	0.6	0.008	0.5	0.004
4	Cytidine- 2',3'-cyclicmonophosphate	221.6	225.0	223.3	246.8	238.9	242.9	252.4	250.7	251.5	0.9	0.045	0.9	0.004
4	D-2-Phospho-Glyceric Acid	232.8	237.0	234.9	261.5	258.7	260.1	265.8	264.6	265.2	0.9	0.010	0.9	0.005
4	Adenosine- 2',3'-cyclicmonophosphate	233.4	230.7	232.1	248.6	249.1	248.9	255.6	253.4	254.5	0.9	0.007	0.9	0.006
4	Uridine- 2',3'-cyclic monophosphate	233.7	229.9	231.8	249.8	252.5	251.2	256.0	253.7	254.9	0.9	0.014	0.9	0.009
4	Trimetaphosphate	232.6	236.7	234.7	249.5	258.9	254.2	254.2	254.7	254.5	0.9	0.063	0.9	0.011
4	Uridine- 3'-monophosphate	232.5	232.7	232.6	254.0	247.6	250.8	260.4	255.1	257.7	0.9	0.029	0.9	0.011
4	Thymidine- 5'-monophosphate	240.5	242.6	241.5	248.6	250.5	249.5	254.6	256.8	255.7	1.0	0.030	0.9	0.011

4	Cytidine- 3',5'-cyclic monophosphate	228.3	224.5	226.4	242.3	243.8	243.0	249.8	246.3	248.1	0.9	0.015	0.9	0.014
4	Phospho-LArginine	230.7	237.5	234.1	254.7	258.4	256.5	261.1	260.9	261.0	0.9	0.028	0.9	0.015
4	D-Glucose-1-Phosphate	241.9	237.1	239.5	253.7	246.1	249.9	258.7	257.7	258.2	1.0	0.146	0.9	0.016
4	Adenosine- 3'-monophosphate	241.2	239.6	240.4	251.2	254.0	252.6	255.4	252.2	253.8	1.0	0.018	0.9	0.017
4	2-Deoxy-Dglucose 6 Phosphate	248.8	252.2	250.5	257.8	258.0	257.9	265.8	264.0	264.9	1.0	0.050	0.9	0.018
4	Cytidine- 3'-monophosphate	233.8	238.3	236.1	247.9	246.4	247.2	252.1	251.7	251.9	1.0	0.044	0.9	0.020
4	Guanosine- 3',5'-cyclicmonophosphate	229.8	234.3	232.1	247.4	236.0	241.7	254.1	250.2	252.2	1.0	0.259	0.9	0.022
4	Phosphoryl Choline	243.7	239.1	241.4	252.2	258.9	255.5	257.2	260.0	258.6	0.9	0.073	0.9	0.023
4	Cytidine- 5'-monophosphate	223.9	231.0	227.5	244.3	237.6	241.0	250.8	249.5	250.1	0.9	0.111	0.9	0.025
4	D,L-α-GlycerolPhosphate	233.1	241.8	237.5	258.2	252.3	255.3	264.0	263.8	263.9	0.9	0.077	0.9	0.026
4	Uridine- 3',5'-cyclic monophosphate	237.0	234.9	235.9	240.5	249.3	244.9	247.7	244.8	246.2	1.0	0.184	1.0	0.029
4	β-GlycerolPhosphate	243.0	249.6	246.3	259.0	262.2	260.6	264.9	264.5	264.7	0.9	0.060	0.9	0.031
4	o-Phospho-LSerine	248.0	254.1	251.1	262.4	257.8	260.1	268.5	267.8	268.2	1.0	0.143	0.9	0.031
4	Adenosine- 3',5'-cyclicmonophosphate	226.3	232.8	229.6	248.6	232.4	240.5	256.9	250.9	253.9	1.0	0.335	0.9	0.031
4	PhosphoenolPyruvate	233.5	227.0	230.2	250.1	245.5	247.8	255.8	250.6	253.2	0.9	0.047	0.9	0.031
4	Adenosine- 2'-monophosphate	239.3	231.6	235.4	250.4	253.3	251.8	255.4	258.0	256.7	0.9	0.057	0.9	0.034

4	6-Phospho-Gluconic Acid	243.8	247.4	245.6	259.6	250.7	255.1	264.3	259.1	261.7	1.0	0.186	0.9	0.037
4	Thymidine 3',5'-cyclic monophosphate	234.2	231.9	233.1	241.2	241.3	241.2	250.1	244.6	247.3	1.0	0.020	0.9	0.041
4	D-Mannose-6-Phosphate	235.0	228.2	231.6	249.2	247.2	248.2	254.2	248.5	251.3	0.9	0.042	0.9	0.046
4	Adenosine- 5'-monophosphate	239.5	232.7	236.1	246.8	254.1	250.5	254.4	251.2	252.8	0.9	0.102	0.9	0.047
4	D-3-Phospho-Glyceric Acid	246.2	242.6	244.4	257.8	255.1	256.5	263.5	257.3	260.4	1.0	0.033	0.9	0.047
4	Guanosine- 3'-monophosphate	238.4	231.8	235.1	250.0	254.1	252.1	255.2	250.6	252.9	0.9	0.049	0.9	0.047
4	O-Phospho-DTyrosine	243.7	237.3	240.5	252.1	255.5	253.8	258.6	254.9	256.8	0.9	0.068	0.9	0.049
4	Dithiophosphate	239.6	235.4	237.5	245.2	240.9	243.0	253.4	248.6	251.0	1.0	0.207	0.9	0.052
4	D-Glucosamine-6-Phosphate	246.7	254.3	250.5	263.5	258.0	260.7	267.0	265.8	266.4	1.0	0.163	0.9	0.055
4	Guanosine- 5'-monophosphate	234.4	241.3	237.9	246.1	247.2	246.6	254.1	251.6	252.8	1.0	0.132	0.9	0.056
4	o-Phospho-LThreonine	241.8	249.0	245.4	260.3	254.2	257.3	266.1	260.8	263.5	1.0	0.127	0.9	0.056
4	D-Mannose-1-Phosphate	220.0	225.6	222.8	228.2	229.9	229.0	233.7	232.8	233.2	1.0	0.167	1.0	0.066
4	Uridine- 5'-monophosphate	226.3	240.1	233.2	251.0	248.4	249.7	258.0	259.0	258.5	0.9	0.143	0.9	0.067
4	O-Phospho-LTyrosine	241.6	233.2	237.4	247.2	254.7	251.0	252.6	251.7	252.2	0.9	0.136	0.9	0.072
4	Phosphocreatine	241.7	238.0	239.8	252.1	250.0	251.1	259.0	250.6	254.8	1.0	0.034	0.9	0.082

4	Guanosine- 2',3'-cyclicmonophosphate	232.3	241.5	236.9	248.7	239.2	243.9	252.1	250.7	251.4	1.0	0.402	0.9	0.090
4	o-Phospho-DSerine	249.6	257.7	253.7	258.7	256.4	257.5	265.3	266.6	265.9	1.0	0.453	1.0	0.095
4	2-Aminoethyl Phosphonic Acid	241.6	244.0	242.8	254.5	254.6	254.5	260.3	251.8	256.1	1.0	0.010	0.9	0.096
4	Thymidine- 3'-monophosphate	239.9	245.2	242.5	253.0	249.1	251.0	259.3	251.2	255.3	1.0	0.122	1.0	0.119
4	Phosphate	245.1	231.6	238.4	246.0	245.9	246.0	256.7	252.3	254.5	1.0	0.376	0.9	0.151
4	D-Glucose-6-Phosphate	245.5	257.9	251.7	258.5	260.5	259.5	264.0	264.5	264.2	1.0	0.343	1.0	0.183
4	Tripolyphosphate	249.5	235.7	242.6	248.9	258.9	253.9	254.8	255.2	255.0	1.0	0.317	1.0	0.214
4	O-Phosphoryl-Ethanolamine	242.8	257.6	250.2	256.6	257.9	257.3	262.8	260.1	261.4	1.0	0.441	1.0	0.272
4	Pyrophosphate	211.2	240.8	226.0	234.4	225.5	230.0	248.8	244.4	246.6	1.0	0.822	0.9	0.303
4	Phosphono Acetic Acid	250.4	253.7	252.0	245.1	242.5	243.8	250.7	248.2	249.5	1.0	0.061	1.0	0.342
4	Thiophosphate	209.8	197.7	203.7	205.1	197.9	201.5	221.8	207.6	214.7	1.0	0.781	0.9	0.361
4	Inositol Hexaphosphate	246.8	242.8	244.8	236.0	238.4	237.2	243.3	240.6	242.0	1.0	0.083	1.0	0.368
4	Triethyl Phosphate	7.4	1.0	4.2	1.0	5.5	3.2	1.0	1.0	1.0	1.3	0.830	4.2	0.423
4	Carbamyl Phosphate	245.7	238.3	242.0	235.2	238.9	237.1	240.2	239.1	239.7	1.0	0.353	1.0	0.594
4	Methylene Diphosphonic Acid	6.6	8.9	7.8	2.3	5.9	4.1	7.9	5.8	6.9	1.9	0.228	1.1	0.613
4	Cysteamine-S-Phosphate	246.8	254.6	250.7	244.0	243.2	243.6	250.3	249.5	249.9	1.0	0.214	1.0	0.856
6	Gly-Thr	5.4	5.4	5.4	1.0	1.0	1.0	1.0	1.0	1.0	5.4	0.000	5.4	0.000
6	Glu-Tyr	18.5	19.1	18.8	5.4	1.0	3.2	1.0	1.0	1.0	5.8	0.020	18.8	0.000
6	Asp-Trp	18.2	17.0	17.6	1.0	1.0	1.0	1.0	1.0	1.0	17.6	0.001	17.6	0.001
6	His-Val	94.1	83.8	88.9	6.4	5.5	5.9	6.9	1.1	4.0	15.0	0.004	22.2	0.005

6	Leu-Met	11.9	10.4	11.2	1.0	1.0	1.0	1.0	1.0	1.0	11.2	0.005	11.2	0.005
6	Ile-Trp	34.7	30.2	32.4	1.0	1.0	1.0	1.0	1.0	1.0	32.4	0.005	32.4	0.005
6	Ala-Leu	50.1	55.7	52.9	9.7	7.7	8.7	10.7	6.9	8.8	6.1	0.005	6.0	0.006
6	Asp-Phe	12.5	10.9	11.7	1.0	1.0	1.0	1.0	1.0	1.0	11.7	0.006	11.7	0.006
6	Ile-Tyr	118.8	102.2	110.5	14.1	2.9	8.5	3.1	3.7	3.4	13.0	0.009	32.4	0.006
6	Ile-Val	91.6	81.0	86.3	7.6	1.0	4.3	9.2	1.0	5.1	20.1	0.006	16.9	0.007
6	Ala-Trp	27.3	23.4	25.4	4.4	1.4	2.9	2.0	1.0	1.5	8.7	0.012	16.7	0.007
6	Glu-Trp	111.4	95.6	103.5	11.7	3.1	7.4	12.2	7.6	9.9	14.0	0.009	10.4	0.008
6	Leu-Phe	62.8	57.6	60.2	26.1	28.0	27.0	32.5	31.2	31.9	2.2	0.007	1.9	0.009
6	Leu-Ile	82.8	72.6	77.7	8.2	11.1	9.6	17.3	9.8	13.6	8.1	0.006	5.7	0.010
6	Ala-Ala	12.9	11.8	12.3	7.5	4.8	6.1	7.1	7.2	7.2	2.0	0.050	1.7	0.010
6	Asp-Leu	17.1	14.0	15.6	1.0	1.0	1.0	1.0	1.0	1.0	15.6	0.011	15.6	0.011
6	Glu-Glu	4.8	4.1	4.4	1.0	1.0	1.0	1.0	1.0	1.0	4.4	0.011	4.4	0.011
6	Leu-Glu	39.9	38.2	39.1	1.0	1.0	1.0	8.6	1.0	4.8	39.1	0.001	8.2	0.013
6	Glu-Val	25.6	20.6	23.1	1.0	1.0	1.0	2.0	1.0	1.5	23.1	0.013	15.4	0.014
6	Ala-Tyr	129.1	119.4	124.2	81.8	78.2	80.0	81.7	84.1	82.9	1.6	0.014	1.5	0.014
6	Leu-Arg	185.2	180.1	182.7	144.7	133.0	138.9	139.8	148.3	144.1	1.3	0.021	1.3	0.016
6	Gly-Lys	12.2	10.5	11.4	1.0	1.0	1.0	2.9	1.0	1.9	11.4	0.007	5.8	0.018
6	Asn-Val	75.5	65.2	70.3	16.8	18.4	17.6	23.4	13.8	18.6	4.0	0.010	3.8	0.018
6	Ile-Ser	33.9	28.0	31.0	1.0	2.1	1.5	9.0	5.0	7.0	20.0	0.010	4.4	0.022
6	Asp-Lys	45.0	37.8	41.4	14.9	14.5	14.7	14.7	17.8	16.3	2.8	0.017	2.5	0.023
6	Ile-His	90.7	66.5	78.6	1.0	1.0	1.0	4.3	1.0	2.6	78.6	0.023	29.8	0.025
6	His-Leu	130.4	112.1	121.3	56.9	59.7	58.3	63.5	54.9	59.2	2.1	0.021	2.0	0.026
6	Asn-Glu	2.1	2.5	2.3	1.0	1.0	1.0	1.0	1.0	1.0	2.3	0.026	2.3	0.026
6	Gly-Leu	14.8	10.8	12.8	1.0	1.0	1.0	1.0	1.0	1.0	12.8	0.028	12.8	0.028
6	Ile-Phe	94.8	67.1	80.9	4.2	1.0	2.6	6.1	1.0	3.6	30.9	0.030	22.8	0.032

6	Leu-Ala	68.6	56.5	62.5	25.4	30.6	28.0	32.6	27.5	30.1	2.2	0.034	2.1	0.038
6	Ala-Phe	85.5	63.7	74.6	29.9	20.1	25.0	22.2	17.6	19.9	3.0	0.054	3.8	0.039
6	Gly-Phe	22.1	15.5	18.8	1.0	1.0	1.0	3.3	1.0	2.1	18.8	0.033	8.7	0.041
6	Arg-Leu	161.6	152.0	156.8	126.1	119.7	122.9	133.2	126.9	130.0	1.3	0.028	1.2	0.043
6	Ile-Gly	36.9	25.8	31.3	1.0	1.0	1.0	5.6	1.0	3.3	31.3	0.032	9.4	0.043
6	His-Tyr	131.6	130.8	131.2	128.4	121.2	124.8	124.2	120.3	122.2	1.1	0.219	1.1	0.047
6	Arg-Tyr	210.4	202.6	206.5	107.8	163.7	135.8	178.5	164.8	171.7	1.5	0.129	1.2	0.048
6	Ile-Ala	77.6	70.5	74.0	13.5	1.0	7.2	27.4	1.0	14.2	10.2	0.011	5.2	0.048
6	Leu-Leu	36.6	25.1	30.8	1.0	1.0	1.0	6.7	1.0	3.8	30.8	0.035	8.1	0.052
6	His-Pro	27.0	16.2	21.6	48.4	1.0	24.7	46.7	43.5	45.1	0.9	0.910	0.5	0.053
6	Ala-Glu	14.0	21.8	17.9	20.1	2.1	11.1	1.4	2.1	1.8	1.6	0.561	10.2	0.055
6	Ile-Gln	114.9	88.6	101.8	46.7	47.8	47.2	49.7	36.2	42.9	2.2	0.054	2.4	0.058
6	Ala-His	54.2	42.9	48.6	19.3	3.8	11.6	10.7	22.2	16.5	4.2	0.061	3.0	0.058
6	His-Trp	69.6	51.1	60.4	21.6	17.5	19.5	26.8	19.6	23.2	3.1	0.050	2.6	0.065
6	Ile-Ile	33.7	19.3	26.5	1.0	1.0	1.0	1.0	1.0	1.0	26.5	0.072	26.5	0.072
6	His-Gly	15.8	9.1	12.5	1.0	1.0	1.0	1.0	1.0	1.0	12.5	0.075	12.5	0.075
6	His-Asp	18.6	10.4	14.5	1.0	1.0	1.0	1.8	1.0	1.4	14.5	0.081	10.3	0.087
6	His-Lys	113.3	93.1	103.2	67.7	58.0	62.8	71.6	54.0	62.8	1.6	0.069	1.6	0.095
6	Gly-Tyr	12.2	6.6	9.4	1.0	1.0	1.0	1.0	1.0	1.0	9.4	0.097	9.4	0.097
6	Arg-Asp	113.9	111.8	112.9	97.3	99.3	98.3	100.8	106.8	103.8	1.1	0.009	1.1	0.104
6	Gly-Trp	9.6	4.9	7.3	1.0	1.0	1.0	1.0	1.0	1.0	7.3	0.119	7.3	0.119
6	Leu-Asp	34.4	20.9	27.6	1.4	1.0	1.2	11.2	1.0	6.1	23.1	0.059	4.5	0.125
6	Arg-Arg	200.5	201.0	200.7	180.2	162.5	171.4	186.7	167.9	177.3	1.2	0.079	1.1	0.130
6	Gly-Ser	17.3	13.4	15.4	1.0	3.4	2.2	9.5	3.5	6.5	6.9	0.028	2.4	0.131
6	Gly-His	6.3	3.1	4.7	1.0	1.0	1.0	1.0	1.0	1.0	4.7	0.147	4.7	0.147
6	His-Met	55.5	38.4	47.0	23.8	23.9	23.9	32.4	16.0	24.2	2.0	0.113	1.9	0.194

6	His-Ser	64.6	29.8	47.2	11.0	34.6	22.8	17.0	10.2	13.6	2.1	0.365	3.5	0.198
6	Leu-Gly	31.9	17.5	24.7	1.0	1.0	1.0	13.2	1.0	7.1	24.7	0.081	3.5	0.204
6	Ala-Gly	5.1	10.0	7.5	1.0	1.0	1.0	1.3	3.7	2.5	7.5	0.117	3.0	0.206
6	Arg-Ser	92.2	75.6	83.9	19.9	64.3	42.1	71.5	60.3	65.9	2.0	0.220	1.3	0.214
6	Glu-Gly	5.5	2.3	3.9	1.0	1.0	1.0	1.0	1.0	1.0	3.9	0.215	3.9	0.215
6	Gly-Arg	96.8	83.0	89.9	72.0	75.1	73.5	81.2	73.7	77.5	1.2	0.148	1.2	0.255
6	Arg-Phe	196.8	137.6	167.2	125.4	101.3	113.4	133.8	101.7	117.8	1.5	0.234	1.4	0.280
6	Gln-Gly	63.4	36.9	50.1	35.6	19.7	27.6	34.0	26.0	30.0	1.8	0.282	1.7	0.283
6	Ala-Lys	59.6	59.0	59.3	57.7	54.8	56.2	29.1	54.2	41.7	1.1	0.171	1.4	0.295
6	Gly-Ala	4.9	1.6	3.2	1.0	1.0	1.0	1.0	1.0	1.0	3.2	0.316	3.2	0.316
6	Arg-Val	161.4	143.1	152.2	129.9	127.0	128.5	144.5	128.7	136.6	1.2	0.125	1.1	0.325
6	Gly-Val	11.5	2.3	6.9	1.0	1.0	1.0	1.0	1.0	1.0	6.9	0.329	6.9	0.329
6	Glu-Ser	8.9	1.8	5.3	1.0	1.0	1.0	1.4	1.0	1.2	5.3	0.346	4.5	0.364
6	Ile-Met	15.0	1.0	8.0	1.0	1.0	1.0	1.0	1.0	1.0	8.0	0.423	8.0	0.423
6	Gly-Gly	1.0	3.7	2.4	1.0	1.0	1.0	1.0	1.0	1.0	2.4	0.423	2.4	0.423
6	Asp-Val	3.5	1.0	2.3	1.0	1.0	1.0	1.0	1.0	1.0	2.3	0.423	2.3	0.423
6	Ala-Asn	7.5	19.7	13.6	6.1	7.1	6.6	1.0	10.8	5.9	2.1	0.367	2.3	0.427
6	Ala-Ser	23.3	14.6	19.0	12.2	13.3	12.7	18.1	9.0	13.6	1.5	0.290	1.4	0.481
6	Gln-Gln	151.4	135.3	143.3	149.2	146.9	148.0	161.7	144.5	153.1	1.0	0.621	0.9	0.495
6	Arg-Met	63.6	53.6	58.6	50.7	64.1	57.4	67.7	59.7	63.7	1.0	0.897	0.9	0.508
6	Ile-Arg	198.2	173.5	185.8	170.9	160.2	165.5	183.6	163.3	173.5	1.1	0.271	1.1	0.520
6	Arg-Trp	94.9	65.0	79.9	60.3	62.8	61.6	75.6	59.8	67.7	1.3	0.344	1.2	0.543
6	Ile-Pro	105.1	94.5	99.8	107.1	105.7	106.4	102.2	105.4	103.8	0.9	0.343	1.0	0.548
6	Arg-Ile	154.3	131.6	142.9	133.3	126.9	130.1	138.7	129.7	134.2	1.1	0.389	1.1	0.548
6	Gly-Pro	96.5	76.6	86.5	75.6	70.5	73.0	82.5	77.1	79.8	1.2	0.320	1.1	0.582
6	Ala-Arg	129.7	130.1	129.9	133.4	125.7	129.6	130.9	126.0	128.4	1.0	0.933	1.0	0.604

6	Ala-Pro	106.9	94.8	100.9	102.0	96.3	99.2	101.7	93.6	97.6	1.0	0.823	1.0	0.701
6	Arg-Gln	147.1	129.9	138.5	142.0	136.3	139.2	150.3	135.8	143.1	1.0	0.948	1.0	0.726
6	Arg-Lys	207.9	180.7	194.3	184.1	165.7	174.9	199.4	176.3	187.9	1.1	0.358	1.0	0.753
6	Arg-Ala	134.6	123.0	128.8	125.7	124.1	124.9	130.7	123.1	126.9	1.0	0.573	1.0	0.806
6	Arg-Glu	169.6	150.6	160.1	164.7	150.7	157.7	167.8	146.0	156.9	1.0	0.857	1.0	0.845
6	Ala-Thr	1.0	1.0	1.0	1.0	1.0	1.0	1.0	1.0	1.0	1.0	N/A	1.0	N/A
6	Asp-Glu	1.0	1.0	1.0	1.0	1.0	1.0	1.0	1.0	1.0	1.0	N/A	1.0	N/A
6	Gly-Met	1.0	1.0	1.0	1.0	1.0	1.0	1.0	1.0	1.0	1.0	N/A	1.0	N/A
6	Gly-Cys	1.0	1.0	1.0	1.0	1.0	1.0	1.0	1.0	1.0	1.0	N/A	1.0	N/A
6	Glu-Asp	1.0	1.0	1.0	1.0	1.0	1.0	1.0	1.0	1.0	1.0	N/A	1.0	N/A
6	Asp-Asp	1.0	1.0	1.0	1.0	1.0	1.0	1.0	1.0	1.0	1.0	N/A	1.0	N/A
6	Cys-Gly	1.0	1.0	1.0	1.0	1.0	1.0	1.0	1.0	1.0	1.0	N/A	1.0	N/A
7	Val-Val	43.3	43.2	43.3	6.1	9.4	7.7	10.8	11.3	11.1	5.6	0.002	3.9	0.000
7	Met-Leu	6.9	7.1	7.0	1.0	1.0	1.0	1.0	1.0	1.0	7.0	0.000	7.0	0.000
7	Val-Leu	123.1	119.2	121.1	10.9	17.0	13.9	16.6	18.5	17.5	8.7	0.001	6.9	0.000
7	Met-Ile	15.8	15.1	15.5	1.0	1.0	1.0	1.0	1.0	1.0	15.5	0.001	15.5	0.001
7	Val-Ile	79.3	82.9	81.1	9.2	13.8	11.5	11.1	13.8	12.5	7.1	0.002	6.5	0.001
7	Phe-Ser	33.9	36.0	34.9	8.7	5.0	6.8	5.8	5.7	5.7	5.1	0.006	6.1	0.001
7	Y-Glu-Gly	32.4	33.2	32.8	12.7	15.9	14.3	23.8	23.1	23.5	2.3	0.007	1.4	0.003
7	Val-Asp	28.0	25.9	27.0	1.0	8.0	4.5	8.2	7.7	7.9	6.0	0.025	3.4	0.003
7	Trp-Leu	25.1	22.5	23.8	2.1	1.0	1.6	1.0	1.6	1.3	15.2	0.004	18.4	0.003
7	Thr-Glu	11.8	11.5	11.6	3.7	4.5	4.1	4.1	3.2	3.6	2.8	0.003	3.2	0.004
7	Lys-Pro	27.8	26.9	27.3	12.9	12.9	12.9	12.2	10.0	11.1	2.1	0.001	2.5	0.005
7	Thr-Ala	17.8	16.7	17.2	2.2	7.4	4.8	7.5	8.3	7.9	3.6	0.043	2.2	0.006
7	Trp-Lys	118.3	105.2	111.7	24.1	29.8	27.0	31.5	31.8	31.6	4.1	0.007	3.5	0.007
7	Trp-Tyr	19.9	16.9	18.4	1.0	1.0	1.0	1.0	1.0	1.0	18.4	0.007	18.4	0.007

7	Lys-Glu	29.6	26.3	27.9	10.4	5.9	8.1	7.6	5.4	6.5	3.4	0.019	4.3	0.008
7	Pro-Gly	12.1	10.3	11.2	1.4	1.0	1.2	1.0	1.0	1.0	9.5	0.009	11.2	0.008
7	Pro-Asp	10.9	9.1	10.0	1.0	1.0	1.0	1.0	1.0	1.0	10.0	0.010	10.0	0.010
7	Ser-Phe	82.6	68.2	75.4	8.1	2.7	5.4	5.2	6.1	5.7	14.0	0.012	13.3	0.011
7	Ser-His	64.1	54.2	59.1	9.0	7.5	8.3	10.6	7.0	8.8	7.2	0.010	6.7	0.011
7	Ser-Val	22.9	19.7	21.3	4.1	4.2	4.1	6.1	6.6	6.3	5.1	0.009	3.4	0.012
7	Tyr-Glu	95.6	87.2	91.4	36.5	54.2	45.4	52.6	54.0	53.3	2.0	0.043	1.7	0.012
7	Met-His	57.1	51.7	54.4	28.3	24.4	26.4	25.0	20.0	22.5	2.1	0.014	2.4	0.013
7	Pro-Ala	47.1	49.5	48.3	31.7	23.1	27.4	17.3	23.4	20.4	1.8	0.042	2.4	0.014
7	Tyr-His	167.8	167.2	167.5	140.2	142.4	141.3	142.0	147.5	144.7	1.2	0.002	1.2	0.014
7	Val-Gly	21.6	20.0	20.8	1.5	7.8	4.6	5.0	8.0	6.5	4.5	0.039	3.2	0.014
7	Phe-Pro	62.1	52.8	57.5	23.1	16.0	19.5	20.8	17.1	18.9	2.9	0.023	3.0	0.017
7	Met-Trp	14.7	11.5	13.1	1.0	1.0	1.0	1.0	1.0	1.0	13.1	0.017	13.1	0.017
7	Trp-Gly	10.1	7.9	9.0	1.0	1.0	1.0	1.0	1.0	1.0	9.0	0.018	9.0	0.018
7	Phe-Gly	24.2	20.4	22.3	10.2	4.2	7.2	7.3	4.9	6.1	3.1	0.051	3.6	0.018
7	Leu-Trp	111.1	92.5	101.8	38.7	38.8	38.8	37.5	36.5	37.0	2.6	0.021	2.8	0.020
7	Leu-Ser	52.5	63.8	58.2	22.8	23.9	23.4	19.3	14.8	17.1	2.5	0.026	3.4	0.021
7	Val-Tyr	124.0	135.3	129.6	81.7	68.7	75.2	63.0	78.0	70.5	1.7	0.024	1.8	0.024
7	Tyr-Gly	75.6	70.7	73.1	12.1	18.9	15.5	11.5	27.8	19.6	4.7	0.005	3.7	0.025
7	Phe-Phe	49.7	47.2	48.5	24.2	20.4	22.3	27.2	19.2	23.2	2.2	0.007	2.1	0.027
7	Trp-Ser	11.5	8.6	10.1	1.0	1.0	1.0	1.5	1.0	1.2	10.1	0.026	8.0	0.028
7	Ser-Ala	19.0	15.0	17.0	3.9	5.1	4.5	6.2	4.6	5.4	3.7	0.026	3.2	0.031
7	Leu-Val	114.4	109.2	111.8	58.9	46.0	52.4	54.1	28.9	41.5	2.1	0.013	2.7	0.032
7	Met-Lys	8.8	6.7	7.8	1.0	3.4	2.2	1.5	2.2	1.8	3.5	0.072	4.2	0.032
7	Val-Arg	108.4	98.4	103.4	135.8	121.3	128.6	130.4	133.9	132.1	0.8	0.103	0.8	0.033
7	Lys-Trp	110.8	101.4	106.1	61.8	50.6	56.2	56.3	35.8	46.0	1.9	0.021	2.3	0.034

7	Trp-Ala	10.9	7.7	9.3	1.0	1.0	1.0	1.0	1.0	1.0	9.3	0.035	9.3	0.035
7	Val-His	88.8	112.2	100.5	23.3	34.1	28.7	26.5	38.1	32.3	3.5	0.031	3.1	0.035
7	Ser-Leu	37.7	55.2	46.4	1.0	1.0	1.0	1.0	1.0	1.0	46.4	0.035	46.4	0.035
7	Met-Gln	10.4	8.1	9.2	10.2	1.0	5.6	2.9	1.0	1.9	1.7	0.521	4.8	0.038
7	Lys-Leu	122.1	123.7	122.9	64.5	61.4	63.0	51.9	15.6	33.8	2.0	0.001	3.6	0.039
7	Lys-Val	83.3	78.9	81.1	41.6	35.8	38.7	34.6	10.9	22.8	2.1	0.007	3.6	0.040
7	Lys-Tyr	175.2	163.8	169.5	149.5	143.8	146.7	137.6	127.2	132.4	1.2	0.070	1.3	0.040
7	Met-Pro	11.8	8.1	9.9	3.6	1.0	2.3	1.0	1.0	1.0	4.3	0.078	9.9	0.041
7	Tyr-Trp	67.3	72.4	69.8	69.2	48.0	58.6	45.4	52.5	48.9	1.2	0.410	1.4	0.041
7	Thr-Gly	4.4	3.2	3.8	1.0	1.0	1.0	1.0	1.0	1.0	3.8	0.044	3.8	0.044
7	Lys-Thr	10.9	10.7	10.8	9.7	2.8	6.3	5.3	2.2	3.8	1.7	0.319	2.9	0.045
7	Pro-Gln	100.5	103.4	101.9	72.8	72.8	72.8	63.9	78.1	71.0	1.4	0.003	1.4	0.051
7	Pro-Pro	102.6	101.8	102.2	113.9	126.4	120.2	115.0	123.4	119.2	0.9	0.102	0.9	0.056
7	Ser-Gly	6.3	4.2	5.2	1.0	1.0	1.0	1.0	1.0	1.0	5.2	0.057	5.2	0.057
7	Thr-Pro	106.5	102.7	104.6	74.6	83.6	79.1	81.5	90.3	85.9	1.3	0.035	1.2	0.060
7	Ser-Ser	8.8	6.0	7.4	1.0	1.0	1.0	2.2	1.0	1.6	7.4	0.047	4.6	0.066
7	Trp-Phe	24.8	14.5	19.6	1.0	1.0	1.0	1.0	1.0	1.0	19.6	0.068	19.6	0.068
7	Phe-Trp	100.3	92.8	96.5	67.3	52.2	59.7	71.3	53.6	62.4	1.6	0.049	1.5	0.071
7	Lys-Ala	36.6	47.9	42.2	42.1	28.9	35.5	22.2	15.1	18.6	1.2	0.519	2.3	0.072
7	Thr-Leu	29.2	16.7	23.0	1.0	1.0	1.0	1.1	1.0	1.1	23.0	0.072	21.8	0.072
7	Tyr-Tyr	118.6	106.1	112.4	90.7	58.9	74.8	82.4	59.7	71.1	1.5	0.158	1.6	0.085
7	Ser-Pro	104.6	103.0	103.8	89.4	91.5	90.4	97.3	100.2	98.8	1.1	0.009	1.1	0.090
7	Ser-Tyr	66.3	62.0	64.2	26.3	16.4	21.4	23.5	45.3	34.4	3.0	0.016	1.9	0.115
7	Met-Val	5.9	3.1	4.5	1.0	1.0	1.0	1.0	1.0	1.0	4.5	0.130	4.5	0.130
7	Lys-Phe	87.1	89.5	88.3	71.5	73.7	72.6	63.0	27.7	45.4	1.2	0.010	1.9	0.136
7	Met-Phe	9.9	7.0	8.4	9.1	1.3	5.2	4.8	1.4	3.1	1.6	0.517	2.7	0.138

7	Pro-Tyr	127.4	119.6	123.5	79.7	88.1	83.9	57.3	96.3	76.8	1.5	0.020	1.6	0.144
7	Met-Glu	8.0	4.4	6.2	10.4	1.0	5.7	2.5	1.0	1.7	1.1	0.925	3.6	0.146
7	Lys-Lys	33.2	29.5	31.4	40.1	31.1	35.6	21.4	6.9	14.1	0.9	0.478	2.2	0.149
7	Lys-Ser	24.8	40.1	32.4	19.3	19.3	19.3	16.2	4.1	10.1	1.7	0.230	3.2	0.150
7	Lys-Ile	142.7	136.9	139.8	120.2	113.5	116.8	109.4	33.9	71.7	1.2	0.035	2.0	0.214
7	Phe-Ile	98.0	94.2	96.1	64.1	77.7	70.9	59.9	86.1	73.0	1.4	0.070	1.3	0.222
7	Tyr-Leu	143.0	134.1	138.6	119.6	125.9	122.7	119.5	132.1	125.8	1.1	0.101	1.1	0.240
7	Tyr-Gln	114.3	107.5	110.9	95.0	105.8	100.4	100.0	109.8	104.9	1.1	0.243	1.1	0.420
7	Trp-Trp	6.0	1.0	3.5	1.0	1.0	1.0	1.0	1.0	1.0	3.5	0.423	3.5	0.423
7	Trp-Glu	2.0	1.0	1.5	1.0	1.0	1.0	1.0	1.0	1.0	1.5	0.423	1.5	0.423
7	Met-Asp	1.8	1.0	1.4	1.0	1.0	1.0	1.0	1.0	1.0	1.4	0.423	1.4	0.423
7	Met-Gly	2.2	1.0	1.6	1.0	1.0	1.0	1.0	1.0	1.0	1.5	0.437	1.6	0.423
7	Thr-Arg	84.9	74.4	79.6	60.8	70.2	65.5	62.8	78.8	70.8	1.2	0.181	1.1	0.451
7	Met-Arg	93.5	86.0	89.7	93.2	87.0	90.1	91.3	43.9	67.6	1.0	0.950	1.3	0.454
7	Tyr-Phe	151.9	98.0	124.9	120.9	71.3	96.1	121.3	77.0	99.1	1.3	0.514	1.3	0.537
7	Pro-Leu	81.3	90.9	86.1	38.2	83.8	61.0	48.9	92.0	70.5	1.4	0.393	1.2	0.552
7	Tyr-Lys	192.8	176.3	184.6	192.8	169.1	181.0	184.8	167.6	176.2	1.0	0.826	1.0	0.555
7	Pro-Phe	128.0	117.9	122.9	122.7	114.8	118.7	122.3	116.8	119.5	1.0	0.581	1.0	0.615
7	Lys-Arg	188.5	182.3	185.4	193.8	178.5	186.2	191.5	163.3	177.4	1.0	0.932	1.0	0.636
7	Trp-Arg	135.8	117.0	126.4	118.6	123.5	121.0	135.8	127.8	131.8	1.0	0.635	1.0	0.652
7	Val-Asn	29.3	1.0	15.2	3.2	10.5	6.8	9.0	10.6	9.8	2.2	0.627	1.5	0.743
7	Phe-Ala	63.8	58.2	61.0	49.6	53.8	51.7	62.6	58.7	60.6	1.2	0.118	1.0	0.932
7	Tyr-Ala	114.2	107.4	110.8	98.8	113.8	106.3	107.0	114.3	110.7	1.0	0.638	1.0	0.984
7	Ser-Met	1.0	1.0	1.0	1.0	1.0	1.0	1.0	1.0	1.0	1.0	N/A	1.0	N/A
7	Trp-Asp	1.0	1.0	1.0	1.0	1.0	1.0	1.0	1.0	1.0	1.0	N/A	1.0	N/A
7	Thr-Met	1.0	1.0	1.0	1.0	1.0	1.0	1.0	1.0	1.0	1.0	N/A	1.0	N/A

7	Pro-Hyp	1.0	1.0	1.0	1.0	1.0	1.0	1.0	1.0	1.0	1.0	N/A	1.0	N/A
7	Met-Met	1.0	1.0	1.0	1.0	1.0	1.0	1.0	1.0	1.0	1.0	N/A	1.0	N/A
8	Val-Tyr-Val	123.2	119.5	121.3	27.1	21.1	24.1	23.4	23.7	23.6	5.0	0.001	5.1	0.000
8	Gln-Glu	94.0	94.6	94.3	64.9	72.3	68.6	74.6	73.1	73.9	1.4	0.021	1.3	0.002
8	Y-Glu-Gly	17.7	19.4	18.6	1.9	4.9	3.4	2.4	2.4	2.4	5.5	0.013	7.8	0.003
8	Val-Lys	88.7	88.1	88.4	38.8	41.9	40.4	47.2	51.5	49.3	2.2	0.001	1.8	0.003
8	Pro-Val	78.7	87.2	82.9	7.2	8.6	7.9	3.7	7.1	5.4	10.5	0.003	15.3	0.003
8	Pro-Arg	81.3	78.7	80.0	109.2	112.0	110.6	115.6	119.3	117.5	0.7	0.004	0.7	0.004
8	Thr-Phe	17.9	20.5	19.2	1.0	1.0	1.0	1.0	1.0	1.0	19.2	0.005	19.2	0.005
8	Val-Gln	78.1	89.2	83.6	7.2	6.4	6.8	8.3	5.5	6.9	12.3	0.005	12.1	0.006
8	Ile-Leu	94.3	109.9	102.1	1.0	1.0	1.0	1.0	1.0	1.0	102.1	0.006	102.1	0.006
8	Ser-Gln	48.1	56.2	52.2	1.3	1.0	1.1	1.0	1.7	1.4	45.9	0.006	38.1	0.006
8	Phe-β-Ala	23.6	20.5	22.1	1.0	1.0	1.0	2.7	1.0	1.9	22.1	0.005	11.8	0.008
8	Val-Met	8.7	10.1	9.4	1.5	1.0	1.2	1.4	1.0	1.2	7.6	0.009	7.8	0.008
8	Tyr-Gly-Gly	82.0	77.0	79.5	42.0	39.2	40.6	36.5	41.9	39.2	2.0	0.005	2.0	0.008
8	Thr-Asp	6.4	5.4	5.9	1.0	1.0	1.0	1.0	1.0	1.0	5.9	0.009	5.9	0.009
8	Lys-Asp	31.4	28.2	29.8	7.5	6.7	7.1	3.5	7.4	5.5	4.2	0.005	5.5	0.010
8	Glu-Ala	34.5	30.4	32.4	20.3	5.8	13.0	7.1	10.0	8.6	2.5	0.123	3.8	0.011
8	Val-Ser	19.6	21.5	20.5	6.9	7.7	7.3	3.1	6.1	4.6	2.8	0.006	4.5	0.012
8	Ser-Glu	12.3	14.3	13.3	1.0	1.0	1.0	3.0	1.0	2.0	13.3	0.006	6.6	0.015
8	Thr-Gln	25.7	23.1	24.4	8.2	5.3	6.8	4.2	8.1	6.2	3.6	0.012	3.9	0.016
8	Leu-Leu-Leu	41.2	52.6	46.9	1.0	1.0	1.0	2.8	1.0	1.9	46.9	0.015	24.7	0.016
8	Pro-Ser	34.8	45.9	40.4	1.0	1.0	1.0	1.0	1.0	1.0	40.4	0.019	40.4	0.019
8	Leu-Gly-Gly	32.9	26.4	29.7	2.4	1.8	2.1	6.3	1.7	4.0	14.2	0.014	7.4	0.023
8	Leu-β-Ala	50.1	65.0	57.5	3.6	4.2	3.9	10.8	2.4	6.6	14.8	0.019	8.8	0.027
8	Gly-Gly-lle	13.8	10.1	12.0	1.0	1.0	1.0	1.0	1.0	1.0	12.0	0.028	11.7	0.028

8	Gly-Gly-Phe	11.0	8.1	9.5	1.0	1.0	1.0	1.0	1.0	1.0	9.5	0.028	9.5	0.028
8	Lys-Gly	21.3	24.7	23.0	8.0	7.7	7.9	11.3	8.2	9.7	2.9	0.012	2.4	0.029
8	Trp-Val	6.9	9.4	8.1	1.0	1.0	1.0	1.0	1.0	1.0	8.1	0.031	8.1	0.031
8	Gly-Gly-Ala	11.2	12.8	12.0	3.9	3.8	3.8	5.2	2.7	4.0	3.1	0.010	3.0	0.031
8	Val-Phe	88.8	79.9	84.4	54.4	29.4	41.9	53.8	43.1	48.5	2.0	0.085	1.7	0.036
8	Pro-Asn	35.5	30.9	33.2	14.7	12.6	13.6	13.5	18.4	16.0	2.4	0.016	2.1	0.036
8	Val-Glu	18.1	26.2	22.1	1.0	1.0	1.0	1.9	1.0	1.4	22.1	0.035	15.5	0.036
8	His-Ala	64.8	77.8	71.3	20.6	8.4	14.5	27.1	8.6	17.8	4.9	0.024	4.0	0.042
8	Ala-Ile	34.4	52.0	43.2	27.7	17.4	22.6	1.0	2.7	1.8	1.9	0.181	23.4	0.043
8	Met-Tyr	29.8	35.7	32.7	17.5	14.8	16.2	12.1	17.2	14.6	2.0	0.036	2.2	0.043
8	Phe-Gly-Gly	38.9	31.7	35.3	13.2	10.3	11.8	17.6	12.6	15.1	3.0	0.026	2.3	0.044
8	Ile-Asn	57.2	72.5	64.8	4.8	4.1	4.5	21.1	4.5	12.8	14.5	0.016	5.1	0.044
8	Pro-Ile	59.9	81.1	70.5	42.2	6.9	24.5	17.2	23.5	20.3	2.9	0.155	3.5	0.045
8	His-Glu	15.4	23.5	19.5	1.0	2.2	1.6	1.0	2.3	1.6	12.1	0.049	11.9	0.049
8	Ala-Gln	43.0	56.9	50.0	16.9	7.5	12.2	6.6	17.6	12.1	4.1	0.046	4.1	0.051
8	Ala-Ala-Ala	56.0	59.8	57.9	10.4	5.1	7.7	5.3	25.1	15.2	7.5	0.004	3.8	0.051
8	β-Ala-Ala	5.2	6.0	5.6	1.0	1.0	1.0	2.6	1.0	1.8	5.6	0.008	3.1	0.054
8	Gly-Asp	4.8	3.2	4.0	1.8	1.0	1.4	1.0	1.1	1.1	2.9	0.096	3.7	0.063
8	Gly-Ile	10.5	17.4	13.9	1.0	1.0	1.0	1.0	1.0	1.0	13.9	0.065	13.9	0.065
8	Phe-Val	84.4	79.8	82.1	72.0	59.2	65.6	72.8	68.6	70.7	1.3	0.137	1.2	0.068
8	D-Leu-Tyr	2.1	1.6	1.8	1.0	1.0	1.0	1.0	1.0	1.0	1.8	0.069	1.8	0.069
8	Asp-Gln	10.6	17.4	14.0	1.2	1.0	1.1	2.3	2.0	2.1	12.7	0.064	6.5	0.074
8	β-Ala-His	6.3	3.9	5.1	1.0	1.0	1.0	1.0	1.0	1.0	5.1	0.075	5.1	0.075
8	His-His	79.9	94.4	87.2	60.2	54.8	57.5	47.9	62.1	55.0	1.5	0.061	1.6	0.087
8	Val-Pro	91.2	92.2	91.7	90.6	91.1	90.8	93.7	93.1	93.4	1.0	0.264	1.0	0.093
8	Ala-Val	13.1	23.8	18.4	2.4	2.6	2.5	3.1	3.0	3.0	7.4	0.098	6.0	0.104

8	Pro-Glu	12.1	23.0	17.6	3.9	2.6	3.2	1.0	3.6	2.3	5.4	0.121	7.7	0.112
8	D-Ala-Leu	6.5	3.5	5.0	1.0	1.0	1.0	1.0	1.0	1.0	5.0	0.117	5.0	0.117
8	Leu-Asn	58.8	72.6	65.7	44.0	49.4	46.7	47.8	46.8	47.3	1.4	0.125	1.4	0.118
8	Val-Ala	23.7	51.5	37.6	1.0	1.0	1.0	1.6	1.0	1.3	37.6	0.119	28.5	0.121
8	Asp-Ala	8.3	15.6	11.9	1.4	1.0	1.2	2.2	2.8	2.5	10.1	0.098	4.8	0.123
8	Gly-Gly-Leu	18.3	8.6	13.5	1.0	1.0	1.0	1.0	1.0	1.0	13.5	0.124	13.5	0.124
8	D-Ala-D-Ala	84.3	80.3	82.3	83.9	92.2	88.1	87.7	92.4	90.0	0.9	0.338	0.9	0.130
8	Lys-Met	3.6	7.3	5.4	1.0	1.0	1.0	1.0	1.0	1.0	5.4	0.135	5.4	0.135
8	Ser-Asp	3.3	7.6	5.5	1.0	1.0	1.0	1.0	1.0	1.0	5.5	0.175	5.5	0.175
8	Pro-Lys	42.7	109.9	76.3	9.5	9.1	9.3	7.0	11.6	9.3	8.2	0.184	8.2	0.185
8	Ala-Asp	5.2	12.9	9.0	1.0	1.2	1.1	2.0	1.0	1.5	8.2	0.173	5.9	0.190
8	β-Ala-Gly	6.4	2.7	4.5	1.0	1.0	1.0	1.0	1.0	1.0	4.5	0.196	4.5	0.196
8	Pro-Trp	24.8	81.2	53.0	1.1	1.0	1.1	1.0	1.1	1.0	49.6	0.207	50.7	0.207
8	Ser-Asn	3.9	11.8	7.9	3.0	3.1	3.0	1.0	1.0	1.0	2.6	0.348	7.9	0.225
8	Leu-His	107.8	127.9	117.9	93.1	94.5	93.8	94.1	104.6	99.3	1.3	0.140	1.2	0.245
8	Phe-Asp	4.7	17.7	11.2	1.0	1.0	1.0	1.0	1.0	1.0	11.2	0.258	11.2	0.258
8	Thr-Ser	1.4	3.2	2.3	1.0	1.0	1.0	1.0	1.0	1.0	2.3	0.273	2.3	0.273
8	Tyr-Ile	113.1	121.1	117.1	107.3	111.3	109.3	104.7	112.9	108.8	1.1	0.223	1.1	0.286
8	Gly-Gly-Gly	13.8	6.9	10.3	1.0	1.2	1.1	7.0	1.0	4.0	9.4	0.117	2.6	0.299
8	Phe-Tyr	96.4	99.8	98.1	76.2	60.7	68.5	97.1	61.7	79.4	1.4	0.065	1.2	0.404
8	Asp-Gly	1.0	3.3	2.1	1.0	1.0	1.0	1.0	1.0	1.0	2.1	0.423	2.1	0.423
8	Gly-D-Ala	1.0	2.8	1.9	1.0	1.0	1.0	1.0	1.0	1.0	1.9	0.423	1.9	0.423
8	Gly-Gly-D-Leu	1.0	1.8	1.4	1.0	1.0	1.0	1.0	1.0	1.0	1.4	0.423	1.4	0.423
8	Tyr-Val	109.3	119.6	114.5	106.6	108.4	107.5	105.3	111.6	108.5	1.1	0.313	1.1	0.424
8	Ala-Met	1.0	8.7	4.9	1.3	1.0	1.1	1.6	1.0	1.3	4.3	0.436	3.7	0.455
8	Leu-Pro	86.0	98.5	92.2	62.7	82.1	72.4	85.4	88.7	87.1	1.3	0.228	1.1	0.509

8	Gly-Asn	15.8	18.1	17.0	20.5	18.5	19.5	1.0	19.0	10.0	0.9	0.246	1.7	0.525
8	Phe-Met	7.1	12.1	9.6	5.7	4.0	4.9	9.5	5.2	7.4	2.0	0.212	1.3	0.564
8	Leu-Tyr	115.2	110.6	112.9	101.6	99.3	100.5	112.4	110.4	111.4	1.1	0.040	1.0	0.607
8	Phe-Glu	11.5	17.2	14.4	25.6	3.8	14.7	16.9	5.7	11.3	1.0	0.977	1.3	0.675
8	D-Ala-Gly-Gly	1.0	1.0	1.0	1.0	1.0	1.0	1.0	1.0	1.0	1.0	N/A	1.0	N/A
8	D-Ala-Gly	1.0	1.0	1.0	1.0	1.0	1.0	1.0	1.0	1.0	1.0	N/A	1.0	N/A
8	Gly-D-Asp	1.0	1.0	1.0	1.0	1.0	1.0	1.0	1.0	1.0	1.0	N/A	1.0	N/A
8	Met-β-Ala	1.0	1.0	1.0	1.0	1.0	1.0	1.0	1.0	1.0	1.0	N/A	1.0	N/A
8	Leu-D-Leu	1.0	1.0	1.0	1.0	1.0	1.0	1.0	1.0	1.0	1.0	N/A	1.0	N/A
8	D-Leu-Gly	1.0	1.0	1.0	1.0	1.0	1.0	1.0	1.0	1.0	1.0	N/A	1.0	N/A
8	β-Ala-Phe	1.0	1.0	1.0	1.0	1.0	1.0	1.0	1.0	1.0	1.0	N/A	1.0	N/A
8	D-Leu-D-Leu	1.0	1.0	1.0	1.0	1.0	1.0	1.0	1.0	1.0	1.0	N/A	1.0	N/A
8	Gly-D-Val	1.0	1.0	1.0	1.0	1.0	1.0	1.0	1.0	1.0	1.0	N/A	1.0	N/A
8	Y-D-Glu-Gly	1.0	1.0	1.0	1.0	1.0	1.0	1.0	1.0	1.0	1.0	N/A	1.0	N/A
8	Met-Thr	1.0	1.0	1.0	1.0	1.0	1.0	1.0	1.0	1.0	1.0	N/A	1.0	N/A
8	Gly-D-Ser	1.0	1.0	1.0	1.0	1.0	1.0	1.0	1.0	1.0	1.0	N/A	1.0	N/A
8	Gly-D-Thr	1.0	1.0	1.0	1.0	1.0	1.0	1.0	1.0	1.0	1.0	N/A	1.0	N/A
8	Gly-Phe-Phe	1.0	1.0	1.0	1.0	1.0	1.0	1.0	1.0	1.0	1.0	N/A	1.0	N/A

8.3   Chapter 4

8.3.1 RNA extaction method optimisation

RNA extraction optimisation performed with the strain PA. Where PCR cycle threshold (CT) values were not shown, PCR was not performed.

Method	Sample	Nanodrop			Tape-station	PCR	Conclusion
		Concentration (ug/ml)	2600/280 nm	260/230 nm	RIN score (RNA integrity)	CT value	
R Neasy extraction with different volumes of cultures	1ml	8.23	0.7	0.5	4	_	The column was not saturated when increased culture volumes was used. Nanodrop integrity scores were very poor. The eluted RNA also visibly appeared cloudy. Perhaps this was due to incomplete cell lysis. Since the RNeasy lysis (RLT) buffer alone was insufficient to lyse all bacterial cells additional cell lysis treatment was required. E.g. mechanical or enzymatic. The RIN score were also low
	2.5 ml	7.23	0.7	0.5	4		
	5 ml	8.45	0.8	0.8	4		
	10 ml	9.32	0.9	0.8	4		
RNAprotect Bacterial reagent was added to the cell pellet and stored at -70 °C overnight	RNA protect Bacterial reagent	10.45	0.9	1.2	7	-	RNA protect bacterial reagent improved the RIN score and increased the RNA concentration.
	Without RNA protect bacterial reagent	10.32	0.8	0.9	4		

RNeasy extraction with bead beating vs roche nucleic lysis buffer using 5 ml culture	Bead beating	10.12	1.2	1.7	6	-	5 ml of culture did not yield the required amount of RNA. Bead beating was carried out as as per the manufacturers protocol, but yielded reduced RNA concentrations compared to treatment with lysis buffer. Nucleic lysis buffer treatment did however reduce the RIN score and caused RNA degradation perhaps due to heating at 65°C for 10 min. The extraction needed to be repeated at room temp to increase RIN scores.
	Roche Nucleic lysis buffer	10.56	1.8	1.7	5		
RNeasy kit extraction with 5ml culture and nucleic lysis buffer with and without heating at 65°C for 10 min.	Nucleic lysis buffer and proteinase K for 10 min at 65°.	12.50	1.5	1.9	5	-	Nanodrop integrity scores and RNA concentrations were still subpar for both samples. However the RIN score for the extraction performed at room temp was good. RNA concentrations from 5 ml of culture were still subpar.
	Nucleic lysis buffer and proteinase K for 10 min at room temp.	10.12	1.9	1.8	6		
RNeasy extraction kits with buffer (either TE buffer or RLT) and lysozyme and proteinase k) using 5 ml culture. TE buffer solubilises contaminants.	TE buffer for 10 min at room temp	15.78	2.0	2.1	8.2	-	Nanodrop quantity and tapestation integrity scores were very good. However RNA concentrations were still below the amount that was required. The initial culture volume needed to be increased i.e. to 10 ml or the the cell lysis step needed to be optimised.
	RLT buffer for 10 min at room temp	11.25	1.9	1.7	7.5		

RNeasy extraction kits with TE buffer and lysozyme and proteinase K 10 min at room temp vs 37 °C	Room temp	12.21	1.9	2.2	8	-	Increasing the incubation temp during the cell lysis step had no effect on RNA concentration and integrity.
	37°C	12.88	2.1	2.2	7.8		
RNeasy extraction with two on-column DNAse treatment vs one treatment with 10 ml of culture	One DNase treatment	35.88	2.1	2.2	8.5	10.5	Increasing the number of on-column DNAse treatments reduced the amount of contaminating DNA but the RNA integrity was also reduced. Perhaps this was due to the RNA being left on the column filter too long. A different type of DNAse treatment was required.
	Two DNase treatments	39.45	2.1	2.4	8	25.7	
RNeasy extraction with Turbo DNase treatment vs without turbo DNase treatment	Tubro DNase treatment	30.48	2.2	2.3	7	32.5	The additional DNase treatment reduced the concentration of DNA contamination. The RIN score dropped yet there seemed to be no contamination present when the RNA was quantified on the nanodrop. Perhaps the reduced RIN score was due to non-enzymatic catalytic degradation caused by contaminating ions found in the DNAse inactivation step. The RNA was likely to have degraded when the samples was heated to 72 °C prior to quantification on the tapestation. Perhaps cleaning the samples by passing through the column may remove contamination ions.
	Without Turbo DNase treatment	32.48	1.9	2.2	8.8	28.5	
RNeasy extraction with and without clean-up.	RNA clean-up	29.48	2.1	2.4	8.8	35.5	RNA samples that were cleaned up by passing the sample through the column again had good quality and quantity results.
	Without RNA-clean up	37.45	2.2	2.3	8	32.8	

8.3.2 SNPS and indels identified among the mexT variants

Strain	Start	End	strand	Reference allele	Variant allele	Quality score	Protein Loci	Gene	Reference codon	Variant codon	Reference amino acid	Variant amino acid
PAdel	5253698	5253698	+	A	C	1.04E-02	314	PA4684	GAG	GCG	E	A
PAnfxC	5253694	5253694	+	T	G	1.31E-05	313	PA4684	TTC	GTC	F	V
PA & PAnfxC	5655220	5655230	+	CCGGCGGCGGC	CCGGCGGCGGCGGC	1.06E-02	222, 225	PA5024	GCCGGCGGCGGC	GCCGGCGGCGGCGGC	AGGG	AGGGG
PAdel & PAnfxC	5253695	5253695	+	T	C	3.52E-04	313	PA4684	TTC	TCC	F	S
PAdel & PAnfxC	5253695	5253695	+	T	C	1.40E-06	313	PA4684	TTC	TCC	F	S

8.3.3. Genes transcriptionally altered in PAdel and PAnfxC

Fold changes in gene expression of PAdel compared to PA. Log2 fold changes over 1 (2 fold) indicated increased expression in PAdel. Log2 fold changes under -1 indicated reduced expression in PAdel.

Gene identifier	Gene	PA RPKM	PAdel RPKM	PAnfxC RPKM	PA vs PAdel log2 fold change	PA vs PAdel P-value	PA vs PAdel log2 fold change	PA vs PAnfxC P-value
PA4211	phzB1	9706	62	52	-7.3	9.3E-26	-7.6	3.8E-27
PA1902	phzD2	17927	142	125	-7	2.0E-10	-7.2	8.3E-11
PA4213	phzD1	17927	142	125	-7	2.0E-10	-7.2	8.3E-11
PA1900	phzB2	10355	69	92	-7.2	4.3E-15	-6.8	2.1E-14
PA4215	phzF1	19063	180	172	-6.7	1.6E-20	-6.8	4.4E-21
PA1904	phzF2	18751	177	170	-6.7	2.6E-20	-6.8	7.6E-21
PA1903	phzE2	44411	418	416	-6.7	4.8E-11	-6.7	3.1E-11
PA4214	phzE1	44411	418	416	-6.7	4.8E-11	-6.7	3.1E-11
PA2069	-	8683	108	109	-6.3	3.6E-20	-6.3	1.8E-20
PA4141	-	89192	1489	1188	-5.9	2.7E-123	-6.2	1.6E-133
PA3361	lecB	6202	99	92	-6	2.9E-68	-6.1	2.6E-70
PA1899	phzA2	2958	41	45	-6.2	2.8E-49	-6	1.6E-48
PA4210	phzA1	1837	24	30	-6.2	3.3E-54	-5.9	9.8E-53
PA4216	phzG1	13759	305	294	-5.5	4.7E-21	-5.5	1.5E-21
PA1905	phzG2	13821	314	296	-5.5	3.4E-21	-5.5	6.9E-22
PA2570	lecA	1343	24	30	-5.8	1.5E-98	-5.5	4.5E-93
PA3479	rhlA	16240	350	372	-5.5	4.6E-109	-5.4	1.2E-108
PA3330	-	5517	232	127	-4.6	1.8E-15	-5.4	5.8E-20
PA0122	-	33340	776	806	-5.4	2.0E-100	-5.4	8.7E-101
PA3332	-	3365	130	93	-4.7	1.2E-17	-5.2	7.3E-21
PA2300	chiC	6422	162	179	-5.3	7.0E-37	-5.2	7.9E-36
PA1901	phzC2	33614	1011	999	-5.1	1.4E-08	-5.1	9.0E-09
PA4212	phzC1	32995	1010	989	-5	1.1E-08	-5.1	6.4E-09
PA4209	phzM	8462	286	258	-4.9	5.0E-91	-5	5.7E-96
PA3329	-	5597	278	176	-4.3	1.8E-25	-5	6.9E-32
PA3333	fabH	4549	237	146	-4.3	1.3E-39	-5	7.3E-50
PA3328	-	4242	181	145	-4.6	2.6E-19	-4.9	1.2E-21

PA3334	-	1531	72	53	-4.4	2.4E-49	-4.8	3.1E-58
PA4140	-	5956	237	221	-4.7	1.4E-69	-4.8	2.0E-73
PA3331	-	7546	351	280	-4.4	6.0E-22	-4.8	2.7E-25
PA4142	-	3427	136	134	-4.7	8.0E-81	-4.7	1.1E-83
PA2068	-	2193	88	90	-4.6	1.2E-14	-4.6	1.0E-14
PA4208	opmD	4260	215	194	-4.3	2.5E-37	-4.5	1.1E-39
PA1906	-	3535	181	168	-4.3	6.3E-31	-4.4	6.2E-32
PA3335	-	2282	150	119	-3.9	2.0E-61	-4.3	2.2E-71
PA3724	lasB	53270	3669	2849	-3.9	4.7E-18	-4.2	1.6E-20
PA3336	-	2821	206	152	-3.8	5.9E-18	-4.2	1.7E-21
PA3478	rhlB	10030	520	574	-4.3	3.0E-72	-4.1	1.3E-70
PA3327	-	14028	1185	993	-3.6	2.2E-08	-3.8	2.5E-09
PA2193	hcnA	1484	124	106	-3.6	4.0E-13	-3.8	2.6E-14
PA2195	hcnC	6287	466	451	-3.8	7.9E-06	-3.8	5.7E-06
PA0123	-	6534	514	478	-3.7	6.6E-55	-3.8	1.8E-57
PA3362	-	1437	117	107	-3.6	8.6E-19	-3.7	6.3E-20
PA1871	lasA	14214	1008	1118	-3.8	8.0E-17	-3.7	4.4E-16
PA2067	-	1772	138	141	-3.7	5.8E-26	-3.7	7.5E-27
PA2194	hcnB	5176	478	423	-3.4	2.4E-04	-3.6	1.3E-04
PA1216	-	995	89	83	-3.5	8.1E-12	-3.6	2.0E-12
PA1914	-	4358	354	369	-3.6	4.0E-54	-3.6	1.4E-54
PA1869	-	1157	102	102	-3.5	1.8E-07	-3.5	1.1E-07
PA3520	-	266	23	24	-3.5	5.5E-37	-3.5	2.3E-35
PA1221	-	698	62	66	-3.5	1.2E-14	-3.4	1.8E-14
PA4143	-	1478	157	146	-3.2	9.1E-43	-3.3	1.7E-46
PA2566	-	3798	294	389	-3.7	8.1E-22	-3.3	6.2E-18
PA4206	mexH	1687	198	178	-3.1	2.0E-09	-3.2	1.9E-10
PA4205	mexG	821	100	89	-3	9.0E-11	-3.2	5.8E-12
PA1215	-	587	67	66	-3.1	2.3E-09	-3.1	2.3E-09
PA4917	-	3313	355	389	-3.2	5.7E-13	-3.1	3.1E-12
PA4294	-	4202	471	499	-3.2	9.3E-08	-3.1	1.5E-07
PA3326	-	12632	1656	1528	-2.9	5.3E-39	-3	1.3E-43
PA0852	cbpD	11412	1416	1406	-3	1.5E-21	-3	1.2E-21
PA1907	-	2055	312	255	-2.7	5.0E-34	-3	3.0E-39
PA1131		1222	144	156	-3.1	6.0E-38	-3	2.2E-38
PA4144	-	591	82	79	-2.9	3.1E-11	-2.9	3.7E-11
PA1214	-	495	67	69	-2.9	1.9E-09	-2.9	4.8E-09
PA4207	mexI	3327	482	464	-2.8	2.6E-08	-2.8	6.3E-09
PA3337	rfaD	1750	247	246	-2.8	4.2E-24	-2.8	3.1E-23
PA0052	-	1014	161	143	-2.7	1.2E-07	-2.8	4.0E-08
PA3734	-	1007	135	142	-2.9	5.5E-08	-2.8	1.2E-07
PA5220	-	1780	241	257	-2.9	4.3E-12	-2.8	1.6E-11
PA0179	-	5259	670	766	-3	4.3E-12	-2.8	4.9E-11
PA1137	-	1407	341	208	-2	1.0E-02	-2.8	1.0E-03
PA2066	-	1105	139	163	-3	1.4E-15	-2.8	2.9E-14

PA4648	-	2860	401	427	-2.8	2.2E-10	-2.7	6.0E-10
PA0200	-	517	99	77	-2.4	1.1E-06	-2.7	2.1E-07
PA1217	-	1850	287	280	-2.7	2.5E-08	-2.7	7.4E-09
PA3719	armR	118	22	18	-2.4	7.4E-04	-2.7	4.2E-04
PA3418	-	4757	685	731	-2.8	1.7E-05	-2.7	3.5E-05
PA1874	-	47257	6712	7316	-2.8	8.2E-18	-2.7	1.2E-16
PA5482	-	430	71	67	-2.6	1.8E-27	-2.7	1.4E-28
PA2565	-	780	92	123	-3.1	3.3E-38	-2.7	2.2E-31
PA3720	-	562	97	91	-2.5	3.4E-05	-2.6	3.2E-05
PA1220	-	298	49	49	-2.6	9.3E-07	-2.6	7.6E-07
PA4078	-	2920	434	494	-2.8	1.4E-10	-2.6	1.0E-09
PA1213	-	259	43	44	-2.6	9.0E-11	-2.6	4.2E-09
PA5170	arcD	10439	1728	1793	-2.6	7.0E-18	-2.5	3.9E-17
PA1656	-	1737	273	299	-2.7	5.1E-20	-2.5	1.5E-18
PA0187	-	217	31	38	-2.8	9.6E-26	-2.5	1.2E-22
PA1218	-	876	143	154	-2.6	1.1E-12	-2.5	8.3E-12
PA1130	rhlC	2007	362	357	-2.5	1.6E-11	-2.5	4.8E-12
PA1930	-	4051	666	721	-2.6	2.6E-10	-2.5	9.2E-10
PA0713	-	1224	161	219	-2.9	2.5E-12	-2.5	5.8E-09
PA3325	-	854	150	155	-2.5	1.9E-27	-2.5	1.6E-28
PA4573	-	1135	188	206	-2.6	3.4E-07	-2.5	1.3E-06
PA4916	-	3325	607	616	-2.5	4.9E-20	-2.4	1.3E-19
PA0178	-	9547	1461	1784	-2.7	7.7E-35	-2.4	7.2E-30
PA1898	qscR	549	96	103	-2.5	2.5E-26	-2.4	2.1E-25
PA5481	-	1262	204	237	-2.6	5.6E-24	-2.4	3.9E-21
PA5027	-	1551	255	294	-2.6	2.5E-16	-2.4	1.0E-14
PA2024	-	1297	247	248	-2.4	3.9E-03	-2.4	4.4E-03
PA3691	-	2340	429	461	-2.4	7.1E-18	-2.3	3.8E-17
PA4133	-	11987	2914	2380	-2	1.3E-09	-2.3	2.5E-13
PA4649	-	732	136	145	-2.4	4.1E-26	-2.3	4.9E-25
PA2937	-	615	133	122	-2.2	1.2E-04	-2.3	1.0E-04
PA3688	-	1682	306	338	-2.5	1.1E-14	-2.3	2.0E-13
PA1784	-	1481	256	298	-2.5	4.5E-15	-2.3	1.8E-13
PA4293	pprA	7640	1436	1546	-2.4	2.2E-28	-2.3	1.7E-27
PA4217	phzS	20452	4593	4217	-2.2	8.6E-15	-2.3	2.6E-16
PA4739	-	3374	591	696	-2.5	6.6E-30	-2.3	5.8E-26
PA4348	-	906	189	188	-2.3	4.4E-14	-2.3	4.2E-13
PA4577	-	461	102	97	-2.2	3.7E-04	-2.3	3.8E-04
PA1894	-	1586	289	334	-2.5	5.7E-08	-2.2	6.6E-07
PA3692	lptF	4010	861	849	-2.2	6.4E-19	-2.2	1.2E-18
PA1877	-	2461	474	523	-2.4	3.4E-26	-2.2	1.4E-23
PA0177	-	3032	519	649	-2.5	2.5E-30	-2.2	6.8E-25
PA2564	-	1376	217	295	-2.7	2.1E-14	-2.2	4.7E-11
PA1870	-	148	26	32	-2.5	6.9E-10	-2.2	1.6E-08
PA1324	-	1650	339	356	-2.3	3.9E-13	-2.2	1.3E-12

PA5475	-	3764	671	813	-2.5	4.5E-17	-2.2	3.2E-13
PA3986	-	1548	333	339	-2.2	6.2E-06	-2.2	1.4E-05
PA4359	-	211	48	46	-2.1	1.0E-02	-2.2	1.1E-02
PA1212	-	302	73	67	-2	3.4E-16	-2.2	1.9E-18
PA4306	-	14011	3103	3107	-2.2	6.6E-09	-2.2	3.9E-09
PA2274	-	203	45	45	-2.2	1.1E-04	-2.2	5.5E-05
PA2788	-	5623	882	1255	-2.7	3.0E-34	-2.2	1.2E-23
PA1323	-	1172	249	262	-2.2	4.4E-23	-2.2	1.4E-22
PA1895	-	2042	427	469	-2.3	1.5E-08	-2.1	8.4E-08
PA3417	-	3698	727	850	-2.3	4.5E-22	-2.1	1.2E-19
PA1557	ccoN	3837	745	887	-2.4	5.0E-09	-2.1	4.6E-07
PA1524	xdhA	938	227	218	-2	1.7E-05	-2.1	1.6E-05
PA2174	-	370	76	86	-2.3	1.2E-06	-2.1	5.2E-06
PA1177	napE	1924	339	447	-2.5	9.9E-10	-2.1	2.9E-07
PA1875	-	3002	602	698	-2.3	1.5E-26	-2.1	1.4E-21
PA0176	-	11560	2092	2701	-2.5	3.2E-29	-2.1	1.2E-22
PA0208	mdcA	3361	689	789	-2.3	1.1E-03	-2.1	2.0E-03
PA2142	-	207	58	49	-1.8	5.2E-14	-2.1	8.7E-17
PA4108	-	1730	409	409	-2.1	8.7E-04	-2.1	9.1E-04
PA0484	-	2509	583	604	-2.1	3.5E-06	-2.1	7.0E-06
PA3945	-	1887	410	454	-2.2	2.8E-06	-2.1	9.4E-06
PA4305	rcpC	6360	1360	1534	-2.2	3.8E-16	-2.1	2.4E-14
PA1415	-	1092	241	267	-2.2	1.2E-06	-2	6.9E-06
PA4311	-	3896	844	962	-2.2	9.2E-25	-2	5.4E-21
PA5429	aspA	7746	1988	1918	-2	1.5E-03	-2	1.5E-03
PA2618	-	1940	481	481	-2	1.3E-02	-2	1.4E-02
PA4352	-	4078	745	1023	-2.5	1.1E-16	-2	1.8E-11
PA2501	-	372	89	93	-2.1	1.0E-03	-2	1.5E-03
PA5383	-	4093	1008	1031	-2	3.3E-02	-2	2.9E-02
PA2573	-	7267	1668	1834	-2.1	3.3E-21	-2	4.9E-19
PA3939	-	707	201	179	-1.8	9.2E-11	-2	4.4E-12
PA1289	-	556	135	141	-2	3.5E-03	-2	5.7E-03
PA3451	-	965	215	248	-2.2	1.0E-06	-2	3.5E-06
PA2192	-	65	18	17	-1.9	1.6E-08	-2	2.2E-08
PA1876	-	4701	1066	1210	-2.1	4.0E-12	-2	2.6E-10
PA1657	-	699	160	180	-2.1	4.7E-14	-2	3.5E-12
PA5446	-	4202	908	1084	-2.2	1.5E-06	-2	1.5E-05
PA4738	-	1626	316	420	-2.4	6.1E-26	-2	6.0E-19
PA1176	napF	1596	312	413	-2.4	2.0E-17	-1.9	1.1E-12
PA0442	-	1	0	0	-1	7.5E-01	-1.9	5.5E-01
PA4651	-	1882	460	491	-2	2.1E-05	-1.9	3.3E-05
PA3930	cioA	5902	840	1541	-2.8	1.9E-37	-1.9	2.9E-19
PA2919	-	222	69	58	-1.7	1.3E-07	-1.9	9.5E-09
PA0451	-	965	220	252	-2.1	1.2E-05	-1.9	3.5E-05
PA4925	-	1575	382	413	-2	1.3E-08	-1.9	7.8E-08

PA4384	-	478	147	126	-1.7	2.8E-07	-1.9	1.8E-08
PA0788	-	3541	881	940	-2	3.8E-09	-1.9	2.1E-08
PA2588	-	1773	479	478	-1.9	6.6E-19	-1.9	3.7E-18
PA4915	-	5014	1261	1356	-2	1.0E-11	-1.9	5.8E-11
PA2747	-	1202	309	326	-2	2.2E-19	-1.9	1.4E-18
PA3974	ladS	2583	711	710	-1.9	1.3E-18	-1.9	1.8E-18
PA1837	-	1203	316	331	-1.9	1.7E-07	-1.9	6.3E-07
PA4130	-	14848	4256	4096	-1.8	6.8E-16	-1.9	2.0E-18
PA5208	-	1623	440	448	-1.9	3.7E-03	-1.9	4.8E-03
PA4781	-	3427	845	954	-2	7.0E-12	-1.8	2.2E-10
PA2071	fusA2	9879	2328	2751	-2.1	1.5E-22	-1.8	3.3E-19
PA3416	-	3430	850	955	-2	1.5E-20	-1.8	4.0E-19
PA2072	-	3407	777	950	-2.1	2.3E-13	-1.8	9.4E-11
PA2571	-	3301	804	922	-2	1.0E-21	-1.8	1.1E-18
PA4650	-	511	127	143	-2	9.9E-13	-1.8	1.4E-10
PA2433	-	306	83	86	-1.9	1.5E-15	-1.8	1.9E-13
PA4129	-	3510	1063	981	-1.7	2.7E-11	-1.8	2.4E-14
PA1551	-	3797	660	1062	-2.5	1.2E-14	-1.8	1.6E-08
PA2779	-	1345	379	377	-1.8	3.8E-09	-1.8	1.4E-09
PA4351	-	1760	359	493	-2.3	3.8E-18	-1.8	6.1E-12
PA0051	phzH	486	117	137	-2.1	7.6E-11	-1.8	1.2E-08
PA1897	-	488	127	138	-1.9	2.8E-16	-1.8	1.9E-15
PA0007	-	3355	816	949	-2	1.2E-21	-1.8	5.8E-18
PA1728	-	4366	1142	1237	-1.9	3.1E-20	-1.8	1.5E-18
PA1878	-	980	275	278	-1.8	2.9E-17	-1.8	2.5E-16
PA4128	-	1566	489	445	-1.7	2.1E-11	-1.8	3.3E-14
PA4523	-	18564	4733	5279	-2	8.4E-18	-1.8	1.4E-15
PA2168	-	59	20	17	-1.5	3.1E-06	-1.8	9.7E-08
PA1355	-	183	51	53	-1.8	1.7E-07	-1.8	2.0E-07
PA2070	-	925	256	266	-1.9	6.2E-17	-1.8	3.2E-17
PA4703	-	319	83	92	-1.9	6.6E-07	-1.8	6.3E-06
PA1896	-	737	193	213	-1.9	1.5E-08	-1.8	8.1E-08
PA4702	-	687	193	200	-1.8	2.8E-11	-1.8	4.0E-11
PA4681	-	607	199	177	-1.6	1.7E-13	-1.8	4.1E-16
PA1673	-	767	228	225	-1.8	6.9E-07	-1.8	1.7E-06
PA1414	-	4045	957	1186	-2.1	5.6E-04	-1.8	4.7E-03
PA4304	rcpA	6902	1778	2039	-2	1.3E-08	-1.8	1.5E-07
PA3369	-	308	95	91	-1.7	5.0E-10	-1.8	7.0E-11
PA2173	-	59	20	17	-1.6	1.4E-03	-1.8	5.8E-04
PA2166	-	121	28	36	-2.1	1.3E-07	-1.7	7.4E-06
PA4682	-	851	265	254	-1.7	6.8E-05	-1.7	6.3E-05
PA3465	-	3224	926	962	-1.8	3.0E-16	-1.7	2.9E-15
PA0588	-	96277	24587	28900	-2	6.7E-21	-1.7	1.2E-17
PA4115	-	3598	1121	1085	-1.7	9.5E-12	-1.7	2.1E-12
PA2572	-	5370	1497	1622	-1.8	7.8E-11	-1.7	6.8E-10

PA2753	-	272	85	82	-1.7	3.7E-04	-1.7	4.5E-04
PA2746	-	671	228	203	-1.6	2.0E-02	-1.7	1.3E-02
PA2939	-	25925	6816	7902	-1.9	1.0E-04	-1.7	5.9E-04
PA0188	-	135	35	41	-1.9	1.1E-10	-1.7	9.0E-10
PA2746	-	674	194	206	-1.8	1.1E-04	-1.7	2.5E-04
PA3311	-	2739	720	841	-1.9	8.3E-19	-1.7	2.0E-15
PA3858	-	3684	1061	1131	-1.8	1.6E-13	-1.7	3.7E-12
PA1659	-	176	49	54	-1.8	2.1E-12	-1.7	8.9E-12
PA1658	-	1804	478	558	-1.9	6.0E-07	-1.7	6.9E-06
PA2799	-	904	285	280	-1.7	5.5E-04	-1.7	7.6E-04
PA1892	-	400	117	124	-1.8	3.1E-14	-1.7	1.1E-13
PA2920	-	2436	723	763	-1.8	1.5E-17	-1.7	3.0E-16
PA5171	arcA	25883	5516	8119	-2.2	2.9E-12	-1.7	4.3E-07
PA0108	col	2360	926	741	-1.3	3.0E-09	-1.7	7.0E-14
PA1129	-	392	128	123	-1.6	1.3E-04	-1.7	4.5E-05
PA0209		417	138	131	-1.6	3.9E-02	-1.7	2.9E-02
PA3723	-	7864	2266	2478	-1.8	1.8E-14	-1.7	4.1E-13
PA3309	-	13233	2344	4176	-2.5	2.6E-17	-1.7	5.5E-08
PA1662	-	1159	357	366	-1.7	7.4E-06	-1.7	1.7E-05
PA1891	-	103	35	32	-1.5	1.9E-08	-1.7	4.5E-09
PA4295	fppA	326	110	103	-1.6	5.1E-11	-1.7	4.1E-12
PA1175	napD	1608	352	514	-2.2	7.9E-21	-1.6	1.2E-12
PA3920	-	1450	426	464	-1.8	3.7E-11	-1.6	2.5E-10
PA0059	osmC	480	153	154	-1.6	3.1E-13	-1.6	3.7E-12
PA2786	-	472	124	152	-1.9	1.6E-02	-1.6	2.9E-02
PA2778	-	1426	497	460	-1.5	7.0E-14	-1.6	1.9E-15
PA3089	-	1058	352	342	-1.6	2.0E-07	-1.6	1.2E-07
PA0109	-	873	307	283	-1.5	1.7E-05	-1.6	2.0E-06
PA2938	-	888	252	288	-1.8	3.8E-07	-1.6	4.0E-06
PA0201	-	2261	768	734	-1.6	2.7E-06	-1.6	1.4E-06
PA2118	-	288	89	94	-1.7	2.7E-07	-1.6	1.3E-06
PA1888	-	4191	1000	1371	-2.1	2.2E-09	-1.6	1.4E-06
PA2182	-	243	68	80	-1.8	2.2E-11	-1.6	1.1E-09
PA2142	-	438	117	144	-1.9	5.3E-17	-1.6	5.3E-14
PA4131	-	5028	1442	1657	-1.8	8.0E-09	-1.6	3.0E-07
PA1118	-	1762	519	581	-1.8	7.6E-06	-1.6	4.5E-05
PA2062	-	3895	1181	1284	-1.7	3.5E-08	-1.6	1.7E-07
PA4084	cupB	724	215	239	-1.8	9.6E-06	-1.6	3.6E-05
PA1860	-	1438	438	476	-1.7	3.2E-14	-1.6	2.7E-13
PA4296	pprB	10253	3512	3475	-1.5	2.1E-14	-1.6	2.8E-15
PA5424	-	2925	808	991	-1.9	1.1E-08	-1.6	1.0E-06
PA4302	tadA	5400	1547	1844	-1.8	2.4E-15	-1.6	2.2E-12
PA3476	rhlI	5470	1895	1869	-1.5	2.8E-03	-1.5	2.4E-03
PA4175	-	31355	10382	10734	-1.6	1.9E-10	-1.5	4.3E-10
PA1730	-	1645	503	565	-1.7	2.6E-15	-1.5	1.4E-12

PA4358	-	3047	910	1047	-1.7	2.3E-08	-1.5	1.7E-06
PA1111	-	85	35	29	-1.3	3.6E-05	-1.5	9.4E-06
PA2504	-	2495	717	861	-1.8	6.8E-06	-1.5	9.8E-05
PA1668	-	355	113	123	-1.7	2.7E-12	-1.5	2.9E-10
PA3370	-	82	24	28	-1.8	1.4E-09	-1.5	2.2E-08
PA3914	moeA	183	70	63	-1.4	7.8E-05	-1.5	3.8E-06
PA5219	-	913	297	316	-1.6	5.9E-09	-1.5	2.0E-08
PA2500	-	743	242	258	-1.6	1.5E-09	-1.5	9.3E-09
PA0355	pfpI	452	151	158	-1.6	9.1E-12	-1.5	3.8E-11
PA5384	-	186	69	65	-1.4	8.9E-02	-1.5	7.2E-02
PA3366	amiE	4208	1666	1479	-1.3	6.3E-12	-1.5	1.0E-12
PA1663	-	460	129	162	-1.8	2.9E-15	-1.5	4.1E-11
PA1664	-	24	6	9	-1.9	1.3E-04	-1.5	8.2E-04
PA1523	xdhB	2059	642	726	-1.7	5.6E-15	-1.5	6.0E-13
PA2146	-	22	6	8	-1.9	3.6E-05	-1.5	1.6E-03
PA1041	-	24101	6598	8538	-1.9	1.2E-15	-1.5	2.5E-11
PA3415	-	2521	815	895	-1.6	1.2E-14	-1.5	1.3E-13
PA3919	-	8947	3027	3175	-1.6	1.4E-14	-1.5	5.3E-14
PA2415	-	170	76	61	-1.2	6.6E-06	-1.5	6.1E-09
PA2310	-	437	137	155	-1.7	9.7E-03	-1.5	1.3E-02
PA4328	-	998	318	355	-1.7	7.6E-11	-1.5	5.0E-09
PA2592	-	4690	1687	1682	-1.5	4.0E-05	-1.5	2.9E-05
PA4236	katA	6604	2186	2372	-1.6	2.7E-11	-1.5	4.2E-10
PA2364	-	1292	427	466	-1.6	1.3E-07	-1.5	1.1E-06
PA2574	alkB	760	247	274	-1.6	2.6E-08	-1.5	2.4E-07
PA4303	tadZ	4638	1426	1675	-1.7	1.1E-07	-1.5	7.3E-07
PA5527	-	1659	590	601	-1.5	1.9E-08	-1.5	2.5E-08
PA0175	-	1328	289	483	-2.2	1.8E-22	-1.5	4.2E-11
PA2754	-	696	217	253	-1.7	1.1E-14	-1.5	5.1E-12
PA1429	-	1196	418	435	-1.5	2.7E-09	-1.5	3.3E-08
PA0830	-	1061	389	388	-1.4	3.4E-12	-1.5	1.8E-12
PA4134	-	807	301	295	-1.4	2.6E-10	-1.5	1.9E-11
PA4680	-	206	81	76	-1.4	1.6E-08	-1.4	2.8E-09
PA1745	-	826	282	303	-1.5	8.6E-06	-1.4	2.6E-05
PA0105	coxB	3723	1575	1369	-1.2	2.7E-06	-1.4	3.0E-08
PA1556	ccoO	1557	360	574	-2.1	5.7E-04	-1.4	3.1E-02
PA0180	cttP	2997	1027	1107	-1.5	1.1E-13	-1.4	1.4E-12
PA5172	arcB	24143	5511	8923	-2.1	1.3E-12	-1.4	6.4E-06
PA3957	-	1338	440	495	-1.6	1.8E-10	-1.4	3.4E-09
PA5207	-	767	254	284	-1.6	4.0E-06	-1.4	3.6E-05
PA3341	-	2587	826	958	-1.6	1.7E-08	-1.4	9.0E-07
PA5261	algR	8397	2935	3111	-1.5	5.8E-14	-1.4	7.3E-13
PA4301	tadB	2371	634	881	-1.9	2.6E-17	-1.4	1.6E-10
PA0506	-	4314	1856	1605	-1.2	1.5E-07	-1.4	5.3E-10
PA0199	exbD	531	169	198	-1.7	3.2E-09	-1.4	6.4E-08

PA3385	amrZ	10756	3853	4024	-1.5	6.3E-13	-1.4	4.5E-12
PA1211	-	136	53	51	-1.4	7.9E-07	-1.4	4.9E-07
PA1660	-	764	260	287	-1.6	2.2E-11	-1.4	1.7E-09
PA3689	-	1137	399	427	-1.5	1.6E-13	-1.4	2.1E-12
PA1174	napA	3334	882	1253	-1.9	2.0E-18	-1.4	3.8E-11
PA0714	-	217	66	81	-1.7	4.3E-04	-1.4	3.4E-03
PA4377	-	2237	774	841	-1.5	3.4E-09	-1.4	5.6E-08
PA0543	-	499	182	188	-1.5	4.1E-11	-1.4	6.7E-11
PA2563	-	761	252	287	-1.6	1.8E-12	-1.4	1.7E-10
PA3877	narK1	193	70	73	-1.5	2.6E-04	-1.4	1.5E-04
PA3846	-	1359	477	512	-1.5	5.5E-13	-1.4	2.5E-11
PA4297	tadG	3850	1263	1455	-1.6	5.5E-14	-1.4	3.0E-11
PA2176	-	126	45	48	-1.5	1.5E-08	-1.4	1.7E-08
PA4369	-	1395	474	529	-1.6	5.6E-04	-1.4	1.3E-03
PA0575	-	2520	847	955	-1.6	1.3E-13	-1.4	2.2E-11
PA3929	cioB	3612	812	1370	-2.2	1.8E-22	-1.4	1.9E-10
PA1872	-	2228	803	848	-1.5	5.8E-12	-1.4	3.1E-11
PA1661	-	379	136	144	-1.5	1.8E-10	-1.4	7.1E-09
PA2633	-	1798	661	686	-1.4	1.1E-03	-1.4	1.4E-03
PA2136	-	28	7	11	-1.9	1.0E-02	-1.4	4.1E-02
PA2312	-	471	154	180	-1.6	1.4E-02	-1.4	2.7E-02
PA0202	-	906	363	346	-1.3	1.4E-05	-1.4	3.3E-06
PA1136	-	465	227	178	-1	3.6E-02	-1.4	8.5E-03
PA1879	-	494	167	189	-1.6	3.3E-12	-1.4	7.1E-10
PA1873	-	235	84	90	-1.5	1.6E-10	-1.4	1.9E-09
PA1887	-	2357	678	906	-1.8	1.5E-08	-1.4	2.5E-06
PA2181	-	203	76	78	-1.4	2.3E-09	-1.4	1.2E-09
PA2787	-	1642	525	632	-1.6	3.5E-14	-1.4	1.1E-10
PA4041	-	834	298	321	-1.5	1.4E-12	-1.4	9.4E-11
PA5427	adhA	5500	1261	2121	-2.1	4.2E-18	-1.4	6.7E-08
PA1881	-	526	167	203	-1.7	4.0E-06	-1.4	5.0E-05
PA5473	-	1560	579	603	-1.4	5.9E-12	-1.4	2.6E-11
PA2170	-	7	5	3	-0.7	3.3E-01	-1.4	3.0E-02
PA3275	-	219	75	85	-1.6	6.1E-05	-1.4	2.2E-04
PA3876	narK2	213	96	83	-1.1	1.4E-06	-1.4	8.3E-08
PA3371	-	304	115	118	-1.4	1.6E-08	-1.4	2.2E-08
PA5262	algZ	4674	1648	1821	-1.5	1.1E-12	-1.4	9.0E-11
PA2231	pslA	3749	1267	1462	-1.6	5.6E-11	-1.4	4.4E-08
PA0121	-	660	273	258	-1.3	1.2E-09	-1.4	3.9E-11
PA0587	-	26619	8807	10408	-1.6	2.7E-14	-1.4	3.6E-12
PA1893	-	1222	411	479	-1.6	1.1E-09	-1.4	1.5E-07
PA4298	-	545	158	214	-1.8	6.1E-08	-1.4	5.1E-05
PA4299	tadD	2555	792	1002	-1.7	2.2E-14	-1.4	1.3E-09
PA1922	-	146	69	57	-1.1	5.3E-05	-1.4	7.3E-07
PA2359	-	1026	381	403	-1.4	4.0E-03	-1.3	5.1E-03

PA1327	-	2812	987	1110	-1.5	6.2E-12	-1.3	5.5E-10
PA2448	-	928	380	367	-1.3	1.2E-05	-1.3	6.1E-06
PA0743	-	2630	1198	1040	-1.1	5.3E-05	-1.3	3.0E-06
PA1951	-	1927	701	764	-1.5	1.4E-12	-1.3	5.7E-11
PA3347	-	2631	928	1045	-1.5	1.1E-06	-1.3	7.6E-06
PA0951	-	718	297	286	-1.3	8.0E-04	-1.3	4.6E-04
PA2167	-	147	46	59	-1.7	1.4E-08	-1.3	1.5E-06
PA0483	-	1040	344	416	-1.6	3.0E-06	-1.3	8.7E-05
PA4312	-	2107	750	843	-1.5	1.1E-11	-1.3	2.1E-09
PA4637	-	14452	4756	5790	-1.6	5.2E-14	-1.3	5.0E-10
PA1666	-	254	92	102	-1.5	1.3E-05	-1.3	7.1E-05
PA4300	tadC	2439	763	980	-1.7	1.0E-13	-1.3	1.3E-08
PA0106	coxA	2402	1210	967	-1	2.7E-04	-1.3	3.7E-07
PA4683	-	479	195	193	-1.3	3.0E-02	-1.3	3.1E-02
PA1880	-	3250	1085	1309	-1.6	1.2E-10	-1.3	1.6E-08
PA5103	-	1860	740	750	-1.3	6.1E-05	-1.3	3.7E-05
PA4876	osmE	1343	460	543	-1.5	1.8E-12	-1.3	8.8E-10
PA3931	-	1178	430	476	-1.5	5.7E-03	-1.3	8.7E-03
PA3446	-	1782	760	723	-1.2	8.3E-03	-1.3	5.7E-03
PA0776	-	222	75	90	-1.6	7.9E-05	-1.3	5.6E-04
PA1550	-	1792	441	730	-2	2.1E-11	-1.3	1.8E-05
PA1191	-	559	206	228	-1.4	1.1E-06	-1.3	1.4E-05
PA2114	-	979	396	400	-1.3	5.2E-09	-1.3	1.5E-08
PA0704	-	1811	697	740	-1.4	3.3E-10	-1.3	2.4E-09
PA0983	-	502	208	205	-1.3	3.3E-08	-1.3	4.5E-08
PA1408	-	1277	453	522	-1.5	8.5E-09	-1.3	2.1E-07
PA5108	-	1334	568	547	-1.2	3.9E-09	-1.3	3.2E-10
PA4127	hpcG	368	158	151	-1.2	2.6E-07	-1.3	6.0E-09
PA2299	-	442	192	182	-1.2	4.1E-09	-1.3	1.2E-09
PA2311	-	285	101	117	-1.5	1.3E-02	-1.3	2.2E-02
PA2620	clpA	37243	14947	15359	-1.3	6.4E-11	-1.3	1.9E-10
PA5379	sdaB	315	131	130	-1.3	1.9E-04	-1.3	2.4E-04
PA2196	-	618	238	255	-1.4	1.0E-09	-1.3	1.7E-08
PA2506	-	20	12	8	-0.7	2.4E-02	-1.3	4.2E-03
PA4653	-	728	287	301	-1.3	1.3E-05	-1.3	5.3E-05
PA3307	-	466	180	193	-1.4	2.0E-06	-1.3	4.1E-06
PA2717	-	1064	375	440	-1.5	9.3E-12	-1.3	1.1E-08
PA0038	-	1466	543	608	-1.4	2.1E-12	-1.3	1.8E-10
PA2119	-	1208	505	501	-1.3	2.7E-09	-1.3	3.5E-09
PA5212	-	786	341	329	-1.2	7.1E-08	-1.3	1.0E-08
PA0732	-	1570	628	658	-1.3	8.3E-11	-1.3	6.3E-10
PA3613	-	2588	882	1089	-1.6	4.1E-06	-1.2	3.7E-04
PA3928	-	444	97	188	-2.2	1.1E-12	-1.2	5.7E-05
PA0173	-	464	140	196	-1.7	1.8E-07	-1.2	4.4E-04
PA2169	-	37	15	16	-1.3	1.0E-04	-1.2	5.0E-04

PA5173	arcC	14535	3467	6140	-2.1	2.8E-08	-1.2	2.1E-03
PA5058	phaC	3688	1370	1562	-1.4	2.3E-07	-1.2	1.1E-05
PA4929	-	2795	1086	1184	-1.4	3.1E-10	-1.2	8.9E-09
PA1561	-	2565	1024	1088	-1.3	1.6E-10	-1.2	2.1E-09
PA5496	nrdJb	8449	1428	3584	-2.6	3.5E-07	-1.2	1.1E-02
PA5304	dadA	5520	2508	2345	-1.1	1.5E-02	-1.2	1.0E-02
PA4139	-	363	172	154	-1.1	1.5E-06	-1.2	1.2E-08
PA2589	-	360	155	153	-1.2	2.9E-07	-1.2	7.5E-08
PA3261	-	2427	921	1038	-1.4	5.7E-07	-1.2	6.1E-06
PA1925	-	42	21	18	-1	2.4E-03	-1.2	2.1E-03
PA0459	-	13304	3893	5705	-1.8	2.3E-11	-1.2	4.4E-06
PA4658	-	1016	407	436	-1.3	1.5E-08	-1.2	3.1E-08
PA4812	fdnG	1973	817	848	-1.3	6.2E-10	-1.2	2.5E-09
PA1546	hemN	4040	1614	1737	-1.3	1.4E-10	-1.2	3.5E-09
PA4652	-	1122	407	483	-1.5	3.5E-10	-1.2	9.0E-08
PA1747	-	138	50	59	-1.4	7.2E-07	-1.2	8.9E-05
PA0174	-	338	93	146	-1.9	2.3E-10	-1.2	5.6E-05
PA3458	-	651	262	281	-1.3	1.7E-06	-1.2	1.3E-05
PA1219	-	167	67	72	-1.3	1.9E-07	-1.2	3.5E-06
PA2059	-	76	28	33	-1.4	7.5E-04	-1.2	3.7E-03
PA1667	-	791	313	342	-1.3	2.9E-09	-1.2	5.0E-08
PA4017	-	2357	1019	1023	-1.2	3.3E-04	-1.2	4.0E-04
PA0656	-	1059	381	460	-1.5	2.0E-12	-1.2	3.2E-09
PA3298	-	105	34	46	-1.6	3.0E-04	-1.2	5.0E-03
PA0256	-	1377	531	600	-1.4	1.3E-11	-1.2	2.2E-09
PA0769	-	2198	872	959	-1.3	2.3E-06	-1.2	1.6E-05
PA1181	-	1986	748	867	-1.4	4.7E-11	-1.2	1.1E-08
PA3431	-	157	68	68	-1.2	7.0E-06	-1.2	8.0E-06
PA1789	-	4139	1603	1809	-1.4	4.8E-08	-1.2	2.2E-06
PA1665	-	356	149	155	-1.3	4.7E-07	-1.2	2.2E-06
PA5439	-	1563	679	684	-1.2	5.5E-05	-1.2	7.6E-05
PA0710	gloA	121	51	53	-1.3	4.6E-05	-1.2	8.7E-05
PA0838	-	2885	1149	1264	-1.3	7.7E-07	-1.2	6.7E-06
PA2179	-	55	25	24	-1.1	7.3E-04	-1.2	5.2E-04
PA5497	nrdJa	26387	5527	11639	-2.3	4.3E-08	-1.2	3.2E-03
PA5213	gcvP1	6020	2310	2670	-1.4	7.6E-06	-1.2	1.1E-04
PA1366	-	1671	667	742	-1.3	1.8E-04	-1.2	4.9E-04
PA4132	-	4658	1798	2076	-1.4	1.7E-05	-1.2	2.1E-04
PA3430	-	318	133	142	-1.3	1.5E-07	-1.2	8.5E-07
PA1562	acnA	6250	2515	2787	-1.3	7.1E-10	-1.2	2.2E-08
PA3216	-	259	109	115	-1.3	4.3E-07	-1.2	3.3E-07
PA2232	pslB	7445	2690	3321	-1.5	1.2E-11	-1.2	8.7E-08
PA2228	-	431	218	193	-1	1.1E-03	-1.2	1.7E-04
PA1931	-	326	125	146	-1.4	2.7E-09	-1.2	2.8E-07
PA4608	-	1616	666	724	-1.3	2.9E-05	-1.2	1.3E-04

PA1670	-	230	103	103	-1.2	3.1E-06	-1.2	1.6E-06
PA2555	-	3335	2075	1496	-0.7	1.1E-03	-1.2	3.3E-07
PA2190	-	168	61	75	-1.5	5.9E-09	-1.2	2.3E-06
PA1753	-	1733	700	780	-1.3	3.5E-06	-1.2	2.4E-05
PA0958	oprD	32077	17958	14466	-0.8	3.4E-03	-1.1	7.9E-05
PA2090	-	362	126	163	-1.5	9.0E-11	-1.1	6.6E-07
PA4067	oprG	20473	4926	9240	-2.1	7.6E-13	-1.1	1.3E-04
PA3432	-	87	35	39	-1.3	2.7E-04	-1.1	2.2E-03
PA3450	-	8628	3847	3899	-1.2	7.0E-03	-1.1	5.7E-03
PA3040	-	5634	1792	2548	-1.7	7.2E-15	-1.1	1.0E-07
PA2621	-	6505	2912	2942	-1.2	2.2E-08	-1.1	2.9E-08
PA5359	-	3864	1563	1748	-1.3	1.9E-10	-1.1	1.2E-08
PA3733	-	387	164	175	-1.2	7.7E-07	-1.1	2.1E-06
PA3449	-	215	67	98	-1.7	1.2E-06	-1.1	1.9E-04
PA4535	-	1969	864	894	-1.2	5.0E-07	-1.1	1.6E-06
PA2092	-	250	100	114	-1.3	2.7E-08	-1.1	3.8E-06
PA0107	-	567	324	258	-0.8	1.2E-03	-1.1	1.1E-06
PA4607	-	83284	31295	37963	-1.4	3.3E-11	-1.1	1.2E-07
PA1167	-	812	322	371	-1.3	1.7E-07	-1.1	7.5E-06
PA3041	-	3072	1005	1405	-1.6	6.6E-14	-1.1	2.0E-07
PA3340	-	4890	2382	2239	-1	2.9E-07	-1.1	5.0E-08
PA2091	-	292	107	134	-1.4	4.5E-04	-1.1	7.4E-03
PA3343	-	1198	552	549	-1.1	8.0E-07	-1.1	4.7E-07
PA2791	-	212	78	98	-1.4	2.2E-10	-1.1	3.6E-07
PA0959	-	3354	1539	1546	-1.1	1.6E-06	-1.1	1.3E-06
PA1774	crfX	966	407	446	-1.2	6.0E-07	-1.1	6.4E-06
PA2475	-	1128	500	521	-1.2	4.9E-08	-1.1	1.7E-07
PA4112	-	6646	2745	3072	-1.3	2.2E-09	-1.1	1.2E-07
PA0854	fumC	3015	1416	1394	-1.1	2.0E-07	-1.1	8.0E-08
PA0276	-	173	79	80	-1.1	4.3E-04	-1.1	2.6E-04
PA3944	-	771	323	357	-1.3	2.1E-09	-1.1	6.0E-08
PA5546	-	11144	4236	5159	-1.4	1.2E-10	-1.1	1.2E-07
PA1732	-	1008	428	468	-1.2	2.1E-08	-1.1	1.3E-07
PA3519	-	64	27	30	-1.3	3.6E-05	-1.1	9.4E-05
PA1208	-	840	355	390	-1.2	1.1E-07	-1.1	2.8E-06
PA0332	-	864	413	402	-1.1	1.3E-06	-1.1	6.6E-07
PA3938	-	2711	1103	1262	-1.3	8.1E-02	-1.1	9.3E-02
PA0468	-	1187	568	554	-1.1	3.2E-07	-1.1	2.2E-07
PA0531	-	278	124	130	-1.2	2.3E-03	-1.1	5.7E-03
PA0191	-	598	240	280	-1.3	1.3E-02	-1.1	2.5E-02
PA2127	-	806	339	378	-1.2	3.1E-09	-1.1	1.1E-07
PA3857	-	1850	861	867	-1.1	1.1E-06	-1.1	1.3E-06
PA2149	-	5	4	3	-0.5	5.5E-01	-1.1	3.2E-01
PA4654	-	213	99	100	-1.1	1.6E-06	-1.1	5.6E-06
PA2375	-	624	251	293	-1.3	3.8E-09	-1.1	3.6E-07

PA0861	-	5182	2204	2438	-1.2	1.6E-09	-1.1	4.0E-08
PA3973	-	641	284	302	-1.2	3.4E-07	-1.1	2.9E-06
PA2562	-	2725	1210	1284	-1.2	1.6E-08	-1.1	1.2E-07
PA0586	-	22379	8614	10574	-1.4	2.0E-10	-1.1	1.7E-07
PA4024	eutB	1228	634	580	-1	3.3E-06	-1.1	2.0E-07
PA4350	-	543	183	257	-1.6	9.6E-09	-1.1	1.6E-04
PA1183	dctA	311	232	147	-0.4	6.0E-01	-1.1	8.7E-02
PA2275	-	258	129	122	-1	8.8E-06	-1.1	8.7E-07
PA0547	-	11372	4523	5383	-1.3	6.6E-11	-1.1	1.3E-07
PA3346	-	4058	1759	1922	-1.2	3.8E-09	-1.1	5.3E-08
PA3932	-	786	325	373	-1.3	4.3E-08	-1.1	8.4E-07
PA2180	-	48	22	23	-1.1	2.2E-02	-1.1	2.8E-02
PA1173	napB	147	52	70	-1.5	6.3E-08	-1.1	6.4E-05
PA4116	bphO	726	349	346	-1.1	5.1E-08	-1.1	5.1E-08
PA3891	-	348	176	166	-1	1.9E-04	-1.1	1.5E-04
PA1166	-	934	390	446	-1.3	2.9E-09	-1.1	3.6E-07
PA3572	-	582	272	278	-1.1	4.2E-03	-1.1	1.2E-02
PA4117	bphP	4061	1942	1941	-1.1	1.4E-07	-1.1	9.6E-08
PA2150	-	57	24	27	-1.2	3.1E-04	-1.1	2.4E-03
PA4636	-	158	76	76	-1	7.0E-06	-1.1	1.4E-05
PA0460	-	2906	1063	1395	-1.5	8.6E-12	-1.1	8.2E-07
PA5107	-	2535	1139	1224	-1.2	1.3E-08	-1	1.1E-07
PA4126	-	231	109	112	-1.1	8.4E-06	-1	4.4E-06
PA4027	-	737	362	356	-1	3.9E-06	-1	1.5E-06
PA1921	-	54	30	26	-0.9	2.3E-03	-1	4.5E-04
PA4877	-	547	218	265	-1.3	7.9E-09	-1	1.7E-06
PA2177	-	1139	537	552	-1.1	3.6E-07	-1	1.4E-06
PA5061	-	5480	2467	2656	-1.2	2.8E-08	-1	2.0E-07
PA3690	-	8351	3901	4055	-1.1	7.6E-08	-1	1.4E-07
PA0788	-	305	164	148	-0.9	2.3E-03	-1	8.6E-04
PA5474	-	3305	1505	1606	-1.1	3.1E-08	-1	6.5E-07
PA4536	-	986	475	479	-1.1	7.0E-07	-1	7.6E-07
PA1107	-	553	228	269	-1.3	1.2E-08	-1	6.4E-07
PA0329	-	4991	2083	2429	-1.3	1.6E-09	-1	8.9E-07
PA2088	-	433	136	211	-1.7	1.3E-08	-1	2.0E-04
PA0436	-	1687	805	822	-1.1	1.2E-05	-1	1.9E-05
PA1430	lasR	12553	5976	6123	-1.1	4.8E-07	-1	6.1E-07
PA4913	-	1270	691	620	-0.9	6.8E-06	-1	5.6E-07
PA2883	-	508	258	248	-1	5.5E-07	-1	2.4E-07
PA0397	-	1143	531	559	-1.1	2.8E-07	-1	1.2E-06
PA0210	mdcC	126	60	61	-1.1	6.0E-06	-1	3.4E-05
PA1349	-	197	74	96	-1.4	9.9E-10	-1	7.1E-06
PA0396	pilU	4048	1966	1987	-1	2.3E-07	-1	4.8E-07
PA4635	-	272	131	134	-1.1	7.0E-05	-1	1.6E-04
PA0452	-	320	148	157	-1.1	2.3E-06	-1	2.5E-06

PA4362	-	1334	613	655	-1.1	1.7E-07	-1	8.4E-07
PA2121	-	509	226	250	-1.2	5.2E-08	-1	1.5E-06
PA3006	psrA	2268	1161	1115	-1	3.2E-02	-1	2.4E-02
PA3910	eddA	183	94	90	-1	1.8E-04	-1	1.9E-04
PA2134	-	62	39	31	-0.7	7.0E-03	-1	5.8E-04
PA1731	-	822	339	404	-1.3	5.3E-06	-1	1.8E-04
PA3274	-	70	34	35	-1	5.8E-04	-1	1.1E-03
PA1915	-	1314	603	650	-1.1	1.6E-07	-1	2.0E-06
PA2632	-	821	388	406	-1.1	7.6E-06	-1	2.4E-05
PA2233	pslC	2453	972	1213	-1.3	3.1E-10	-1	1.2E-06
PA0284	-	1600	784	793	-1	6.3E-02	-1	5.4E-02
PA3305	-	1208	547	601	-1.1	1.0E-07	-1	1.6E-06
PA2781	-	681	321	339	-1.1	1.1E-07	-1	1.3E-06
PA1920	nrdD	467	179	233	-1.4	1.4E-08	-1	5.0E-05
PA4049	-	750	371	375	-1	9.4E-07	-1	4.0E-06
PA1979	eraS	55	26	27	-1.1	3.9E-03	-1	1.0E-02
PA2302	ambE	20130	9979	10111	-1	5.2E-06	-1	1.1E-05
PA4048	-	653	347	329	-0.9	1.7E-05	-1	9.4E-06
PA2864	-	1855	848	938	-1.1	3.6E-08	-1	4.9E-07
PA4368	-	1554	731	786	-1.1	5.3E-07	-1	2.5E-06
PA5408	-	171	92	87	-0.9	9.9E-04	-1	7.5E-05
PA0843	plcR	65	28	33	-1.2	2.0E-05	-1	1.8E-04
PA5428	-	1149	519	584	-1.1	2.1E-08	-1	1.6E-06
PA1555	ccoQ	690	215	351	-1.7	6.2E-03	-1	1.6E-01
PA5409	-	899	480	457	-0.9	1.6E-05	-1	7.6E-06
PA5060	phaF	27997	14323	14242	-1	2.5E-06	-1	2.7E-06
PA0366	-	809	419	412	-0.9	6.5E-06	-1	2.4E-06
PA3042	-	1467	497	748	-1.6	6.7E-13	-1	1.2E-05
PA2591	-	2537	1243	1294	-1	7.7E-07	-1	1.5E-06
PA0250	-	1480	713	756	-1.1	5.5E-06	-1	1.2E-05
PA2175	-	118	55	61	-1.1	8.3E-06	-1	5.7E-05
PA1385	-	442	203	226	-1.1	1.4E-06	-1	6.3E-06
PA2606	-	736	359	377	-1	1.3E-04	-1	3.2E-04
PA3354	-	1799	929	922	-1	2.0E-06	-1	3.4E-06
PA2047	-	643	359	330	-0.8	1.1E-05	-1	2.8E-06
PA0736	-	97	55	50	-0.8	5.4E-03	-1	7.9E-04
PA3459	-	1536	683	790	-1.2	6.1E-08	-1	3.0E-06
PA0960	-	796	421	410	-0.9	9.6E-05	-1	8.1E-05
PA3677	-	874	568	450	-0.6	3.5E-03	-1	4.7E-05
PA3460	-	1451	725	747	-1	5.5E-04	-1	6.0E-04
PA0806	-	151	71	78	-1.1	2.1E-06	-1	6.3E-05
PA3461	-	1173	548	605	-1.1	5.9E-07	-1	8.5E-06
PA2600	-	446	241	230	-0.9	3.3E-03	-1	1.9E-03
PA2780	-	583	289	301	-1	1.0E-06	-1	4.9E-06
PA3289	-	541	241	280	-1.2	2.0E-06	-1	5.5E-05

PA4717	-	2178	1149	1127	-0.9	2.0E-06	-1	1.3E-06
PA2303	ambD	2665	1391	1380	-0.9	1.7E-05	-0.9	1.7E-05
PA2178	-	179	90	93	-1	3.5E-04	-0.9	9.0E-04
PA4610	-	279	146	145	-0.9	2.6E-05	-0.9	1.6E-05
PA2087	-	241	95	125	-1.3	2.0E-07	-0.9	3.8E-04
PA3386	-	184	84	96	-1.1	3.6E-06	-0.9	1.1E-04
PA0853	-	822	403	427	-1	6.2E-06	-0.9	2.5E-05
PA3420	-	252	128	131	-1	3.7E-05	-0.9	5.3E-05
PA1431	rsaL	9124	4461	4746	-1	1.5E-07	-0.9	1.1E-06
PA1473	-	478	235	249	-1	2.4E-03	-0.9	6.1E-03
PA3273	-	47	23	25	-1	1.2E-03	-0.9	1.6E-03
PA0198	exbB	483	224	252	-1.1	8.2E-06	-0.9	1.0E-04
PA5211	-	433	190	226	-1.2	1.8E-07	-0.9	4.3E-05
PA2007	maiA	2462	1047	1287	-1.2	3.3E-04	-0.9	1.8E-02
PA3462	-	961	453	503	-1.1	5.8E-07	-0.9	1.3E-05
PA0982	-	642	312	336	-1	1.2E-06	-0.9	1.6E-05
PA1356	-	611	284	320	-1.1	1.0E-06	-0.9	2.7E-05
PA0195	pntA	2277	1010	1198	-1.2	1.0E-08	-0.9	3.0E-06
PA2771	-	2085	998	1097	-1.1	3.1E-07	-0.9	8.8E-06
PA5101	-	609	301	321	-1	3.2E-04	-0.9	1.1E-03
PA5210	-	4575	2162	2413	-1.1	2.2E-07	-0.9	1.6E-05
PA0742	-	256	114	135	-1.2	2.9E-07	-0.9	1.8E-05
PA3323	-	185	95	98	-1	7.6E-05	-0.9	1.4E-04
PA1669	-	954	494	507	-1	1.2E-05	-0.9	3.6E-05
PA2301	-	806	396	428	-1	1.8E-06	-0.9	1.4E-05
PA1348	-	710	305	378	-1.2	5.4E-07	-0.9	6.3E-05
PA1555	ccoP	2492	752	1337	-1.7	1.8E-03	-0.9	1.4E-01
PA2183	-	77	36	41	-1.1	8.5E-05	-0.9	8.0E-04
PA3049	-	46083	15590	24789	-1.6	1.3E-11	-0.9	2.4E-04
PA4611	-	1685	718	908	-1.2	1.7E-09	-0.9	1.4E-05
PA2605	-	1301	598	702	-1.1	4.3E-06	-0.9	1.7E-04
PA3316	-	731	375	396	-1	7.3E-05	-0.9	4.3E-04
PA3839	-	749	380	406	-1	3.5E-06	-0.9	3.1E-05
PA5495	thrB	4503	1667	2460	-1.4	6.6E-12	-0.9	3.2E-05
PA2699	-	811	355	443	-1.2	2.7E-06	-0.9	1.1E-03
PA2534	-	473	235	259	-1	2.5E-04	-0.9	6.7E-04
PA2360	-	1921	797	1054	-1.3	8.3E-09	-0.9	1.7E-04
PA0424	mexR	2040	949	1123	-1.1	3.4E-07	-0.9	2.1E-05
PA3678	-	1780	892	982	-1	4.9E-07	-0.9	4.4E-06
PA1470	-	613	314	339	-1	8.1E-06	-0.9	1.2E-04
PA4111	-	652	293	363	-1.2	1.2E-07	-0.8	5.8E-05
PA5178	-	15374	6911	8554	-1.2	2.7E-08	-0.8	5.0E-05
PA2086	-	360	155	201	-1.2	5.9E-04	-0.8	1.7E-02
PA2607	-	878	415	490	-1.1	7.8E-06	-0.8	2.1E-04
PA0585	-	306	157	171	-1	7.8E-05	-0.8	1.3E-03

PA5358	ubiA	3551	1775	1989	-1	1.4E-06	-0.8	3.6E-05
PA1886	polB	1963	1001	1100	-1	7.1E-06	-0.8	6.4E-05
PA1350	-	390	200	219	-1	4.6E-05	-0.8	3.9E-04
PA3304	-	521	266	293	-1	8.5E-06	-0.8	1.5E-04
PA3051	-	1396	550	787	-1.3	1.3E-10	-0.8	2.6E-04
PA1733	-	1322	674	746	-1	8.4E-06	-0.8	8.6E-05
PA1290	-	208	102	118	-1	2.4E-05	-0.8	1.7E-04
PA3023	-	827	428	468	-1	5.0E-06	-0.8	8.1E-05
PA2474	-	184	94	104	-1	1.5E-02	-0.8	4.2E-02
PA3875	narG	496	236	281	-1.1	2.7E-06	-0.8	6.2E-04
PA2234	pslD	2287	1135	1296	-1	1.3E-06	-0.8	2.4E-04
PA2918	-	725	365	411	-1	2.4E-06	-0.8	3.8E-05
PA2371	-	7570	2955	4301	-1.4	1.5E-09	-0.8	4.0E-04
PA2240	pslJ	1635	798	930	-1	5.5E-05	-0.8	4.3E-03
PA3874	narH	314	131	179	-1.3	4.8E-06	-0.8	6.4E-03
PA1076	-	2688	1266	1536	-1.1	1.2E-07	-0.8	6.9E-05
PA2239	pslI	1662	812	951	-1	1.6E-05	-0.8	1.9E-03
PA2593	qteE	344	166	197	-1.1	7.8E-06	-0.8	2.4E-04
PA1643	-	842	430	484	-1	3.9E-06	-0.8	1.0E-04
PA5303	-	2023	932	1163	-1.1	1.6E-03	-0.8	2.5E-02
PA2008	fahA	5457	2436	3138	-1.2	7.5E-04	-0.8	1.7E-02
PA2700	opdB	368	176	213	-1.1	6.4E-04	-0.8	1.1E-02
PA2236	pslF	2543	1247	1475	-1	9.8E-07	-0.8	7.2E-04
PA2370	-	2055	844	1192	-1.3	2.0E-04	-0.8	2.9E-02
PA0197	tonB	174	88	101	-1	2.0E-04	-0.8	1.0E-03
PA2094	-	259	133	151	-1	8.4E-05	-0.8	6.9E-04
PA4736	-	1162	577	679	-1	2.7E-06	-0.8	8.6E-05
PA4874	-	4441	2118	2603	-1.1	4.8E-07	-0.8	2.6E-04
PA2093	-	184	90	108	-1	1.1E-05	-0.8	1.7E-03
PA2368	-	1817	790	1072	-1.2	8.8E-05	-0.8	1.2E-02
PA1746	-	1842	883	1087	-1.1	4.1E-03	-0.8	1.0E-01
PA0141	-	2808	844	1661	-1.7	1.8E-08	-0.8	3.2E-02
PA3786	-	554	283	329	-1	3.0E-05	-0.8	1.4E-03
PA2608	-	1021	516	609	-1	9.8E-03	-0.7	3.3E-02
PA2089	-	1171	589	701	-1	1.1E-05	-0.7	7.5E-04
PA5059	-	837	426	503	-1	1.8E-05	-0.7	1.1E-03
PA2238	pslH	1996	1031	1214	-1	7.6E-06	-0.7	1.8E-03
PA1344	-	2147	1108	1310	-1	4.3E-04	-0.7	1.1E-02
PA0546	metK	26569	13462	16248	-1	1.0E-04	-0.7	8.3E-03
PA2374	-	707	327	433	-1.1	1.2E-06	-0.7	1.9E-03
PA0026	plcB	3652	1881	2242	-1	5.1E-06	-0.7	4.5E-04
PA2009	hmgA	5543	2707	3410	-1	2.6E-03	-0.7	2.0E-02
PA2237	pslG	2136	1084	1317	-1	7.1E-06	-0.7	3.8E-03
PA3032	-	536	245	331	-1.1	3.5E-06	-0.7	2.0E-03
PA2369	-	4924	2260	3058	-1.1	2.5E-04	-0.7	3.0E-02

PA2235	pslE	6966	3556	4369	-1	1.1E-04	-0.7	1.8E-02
PA5395	-	287	147	181	-1	7.4E-05	-0.7	3.8E-03
PA0049	-	822	382	519	-1.1	2.3E-02	-0.7	2.2E-01
PA2367	-	4029	1862	2555	-1.1	7.3E-04	-0.7	4.0E-02
PA2365	-	3491	1761	2231	-1	9.3E-06	-0.6	2.5E-03
PA2366	-	11151	5753	7125	-1	4.3E-02	-0.6	1.7E-01
PA2061	-	205	106	132	-1	1.1E-04	-0.6	1.9E-03
PA0050	-	918	311	593	-1.6	8.3E-13	-0.6	8.7E-03
PA5115	-	151	75	99	-1	9.4E-04	-0.6	5.9E-02
PA1544	-	9194	4343	6073	-1.1	5.5E-04	-0.6	5.3E-02
PA4495	-	6808	3398	4509	-1	2.1E-06	-0.6	6.0E-03
PA1172	napC	240	124	163	-1	4.3E-05	-0.6	2.4E-02
PA1919	nrdG	413	184	281	-1.2	2.5E-07	-0.6	1.7E-02
PA2373	-	4618	2216	3190	-1.1	8.2E-06	-0.5	3.4E-02
PA1924	-	38	19	26	-1	1.3E-02	-0.5	2.0E-01
PA3788	-	306	138	215	-1.1	5.4E-04	-0.5	1.7E-01
PA2381	-	1612	509	1164	-1.7	5.8E-07	-0.5	2.9E-01
PA0135	-	6	2	4	-1.3	1.3E-01	-0.4	8.0E-01
PA0572	-	13036	6506	9948	-1	5.9E-04	-0.4	3.5E-01
PA5169	-	481	1022	422	1.1	5.6E-02	-0.2	8.6E-01
PA1123	-	525	241	464	-1.1	7.2E-03	-0.2	9.1E-01
PA1155	nrdB	28942	11035	27918	-1.4	6.6E-04	-0.1	8.3E-01
PA1156	nrdA	42491	21426	41150	-1	1.5E-02	0	8.0E-01
PA0793	-	706	1386	746	1	4.3E-02	0.1	1.0E+00
PA3569	mmsB	2480	4906	2689	1	6.4E-02	0.1	9.1E-01
PA3570	mmsA	6015	11723	7205	1	2.1E-02	0.3	5.6E-01
PA3186	oprB	8350	21895	10331	1.4	1.8E-02	0.3	5.6E-01
PA0516	nirF	337	730	424	1.1	1.2E-03	0.3	2.4E-01
PA0513	-	99	201	127	1	1.2E-02	0.4	3.2E-01
PA0519	nirS	2014	5407	2583	1.4	1.5E-03	0.4	3.6E-01
PA0512	nirJ	149	292	193	1	8.3E-03	0.4	2.4E-01
PA1073	braD	892	1899	1155	1.1	2.8E-05	0.4	1.6E-01
PA0517	nirC	127	316	167	1.3	5.5E-04	0.4	2.5E-01
PA0753	-	40	79	53	1	1.3E-02	0.4	2.3E-01
PA0866	aroP	365	810	488	1.2	1.1E-02	0.4	3.5E-01
PA1071	braF	956	1978	1282	1	2.6E-04	0.4	1.3E-01
PA0522	-	51	177	68	1.8	5.4E-03	0.4	5.5E-01
PA0521	-	80	225	109	1.5	7.2E-04	0.4	4.3E-01
PA3568	-	857	2062	1161	1.3	9.9E-03	0.4	3.4E-01
PA1072	braE	1107	2518	1499	1.2	9.4E-05	0.4	8.4E-02
PA0518	nirM	192	539	265	1.5	6.6E-05	0.5	1.2E-01
PA0523	norC	600	1862	838	1.6	1.2E-03	0.5	3.9E-01
PA3811	hscB	1109	2291	1550	1	5.3E-03	0.5	2.3E-01
PA3812	iscA	1261	2607	1765	1	1.0E-03	0.5	1.5E-01
PA1070	braG	567	1354	797	1.3	9.9E-06	0.5	7.5E-02

PA2459	-	84	203	117	1.3	2.7E-01	0.5	6.1E-01
PA0795	prpC	2801	6362	3991	1.2	8.7E-03	0.5	1.8E-01
PA5096	-	531	1264	756	1.3	5.7E-02	0.5	5.4E-01
PA0525	-	929	3123	1336	1.7	9.5E-05	0.5	1.6E-01
PA3814	iscS	6679	14428	9620	1.1	3.8E-05	0.5	5.4E-02
PA3392	nosZ	447	1376	661	1.6	3.4E-04	0.6	1.4E-01
PA3809	-	552	1249	816	1.2	1.4E-06	0.6	2.7E-02
PA3810	hscA	2413	5423	3585	1.2	9.3E-06	0.6	1.7E-02
PA3813	iscU	2025	4576	3038	1.2	3.8E-05	0.6	4.2E-02
PA5530	-	330	819	502	1.3	2.9E-04	0.6	8.3E-02
PA3182	-	1586	3243	2434	1	1.5E-03	0.6	5.6E-02
PA0235	pcaK	29	58	45	1	1.7E-02	0.6	1.4E-01
PA3187	-	3834	11759	6003	1.6	7.1E-04	0.6	1.4E-01
PA0524	norB	1321	5031	2094	1.9	5.7E-05	0.7	1.5E-01
PA3192	gltR	512	1055	816	1	2.0E-04	0.7	5.5E-03
PA5098	hutH	963	2596	1538	1.4	4.9E-03	0.7	1.9E-01
PA1588	sucC	19020	38478	30560	1	2.9E-07	0.7	2.7E-04
PA3836	-	1831	3742	2985	1	2.0E-04	0.7	1.0E-02
PA1911	femR	1005	1970	1664	1	5.2E-07	0.7	4.9E-05
PA5153	-	2778	7264	4616	1.4	1.5E-03	0.7	7.4E-02
PA5099	-	643	1516	1071	1.2	2.8E-06	0.7	4.2E-03
PA2129	cupA	20	45	34	1.2	1.1E-03	0.7	3.3E-02
PA5137	-	521	1129	886	1.1	7.8E-07	0.8	4.1E-04
PA4170	-	146	322	248	1.1	1.6E-05	0.8	2.4E-03
PA4588	gdhA	661	1498	1126	1.2	1.6E-07	0.8	3.4E-04
PA2322	-	257	600	446	1.2	3.5E-03	0.8	5.1E-02
PA3554	arnA	397	817	689	1	6.7E-06	0.8	4.1E-04
PA5097	-	481	1446	838	1.6	2.7E-03	0.8	1.2E-01
PA2951	etfA	11300	22630	19686	1	1.8E-07	0.8	1.2E-05
PA0707	toxR	975	1912	1702	1	7.8E-06	0.8	2.1E-04
PA1696	pscO	37	74	65	1	9.5E-03	0.8	2.0E-02
PA2391	opmQ	2792	5460	4919	1	6.4E-06	0.8	6.3E-05
PA3188	-	1299	4464	2299	1.8	6.2E-06	0.8	2.1E-02
PA1276	cobC	238	470	423	1	6.7E-06	0.8	2.0E-04
PA4169	-	175	401	313	1.2	1.8E-06	0.8	4.8E-04
PA0168	-	280	551	502	1	2.2E-06	0.8	2.4E-05
PA2450	-	493	954	887	1	8.3E-06	0.8	6.2E-05
PA2411	-	15893	32938	28699	1.1	5.8E-07	0.9	2.4E-05
PA4823	-	1	0	3	-1.9	1.0E+00	0.9	3.6E-01
PA3642	rnhB	187	384	338	1	1.4E-04	0.9	1.3E-03
PA1273	cobB	354	686	640	1	2.4E-03	0.9	2.7E-03
PA5127	-	283	558	512	1	4.5E-06	0.9	3.0E-05
PA3887	nhaP	627	1227	1139	1	5.3E-06	0.9	4.7E-05
PA3553	arnC	162	340	296	1.1	5.0E-06	0.9	7.8E-05
PA5100	hutU	4427	10975	8081	1.3	1.4E-04	0.9	8.4E-03

PA5074	-	464	944	847	1	2.5E-04	0.9	8.4E-04
PA3263	-	627	1320	1145	1.1	2.9E-06	0.9	6.6E-05
PA0552	-	1540	3010	2826	1	9.6E-06	0.9	2.4E-05
PA3283	-	131	273	241	1.1	2.6E-06	0.9	9.2E-05
PA5052	-	383	764	706	1	4.5E-03	0.9	6.4E-03
PA5135	-	255	507	470	1	1.1E-05	0.9	4.3E-05
PA0996	pqsA	9781	19565	18067	1	1.6E-07	0.9	1.9E-06
PA4370	icmP	18850	36738	34995	1	6.7E-07	0.9	2.2E-06
PA2385	pvdQ	7093	14739	13188	1.1	1.0E-04	0.9	3.4E-04
PA0757	-	260	503	487	1	2.1E-05	0.9	2.2E-05
PA3470	-	182	360	340	1	7.9E-06	0.9	2.9E-05
PA4259	rpsS	4346	8443	8146	1	4.2E-03	0.9	2.8E-03
PA4934	rpsR	2489	4850	4701	1	1.2E-03	0.9	9.0E-04
PA1909	-	151	331	286	1.1	5.9E-07	0.9	3.1E-05
PA2019	-	259	523	490	1	1.3E-06	0.9	3.4E-06
PA2466	foxA	550	1063	1042	1	1.4E-06	0.9	1.7E-06
PA1805	ppiD	5057	9942	9589	1	1.3E-06	0.9	3.9E-06
PA2952	etfB	8897	18379	16875	1	1.4E-07	0.9	1.6E-06
PA2998	nqrB	1152	2293	2186	1	2.4E-03	0.9	2.5E-03
PA0659	-	2215	4410	4204	1	8.7E-07	0.9	3.9E-06
PA4389	speA	1641	3378	3120	1	7.1E-07	0.9	1.1E-05
PA4229	pchC	15235	32579	28963	1.1	2.5E-05	0.9	1.2E-04
PA3666	dapD	1378	2730	2621	1	1.2E-06	0.9	2.5E-06
PA1725	pscL	131	289	251	1.1	2.9E-07	0.9	3.3E-05
PA0930	-	545	1097	1039	1	5.4E-07	0.9	2.9E-06
PA5076	-	914	1860	1749	1	1.6E-06	0.9	6.3E-06
PA0341	-	529	1042	1013	1	1.8E-06	0.9	4.1E-06
PA2945	-	1538	3234	2950	1.1	8.7E-08	0.9	1.2E-06
PA2948	cobM	415	848	796	1	4.9E-07	0.9	3.6E-06
PA1580	gltA	8993	18264	17275	1	1.5E-07	0.9	1.1E-06
PA2634	aceA	4101	8003	7887	1	2.5E-07	0.9	1.0E-06
PA1274	-	172	345	332	1	1.4E-05	0.9	2.0E-05
PA3483	-	319	621	614	1	1.1E-05	0.9	8.2E-06
PA4705	prrF	573	1244	1105	1.1	1.4E-05	0.9	7.0E-05
PA3807	-	3406	6903	6576	1	4.1E-05	0.9	5.3E-05
PA4274	rplK	6966	14789	13450	1.1	3.3E-05	0.9	1.1E-04
PA3117	-	1143	2497	2207	1.1	1.0E-07	0.9	3.4E-06
PA2900	-	653	1183	1262	0.9	1.3E-05	1	6.1E-07
PA5049	rpmE	1730	3227	3345	0.9	1.2E-03	1	7.0E-04
PA0047	-	141	273	274	0.9	3.4E-04	1	2.7E-04
PA2774	-	208	410	403	1	1.2E-05	1	1.4E-05
PA3865	-	747	1407	1449	0.9	3.8E-05	1	4.0E-05
PA1365	-	714	1268	1385	0.8	3.7E-05	1	2.7E-06
PA3980	-	1477	2654	2865	0.8	3.9E-04	1	5.3E-05
PA1812	mltD	2833	5586	5512	1	3.9E-05	1	2.7E-05

PA1012	-	1066	1959	2075	0.9	9.3E-04	1	1.8E-04
PA2660	-	443	915	862	1	8.6E-07	1	3.5E-06
PA4724	-	212	418	412	1	4.8E-05	1	2.2E-05
PA0085	-	1553	2929	3024	0.9	3.4E-05	1	1.9E-05
PA1011	-	4153	7956	8091	0.9	1.6E-06	1	5.6E-07
PA5154	-	342	1146	667	1.7	9.1E-11	1	7.9E-04
PA2467	foxR	902	1816	1760	1	2.1E-07	1	4.8E-07
PA1702	-	14	32	27	1.2	1.8E-02	1	5.1E-02
PA4802	-	63	123	123	1	7.8E-05	1	1.3E-04
PA3635	-	5024	9895	9823	1	4.9E-03	1	2.5E-03
PA4234	uvrA	2766	5483	5418	1	5.2E-07	1	2.5E-07
PA4439	trpS	1504	2968	2946	1	1.6E-06	1	1.6E-06
PA4686	-	1697	3278	3328	0.9	5.1E-03	1	2.6E-03
PA2977	murB	633	1143	1241	0.9	3.5E-04	1	6.1E-05
PA0009	glyQ	1378	2634	2706	0.9	3.1E-06	1	7.5E-07
PA1790	-	211	380	416	0.8	2.6E-03	1	5.0E-04
PA4730	panC	640	1223	1261	0.9	2.8E-07	1	8.2E-08
PA1721	pscH	139	352	274	1.3	7.9E-09	1	6.1E-05
PA1720	pscG	214	535	422	1.3	1.6E-07	1	2.0E-04
PA3603	dgkA	116	181	229	0.6	3.5E-03	1	1.9E-05
PA0390	metX	1140	2102	2254	0.9	2.6E-05	1	2.7E-06
PA3284	-	190	384	375	1	9.9E-06	1	1.0E-04
PA0955	-	1007	1914	1993	0.9	4.5E-06	1	1.2E-06
PA2964	pabC	393	775	778	1	4.0E-03	1	2.2E-03
PA3769	guaA	2368	4396	4692	0.9	3.3E-04	1	4.8E-05
PA2390	pvdT	3699	7846	7337	1.1	1.6E-08	1	1.6E-07
PA3134	gltX	2315	4395	4597	0.9	1.8E-06	1	1.9E-07
PA2876	pyrF	255	468	507	0.9	3.2E-03	1	4.6E-04
PA3716	-	1390	2772	2764	1	3.3E-06	1	2.3E-06
PA1159	-	1863	3539	3718	0.9	4.9E-06	1	9.2E-07
PA4849	-	86	148	172	0.8	4.0E-03	1	2.1E-04
PA4271	rplL	6874	15303	13726	1.2	9.6E-08	1	2.0E-06
PA5155	-	178	572	356	1.7	2.1E-09	1	4.3E-04
PA0944	purN	825	1548	1652	0.9	1.4E-04	1	1.4E-05
PA0088	-	403	797	806	1	3.0E-06	1	3.2E-06
PA0888	aotJ	7411	15789	14845	1.1	1.7E-07	1	8.0E-07
PA3189	-	1248	4944	2509	2	1.2E-07	1	4.0E-03
PA3736	-	1502	3032	3022	1	6.4E-07	1	4.7E-07
PA2446	gcvH	555	1086	1118	1	1.5E-03	1	2.5E-04
PA4897	-	725	1464	1460	1	2.7E-06	1	1.8E-06
PA4228	pchD	53874	118883	108856	1.1	1.5E-08	1	7.9E-08
PA4054	ribB	826	1688	1670	1	2.1E-02	1	1.4E-02
PA0350	folA	276	544	559	1	3.3E-05	1	1.8E-05
PA0377	-	215	435	436	1	3.0E-06	1	2.0E-06
PA4244	rplO	8037	16730	16267	1.1	1.1E-03	1	7.7E-04

PA1475	ccmA	350	663	710	0.9	5.8E-04	1	1.3E-04
PA1723	pscJ	262	612	532	1.2	1.4E-08	1	1.2E-05
PA4894	-	338	774	687	1.2	4.2E-04	1	9.1E-04
PA0889	aotQ	908	1964	1846	1.1	6.8E-05	1	1.3E-04
PA1272	cobO	430	857	875	1	1.7E-03	1	6.1E-04
PA3925	-	565	1552	1151	1.5	1.3E-07	1	6.0E-05
PA5342	-	212	426	432	1	4.2E-07	1	1.2E-07
PA3471	-	2834	5975	5784	1.1	3.6E-08	1	7.1E-08
PA3604	erdR	654	1260	1337	0.9	3.6E-05	1	4.0E-06
PA5426	purE	509	971	1040	0.9	4.7E-04	1	7.5E-05
PA5391	-	17	34	35	1	1.4E-02	1	6.9E-03
PA3019	-	1173	2170	2406	0.9	3.7E-04	1	2.8E-05
PA3968	-	208	419	428	1	5.9E-06	1	2.3E-06
PA4266	fusA1	42026	87901	86242	1.1	2.1E-06	1	1.6E-06
PA2321	-	127	313	260	1.3	3.3E-06	1	9.3E-05
PA2063	-	284	572	585	1	7.1E-07	1	2.5E-07
PA1722	pscI	158	408	326	1.4	8.3E-09	1	1.9E-05
PA5136	-	848	1863	1748	1.1	1.7E-08	1	1.2E-07
PA5569	rnpA	2856	5449	5891	0.9	1.6E-03	1	4.2E-04
PA3552	arnB	226	520	467	1.2	7.7E-08	1	3.9E-06
PA2395	pvdO	7418	16595	15328	1.2	4.7E-09	1	5.4E-08
PA4568	rplU	4335	9011	8963	1.1	3.2E-05	1	3.2E-05
PA0660	-	2752	6114	5691	1.2	2.8E-09	1	4.3E-08
PA2203	-	211	470	436	1.2	2.0E-05	1	2.5E-04
PA4260	rplB	9767	21759	20215	1.2	3.7E-03	1	3.9E-03
PA4855	purD	708	1533	1465	1.1	1.8E-02	1	1.2E-02
PA0083	-	496	1154	1027	1.2	5.6E-09	1	2.4E-07
PA0040	-	574	1137	1189	1	1.2E-06	1.1	3.9E-07
PA4852	-	2538	4588	5257	0.9	1.1E-03	1.1	5.4E-05
PA4731	panD	183	374	380	1	3.4E-06	1.1	2.2E-06
PA4390	-	901	1971	1869	1.1	1.3E-07	1.1	1.6E-06
PA0945	purM	1679	3301	3488	1	1.2E-04	1.1	1.7E-05
PA5046	-	6292	14503	13071	1.2	2.7E-09	1.1	3.9E-08
PA0347	glpQ	447	1002	928	1.2	5.6E-08	1.1	4.6E-07
PA1700	-	31	78	64	1.3	8.1E-07	1.1	3.7E-05
PA3245	minE	1769	3415	3677	0.9	5.0E-07	1.1	1.0E-07
PA4706	-	762	1669	1585	1.1	2.2E-06	1.1	2.6E-06
PA4853	-	702	1322	1462	0.9	5.0E-04	1.1	4.6E-05
PA4372	-	1445	2867	3010	1	6.7E-05	1.1	8.4E-06
PA0948	-	278	567	579	1	1.7E-04	1.1	7.1E-05
PA5570	rpmH	1940	3577	4047	0.9	2.5E-05	1.1	2.8E-07
PA1767	-	2315	4742	4836	1	1.4E-06	1.1	6.4E-07
PA1620	-	22	37	47	0.7	3.6E-02	1.1	6.9E-04
PA0245	aroQ	17	35	35	1.1	6.9E-04	1.1	1.3E-03
PA2320	gntR	573	1275	1202	1.2	1.1E-07	1.1	3.3E-07

PA3866	-	10620	23470	22320	1.1	1.1E-08	1.1	1.4E-07
PA0381	thiG	1181	2264	2484	0.9	1.5E-05	1.1	5.8E-07
PA1275	cobD	136	349	287	1.4	1.5E-08	1.1	3.5E-06
PA2202	-	198	451	416	1.2	7.5E-08	1.1	9.9E-07
PA0756	-	172	356	363	1	5.1E-06	1.1	2.2E-06
PA1674	folE	1276	2462	2695	0.9	2.1E-04	1.1	3.6E-05
PA0903	alaS	3254	6700	6873	1	2.3E-05	1.1	7.7E-06
PA4684	-	488	959	1031	1	5.3E-04	1.1	8.3E-05
PA5425	purK	703	1390	1490	1	4.2E-04	1.1	6.4E-05
PA0750	-	633	1340	1340	1.1	9.0E-08	1.1	6.8E-08
PA4745	nusA	5955	12129	12643	1	2.2E-03	1.1	7.7E-04
PA2662	-	487	1022	1035	1.1	4.5E-06	1.1	2.0E-06
PA5129	-	634	1338	1349	1.1	7.0E-07	1.1	3.1E-07
PA5118	thiI	793	1493	1690	0.9	3.4E-03	1.1	4.6E-04
PA2619	infA	668	1236	1423	0.9	2.5E-02	1.1	4.4E-03
PA0151	-	185	394	395	1.1	5.9E-07	1.1	1.9E-07
PA3837	-	424	1191	910	1.5	2.7E-11	1.1	6.1E-07
PA4055	ribC	543	1088	1166	1	1.9E-02	1.1	6.6E-03
PA1193	-	299	602	642	1	3.5E-06	1.1	2.7E-07
PA2792	-	127	263	273	1	9.6E-07	1.1	5.7E-07
PA1161	rrmA	564	1267	1214	1.2	3.7E-09	1.1	1.3E-08
PA1714	exsD	952	2448	2054	1.4	5.6E-10	1.1	6.1E-07
PA1717	pscD	231	696	499	1.6	4.2E-06	1.1	7.9E-04
PA3746	-	2421	4678	5233	1	8.2E-07	1.1	7.5E-09
PA0169	-	230	605	498	1.4	7.4E-11	1.1	3.8E-08
PA3232	-	192	395	416	1	2.0E-05	1.1	1.1E-05
PA4272	rplJ	7125	17500	15426	1.3	3.5E-10	1.1	5.6E-08
PA4632	-	1043	2203	2262	1.1	6.3E-08	1.1	7.3E-09
PA2392	pvdP	9330	20996	20257	1.2	1.1E-09	1.1	4.8E-09
PA5075	-	485	1126	1055	1.2	9.0E-05	1.1	1.2E-04
PA5128	secB	3546	8301	7722	1.2	4.9E-10	1.1	8.1E-09
PA1638	-	117	226	254	1	9.0E-05	1.1	7.1E-06
PA4709	-	3110	7119	6783	1.2	5.2E-09	1.1	1.5E-08
PA3790	oprC	1406	1747	3067	0.3	4.3E-01	1.1	1.2E-02
PA3838	-	376	1024	821	1.4	1.2E-09	1.1	1.4E-06
PA3824	queA	371	776	811	1.1	7.4E-04	1.1	2.1E-04
PA4567	rpmA	2452	4874	5360	1	7.4E-06	1.1	1.3E-07
PA4774	-	228	605	500	1.4	1.8E-08	1.1	1.8E-06
PA3408	hasR	4165	9626	9126	1.2	6.9E-10	1.1	1.6E-08
PA1293	-	988	2228	2166	1.2	3.6E-09	1.1	1.3E-08
PA4664	hemK	467	1022	1024	1.1	3.8E-03	1.1	2.1E-03
PA2463	-	702	1570	1543	1.2	1.5E-08	1.1	2.8E-08
PA3162	rpsA	29676	65638	65590	1.1	1.3E-06	1.1	1.1E-06
PA0774	-	337	696	747	1	8.8E-05	1.1	1.2E-05
PA4264	rpsJ	9000	18190	19954	1	4.3E-04	1.1	7.6E-05

PA0802	-	75	161	167	1.1	3.5E-04	1.2	1.8E-04
PA0389	-	463	1011	1028	1.1	7.0E-09	1.2	1.6E-09
PA4245	rpmD	3896	8612	8657	1.1	3.5E-04	1.2	1.6E-04
PA0800	-	192	452	426	1.2	5.0E-05	1.2	9.9E-05
PA3823	-	535	1147	1191	1.1	7.7E-03	1.2	3.6E-03
PA4708	phuT	2085	5461	4641	1.4	1.5E-05	1.2	9.7E-05
PA2828	-	843	1751	1882	1.1	9.7E-07	1.2	8.1E-08
PA2663	ppyR	103	230	232	1.2	1.0E-04	1.2	6.7E-05
PA4895	-	1047	2618	2348	1.3	2.9E-06	1.2	1.4E-05
PA2397	pvdE	6632	15316	14938	1.2	2.4E-10	1.2	1.6E-09
PA3237	-	68	160	154	1.2	8.7E-07	1.2	4.1E-06
PA1743	-	19	43	43	1.2	1.9E-04	1.2	2.9E-04
PA5117	typA	997	2542	2253	1.4	3.0E-03	1.2	4.4E-03
PA5296	-	1071	2195	2423	1	1.1E-05	1.2	9.4E-07
PA1687	speE	299	636	678	1.1	5.0E-04	1.2	9.7E-05
PA2969	plsX	654	1237	1484	0.9	3.4E-02	1.2	5.7E-03
PA2413	pvdH	22318	58299	50747	1.4	3.0E-12	1.2	7.2E-10
PA1724	pscK	64	171	145	1.4	6.2E-09	1.2	1.5E-06
PA0421	-	1568	3755	3586	1.3	6.9E-10	1.2	2.5E-09
PA5204	argA	2769	6266	6348	1.2	5.5E-09	1.2	4.1E-09
PA4263	rplC	11828	26269	27119	1.2	9.0E-04	1.2	3.1E-04
PA4249	rpsH	6709	14538	15403	1.1	1.0E-05	1.2	2.2E-06
PA2971	-	3078	6246	7094	1	9.9E-03	1.2	2.6E-03
PA4707	-	781	1952	1801	1.3	5.4E-06	1.2	1.0E-05
PA4333	-	978	2039	2257	1.1	4.0E-06	1.2	1.6E-07
PA1713	exsA	1831	4435	4240	1.3	8.6E-10	1.2	2.2E-08
PA0970	tolR	1679	3975	3890	1.2	1.0E-04	1.2	1.0E-04
PA4602	glyA3	2006	4470	4658	1.2	4.4E-05	1.2	8.6E-06
PA4246	rpsE	9014	21277	20972	1.2	1.7E-04	1.2	1.1E-04
PA2664	-	731	1564	1702	1.1	4.2E-06	1.2	1.9E-07
PA0346	-	313	861	729	1.5	3.2E-11	1.2	8.8E-09
PA3984	-	768	1842	1795	1.3	3.9E-10	1.2	6.9E-10
PA1757	thrH	277	641	647	1.2	3.1E-06	1.2	1.3E-06
PA1718	pscE	142	416	332	1.6	2.0E-06	1.2	2.6E-04
PA2393	-	8324	20396	19496	1.3	5.3E-11	1.2	4.0E-10
PA2913	-	258	670	605	1.4	3.8E-07	1.2	1.9E-06
PA0801	-	501	1277	1177	1.4	7.2E-08	1.2	2.7E-07
PA0796	prpB	1147	3195	2700	1.5	1.5E-03	1.2	4.2E-03
PA3903	prfC	1530	3419	3604	1.2	2.4E-07	1.2	3.0E-08
PA4031	-	2444	5684	5768	1.2	5.4E-09	1.2	9.5E-10
PA4854	purH	1407	3172	3326	1.2	1.3E-02	1.2	5.0E-03
PA0969	tolQ	3199	7906	7585	1.3	2.9E-05	1.2	3.9E-05
PA4481	mreB	2559	6086	6076	1.3	8.7E-07	1.2	4.9E-07
PA3174	-	136	278	323	1	2.3E-05	1.2	2.7E-06
PA3822	-	1221	2776	2907	1.2	5.5E-07	1.3	1.3E-07

PA1715	pscB	83	252	198	1.6	1.7E-11	1.3	9.0E-08
PA4438	-	806	1663	1944	1	5.7E-04	1.3	3.9E-05
PA3406	hasD	1047	2417	2533	1.2	2.2E-09	1.3	7.3E-10
PA1228	-	35	77	84	1.2	3.0E-03	1.3	1.1E-03
PA4267	rpsG	7683	18941	18698	1.3	1.2E-08	1.3	7.1E-09
PA4247	rplR	4840	11778	11792	1.3	5.0E-04	1.3	2.1E-04
PA2851	-	4694	11067	11445	1.2	1.1E-06	1.3	3.3E-07
PA3308	hepA	1413	3080	3447	1.1	2.4E-03	1.3	4.1E-04
PA0170	-	154	421	375	1.5	3.7E-09	1.3	3.4E-08
PA3165	hisC	1850	4909	4516	1.4	1.1E-08	1.3	6.8E-08
PA2394	pvdN	6107	15580	14932	1.4	1.3E-08	1.3	4.8E-08
PA4262	rplD	10128	24263	24808	1.3	1.2E-03	1.3	4.7E-04
PA5201	-	1412	3274	3458	1.2	1.2E-03	1.3	3.4E-04
PA3409	-	1109	2872	2719	1.4	1.8E-11	1.3	2.1E-10
PA4268	rpsL	6820	16056	16725	1.2	1.2E-08	1.3	1.4E-09
PA3405	hasE	701	1584	1720	1.2	1.8E-07	1.3	1.1E-08
PA5316	rpmB	2920	7066	7178	1.3	9.9E-05	1.3	3.7E-05
PA4773	-	127	346	312	1.5	2.2E-09	1.3	6.1E-08
PA5194	-	378	923	930	1.3	1.1E-09	1.3	5.0E-10
PA4248	rplF	8062	19877	19894	1.3	5.6E-05	1.3	2.6E-05
PA3176	gltS	88	234	218	1.4	1.6E-08	1.3	4.5E-07
PA0797	-	512	1246	1266	1.3	9.9E-04	1.3	6.5E-04
PA2970	rpmF	1078	2209	2664	1	2.8E-03	1.3	2.7E-04
PA1271	-	808	1992	2004	1.3	1.1E-05	1.3	4.2E-06
PA4513	-	684	1752	1702	1.4	2.4E-05	1.3	1.9E-05
PA1719	pscF	250	750	624	1.6	1.8E-10	1.3	1.6E-07
PA3700	lysS	1694	4176	4243	1.3	2.3E-04	1.3	8.8E-05
PA4896	-	1004	2618	2516	1.4	7.4E-11	1.3	2.2E-10
PA2661	-	242	607	608	1.3	1.6E-07	1.3	1.3E-07
PA3745	rpsP	1848	4036	4652	1.1	9.7E-04	1.3	1.1E-04
PA4261	rplW	4788	11388	12072	1.2	2.2E-03	1.3	6.4E-04
PA3744	rimM	4692	10047	11849	1.1	7.3E-03	1.3	1.0E-03
PA4673	-	1329	3312	3371	1.3	2.1E-05	1.3	6.9E-06
PA5192	pckA	3100	7898	7884	1.3	3.2E-07	1.3	1.5E-07
PA2042	-	1395	3581	3548	1.4	1.4E-08	1.3	7.7E-09
PA5131	-	3138	8667	8003	1.5	8.6E-14	1.4	2.2E-12
PA4433	rplM	6234	15233	15989	1.3	2.2E-05	1.4	4.3E-06
PA0931	pirA	1237	3251	3176	1.4	2.3E-05	1.4	1.4E-05
PA2490	-	46	110	118	1.3	1.4E-07	1.4	2.0E-08
PA0578	-	401	843	1032	1.1	8.0E-03	1.4	8.8E-04
PA0382	micA	265	654	684	1.3	3.3E-04	1.4	1.0E-04
PA2758	-	226	585	583	1.4	1.1E-10	1.4	2.4E-10
PA1363	-	382	945	992	1.3	1.4E-07	1.4	3.7E-08
PA4432	rpsI	4160	9878	10804	1.2	2.0E-04	1.4	2.6E-05
PA3001	-	5763	14449	14980	1.3	5.2E-10	1.4	7.8E-11

PA4669	-	2730	6022	7105	1.1	3.3E-03	1.4	3.6E-04
PA4840	-	180	414	469	1.2	8.7E-08	1.4	2.7E-10
PA3743	trmD	4139	9826	10823	1.2	8.8E-03	1.4	2.7E-03
PA5139	-	158	366	413	1.2	2.3E-06	1.4	2.0E-08
PA0172	-	347	1015	911	1.5	1.1E-13	1.4	4.2E-12
PA0775	-	309	699	812	1.2	2.9E-04	1.4	2.0E-05
PA3209	-	28	58	75	1	9.2E-05	1.4	1.3E-06
PA4672	-	358	887	952	1.3	5.9E-03	1.4	2.1E-03
PA2445	gcvP2	3106	8545	8266	1.5	6.9E-09	1.4	4.3E-09
PA0968	-	1678	4314	4477	1.4	1.3E-04	1.4	5.6E-05
PA2629	purB	1128	2682	3012	1.2	9.2E-05	1.4	7.6E-06
PA1800	-	9793	24702	26403	1.3	8.1E-07	1.4	9.8E-08
PA4665	prfA	633	1554	1710	1.3	1.6E-07	1.4	4.3E-09
PA1697		93	274	251	1.6	2.7E-04	1.4	4.0E-04
PA4640	mqoB	2379	6684	6442	1.5	4.8E-06	1.4	4.7E-06
PA1716	pscC	349	1079	947	1.6	4.0E-14	1.4	8.4E-12
PA1701	-	15	42	41	1.5	4.4E-04	1.4	3.0E-04
PA5315	rpmG	366	767	997	1.1	1.3E-03	1.4	3.8E-05
PA4480	mreC	458	1254	1259	1.5	6.2E-04	1.5	3.5E-04
PA2760	-	9579	34269	26328	1.8	1.6E-12	1.5	5.8E-09
PA5568	-	2347	6451	6494	1.5	2.4E-04	1.5	1.4E-04
PA2911	-	617	1921	1709	1.6	9.6E-08	1.5	5.5E-07
PA1771	estX	140	340	387	1.3	1.6E-02	1.5	5.1E-03
PA2759	-	341	1016	948	1.6	8.0E-07	1.5	2.2E-06
PA2396	pvdF	11305	34063	31636	1.6	3.2E-15	1.5	1.0E-13
PA0579	rpsU	1637	3629	4621	1.1	8.5E-03	1.5	7.1E-04
PA2487	-	60	158	169	1.4	4.5E-08	1.5	2.8E-09
PA0789	-	596	1926	1684	1.7	1.5E-10	1.5	5.3E-09
PA4671	-	3319	9976	9396	1.6	3.5E-08	1.5	5.6E-08
PA3411	-	90	280	259	1.6	1.7E-06	1.5	7.2E-06
PA3231	-	20	51	58	1.3	9.3E-05	1.5	5.1E-06
PA0046	-	90	266	259	1.6	9.8E-05	1.5	6.9E-05
PA3656	rpsB	6638	18092	19193	1.4	3.5E-06	1.5	4.3E-07
PA4622	-	149	489	434	1.7	4.7E-14	1.5	3.1E-11
PA4563	rpsT	2071	5359	6053	1.4	1.2E-03	1.5	1.9E-04
PA2912	-	135	464	395	1.8	2.9E-06	1.5	2.0E-05
PA0171	-	182	623	533	1.8	9.3E-16	1.6	1.0E-12
PA1699	pcr1	31	105	92	1.7	2.1E-06	1.6	9.4E-06
PA4355	-	246	658	728	1.4	2.8E-10	1.6	9.4E-13
PA3820	secF	922	2904	2742	1.7	1.3E-04	1.6	1.5E-04
PA2326	-	119	317	356	1.4	6.2E-10	1.6	1.5E-11
PA0045	-	205	580	612	1.5	7.1E-06	1.6	1.3E-06
PA1364	-	170	490	514	1.5	1.8E-12	1.6	5.3E-13
PA4479	mreD	88	277	268	1.7	1.0E-03	1.6	1.0E-03
PA4670	-	4523	12171	13965	1.4	2.0E-04	1.6	1.7E-05

2PA2492	-	488	1573	1516	1.7	3.8E-14	1.6	3.1E-13
PA3641	-	1161	3605	3623	1.6	4.6E-08	1.6	2.3E-08
PA3655	-	3915	11853	12241	1.6	4.6E-04	1.6	1.7E-04
PA4675	-	1730	6745	5540	2	1.6E-11	1.7	1.2E-09
PA2444	glyA2	438	1355	1425	1.6	1.8E-03	1.7	5.5E-04
PA1333	-	104	354	340	1.8	2.1E-13	1.7	1.4E-12
PA1791	-	298	816	978	1.5	7.8E-12	1.7	1.0E-15
PA4356	xenB	1710	4808	5632	1.5	1.2E-12	1.7	3.1E-16
PA3821	secD	2267	7748	7501	1.8	2.6E-07	1.7	2.5E-07
PA1698	popN	72	235	239	1.7	1.1E-06	1.7	3.8E-07
PA2496	-	85	306	295	1.8	6.5E-15	1.8	3.1E-14
PA2398	fpvA	21716	83134	76262	1.9	2.0E-21	1.8	1.9E-19
PA1744	-	22	67	84	1.6	5.6E-06	1.9	8.9E-09
PA3410	-	749	2955	2817	2	1.4E-17	1.9	2.1E-16
PA4168	fpvB	2156	11650	8293	2.4	4.3E-12	1.9	4.5E-09
PA4354	-	87	295	348	1.8	1.4E-12	2	3.4E-15
PA2812	-	1140	4314	4712	1.9	3.4E-20	2	4.3E-22
PA2333	-	161	674	674	2.1	2.9E-15	2.1	2.0E-14
PA2811	-	633	2601	2731	2	1.2E-24	2.1	1.3E-25
PA2813	-	672	2924	2966	2.1	1.7E-22	2.1	4.5E-23
PA2327	-	459	1970	2063	2.1	6.4E-16	2.2	4.4E-16
PA3268	-	457	1961	2200	2.1	1.0E-03	2.3	3.0E-04
PA4710	phuR	4537	26773	25760	2.6	8.1E-09	2.5	6.0E-09
PA2328	-	831	4981	5151	2.6	6.8E-13	2.6	1.6E-12
PA2485	-	146	1023	1062	2.8	2.1E-33	2.9	1.3E-34
PA2491	-	1765	12975	13941	2.9	2.5E-38	3	8.6E-42
PA2329	-	614	5135	4964	3.1	4.6E-16	3	5.4E-15
PA1970	-	61	404	504	2.7	1.4E-30	3	2.5E-37
PA2330	-	1133	10245	9752	3.2	3.1E-23	3.1	8.9E-22
PA2331	-	1109	9950	9748	3.2	1.6E-22	3.1	1.8E-21
PA2486	-	71	603	731	3.1	6.3E-35	3.4	1.4E-41
PA3230	-	592	6615	6562	3.5	1.7E-53	3.5	7.5E-53
PA1942	-	113	1953	1867	4.1	3.8E-38	4	4.8E-38
PA4623	-	53	3200	2461	5.9	3.8E-110	5.5	1.3E-98
PA4881	-	23	1162	1167	5.7	1.3E-35	5.7	1.6E-36
PA3229	-	123	12131	11934	6.6	9.1E-140	6.6	1.8E-138
PA2494	mexF	356	74861	62437	7.7	5.5E-177	7.5	3.5E-169
PA2495	oprN	117	26480	21369	7.8	5.7E-178	7.5	3.4E-169
PA2493	mexE	76	43561	37687	9.2	1.2E-213	8.9	1.3E-207

8.3.4 Genes assoicated with pathways

Up regulated genes in PAdel and associated genes, compared to PA:

Two-component system: nirM PA0753 PA0756 PA0757 amrA maeA arnB phaA PA5169 dnaA PA0112 dctA1 cheB2 cheR2 aer2 PA0177 PA0178 PA0179 cttP spuI spuB pilG pilH pilI pilJ pilK chpA chpB chpC creB creC vfr PA0749 PA0752 PA0754 PA0885 PA0886 csrA gacS oprD flaC fleQ fleS fleR PA1157 PA1158 phoP phoQ dctA2 PA1335 PA1336 ansB PA1339 PA1340 PA1341 PA1342 bdlA PA1437 PA1438 fliA cheY cheA cheB1 motC orf4 cheW ccoP1 ccoQ1 ccoO1 ccoN1 ccoP2 ccoO2 ccoN2 aer PA1566 PA1608 kdbF kdpA kdpB kdpC kdpD kdpE PA1646 PA1736 parS parR PA1856 PA1930 eraR atoB PA2002 amrB PA2040 czrR czcS PA2526 PA2527 PA2528 PA2548 PA2553 ctpH PA2573 PA2583 PA2652 PA2654 copR copS PA2920 PA3045 phoA cheR1 PA3349 PA3356 algD PA3589 glnD wspR cheB3 wspE wspD wspC wspB wspA PA3714 narI narJ narH narG narX narL eddA cioB cioA rocS1 rocA1 PA4080 ampC PA4133 PA4290 pctC pctA pctB PA4429 PA4430 PA4431 rpoN roxR roxS PA4520 pil pilS pilR PA4633 O1O_06561 PA4785 irlR PA4886 PA4915 motA PA5072 PA5082 glnA ntrB ntrC PA5165 PA5166 PA5167 PA5168 amgS amgR algR O1O_17699 phoB phoR O1O_21737 algB kinB PA5508 mifR mifS PA5522

Purine metabolism: purM purB PA3232 ndk prs purH purD purK dnaN PA0134 nuh PA0148 PA0387 apaH relA mazG purN purC dgt PA1140 nrdB nrdA cysC pykF allA alc PA1518 PA1521 xdhB xdhA dnaX apt dnaQ nrdD PA1931 PA1932 PA1933 holB dgt2 purF PA3516 PA3517 surE dnaE adk purT purL guaA guaB holC amn holA rpoA rpoC rpoB pykA cysNC cysD PA4645 pnp ureA ureB ureC purA aspP arcC nudE ppx cyaA xpt algC gmk rpoZ spoT purE polA nrdJa

Arginine and proline metabolism: PA0421 glsA speE1 gdhA speH speE2 argA PA0202 PA0219 gpuA aguA aguB spuI spuB spuC proC codA PA0530 speD argC PA0704 putA argD astA aruG astD astB astE PA1027 PA1268 ansB gbuA PA1566 ldcA PA2040 PA2317 PA2776 gdhB PA3356 amiE argG argF spdH dauB proA

PA4114   PA4163   PA4189   PA4342   argJ   speC   proB   PA4839   ureA ureB   ureC   PA4899   PA4908   aruH   aruI   PA5080   glnA   arcA   arcB arcC   argE   argH   PA5312   argB   PA5390   PA5508   PA5522

Protein export: ffh   secF   secD   yajC   secB   yidC   ftsY   lepB PA1303   secY   secE   secA   lspA   secG   tatA   tatB   tatC

Inter-pathway connection between 'Pyruvate metabolism' and 'Glyoxylate and dicarboxylate metabolism':   gltA   maeA   PA4333   mqo2 PA5046   pckA   glcB   fumC2   kynB   mqo1   ppc   purU   fumC1   fdnI fdnH   fdnG   purU2   PA5435   PA5436

Nitrogen metabolism   nir   norC   norB   PA0660   nosZ   gdhA   PA0102 spuI   spuB   PA0440   PA1024   napB   napA   PA1566   PA1779   O1O_12798 nasR   nasA   PA1786   PA2040   cynS   cynT   gdhB   PA3356   narI   narJ narH   narG   narK2   narK1   PA4202   PA4676   gltD   gltB   glnA   arcC PA5508   PA5522

Propanoate metabolism   prpC   prpB   sucC   PA3568   mmsA   phaA PA0130   PA0132   PA0494   PA0747   prpD   pta   ackA   PA0879   acsA1 PA1027   PA1187   PA1535   sucD   PA1736   PA1737   PA1748   acnB PA1821   exaA   atoB   PA2550   PA2553   PA2555   fadB   accD   PA3426 PA3589   accA   PA4435   acsA2   PA4785   accB   accC   PA4899   PA4994 PA5313

Glyoxylate and dicarboxylate metabolism   gltA   O1O_08108   gcvH1 PA2634   phaA   glyA3   PA0065   spuI   spuB   glcB   PA0550   gph1 PA0794   PA1052   PA1499   PA1500   PA1501   gcl   acnA   PA1566 PA1736   acnB   atoB   PA2040   kynB   katE   PA2553   PA2974   PA3131 gph2   eda   PA3356   PA3589   katA   purU   katB   hprA   PA4785   fdnI fdnH   fdnG   glnA   gcvH2   glcF   glcE   glcD   glyA1   purU2   PA5508 PA5522

Pyruvate metabolism   maeA   phaA   PA4333   mqo2   PA5046   pckA   glcB PA0494   gloA2   pta   ackA   fumC2   acsA1   ldhA   acyP   PA1027   hchA PA1217   pykF   lpd   PA1736   ppsA   gloB   exaC   atoB   PA2108   lpdV lldA   PA2553   PA2555   accD   PA3415   PA3416   PA3417   mqo1   gloA1 PA3589   accA   ppc   leuA   PA4022   PA4150   acoB   PA4152   pykA fumC1   acsA2   lldD   PA4785   lpd3   accB   accC   PA4899   aceE   aceF gloA   O1O_21382   PA5435   PA5436   PA5445

Inter-pathway connection between 'Citrate cycle (TCA cycle)' and 'Alanine, aspartate and glutamate metabolism'   gltA   purB   gdhA   mqo2 pckA   gabD   PA0440   O1O_19361   sucA   icd   idh   gdhB   mqo1   PA3516 PA3517   gltD   gltB   argH   aspA   PA5435   PA5436

Down regulated pathways in PAdel and associated genes (compared to PA):

Oxidative phosphorylation coxB coxA coIII ccoP2 ccoO2 ccoN2 cioB cioA PA4133 PA0107 PA0112 cyoE1 cyoA cyoB cyoC cyoD cyoE2 ccoP1 ccoQ1 ccoO1 ccoN1 sdhC sdhD sdhA sdhB PA1856 nuoA1 nuoA2 nuoB nuoC nuoE nuoF nuoG nuoH nuoI nuoJ nuoK nuoL nuoM nuoN PA2691 ppa PA4429 PA4430 PA4431 ndh ppk atpC atpD atpG atpA atpH atpF atpE atpB

Bacterial secretion system PA1662 PA1666 PA1668 PA1669 stp1 PA2367 PA2371 PA4144 PA5210 O1O_24470 pppA icmF1 PA0078 PA0080 fha1 hcp1 clpV1 PA0262 PA0263 ftsY PA0677 PA0678 PA0679 PA0680 PA0681 PA0682 PA0683 PA0684 PA0685 PA0686 PA0687 PA1382 PA1511 PA1512 pscU pscT PA1692 pscR pscQ pscP pscO pscN popN pcr3 pcrD pscC pscF pscJ pscL xphA xqhA PA2361 PA2362 PA2672 PA2673 PA2674 PA2675 PA2676 PA2677 xcpZ xcpY xcpX xcpW xcpV xcpU xcpT xcpS xcpR xcpP xcpQ PA3294 PA3486 ffh secF secD yajC secY secE secA secG opmH tatA tatB tatC secB PA5266 hcpA yidC

Biosynthesis of amino acids metK PA1217 acnA PA1901 phzC arcB sdaB thrB PA0025 trpA trpB PA0223 O1Q_16377 aroQ2 spuI spuB serA rpiA ilvA1 ilvD proC PA0399 PA0400 PA0440 PA0530 tktA pgk fba rpe trpE trpG trpD trpC argC PA0794 PA0851 phhC phhA argD gly1 lysC cysM phnA phnB dapA PA1061 dapE PA1254 ilvA2 PA1417 pykF PA1566 gltA aroC PA1750 thrH acnB metH metE PA2035 PA2040 PA2104 PA2105 pvdH sdaA O1O_08108 PA2531 icd idh PA2683 cysK tal PA2828 PA2843 PA2943 PA3001 trpF asd leuB leuD leuC aspC hisF2 hisH2 hisC2 pheA serC gap PA3356 pheC PA3506 argG argF eno PA3659 dapD thrC hom leuA cysE dauB proA PA4180 PA4188 pykA argJ hisC1 hisD hisG proB glyA3 prs ilvC ilvH ilvI tpiA dapB aroQ1 PA4908 hisZ PA4960 ilvE gltD gltB aroB aroK hisI hisE glnA gpmI hisF hisA hisH1 hisB O1O_18099 argA argE argH lysA dapF argB PA5390 ltaE glyA1 PA5435 PA5436 PA5508 PA5522

Purine metabolism nrdB nrdA xdhB xdhA nrdD PA1931 arcC nrdJa dnaN PA0134 nuh PA0148 PA0387 apaH relA mazG purN purM purC dgt PA1140 cysC pykF allA alc PA1518 PA1521 dnaX apt dnaQ PA1932 PA1933 purB holB dgt2 purF PA3232 PA3516 PA3517 surE dnaE adk purT purL guaA guaB ndk holC

amn holA rpoA rpoC rpoB pykA cysNC cysD PA4645 prs pnp purH purD ureA ureB ureC purA aspP nudE ppx cyaA xpt algC gmk rpoZ spoT purK purE polA

Nitrogen metabolism   napB napA narH narG narK2 narK1 arcC PA0102 spuI spuB PA0440 nir norC norB PA0660 PA1024 PA1566 PA1779 O1O_12798 nasR nasA PA1786 PA2040 cynS cynT gdhB PA3356 nosZ narI narJ PA4202 gdhA PA4676 gltD gltB glnA PA5508 PA5522

Styrene degradation PA0202 PA0704 maiA fahA hmgA amiE PA0226 PA0227 PA2473 PA4073 PA4163 PA4342

Aminobenzoate degradation   PA0202 PA0704 PA2475 PA3331 amiE eddA acyP PA1748 PA1821 antA antB antC phoA PA3426 PA4163 PA4342 mdlC vanA vanB

Tyrosine metabolism maiA fahA hmgA hpcG PA4128 adhA PA0242 gabD PA0421 hpd phhC PA1200 PA1966 gtdA PA2471 PA2473 PA2531 aspC hisC2 adhC hpaA hpaC PA4121 PA4122 hpcC hpcB hpcD hisC1

Sulfur metabolism   PA2310 CP84 PA3446 PA3449 PA3938 PA4130 atsC PA0185 atsR PA0193 cysA cysW cysT O1O_06686 nirM glpE cysM PA1061 sseA cysC cysP cysH cysI PA2104 PA2105 PA2345 msuD algY PA2594 PA2595 PA2596 PA2598 PA2600 cysK metZ ssuB PA3443 PA3444 PA3445 ssuB2 PA3448 cysE tauD PA3936 tauB PA3954 cysNC cysD piuB rhdA cysQ

Pyruvate metabolism gloA2 fumC2 PA1217 PA3415 PA3416 PA3417 glcB PA0494 pta ackA acsA1 ldhA acyP PA1027 hchA pykF lpd PA1736 ppsA gloB exaC atoB PA2108 lpdV lldA PA2553 PA2555 accD mqo1 maeA gloA1 PA3589 accA ppc leuA phaA PA4022 PA4150 acoB PA4152 pykA PA4333 fumC1 mqo2 acsA2 lldD PA4785 lpd3 accB accC PA4899 aceE aceF PA5046 gloA pckA O1O_21382 PA5435 PA5436 PA5445

Up regulated pathways 9and associated genes) in PAnfxC:

Glycine, serine and threonine metabolism: PA0421   thrH   pvdH O1O_08108 gcvP1 gcvH1 hom glyA3 gpmI trpA trpB serA ilvA1 PA0399 PA0400 PA0851 gly1 lysC PA1052 ilvA2 PA1499 lpd lpdV gcvT2 sdaA PA2683 asd serC dsdA PA3504 PA3710 thrC hprA pssA lpd3 PA4960 gcvP2 gcvH2 gcvT betA betB sdaB ltaE glyA1 soxB soxD soxA soxG thrB

Protein export: ffh   secF   secD   yajC   secB   yidC   ftsY   lepB PA1303   secY   secE   secA   lspA   secG   tatA   tatB   tatC

Pyruvate metabolism: maeA   phaA   PA4333   mqo2   PA5046 pckA   glcB   PA0494   gloA2   pta   ackA   fumC2   acsA1   ldhA   acyP PA1027   hchA   PA1217   pykF   lpd   PA1736   ppsA   gloB   exaC   atoB PA2108   lpdV   lldA   PA2553   PA2555   accD   PA3415   PA3416   PA3417 mqo1   gloA1   PA3589   accA   ppc   leuA   PA4022   PA4150   acoB PA4152   pykA   fumC1   acsA2   lldD   PA4785   lpd3   accB   accC   PA4899 aceE   aceF   gloA   O1O_21382   PA5435   PA5436   PA5445

Arginine and proline metabolism: PA0421   glsA   speE1   speH   speE2 argA   PA0202   PA0219   gpuA   aguA   aguB   spuI   spuB   spuC   proC codA   PA0530   speD   argC   PA0704   putA   argD   astA   aruG   astD astB   astE   PA1027   PA1268   ansB   gbuA   PA1566   ldcA   PA2040 PA2317   PA2776   gdhB   PA3356   amiE   argG   argF   spdH   dauB   proA PA4114   PA4163   PA4189   PA4342   argJ   speC   proB   gdhA   PA4839 ureA   ureB   ureC   PA4899   PA4908   aruH   aruI   PA5080   glnA   arcA arcB   arcC   argE   argH   PA5312   argB   PA5390   PA5508   PA5522

Catalytic complex: ccmA   macB   gcvH1   eno   uvrA   hmuV   dnaN   potA1 cysA   ruvA   sucB   gpsA   modC   metN1   uvrC   nuoC   nuoE   lolD   accD leuD   phnC1   phnC2   ssuB   ssuB2   glpD   potA2   accA   xseA   tauB xseB   ribH   rpoC   rpoB   accB   msbA   aceF   gcvH2   ppk   pstB   znuC metN

One carbon pool by folate: folA   purN   O1O_08108   glyA3   purH   fmt thyA   metF   folD   metH   gcvT2   folM   purT   purU   gcvT   PA5228 glyA1   purU2

Methane metabolism: thrH   O1O_08108   eno   glyA3   gpmI   serA fba   pta   ackA   acsA1   ppsA   PA2555   serC   PA3628   adhC   ppc   hprA acsA2   fdnI   fdnH   fdnG   PA4960   fbp   glyA1   fdhA

Aminoacyl-tRNA biosynthesis: glyQ   alaS   gltX   lysS   trpS   glyS fmt   tyrS2   proS   aspS   glnS   cysS   serS   pheT   pheS   thrS   metG hisS   valS   leuS   tyrS1   gatC   gatA   gatB   ileS   selA   argS

Cysteine and methionine metabolism metX   speE1   hom   speH speE2   PA0399   PA0400   ahcY   metK   speD   phhC   lysC   cysM   PA1061 sseA   mtnB   mtnD   mtnC   metH   metE   PA2104   PA2105   sdaA   cysK nucP   metZ   asd   aspC   mtnA   cysE   rhdA   metY   sdaB

Two-component system: PA0756   maeA   arnB   phaA   dnaA   PA0112 dctA1   cheB2   cheR2   aer2   PA0177   PA0178   PA0179   cttP   spuI spuB   pilG   pilH   pilI   pilJ   pilK   chpA   chpB   chpC   creB   creC   nirM

vfr   PA0749   PA0752   PA0753   PA0754   PA0757   PA0885   PA0886
csrA   gacS   oprD   flaC   fleQ   fleS   fleR   PA1157   PA1158   phoP   phoQ
dctA2   PA1335   PA1336   ansB   PA1339   PA1340   PA1341   PA1342
bdlA   PA1437   PA1438   fliA   cheY   cheA   cheB1   motC   orf4   cheW
ccoP1   ccoQ1   ccoO1   ccoN1   ccoP2   ccoO2   ccoN2   aer   PA1566
PA1608   kdbF   kdpA   kdpB   kdpC   kdpD   kdpE   PA1646   PA1736   parS
parR   PA1856   PA1930   eraR   atoB   PA2002   amrB   amrA   PA2040
czrR   czcS   PA2526   PA2527   PA2528   PA2548   PA2553   ctpH   PA2573
PA2583   PA2652   PA2654   copR   copS   PA2920   PA3045   phoA   cheR1
PA3349   PA3356   algD   PA3589   glnD   wspR   cheB3   wspE   wspD
wspC   wspB   wspA   PA3714   narI   narJ   narH   narG   narX   narL   eddA
cioB   cioA   rocS1   rocA1   PA4080   ampC   PA4133   PA4290   pctC   pctA
pctB   PA4429   PA4430   PA4431   rpoN   roxR   roxS   PA4520   pil   pilS
pilR   PA4633   O1O_06561   PA4785   irlR   PA4886   PA4915   motA
PA5072   PA5082   glnA   ntrB   ntrC   PA5165   PA5166   PA5167   PA5168
PA5169   amgS   amgR   algR   O1O_17699   phoB   phoR   O1O_21737
algB   kinB   PA5508   mifR   mifS   PA5522